Functional involvement of two histone-methyltransferases in response to stress and in regulation of flowering time in Arabidopsis thaliana

Xue Zhang

Université de Strasbourg

UNIVERSITÉ DE STRASBOURG

École Doctorale des Sciences de la Vie et de la Santé STRASBOURG

ÉCOLE DOCTORALE DES SCIENCES DE LA VIE ET DE LA SANTÉ

[Institut de Biologie Moléculaire des Plantes, UPR2357 CNRS]

THÈSE présentée par :

Xue ZHANG

soutenue: **le 27 Septembre 2019**

pour obtenir le grade de : **Docteur de l'université de Strasbourg**

Discipline/ Spécialité : Aspects Moléculaires et Cellulaires de la Biologie

Implications fonctionnelles de deux histone méthyltransferases dans les réponses aux stress et la régulation de la floraison chez *Arabidopsis thaliana*

THÈSE dirigée par :

Dr. SHEN Wen-Hui	DR CNRS, Université de Strasbourg

Rapporteurs externes :

Dr. CARLES Cristel	MdC, Université Joseph Fourier, Grenoble
Dr. BARNECHE Fredy	DR CNRS, ENS, Paris

Examinateur interne :

Dr. CHABOUTE Marie-Edith	DR CNRS, IBMP, Strasbourg

Autres membres du jury :

Dr. TREMOUSAYGUE Dominique	CRCN CNRS, LIPM, Toulouse
Dr. BERR Alexandre	CRCN CNRS, IBMP, Strasbourg

Acknowledgments

Firstly, I would like to thank **Dr. Alexandre Berr** for supervising and helping my research work along these four years. I am particularly indebted to **Alexandre** for his excellent advices and helps on my experiments, data analyzing, and thesis writing during my PhD study. I would like also to thank **Dr. Wen-Hui Shen** for acceptance as official director of my thesis and for providing helps and advices to my PhD work.

I acknowledge all members of my PhD jury: **Dr. Cristel Carles**, **Dr. Fredy Barneche**, **Dr. Dominique Tremousaygue**, and **Dr. Marie-Edith Chabouté**, who have kindly accepted to evaluate my PhD work.

I also express many thanks to my previous laboratory members for their help. I am deeply grateful to all colleagues in IBMP, in particular **Dr. Marion Clavel**, **Dr. Marie-Claire Criqui, Dr.Thibaut Hacquard, Dr. Esther Lechner** and **Dr. Thomas Potuschak** from Lab 612, **Dr. Amelia Felipo** and PhD student **Lucas Jilli** from Lab 626, **Dr. Marco Incarbone** from lab 309, **Dr. Yihan Dong** from Lab 456, and the principal investigator **Dr. Todd Blevins** from Lab 426 for their generous research help. I also acknowledge **Dr. Patrick Achard** from IBMP, **Dr. Kosmas Haralampidis** from Molecular Plant Development, National and Kapodistrian University of Athens, **Dr. Keqiang Wu** from Institute of plant biology, National Taiwan University, **Dr. Yuehui He** from CAS Center for Excellence in Molecular Plant Sciences and **Dr. Ilha Lee** from School of Biological Sciences, Seoul National University for their kindly providing plant mutant seeds. Moreover, I would like to thank my collaborators: **Mathieu ERHARDT** from the Microscopy and cellular imaging platform, **Julie ZUMSTEG** from Plant Imaging and Mass Spectrometry platform, **Dr. Thierry HEITZ** from IBMP, **Philippe Hammann** and **Johana Chicher** from the IBMC/IBMP proteomic platform, **Dominique Eeckhout** and **Geert De Jaeger** from VIB Center for Plant Systems Biology.

I am grateful to the **Chinese Scholarship Council (CSC)** for financial support over my PhD study.

Lastly, special thanks are reserved for my parents and all my friends for their support, encouragement and understanding.

CHAPTER I

GENERAL INTRODUCTION

I.1. The origin and definition of ‘epigenetics’

In the early 1940s, the term” epigenetics” was firstly defined by Conrad Waddington

and originally referred to heritable variations that can give rise to distinct patterns of terminal differentiation phenotypes in a reversible and often self-perpetuating way (Nicoglou and Merlin, 2017). Afterwards, new definitions of epigenetics started to emerge. David L. Nanney, in his paper published in 1958, explained epigenetics as mitotically stable, which is considered as a striking feature later (Nanney, 2006). The emerging hypothesis that chromatin state may influence gene expression based on McClintock's study on chromosome conformation in the 1950s and the discovery of DNA structure opens the door to investigate epigenetics at the molecular level (McClintock, 1951; Watson and Crick, 1953). With the help of epigenetics study progress in molecular and cellular biology, in 1996, Riggs and colleagues gave a more precise definition about epigenetics as "the study of mitotically and/ or meiotically heritable changes in gene function that can't be explained by changes in DNA sequence" (Riggs et al., 1996). Our view of epigenetics has considerably evolved during the past two decades, and thus in 2017, Antonine Nicoglou and Francesca Merlin gave a more general definition: "Epigenetics is the study of various intracellular factors that affect the stability of developmental process through their action on genome potentialities" (Nicoglou and Merlin 2017). Nowadays, epigenetic mechanisms classically comprise covalent post-translational modifications of histones, ATP-dependent chromatin remodeling, DNA methylation, nucleosome assembly/disassembly, histone variant incorporation, and non-coding RNAs regulation. All these mechanisms affect and control gene expression at the chromatin level (Feng and Lazar, 2012; Kumar, 2018).

I.2. Chromatin structure

In eukaryotic cells, the DNA-protein complex found inside the nucleus is called chromatin. Nucleosomes constitute the basic unite of chromatin. A single nucleosome contains about 147 base pairs (bp) of DNA wrapped around a histone octamer complex, which consists of 2 copies of each of the four core histone proteins H2A, H2B, H3 and H4 (Figure 1; Andrews and Luger, 2011; Bentley et al., 1984; Richmond et al., 1997). Nucleosomes are interconnected by a short stretch of about 20-60 bp of linker DNA forming a 'beads-on-a-string' chromatin fiber structure, also named the '10 nm chromatin fiber'. The beads-on-a-string structure can be further compacted with the addition of the linker histone H1 into a 30 nm diameter helical structure (Andrews and Luger, 2011;

Hansen, 2002).

Chromatin structure is not static but dynamic. Indeed, nucleosomes can move and be stabilized/destabilized or disassembled/reassembled in response to specific environmental signals or developmental cues (Andrews and Luger, 2011; Berr et al., 2011). Under light microscope, interphase chromatin exhibits two different forms named heterochromatin and euchromatin. Heterochromatin appears as electron-dense and darkly stained, with irregular particles scattered throughout the nucleus or found accumulated adjacent to the nuclear envelope. Inversely, euchromatin appears lightly stained and dispersed in the whole nucleus (Solovei et al., 2002). Because heterochromatin is tightly packed, it often correlates with gene silencing while euchromatin is loosely packed and associates with gene transcription. Dynamic changes in chromatin structure affects all DNA-based processes like transcription, DNA replication, DNA repair, chromosome segregation and transposon transposition.

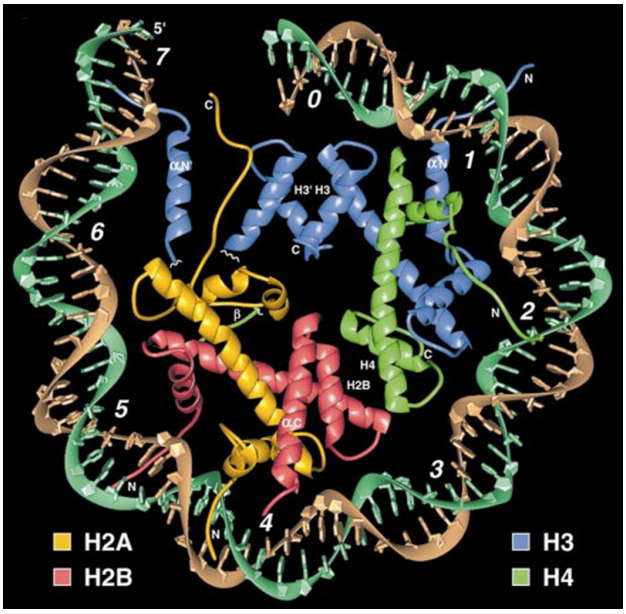

Figure 1: The nucleosome core particle. About 147-bp of DNA are wrapped around an octamer complex comprising two copies of each of histones H2A, H2B, H3 and H4 (Luger et al., 1997).

I.3. Histone modifications

Histones are water-soluble and contain a large number of basic amino acids, particularly lysine and arginine. The nucleosome core histones H2A, H2B, H3 and H4 are highly conserved in eukaryotes in terms of sequence and structure organization. Each histone in the octamer has a structured domain named histone fold and unstructured N- and C-terminal tails. Histone tails protrude from the nucleosome core, and they are subjected to diverse types of post-translational modifications (PTMs), usually referred as histone marks, including methylation, acetylation, phosphorylation, ubiquitination, and among others (Feng and Jacobsen, 2011; Kouzarides, 2007; Musselman et al., 2012). These modifications are established by so-called 'writers', and removed by 'erasers'. Functionally, these marks (in combination or not) can either modify the local electrostatic behavior (e.g. histone acetylation and histone deacetylation) and/or act as specific docking sites for secondary effectors named 'readers' (Rothbart and Strahl, 2014). Moreover, distinct marks can act sequentially or in a combined way to bring about different outcomes, thus constituting a histone code that considerably extends the information potential of the genetic code (Jenuwein and Allis, 2001). Here, I will mainly focus on histone methylation at lysine residues.

I.3.1. Histone methylation

Histone methylation drew attention in 1964 when it was firstly discovered (Allfrey and Mirsky, 1964) and then correlated with gene expression (Allfrey and Mirsky, 1964). Nowadays, histone methylation has been well documented in yeast, animals and plants. Methylation of histone can occur on lysine (K) and arginine (R) residues. Lysine methylation of H3 and H4 is implicated in both transcriptional activation and repression. Lysine methylation of H3 is one of the best-studied modifications and can be either mono-, di-, or tri-methylated, providing functional diversity to each site of methylation (Figure2; Bannister and Kouzarides, 2011; Kouzarides, 2007).

In the model organism *Arabidopsis thaliana*, at euchromatin region, histone H3 particularly carries methyl group on K4, K36 and K27. Among them, histone H3 methylations on K4 and K36 are associated with gene transcription activation, whereas methylation on K27 is generally associated with gene transcription repression (Bannister

and Kouzarides, 2011; Bemer, 2018; Deal and Henikoff, 2011).

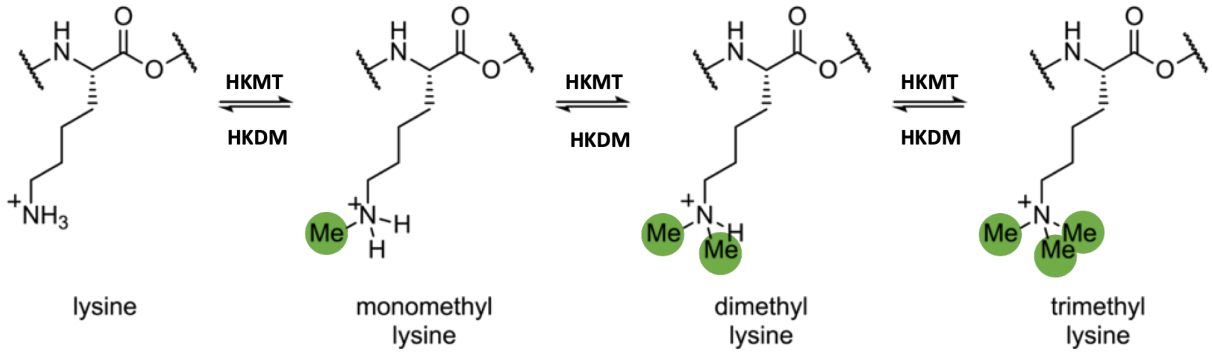

Figure 2: Histone methylation and demethylation. Schematic representation of histone methylation and histone demethylation processes by adding or removing one, two or three methyl group at ε-amine group of a particular histone lysine residue.

I.3.1.1. Genome-wide distribution of histone methylation H3K4me3, H3K36me3 and H3K27me3

During recent years, the genome-wide landscape of histone lysine methylation together with other histone modifications, histone variants and DNA methylation were gradually established in various organisms. Correlating transcription activation within the euchromatin, H3K4me3 forms a narrowed symmetric peak around the transcription start site (TSS) in animals and plants (He et al., 2011; Rowe et al., 2019; Xiao et al., 2016). In yeast and mammals, H3K4me3 is found associated with the initiation form of RNA Polymerase II (RNAPII), which is phosphorylated at serine 5 of its C-terminal domain (Collins et al., 2019; Deal and Henikoff, 2011; Kouzarides, 2007). H3K36me3 distributes towards the 3' end of transcribe regions in animals and yeast and is generally tightly associated with transcription rate by regulating RNAPII elongation (Kouzarides, 2007; Zhang et al., 2015). While in both rice and Arabidopsis, H3K36me3 was found across gene body with a peak towards the 5' end of transcribed regions (Liu et al., 2019; Xiao et al., 2016). Correlating with transcription repression, H3K27me3 has been found to distribute across the whole transcribed regions in Arabidopsis, unlike its enrichment at promoter regions in animals (Figure3; He et al., 2011; Xiao et al., 2016; Young et al., 2011; Zhang et al., 2007). In general, H3K27me3 and H3K4me3 are separately involved in gene silencing and active transcription, respectively. However, at some bivalent

genomic loci, H3K27me3 and H3K4me3 can co-exist (Jiang et al., 2008; Luo et al., 2013; Sequeira-Mendes et al., 2014).

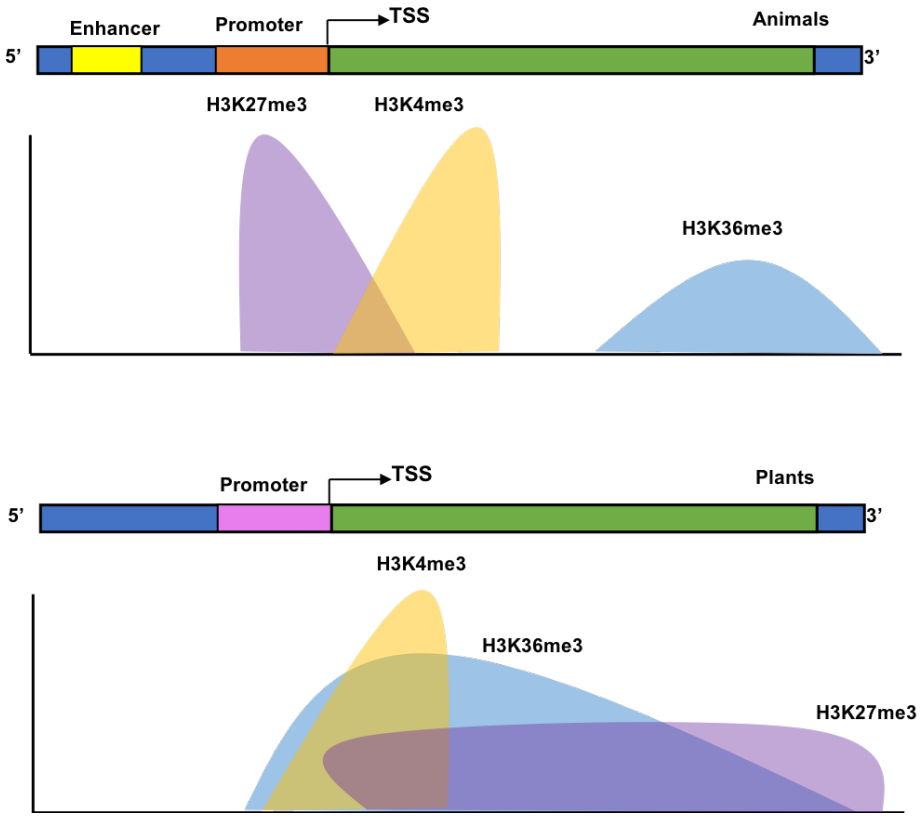

Figure 3: Histone lysine methylation distribution in animals (top) and plants (Adapted from Xiao et al., 2016). The definition of 'promoter' is different in animals and plants. In animals, promoter include about 100 bp upstream of the TSS. In Arabidopsis, promoter was located about the upstream intergenic region (1–2 kb or more) and includes the core promoter as well as enhancers. TSS: transcription start site; TTS: transcription termination site.

I.3.1.2. Histone lysine methylation 'writers'

Histone lysine methyltransferases (HKMTs) are evolutionarily conserved in eukaryotes. They usually have a conserved 130-150 amino acids catalytic domain SET, named after SUPPRESSOR OF VARIEGATION3–9 [SU(VAR)3–9], ENHANCER OF ZESTE [E(Z)] and TRITHORAX (TRX) in Drosophila (Berr et al., 2011; Dillon et al., 2005). Unlike other HKMTs, Dot1 in animal and yeast does not contain a SET domain, and it specifically methylates nucleosome histone H3 on lysine 79 (Min et al., 2003).

In Arabidopsis, approximately 47 genes encoding putative SET domain group (SDG)

proteins have been identified and assigned to distinct phylogenetic classes (Ng et al., 2007). SU(VAR)3–9 proteins generally govern H3K9 methylation activity and are associated with heterochromatinization, whereas others associate with euchromatin (Thorstensen et al., 2011). The Trithorax (Trx) family comprises five Trx homologs (ATX1/SDG27, ATX2/SDG30, ATX3/SDG14, ATX4/SDG16, and ATX5/SDG29), seven Trx-related proteins (ATXR1/SDG35, ATXR2/SDG36, ATXR3/SDG2, ATXR4/SDG38, ATXR5/SDG15, ATXR6/SDG34, and ATXR7/SDG25) and four ASH1 homologs (ASHH1/SDG26, ASHH2/SDG8, ASHH3/SDG7, and ASHH4/SDG24) (Berr et al., 2011). These SDGs associate with active gene transcription. The E(z)-family homologs (CLF/SDG1, MEA/SDG5, and SWN/SDG10) belong to the Polycomb Group (PcG) and are responsible for catalyzing H3K27 methylation involved in repression of gene transcription (Figure 4; Xiao and Wagner, 2015).

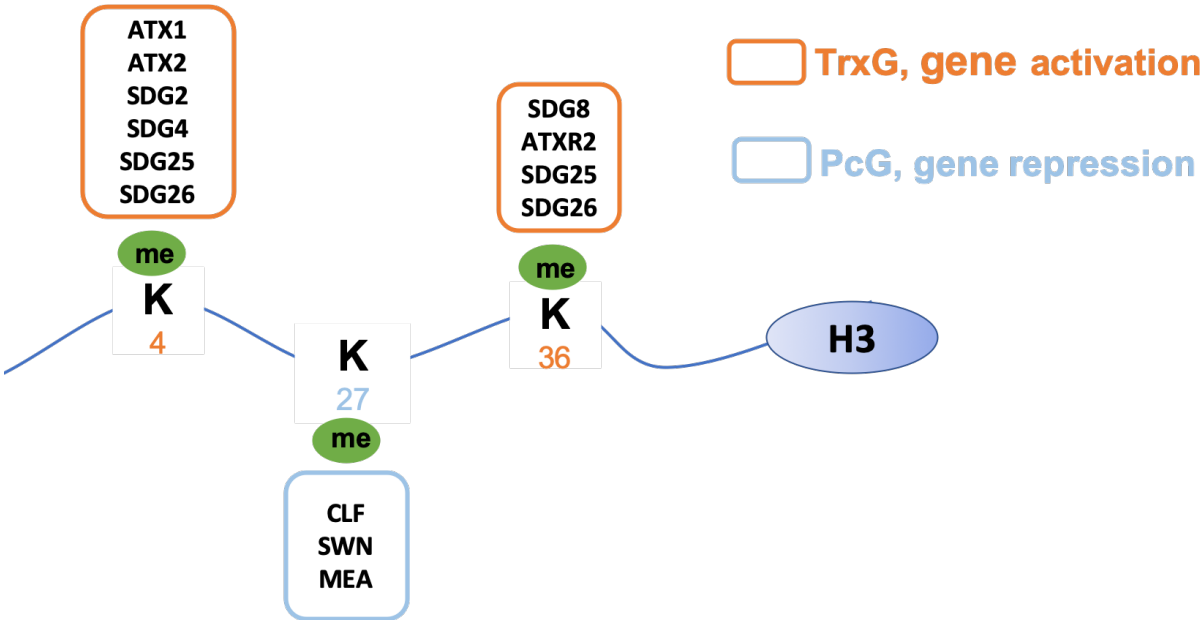

Figure 4: Histone 'Writers' in Arabidopsis, TrxG and PcG proteins. TrxG proteins methylate histone H3 at lysine 4 or 36 and contribute to gene activation; PcG proteins methylate histone H3 at lysine 27 and contribute to gene repression.

I.3.1.2.1. H3K4me3 writers

Set1 was the first H3K4 methyltransferase identified in yeast (Miller et al., 2001). It forms a complex, called COMPASS (Complex of Proteins Associated with Set1), and

exerts the enzyme activity to deposit one, two and up to three methyl groups at H3K4 (Miller et al., 2002). In Drosophila, three Set1 homologs were identified: dSet1, Trithorax (Trx), and Trithorax-related (Trr; Mohan et al., 2011). In Mammals, six Trx-related H3K4 methyltransferases were found: Set1A, Set1b, MLL, MLL2, MLL3 and MLL4 (Eissenberg and Shilatifard, 2010). All of them are associated with COMPASS or COMPASS-LIKE complexes containing the other core subunits WDR5 (WD repeat domain5), RbBP5 (Retinoblastoma binding protein 5), ASH2L (absent, small or homeotic 2-like), and DPY30 (Dumpy-30; Eissenberg and Shilatifard, 2010).

In Arabidopsis, ARABIDOPSIS HOMOLOG of TRITHORAX1 (ATX1/SDG27) was the first TrxG member reported in plants (Alvarez-Venegas et al., 2003). The *atx1* mutant show about 6-8% decrease of H3K4me2 and 15% reduction of H3K4me3 at the global level (Alvarez-Venegas and Avramova, 2005). Mutations in *ATX1* affects floral organ identity (Alvarez-Venegas et al., 2003a; Saleh et al., 2007, 2008), seed germination (Xu et al., 2018), flowering time regulation (Pien et al., 2008; Shafiq et al., 2014; Tamada et al., 2009; Xing et al., 2018), root development (Napsucialy-Mendivil et al., 2014), and biotic and abiotic stress responses (Ding et al., 2009, 2011; Ndamukong et al., 2010). By studying ATX1-dependent genes, several results suggested that:

1) the assembly of the Pre-Initiation Complex (PIC) at the promoter of ATX1-regulated genes requires ATX1 and AtCOMPASS (Ding et al., 2012, 2011; Fromm and Avramova, 2014).

2) the absence of H3K4me3 in *atx1* mutant does not affect the recruitment of TATA-binding proteins and RNAPII to its target gene promoters (Ding et al., 2011; Fromm and Avramova, 2014).

3) H3K4me3 is essential for transcription elongation (Fromm and Avramova, 2014).

ATX2/SDG30 is the closest ATX1 homolog, it shows 65% identity and 75% similarity with ATX1 at the amino acid level. While ATX1 appears responsible for the deposition of H3K4me3, ATX2 is defined as an H3K4 di-methyltransferase (Saleh et al., 2008). Surprisingly, the mutation of *ATX2* doesn't cause any visible phenotype. Nevertheless, the introducing of the loss function of *ATX2* into *atx1* mutant further enhances the early-flowering phenotype of the *atx1* single mutant, indicating partially redundant functions between ATX1 and ATX2 in flowering time regulation (Avramova,

2015; Berr et al., 2011).

SDG2/ATRX3 is a major H3K4-methyltransferase in Arabidopsis. It is capable of catalyzing H3K4me1, H3K4me2, H3K4me3 *in vitro* and its loss of function leads to severely decreased H3K4me3 level globally (Berr et al., 2010; Guo et al., 2010). SDG2 has very important role in multiple plant developmental process including root growth, circadian clock, male gametogenesis and vernalization (Berr et al., 2010; Guo et al., 2010; Malapeira et al., 2012; Pinon et al., 2017; Yao et al., 2013; Yun et al., 2012). Recently, SDG2 was shown to interact with the COMAPSS component S2Lb in vivo and they act coordinately to regulate a number of highly transcribed genes (Fiorucci et al., 2019).

SDG25/ATXR7 also belongs to the Arabidopsis TrxG family (Berr et al., 2009). It has been shown that SDG25 affects the expression of the major floral repressor *FLOWERING LOCUS C* (*FLC*) via H3K4 methylation (Berr et al., 2015; Berr et al., 2009; Shafiq et al., 2014; Tamada et al., 2009; Yun et al., 2011, 2012). It was also reported to be involved in plant immunity, a topic I will describe in later section of my manuscript thesis.

Loss-of-function of *SDG4* (*ASHR3*) leads to the decrease of the H3K4me2, H3K4me3 and H3K36me3 immunostaining signals in pollen vegetative nuclei. However, its precise enzyme activity was not defined *in vitro* (Cartagena et al., 2008). SDG4 was reported to play roles in pollen, stamen and root development, as well as in the regulation of disease-responsive genes (De-La-Peña et al., 2012; Kumpf et al., 2014; Thorstensen et al., 2008).

The biological function of ATX3, ATX4 and ATX5 was investigated more recently (Chen et al., 2017) . The mutation of a single of these genes does not display any apparent phenotypic defect. Strikingly, the developmental growth was significantly affected in the triple mutant *atx3/4/5*, which exhibits dwarf plants with small rosette leaves and reduced seed production. According to western blot analysis, *atx3/4/5* triple mutants presented a marked decrease of H3K4me2 and H3K4me3 levels. Chromatin immunoprecipitation assays with sequencing (ChIP-seq) combined with RNA-seq analysis demonstrate that ATX3, ATX4 and ATX5 most likely act redundantly to load H3K4me2/3 at a large number of genomic loci. However, authors reported a lack of constitutive correlation between the reduction in H3K4me2/3 and gene transcription since the majority of the genes with a decrease in H3K4me2/3 levels to show no change in transcript levels. The analysis of the genetic crosstalk between ATX3/4/5 and ATX1, ATX2 as well as SDG2 suggested

ATX3/4/5 likely function in the same pathway as ATX1, but in a separate pathway then ATX2 and SDG2 (Chen et al., 2017).

Related to the TrxG family, the COMPASS complex seems also highly conserved in Arabidopsis. Indeed, in addition to ATX1, other core COMPASS components were identified, including ARABIDOPSIS Ash2 RELATIVE (ASH2R), AtWDR5a/b, RETINOBLASTOMA-LIKE PROTEIN (RBL; jiang et al., 2011). It has been shown that COMPASS activates the transcription of several flowering genes through the deposition of H3K4me3 (Jiang et al., 2011). Liu and colleagues also found that under endoplasmic reticulum stress, two sequence-specific membrane-associated basic leucine zipper (bZIP) transcription factors bZIP28 and bZIP60 interact with COMPASS-like components WDR5 and ASH2R and result in the PIC assembly and the deposition of H3K4me3 at target genes (Song et al., 2015). Together, these findings indicate that H3K4me3 writers might be recruited to target loci by sequence-specific DNA binding factors. Additionally, a study from the He's group demonstrates that a COMPASS-like complex forming a super complex with an H3K36 methyltransferase and the nuclear mRNA cap-binding complex involve in RNA-processing-related events (Li et al., 2016). Their more recent work further illustrates that COMPASS-like and other chromatin modifiers, together with the primary determinant of natural variation in Arabidopsis flowering time named FRIGIDA (FRI), form a super-complex which establishes a local chromosomal environment at *FLC* to promote transcriptional initiation, fast elongation and efficient pre-messenger RNA splicing, leading to high-level of *FLC* mRNAs (Li et al., 2018). More recently, S2Lb, a homolog of the Swd2 COMPASS-associated subunit, which acts as a vital component of the H2Bub-H3K4me3 trans-histone crosstalk in *S. cerevisiae*, was identified in Arabidopsis. It co-regulates a large set of genes together with the AtCOMPASS-like core component WDR5, as well as with SDG2 through H3K4me3 deposition (Fiorucci et al., 2019).

I.3.1.2.2. H3K36me3 writers

In yeast, Set2, a RNAPII-associated methyltransferase, is responsible for adding one, two, or three methyl groups to lysine 36 of H3 (Venkatesh and Workman, 2013). Set2-mediated H3K36me functions to promote transcription elongation, repress histone exchange, impede hyperacetylation, and maintain the well-spaced chromatin structure

over the coding regions (Venkatesh and Workman, 2013). Set2 protein and its lysine methyltransferase activity are conserved in eukaryotes. In human, multiple proteins are capable of H3K36 methylation, including NSD1/2/3, ASH1L, SMYD2, SETMAR and SETD2. Among them, only SETD2 has been experimentally demonstrated to tri-methylate H3K36 (Wagner and Carpenter, 2012; Zhang et al., 2015). H3K36 methylation not only associates with transcription activation but also shows function in alternative splicing, dosage compensation, transcription initiation, transcription repression as well as DNA replication, recombination and repair (Wagner and Carpenter, 2012).

In Arabidopsis SDG4, SDG26, ATXR2/SDG36 and SDG8 (EFS/ASHH2) have been shown to regulate H3K36 methylation, with SDG8 being the most studied (Berr et al., 2015; Cartagena et al., 2008; Lee et al., 2017; Xu et al., 2007). Mutation of *SDG8* resulted in a reduced level of H3K36me2/me3 at the global level (Li et al., 2015; Xu et al., 2007; Zhao et al., 2005). SDG8 was involved in the regulation of multiple processes including temperature-induced RNA splicing (Pajoro et al., 2017), shoot branching (Bian et al., 2016; Cazzonelli et al., 2009; Dong et al., 2008), flowering time regulation (Kim, 2005; Kim and Michaels, 2006; Ko et al., 2010; Liu et al., 2016; Soppe et al., 1999; Xu et al., 2007; Zhao et al., 2019, 2005; Zhong et al., 2019), ovule and anther development (Grini et al., 2009), defense response against pathogens (Berr et al., 2010; Chen et al., 2009; Lee et al., 2016; Palma et al., 2010), carotenoid biosynthesis (Cazzonelli et al., 2010; Cazzonelli et al., 2009), seed development (Cheng et al., 2018; Tang et al., 2012), brassinosteroid response (Dong, 2014; Wang et al., 2014), and light and carbon response (Li et al., 2015). Interestingly, besides its H3K36me activity, SDG8 possesses a CW domain in the middle of its amino acid sequence that enables recognition of H3K4me (Hoppmann et al., 2011; Liu and Huang, 2018)

SDG26 (ASHH1) was first described as a flowering time promoter (Xu et al., 2008). Despite homology with SDG8 and similar histone methyltransferase activity *in vitro*, loss-of-function mutation of *SDG26* did not affect H3K36 methylation globally. Moreover, *sdg26* presents a late flowering phenotype, which is unusual compared to other HKMT mutants (Xu et al., 2008). The characterization of the genetic interaction between SDG26 and SDG8 further indicated that *SDG8* is epistatic to *SDG26* (Liu et al., 2016). The study of the involvement of *SDG26* in flowering time regulation further revealed that SDG26 activates specifically the expression of the floral integrator *SUPPRESSOR OF*

OVEREXPRESSION OF CONSTANS 1 (*SOC1*) *via* the deposition of H3K4me3 and H3K36me3 at its chromatin to promote floral transition (Berr et al., 2015). In parallel, the study of the double mutant *sdg8 sdg26* further reveals the involvement of SDG26 in H3K36me1 deposition at *FLC* (Liu et al., 2016). Finally, apart from its role in flowering time regulation, *SDG26* was also found to participate in DNA damage response and repair (Campi et al., 2012; MA et al., 2013; Roitinger et al., 2015).

The last characterized one was ARABIDOPSIS TRITHORAX-RELATED 2 (ATXR2). This HKMT was involved in the H3K36me3 deposition at *LATERAL ORGAN BOUNDARIES DOMAIN* (*LBD*) genes for their efficient transcriptional induction during cellular dedifferentiation (Lee et al. 2017). Loss-of-function mutation of *ATXR2* resulted in callus formation defect and global loss of H3K36me3 upon callus induction (Lee et al., 2017).

I.3.1.2.3. H3K27me3 writers

Unlike the association with transcription activation of TrxG proteins, PcG contributes to the maintenance of transcriptional repression (Montavon and Duboule, 2013). In animals, PcG proteins assemble in large protein complexes to exert their enzyme activity. Polycomb Repressive Complex 1 (PRC1) and PRC2 are the best-characterized PcG complexes. PRC1 catalyzes mono-ubiquitylation on the histone H2A lysine 119 residue (H2Aub1) *via* its ring-finger subunits, the RING1 and BMI1 ubiquitin ligases. PRC2 catalyzes mono-, di- and tri-methylation on lysine 27 of histone H3 (H3K27me1, H3K27me2, H3K27me3; Laugesen et al., 2019). In Drosophila, four core subunits: E(z), Su(z)12 (Suppressor of zeste 12), Esc (Extra sex combs) and N55 (a 55 kDa WD40 repeat protein also named p55), constitute the PRC2 (Pu and Sung, 2015). In Arabidopsis, CURLY LEAF (CLF), MEDEA (MEA) and SWINGER (SWN) are H3K27me3 methyltransferases, and are the homologs of E(Z). EMBRYONIC FLOWER 2 (EMF2), FERTILISATION INDEPENDENT SEED2 (FIS2) and VERNALIZATION2 (VRN2) are homologs of Su(z)12 and are necessary for H3K27me3 deposition. A similar function was later reported for FERTILIZATION INDEPENDENT ENDOSPERM (FIE) as the homolog of Esc. MULTICOPY SUPPRESSOR OF IRA 1 (MSI1) to MSI5 are homologs of N55 and they are able to bind histones (Pu and Sung, 2015; Xiao and Wagner, 2015). Together, these subunits have been reported to form at least three different PRC2

complexes, with histone methyltransferases acting partially redundantly:

1) the EMF2 complex (CLF or SWN, EMF2, MSI1 and FIE) contributes to regulating the vegetative-to-reproductive transition by repressing key developmental genes such as *LEAFY* and *AGAMOUS* (Chanvivattana, 2004; Kim and Sung, 2014; Kim et al., 2012, 2009; Yoshida et al., 2007).

2) the FIS2 complex (MEA, FIE, FIS2 and MSI1) functions in the female gametophyte and endosperm to repress *PHERES* (Hehenberger et al., 2012; Kim and Sung, 2014; Luo et al., 2002; Wang et al., 2006).

3) the VRN2 complex (CLF or SWN, VRN2, FIE and MSI1) represses *FLC* to accelerate flowering in response to vernalization (Chanvivattana, 2004; Dean et al., 2008; Finnegan and Dennis, 2007; Kim and Sung, 2014).

CLF was the first PcG functionally characterized in Arabidopsis (Goodrich et al., 1997). Nowadays, CLF appears to play multiple important roles in plants. It represses homeotic gene expression such as *AGAMOUS* (*AG*) and the Class I KNOX gene *SHOOTMERISTEMLESS* (*STM*) during leaf and flower development (Goodrich et al., 1997; Jiang et al., 2008; Kim et al., 1998; Liu et al., 2011, 2018; Saleh et al., 2007). It is involved in the silencing of *FLC* and its paralogs *MADS AFFECTING FLOWERING 4* and *5* (*MAF4* and *MAF5*), resulting in the induction of the floral pathway integrator *FLOWERING LOCUS T* (*FT*; Doyle and Amasino, 2009; Jiang et al., 2008; Liu et al., 2018; Shafiq et al., 2014). It suppresses homeobox gene by interacting with FIE during sporophyte development (Katz et al., 2004). It was implicated in seed size regulation and lipid biosynthesis (Liu et al., 2016), and it was required for proper somatic recombination (Chen et al., 2014), meristem activity in root (Aichinger et al., 2011) and cellular differentiation (Schatlowski et al., 2010).

The loss-of-function mutation of the maternal MEA allele exhibited embryo abortion and prolonged endosperm development (Grossniklaus et al., 1998; Jullien et al., 2006; Kinoshita et al., 2007; Kiyosue et al., 2002; Luo et al., 2002; Vielle-Calzada et al., 1999). It has been shown that MEA, together with DNA methylation, regulates cell proliferation during seed development (Schmidt et al., 2013; Wöhrmann et al., 2012; Xiao et al., 2003).

The mutation of *SWN* has no distinct phenotype, but can enhance the phenotype of

clf and *mea* single mutants (Chanvivattana, 2004; He et al., 2012; Wang et al., 2006). In addition, SWN showed partial redundant function with MEA in controlling the initiation of seed development (Wang et al., 2006). Recently, SWN was reported to function redundantly with CLF in seed development and vegetative phase transition (Footitt et al., 2015; Xu et al., 2015). This redundancy was further supported by recent genome-wide ChIP data (Shu et al., 2019).

I.3.1.3. Histone methylation 'Erasers'

Owing to the reversibility of histone modifications, methylated histone lysine residue can be demethylated by 'erasers' named histone demethylases (KDMs). The first human histone lysine-specific demethylase 1 (LSD1/KDM1A) was identified in 2004 as being able to remove dimethyl groups from lysine 4 on H3 (Shi et al., 2004). Later, proteins containing JmjC domain were found to be able to remove histone methyl groups in the presence of alpha-ketoglutarate, molecular oxygen (O2) and Fe(II) as cofactors (Tsukada et al., 2006). Based on sequence similarities, several sub-groups were defined as KDM5/JARID, JMJD1/JHDM2/KDM3, JMJD3/KDM6, JHDM1/FBX/KDM2 and 'JmjC domain-only' (Chen et al., 2011; Fodor et al., 2006; Klose et al., 2006; Mosammaparast and Shi, 2010; Tsukada et al., 2006; Whetstine et al., 2006). Meanwhile, histone lysine demethylases were also identified in plants and separated into two types: lysine-specific demethylase 1 (LSD) homologs and JUMONJI (JMJ) domain-containing proteins. The former is responsible for demethylation of mono-/di-methylated lysine residues, and the latter is responsible for demethylation of mono-/di-/tri-methylated lysine residues (Gan et al., 2015). In Arabidopsis, four LSD homologs were found and named LYSINE SPECIFIC DEMETHYLASE LIKE 1 (LDL1), LDL2, LDL3 (Jiang et al., 2007), and FLOWERING LOCUS D (FLD; Liu et al., 2007). In addition, 21 genes encode JMJ proteins in Arabidopsis, which were clarified as KDM5/JARID1, KDM4/JHDM3/JMJD2, KDM3/JHDM2, JMJD6 and JmjC domain-only group, based on their JmjC domain sequences and domain architectures (Hong et al., 2009; Lu et al., 2008). Here, I will mainly focus on FLD.

FLD has 60% similarity in amino acids with the human protein LSD1, which was previously reported to associate with deacetylase complexes (He et al., 2003). *fld* mutant exhibited hyperacetylation of histone H4 at *FLC* chromatin. According to this two

observations, FLD was originally considered as a histone deacetylase (He et al., 2003). Afterwards, FLD together with LDL1 and LDL2 were found to redundantly promote the floral transition by repressing *FLOWERING WAGENINGEN* (*FWA*) and *FLC* (Jiang et al., 2007). In 2007, Dean's group defined FLD as an H3K4me2 demethylase because of the global increase of H3K4me2 observed in the *fld-3* mutant (Liu et al., 2007). Many studies have established the essential role of FLD in flowering time regulation. The loss-of-function mutation of *FLD* results in a late flowering phenotype, which can be suppressed by vernalization treatment and by introducing *fld* in *flc-3* mutant background (He et al., 2003). FLD is demonstrated to repress sense *FLC* transcript *via* histone modifications (He et al., 2003; Jiang et al., 2007, 2009; Liu et al., 2007; Wu et al., 2015; Yu et al., 2011). Besides its function in flowering time regulation, FLD was recently shown to be required for systemic-acquired-resistance (SAR) by regulating the basal and SAR-induced expression of *WRKY* genes (Singh et al., 2013; Singh et al., 2014).

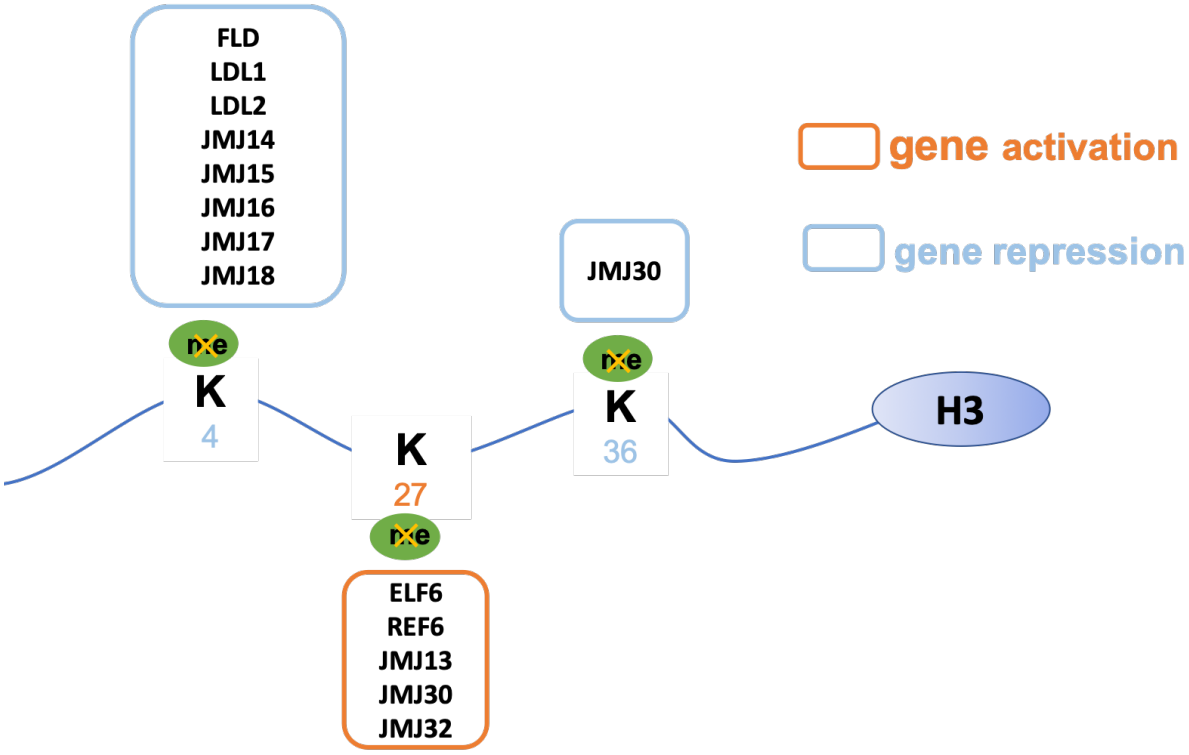

Figure 5: Reported histone methylation 'erasers' at euchromatin in Arabidopsis. Demethylases for the removal of H3K27me contribute to gene activation while ones for the removal of H3K4me and H3K36me contribute to gene repression.

I.4. Histone methyltransferases and plant development

Over the last ten years, the use of reverse genetic, and the development and improvement of methods for analyzing local/global changes of histone methylations had unraveled fundamental and multiple roles of histone methylations in regulating broad aspects of plant development. Here, I will focus on histone methyltransferases to gain insight about histone methylation contributions to biotic/abiotic stress responses and flowering time regulation.

I.4.1. Histone methylations in plant stress responses

Due to their sessile lifestyle, plants have to cope with an ever-changing environment and endure a broad spectrum of biotic (e.g. herbivorous insects or pathogens such as fungi, bacteria and viruses) or abiotic (e.g. high or low temperature, submergence or drought, and salinity) stresses that under field conditions usually occur concomitantly. Plants mainly rely on two different strategies to minimize the deleterious effects of stresses, either resist or tolerate. Therefore, in the course of evolution, plants have developed specific and very efficient multicomponent mechanisms to precisely perceive different environmental stresses and respond and/or adapt to them (Osakabe et al., 2013; Pieterse et al., 2009). These mechanisms allow plants to colonize even extreme habitats. In addition to pre-existing defense mechanisms (e.g. pre-existing physical and/or biochemical impediments such as the cuticle), plants have evolved inducible defense strategies for tolerance and/or resistance. Indeed, upon the perception of stressful conditions, a signal will induce a complex, rapid, and more or less specific repertoire of cellular and molecular responses to minimize or prevent damage. After detection, the stimulation of a given stress-signaling pathway will be integrated into the plant cell nucleus through a set of regulatory transcription factor cascades, which prioritizes defense over growth-related cellular functions, while conserving enough valuable resources for survival and reproduction (Nakashima et al., 2009; Verk et al., 2009). After stress detection, an essential component of all stress response strategies relies on the plant capacity to rapidly modify its transcriptome. Indeed, all plant stress responses ultimately result in a massive transcriptional reprogramming (Glazebrook et al., 2003; Huang et al., 2008; Moore et al., 2011; Riechmann and Ratcliffe, 2000; Tao et al., 2003). Among mechanisms able to achieve rapid and severe changes in gene expression, the impact of chromatin remodeling on the vital transcriptional reprogramming of stress responsive

genes is receiving more and more attention, especially because chromatin modifications can be mitotically or meiotically inherited (Figure 6). Chromatin changes can occur through different processes (DNA methylation, histone variants exchange, nucleosome occupancy, etc.) and I will here focus in particular on histone lysine methylations applied by histone methyltransferases.

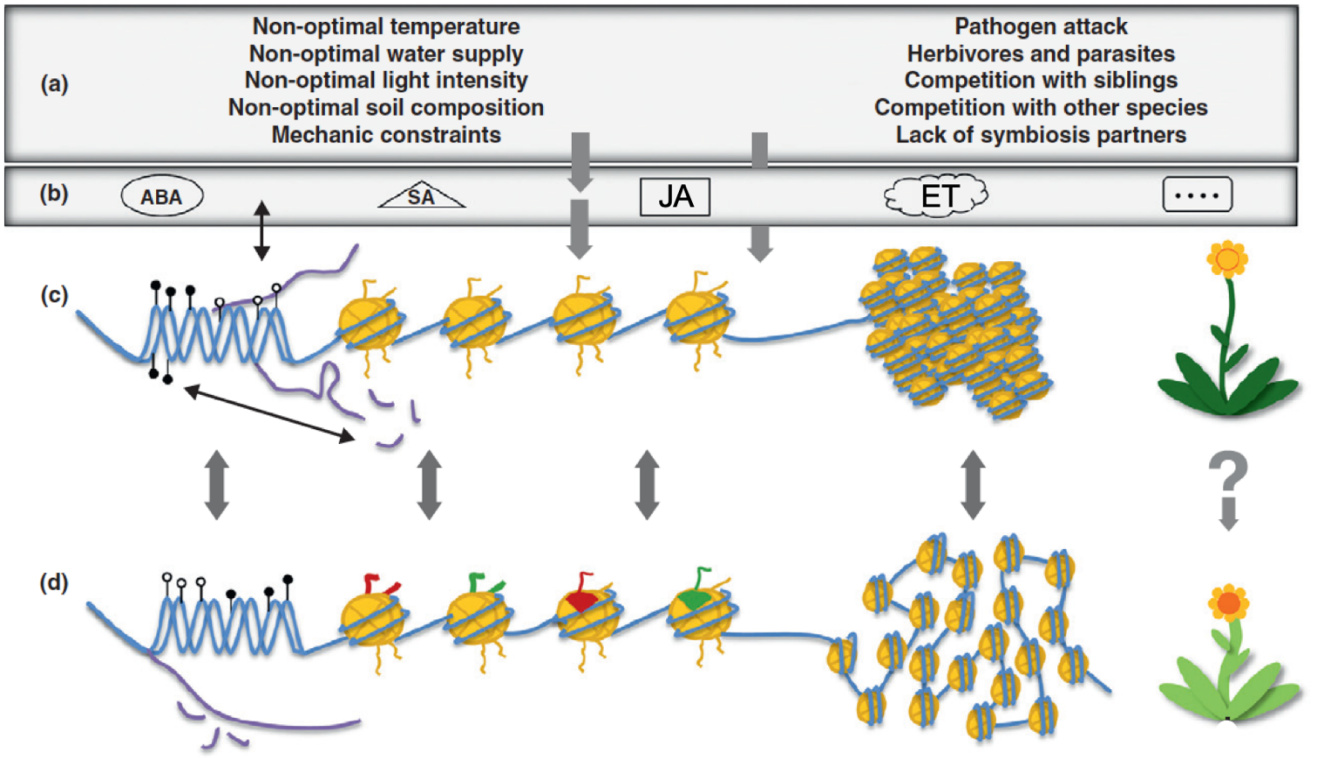

Figure 6: Model of stress etching on chromatin. Plants use a wide range of different sensing and signaling mechanisms to induce dynamic responses when challenged by a type of abiotic and biotic stresses (**a**). Signaling mainly goes through different plant stress hormones (**b**), including abscisic acid (ABA) in case of biotic stress, and salicylic acid (SA), jasmonic acid (JA) and ethylene (ET) upon biotic stress. Stress signaling then leads to stress-adapted gene expression by directly or indirectly affecting chromatin structure *via* DNA methylation, histone tail modifications such as methylation or acetylation (indicated in red and green, respectively), histone variant replacements or nucleosome addition/loss leading to chromatin condensation/de-condensation at responsive genes (**c**, **d**). These changes will modify metabolic or morphologic plant features under stress conditions, enabling the plant to resist or tolerate stressful conditions. (Adapted from Gutzat and Mittelsten Scheid, 2012).

I.4.1.1. Histone methylations during biotic stress responses

Biotic stress usually refers to the damage inflected by insects or pathogens (viruses, bacteria or fungi) to plants. In addition to passive defense mechanisms (i.e. pre-existing

physical and/or biochemical impediments), tolerance and/or resistance can be acquired from rapidly inducible defense mechanisms (Lee et al., 2017). The phenomenon of non-host resistance (NHR) is defined as the resistance of an entire plant species against a specific pathogen. NHR is the most durable resistance in plants, and it relies on a complex combination of constitutive and inducible defense components. In addition to NHR, plants possess other elaborated defense components to protect themselves against infection and can recognize pathogens using specific receptors that induce two layers of defense. Firstly, surface-localized receptors can perceive conserved pathogen structures called pathogen-associated molecular patterns (PAMPs). PAMPs are recognized *via* pattern-recognition receptors (PRRs) that induce the first rise in plant defense level generally termed PAMP-triggered immunity (PTI). To suppress PTI, successful pathogens will secrete effector proteins into host cells. In turn, plants induce the second rise in defense level termed effector-triggered immunity (ETI), *via* the pathogen strain or race-specific recognition of effectors by intracellular immune receptors called resistance (R) proteins, which often belong to the nucleotide-binding site–leucine-rich repeat (NBS-LRR, also known as NLR) family. Typically, ETI is associated with rapid programmed cell death at the infection site to restrict the spread of pathogens, a response which is referred to as the hypersensitive response (HR), and systemic acquired resistance (SAR) in the host, while PTI is not.

To defend themselves and build-up effective defensive reactions against various pathogens, plants have evolved complex defense strategies in which the pathogen-sensing machinery will provoke, though specific signaling cascades, the biosynthesis of several phytohormones, including salicylic acid (SA), jasmonic acid (JA) and ethylene (ET; Bari and Jones, 2009; Pieterse et al., 2009; Figure 7). Accumulating evidence shows that defense hormones also contribute to NHR. These hormones will then orchestrate the overall plant defense reaction locally but also systemically by inducing defense genes through intricate regulatory networks.

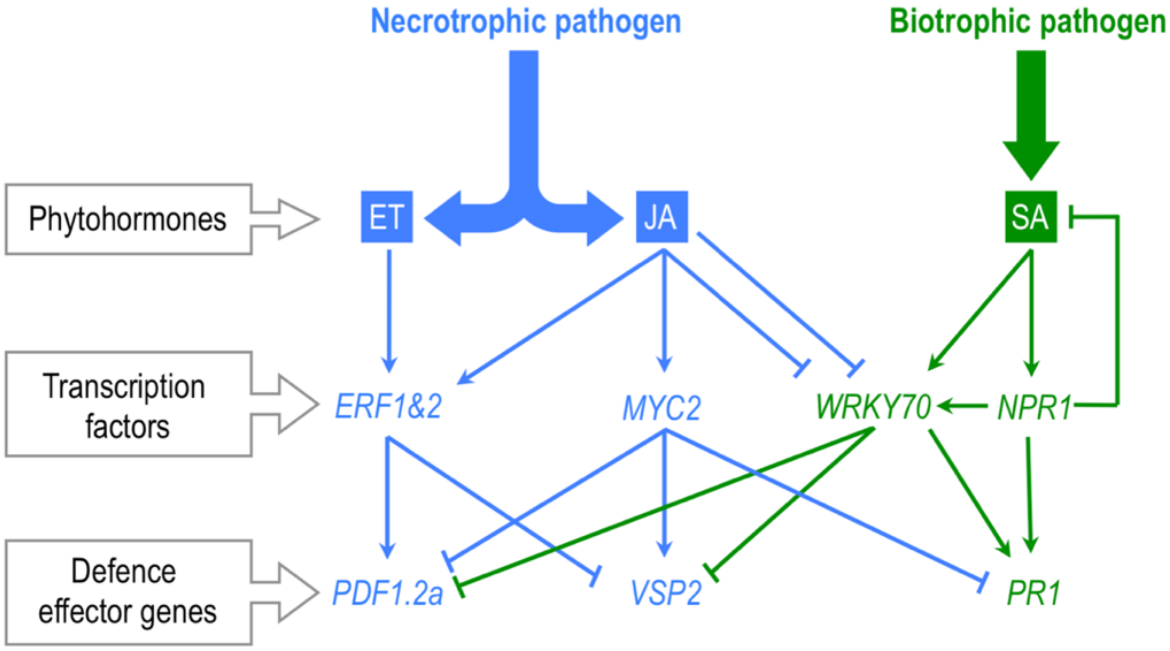

Figure 7: A simplified model for the regulation of plant defense networks in response to biotrophic and necrotrophic pathogenic infection. Upon infection, accumulation of plant defense hormones like ET, JA or SA further activates the expression of specific plant defense genes such as *PDF1.2* (*PLANT DEFENSIN1.2*), *VSP2* (*VEGETATIVE STORAGE PROTEIN 2*) and *PR1* (*PATHOGENESIS-RELATED-1*) through selective transcription factor dependent pathways. Positive (arrows) and negative (bars) regulations are depicted. (Adapted from Berr et al., 2012)

I.4.1.1.a. Histone methyltransferases and the SA signaling pathway

SA is a non-mobile signal agent playing an important role in defense against pathogens with a biotrophic lifestyle such as *Hyaloperonospora parasitica* and *Erysiphe orontii* fungi or with a hemibiotrophic lifestyle such as *Pseudomonas syringae* (Figure 7; Jones and Dangl, 2006). SA accumulation is required for both local and SAR and is considered as the first chemical in the induction of Pathogenesis-Related (PR) genes, such as *PR1*, which play important roles in preventing or slowing colonization of pathogens in the host (Sudisha et al., 2012). While to tackle biotrophic pathogens infection Arabidopsis relies primarily on the SA signaling pathway, JA together with ET are prominent to mediate efficient responses upon necrotrophic pathogens infection, such as *Botrytis cinereal* or *Alternaria brassicicola*, or wounding for example during herbivorous insect attacks (Figure 7;Pieterse, 2013). SA, JA and ET signaling pathways are extensively cross-talking,

providing the plant with a powerful regulatory plasticity essential to quickly and efficiently cope with its hostile environment (Figure 7; Grant and Jones, 2009; Pieterse et al., 2009; Spoel and Dong, 2008).

In the past decade, several studies in Arabidopsis have suggested the involvement of histone methylations in the control of the SA-related signaling network. Indeed, an increased level of H3K4me2 was detected at the chromatin of *PR1* in mutants for the negative regulator of SAR *SNI1* (*Suppressor of NPR1, Inducible*) and 48 h after stimulation with the SA-analogue S-methyl benzo [1,2,3] thiadiazole-7-carbothioate (BTH; Mosher et al., 2006). Interestingly, it is crucial to notice that H3K4me3 is present on *PR1* chromatin before any stimulation. Surprisingly, no changes in both H3K4me2 and H3K4me3 were reported on *PR1* 24 h after SA treatment. These contradicting results probably reflect several thinks, first, the action of the so-called "SA-analogue" BTH on gene induction is broader than the action of SA itself (Gruner et al., 2013), and second, the sampling timing (48 h after stimulation versus 24 h). Together, it seemed that H3K4 methylation is required not precociously for the transcriptional induction of *PR1*, but later, for its maintenance. The results also suggest that H3K4me3 is preliminarily in place before stimulation, probably to provide *PR1* with the appropriate chromatin state for efficient induction upon need.

SAR is a global response induced at the site of infection that leads to long-lasting and broad-spectrum disease resistance at distal uninfected tissues (Fu and Dong, 2013). In the SAR, gene priming corresponds to the capacity of a gene to respond faster and stronger to a subsequent challenge and benzothiadiazole (BTH) is known to induce priming (Kohler et al., 2002). Using BTH, H3K4 tri-methylation (i.e. together with H3 acetylation) was systemically found to set during a priming event at the promoter region of several *WRKY* genes, which are known to be induced by PAMP (Dong et al., 2003) and maintained after of lag phase of several days . In line with the systemic nature of SAR, the methylation increase was also found in adjacent non-primed leaves. Together, it was proposed that H3K4 methylation might create a memory of the primary stimulation that will be associated with an amplified reaction to a second stress stimulus (Jaskiewicz et al., 2011). However, nothing is yet known about the histone-methyltransferase(s) involved in this priming process and about how a particular histone methyltransferase would be recruited at these primed genes.

Few histone methyltransferases were involved in the defense against biotrophic pathogens. The H3K4 tri-methyltransferase ATX1 positively and directly regulates the expression of the transcription factor WRKY70, a factor involved in regulating cross-talk between the SA and JA signaling pathway (Alvarez-Venegas et al., 2006). The expression of *WRKY70* is decreased in *atx1*, and this provokes a decrease in the expression of *PR1*, resulting in impaired resistance to *Pst* infection. Because the SA-induced *PR1* transcription is not affected in *wrky70* mutant (Ren et al., 2008), ATX1 may also regulate *PR1* expression through a yet unknown mechanism. The major H3K36-methyltransferase SDG8 is also involved in plant defense against *Pst*. SDG8 maintains the basal H3K36me3 level at the chromatin of *RPM1* and *LAZ5*, two genes encoding nucleotide-binding site–leucine-rich repeat (NBS-LRR) proteins (Palma et al., 2010). The basal H3K36me3 level is required for both the basal transcription and the transcriptional induction upon stimulation of these resistance genes. Also, the mutation of *SDG37/ASHR1*, another *ASH1*-related gene encoding a putative HKMT, results in more sensitive to *Pst* infection than wild-type plants (De-La-Peña et al., 2012). Interestingly, *SDG8* and *SDG37* are both induced by the non-pathogenic *Pst* DC3000 *hrpA* mutant and repressed by the virulent *Pst* DC3000. Because the *hrpA* gene encodes the major subunit of the Hrp pilus, which is required for secretion of putative virulence proteins, this result suggests the existence of a yet unknown mechanism through which virulent bacteria repress specific histone methyltransferases to promote host susceptibility. This hypothesis is very exciting since there is few examples of pathogens able to produce histone-modifying enzyme inhibitors. Indeed, the HC-toxin produced by the maize pathogen *Cochliobolus carbonum* and required for its pathogenicity causes histone hyperacetylation, making it a potential histone deacetylase (HDACs) inhibitor (Brosch et al., 1995; Ransom and Walton, 1997). Similarly, *Alternaria brassicicola* produces a toxin called depudecin, known to inhibit HDAC activity both *in vitro* and *in vivo* (Kwon et al., 2003, 1998; Matsumoto et al., 1992; Oikawa et al., 1995). Finally, SDG8 and also SDG25/ATXR7 were recently found to contribute together to plant immunity (Lee et al., 2016). Indeed, the enhanced susceptibility of the corresponding loss-of-function mutants was explained, at least in part, by the reduced expression of *CAROTENOID ISOMERASE2* (*CCR2*) and *ECERIFERUM3*, two genes encoding enzymes involved in the biosynthesis of carotenoids and cuticular wax, respectively, and involved in plant immunity. The reduced expression of these two genes was correlated with the lower than wild-type level of H3K4 and H3K36 methylation

and of H3K4 at their chromatin in *sdg8* and *sdg25*, respectively (Lee et al., 2016).

I.4.1.1.b. Histone methyltransferases and the JA/ET signaling pathway

The involvement of histone methylation in the defense against necrotrophic pathogens is far less documented as compared with the defense against biotrophic pathogens. Besides being more susceptible to *Pst*, the *sdg8* mutant also presents an increased susceptibility to necrotrophic fungal pathogens as a consequence of the inefficient transcriptional induction of different genes in the JA/ET signaling pathway (Berr et al., 2010). While in the mutant this lack of induction was correlated to a weak level of H3K36me3 at the chromatin of these genes, in wild-type plants, H3K36me3 and gene expression were together increased upon infection or stimulation with exogenous methyl jasmonate (MeJA, an active derivative of JA). Because H3K36me3 was readily in place at a subset of JA/ET signaling-related genes under resting conditions, H3K36 methylation was proposed to act as a "permissive" mark enabling the more rapid and efficient transcriptional induction of JA/ET-related genes when challenged (Berr et al., 2012). In addition, the repressive mark H3K27me3 was detected at a stably low level at defense effector genes, which may participate in the reactivity of plants to pathogen infections since H3K27 demethylation is not required. The higher sensitivity of *sdg8*, and also *sdg25*, to necrotrophic fungi was independently confirmed by Lee and colleagues (Lee et al., 2016), further supporting the important role played by SDG8 in regulating plant immunity genes. More recently, the pre-deposition of SDG8-mediated H3K36me3 was found required for the upregulation of many genes induced by a JA-mediated wound signal (Zhang et al., 2019). Because wounding is the first event triggering regeneration, the authors further proposed that JA may cooperate with histone methylation to promote regeneration in response to wounding.

I.4.1.2. Histone methylations during abiotic stress responses

Heat, cold, drought, salinity and nutrient deficiency represent different types of abiotic stresses that are related to every ecosystem and their impacts on plants are inevitable. These environmental stresses influence plant yield and quality by affecting various cellular and organ processes (Wang et al., 2003). Abiotic stresses also induce the production of reactive oxygen species (ROS), which will cause irreversible damages to

tissues and cells, ultimately leading to reduced growth, fertility and premature senescence (Krasensky and Jonak, 2012). Like biotic stresses, plants have evolved adaptive and dynamic mechanisms to circumvent biotic stresses. One of the early events following the perception of abiotic stress is the local biosynthesis of the phytohormone abscisic acid (ABA; Jones, 2016). ABA regulates many aspects of plant growth in response to unfavorable abiotic stress conditions, allowing the plant to tolerate and survive in adverse conditions (Fujita et al., 2006). For example, drought, firstly perceive at the root level, triggers ABA biosynthesis, and increased tissue ABA accumulation. ABA is then transported to the upper parts of the plant to provoke stomatal closure and reduced transpiration. In addition, ABA can integrate both biotic and abiotic stresses in a complex network of interacting pathways with crosstalk at many different levels in order to control the switch in priority between stress responses, promoting the response to the most severe threat (Fujita et al., 2006). Despite their very harmful effects on crop growth and productivity worldwide, particularly when they occur in combination (Asselbergh et al., 2008; Atkinson and Urwin, 2012; Yasuda et al., 2008), only little is known about the functional involvement of a particular histone methyltransferase as a potential regulator of plant responses to abiotic stresses.

I.4.1.2.a. Histone methyltransferases and water stress

Water stress is a term which reflects two extremes regarding the water availability, with on one side a lack and on the other side an excess. Drought reduces the water availability for fundamental cellular functions and maintenance of turgor pressure. The resulting osmotic shock will then reduce photosynthetic carbon assimilation. In Arabidopsis, while several drought-inducible genes (*RD29A*, *RD29B*, *RD20* and *RAP2.4*) were upregulated in response to dehydration, the level of H3K4me3 at their chromatin was simultaneously found increased (Gao et al., 2007; Mittler, 2006). Interestingly, the RNAPII level was quickly reaching a plateau upon stress exposure, while H3K4me3 was still growing. Later, another group demonstrated that ATX1, through its H3K4 methyltransferase activity, was necessary for the efficient induction of genes involved in dehydration stress signaling in both ABA-dependent and ABA-independent pathways (Kim et al., 2008). More globally, the whole-genome distribution patterns of H3K4me1/me2/me3 were established using ChIP-Seq in 4-week-old Arabidopsis rosette leaves under dehydration stress conditions, and a strong correlation was found between

H3K4me3 and transcripts levels of stress-responding genes (Ding et al., 2011). Surprisingly, in contrast to the classical enrichment of H3K4me3 around the transcriptional start site of actively transcribed genes observed in different eukaryotes (Rando and Chang, 2009; Roudier et al., 2011), H3K4me3 displayed a broader distribution on dehydration and ABA-inducible genes which may reflect a function not strictly related to transcription initiation (Dijk et al., 2010). In line with an evolutionarily conserved process, a positive correlation between H3K4 methylation and drought stress was also found in rice (Zong et al., 2013). In a time-course study where Arabidopsis seedlings were exposed to cycles of dehydration stress followed by recovery under normal conditions, "trainable" and "not trainable" genes were identified (Ding et al., 2012). While "not trainable" genes showed during the recovery period H3K4me3 levels similar to those in control conditions, "trainable" ones displayed an additive increase after each cycle accompanied by an accumulation of RNAPII, suggesting a putative transcriptional stress memory.

Compare to drought, the impact of histone methylation on submergence tolerance is far less documented. Like drought, submergence is also a complex stress that encompasses many changes in environmental factors, including light intensity, pH and dissolved oxygen concentration. Alcoholic fermentation is essential for the survival of plants under anaerobic environments and the expression of two genes involved in this anaerobic metabolism was found correlated to the increased H3K4 methylation level on their chromatin in rice (Tsuji et al., 2006). This change was reverted to its initial level following re-aeration, indicating that in this particular case, H3K4me3 does not serve as a memory mark of prior transcriptional activity.

I.4.1.2.b. Histone methyltransferases and salt stress

Salinity is also a severe stress factor that can limit plant growth and development by stimulating water stress, ion toxicity, nutritional disorders, oxidative stress, alteration of metabolic processes, membrane disorganization, genotoxicity, reduction of cell division and expansion (Carillo et al., 2011). In Arabidopsis, the induction of several ABA and salt (NaCl) stress responding genes were found correlated to an increase in H3K4me3 and a decrease in H3K9me2 (Chen et al., 2010). Whether a specific histone methyltransferase responsible for the H3K4 methylation increase contributes to the

processes is still unknown. The decrease in the repressive histone modification H3K9me2 might reflect either the removal of methyl groups by a histone demethylase or the dilution of the marked nucleosomes. Interestingly, when the histone deacetylase HDA6 was mutated, the observed increase in H3K4me3 was partially suppressed in response to stress, while the H3K9me2 decrease was unaffected. Because H3K4me3 and histone acetylation are typically together associated with transcribed regions and transcription start sites (Roudier et al., 2011; Sequeira-Mendes et al., 2014), this last observation may suggest that histone acetylation is preliminary required for H3K4 methylation. Supporting the conserved role played by histone methylation in regulating the expression of some transcription factors crucial for salinity tolerance in plants, this histone mark was found altered at some salinity-induced genes in soybean (Song et al., 2012).

Like in biotic stress, priming can also be observed when plants exposed to abiotic stress. Indeed, if plants have previously undergone an acclimation process, their reaction to the following stress could be more successful (Knight et al., 1998; Lang and Palva, 1992). While studying chromatin changes after low salt priming globally, H3K4me3 and H3K27me3 were found increased and decreased at some genes, respectively (Sani et al., 2013). Suggesting a somatic process of stress memory, some of these methylation changes continue apparent 10 days after at some genes resulting in a long-lasting transcriptional change.

I.4.1.2.c. Histone methylations and temperature stresses

Due to global warming and the fact that temperature stress severely affects flowering time and reproductive success of plants, the genetic mechanisms of plant responses to temperature changes have been extensively studied. Plants exposed to temperature stresses modulate the transcription of a large number of genes involved in distinct biochemical and physiological response pathways and networks of phytohormones or secondary metabolites, ultimately leading to increased tolerance to hazardous temperature stresses (Chinnusamy et al., 2007; Qu et al., 2013). In Arabidopsis, some histone methylation marks were involved in the setting up of the temperature stress response, but corresponding histone-modifying enzymes were not yet identified. In a heat stress study, H3K27me3 was found decreased at *FLC* locus when plants were exposed to heat, resulting in its up-regulation and preventing precocious flowering (Gan et al., 2014).

Similar to other stress, a heat stress memory, during which acquired thermotolerance is actively maintained, also exists and was associated with the sustained accumulation of H3K4me2 and H3K4me3 at some memory genes that would be maintained for at least 2 days after the end of the heat stress (Lämke et al., 2016). Interestingly but through an unknown mechanism, the sustained accumulation of H3K4 methylation was found dependent on the hit-and-run functioning of the heat-shock transcription factor HsfA2 (Lämke et al., 2016).

Similar to heat stress, cold stress also positively regulates several specific downstream transcription factors and their target genes (Banerjee et al., 2017). Upon cold stress, the repressive mark H3K27me3 was decreased at the cold-responsive genes *COLD REGULATED 15A* (*COR15A*) and *GALACTINOL SYNTHASE 3* (*ATGOLS3*), in both a histone occupancy-dependent and -independent manner (Kwon et al., 2009). Interestingly, the resulting transcriptional induction was more rapid than the H3K27me3 decrease, and the H3K27me3 decrease was maintained upon plants back to normal growth conditions. However, the maintenance of a low H3K27me3 level at *COR15A* and *ATGOLS3* cannot be regarded as a short-term memory since re-exposure to cold temperatures does not cause the stronger and/or faster transcriptional induction of these genes.

I.4.1.3. Histone methylations at the junction between abiotic and biotic stresses

In nature, plants are exposed to a multitude of stresses during their lifetime, while in the controlled laboratory environment, stresses are usually applied separately. To approach as close as possible natural growth conditions in a controlled manner, the effect of recurrent abiotic stresses on the resistant to *Pst* was measured (Singh et al., 2014). Interestingly, plant exposed prior to abiotic stresses were more resistant to *Pst* than plants grown in a stable environment. This enhanced resistance was due to the priming of commonly used marker genes of PTI. Interestingly, an increase in H3K4me2 and H3K4me3 at the chromatin of these genes was observed (Singh et al., 2014). Even if the histone methyltransferase involved in this process remains to be identified in future, this work readily indicates that the environmental history of plants is recorded in its chromatin under certain conditions and can shape/modulate the response to abiotic/biotic stresses.

I.4.1.4. Toward a unifying model of stress response regulation by histone methylations

Stressful conditions for plants can originate from numerous physical, chemical and biological factors, and plants have developed a plethora of survival strategies including developmental and morphological adaptations, specific signaling and defense pathways as well as innate and acquired immunity. Current information implicates that histone methylations and some stress responses meet at different levels. Although connections still resemble a puzzle for which many pieces are still missing, a preliminary model is emerging (Figure 8). In this model, histone methylation changes involved in stress responses can be classified into three, most likely, interrelated categories:

- histone methylation marks can be basally present on some stress-related genes and establish a "permissive" chromatin context that may potentiate a rapid transcriptional induction upon need.
- upon stress perception, histone methylation marks can be transiently changed enabling chromatin to change from a transcriptionally inactive/permissive state to a transcriptionally active state in order to allow the transcription initiation and/or to reinforce an ongoing transcription of stress-responding genes.
- finally, the methylation change can be maintained for a certain time during the lifespan of an individual as a kind of somatic memory to enable a faster/stronger induction upon a subsequent stimulation (gene priming).

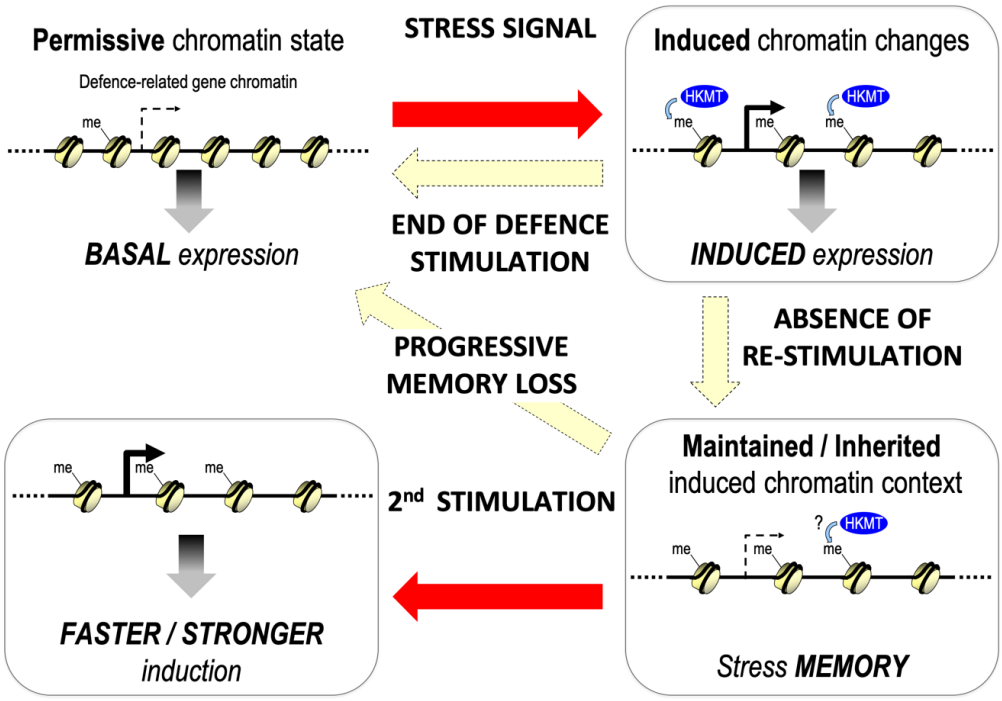

Figure 8: Simplified model for the involvement of histone methylation in establishing a transcriptional response to different kind of stress. Methylation changes can be classified in three different but related categories:

- A permissive chromatin context, with a low level of histone methylation indispensable to establish the basal transcription level of certain stress-responding gene and maintain the chromatin in a permissive context for efficient transcriptional induction if needed.

- An increase of the histone methylation level will be involved in the transcriptional induction and/or the transcriptional reinforcement of stress-responding genes upon signal perception.

- The histone methylation change can be maintained as a somatic memory allowing a faster and/or stronger transcriptional induction of stress-responding genes upon a subsequent stimulation (Adapted from Berr et al., 2012).

I.4.2. Histone methylation in flowering time regulation

I.4.2.1. Flowering time regulation pathways

The flowering transition from vegetative to reproductive development ensures reproductive success under given environmental conditions (Wilczek et al., 2009).

Genetic analyses have identified several sophisticated molecular pathways that perceive and integrate multiple internal and external cues to modulate the floral transition (Montaigu et al., 2015). Those pathways comprised the photoperiod pathway and circadian clock, aging pathway, ambient temperature pathway, gibberellin pathway, vernalization pathway and autonomous pathway. Among them, aging, gibberellin and autonomous pathway are developmental, whereas the other three pathways are key in the control of plant flowering in response to environmental cues (Blümel et al., 2015; Fornara et al., 2010; Theißen et al., 2018). Those pathways converge to regulate essential floral integrator genes. Floral pathway integrators, including SUPPRESSOR OF OVEREXPRESSION OF CONSTANS 1/AGAMOUS-LIKE 20 (SOC1/AGL20) and FT, activate floral meristem identity genes such as *LEAFY(LFY)*, *APETALA 1(AP1)*, *SEPALLATA3 (SEP3)* and *FRUITFULL (FUL)*, which irreversibly result in the transition from a vegetative to a floral meristem (Blümel et al., 2015; Fornara et al., 2010; Simpson and Dean, 2002; Theißen et al., 2018). *FT* encodes a mobile protein (florigen), synthesized in the leaf and able to move to the shoot apex to promote flowering under inductive day length conditions (He, 2009; Shim et al., 2016; Wagner, 2017). *FT* is mainly induced by the transcription factor CO (CONSTANS) under long-day photoperiods (Song et al., 2014). *SOC1* encodes a floral activator and is partially activated by FT (He, 2009). Both *FT* and *SOC1* are repressed by the MADS-box transcription factor FLC, which is a central player in the vernalization and autonomous pathway in Arabidopsis. *FLC* has 5 paralogs, *MAF1* to *MAF5*, all of which are involved in repressing flowering (Gu et al., 2013; Lee et al., 2013; Li et al., 2008; Mateos et al., 2015; Posé et al., 2013; Sureshkumar et al., 2016). Here, I will mainly focus on the vernalization and autonomous pathway.

I.4.2.1.a. Vernalization pathway

Winter-annual plants require to be exposed to prolonged cold winter (or 4 °C for 6 to 12 weeks) to flower during spring. This prolonged cold to accelerate the flowering process is called vernalization (Amasino and Michaels, 2010). Classically, Arabidopsis accessions are classified into summer-annual and winter-annual ecotypes (Michaels and Amasino, 2007). By using crosses between winter- and summer-annual plants, the promotion of flowering was found determined by two dominant genes: *FLC* and *FRIGIDA (FRI)* (Bloomer and Dean, 2017; Ding et al., 2013; He et al., 2004; Lee and Amasino, 2013). *FRI* encodes a coiled-coil protein that elevates *FLC* expression to the levels that inhibit

flowering, resulting in the winter-annual growth habit (Johanson et al., 2000). Summer-annuals carry inactive *fri* allele and thus express low *FLC* transcript, resulting in flowering promotion. Winter annuals only flower rapidly after vernalization treatment (mimicking the transition from winter to spring), during which *FLC* transcription is turn-off gradually and maintained stably silenced later-on (Amasino, 2004; Sung 2005; Sung and Amasino, 2005; Kim et al., 2009).

I.4.2.1.b. Autonomous pathway

Analysis of mutants that flower very late under either long-day or short-day photoperiod defined the autonomous pathway (Koornneef et al., 1998). To date, a number of autonomous pathway components have been identified, making up an epistatic group: *FLOWERING CONTROL LOCUS A (FCA), FLOWERING LOCUS Y (FY), cleavage stimulation factor 64* (*CstF64*), *CstF77, Pcf11p-similar protein 4* (*PCFS4*), *pre-mRNA processing protein 8* (*PRP8*), *cyclin-dependent kinase C;2* (*CDKC;2*), *FLOWERING LOCUS PA (FPA), FLOWERING LATE KH MOTIF(FLK), TBP-associated factor 15b* (*TAF15b*), *LUMINIDEPENDEN (LD), MULTIPLE SUPPRESSOR OF IRA14/FLOWERING LOCUS VE (MSI4/FVE), FLOWERING LOCUS D* (*FLD*; Ausín et al., 2004; Eom et al., 2018; Liu et al., 2010; Koornneef et al., 1998; Lee et al., 1994; Lim, 2004; Liu et al., 2007; Marquardt et al., 2014; Quesada et al., 2003; Wang et al., 2014; Xing et al., 2008). Autonomous pathway genes have canonical characteristics:

1) their mutations lead to a late-flowering phenotype independent of the day length.

2) The late-flowering phenotype of their loss-of-function mutants could be reverted to wild type after either vernalization or through introgression into the *flc-3* mutant background (Michaels, 2001; Simpson et al., 2002).

3) As evidenced by histochemical analysis, the autonomous pathway genes are preferentially express in shoot and root apical regions which contain mainly dividing cells (Simpson, 2004).

4) they act upstream of *FLC* to repress flowering (He et al., 2004).

Numerous studies have revealed that autonomous pathway factors FCA, FPA, FY, CstF64, CstF77 and PRP8 trigger *FLC* sense strand transcriptional silencing by promotion of antisense *COOLAIR* processing (Henderson, 2005; Manzano et al., 2009; Marquardt et

al., 2006; Quesada et al., 2003; Simpson et al., 2003; Swiezewski et al., 2009). They facilitate the usage of both the proximal *COOLAIR* splice acceptor site and the proximal polyadenylation site. And this *COOLAIR* processing results in the change of chromatin state of *FLC* via FLD-mediated H3K4me2 removal. The loss-of-function of *CDKC;2*, encoding a component of transcription elongation factor b (P-TEFb), results in a global loss of RNAPII Ser2 phosphorylation levels. It has been proposed that CDKC;2 negatively affects *FLC* sense transcription via promoting the production of *COOLAIR* transcripts (Wang et al., 2014). *LD* encodes a homeobox domain transcription factor, yet its transcriptional activity on *FLC* has not been revealed. Moreover, FLD and FVE transcriptionally suppress *FLC* via histone modifications (Figure9; Doyle and Amasino, 2009; He et al., 2003; Jiang et al., 2008; Liu et al., 2007; Pazhouhandeh et al., 2011; Tian et al., 2019; Wu et al., 2015; Yu et al., 2016).

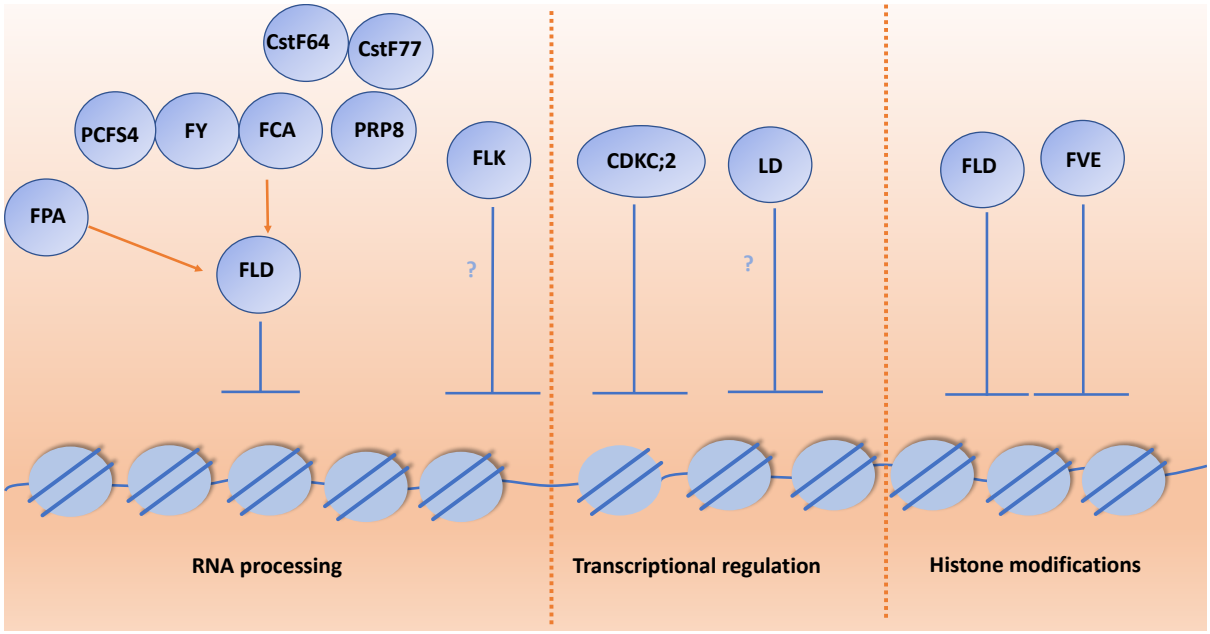

Figure 9: RNA processing, transcriptional regulation and Histone modifications mediate *FLC* silencing in autonomous pathway. RNA processing contains PCFS4, FY, FCA, PRP8, FPA, FLK, CstF64 and CstF77; Transcriptional regulation group contains CDKC;2 and LD; Histone modifications group contains FLD and FVE.

I.4.2.2. *FLC* regulation by histone methylations in flowering time control

FLC is a key repressor of Arabidopsis flowering and the essential role of histone methylations for its regulation was extensively studied. Here, I will briefly summarize how *FLC* transcription is positively or negatively affected by histone methylations.

I.4.2.2.a. *FLC* epigenetic silencing in vernalization by histone methylations

The repressive mark H3K27me3 is a key factor to quantitively determine the *FLC* chromatin state as either active or repressive along the vernalization process (Figure 10). The PHD-PRC2 complex promotes H3K27me3 deposition initiation at the "nucleation" region located at the *FLC* 1st intron upon prolonged cold exposure, and continuously spreading H3K27me3 across the entire *FLC* locus upon back to warm temperature, leading to *FLC* epigenetic silencing (Hepworth and Dean, 2015). The PHD-PRC2 complex contains PHD-domain proteins such as VIN3 and its three homologs [VIN3-LIKE 1(VIL1)/VERNALIZATION5 (VRN5), VIL2/VIN3-LIKE1 (VEL1) and VIL3/VEL2] and the PRC2 components SWN, FIE, VRN2, MSI1 (He, 2009). Among them, VIN3 is the only component known to be inducibly produced in response to cold, which then quickly go down to vanish after plants are put back to warm temperature (Heo and Sung, 2011; Sung and Amasino, 2004). Mutations in the PHD-PRC2 components impair cold-induced H3K27me3 deposition in the "nucleation" region and subsequent spreading across the *FLC* locus (Lucia et al., 2008; Greb et al., 2007). Additionally, during cold exposure, PRC2 acts coordinately with long non-coding RNAs (lncRNAs) to downregulate *FLC*. Indeed, the *FLC* chromatin active state is inhibited by both elevated antisense transcript *COLD ASSISTED INTRONIC NONCODING RNA* (*COLDAIR*), produced from *FLC* intron 1, and *COLD OF WINTER-INDUCED NONCODING RNA FROM THE PROMOTER (COLDWRAP)*, originated from the *FLC* promoter. Both *COLDAIR* and *COLDWRAP* physically interact with the *PRC2* subunit CLF and promote PRC2 recruitment to the nucleation region of *FLC* to finally establish stable chromatin silencing (Heo and Sung, 2011; Kim et al., 2017; Kim and Sung, 2017). Upon back to warmth, the maintenance of this "epigenetic" memory rely on the DNA replication machinery to correctly duplicate PRC2-mediated H3K27me3. Indeed, mutation of the DNA polymerase α subunit *INCURVATA2* (*ICU2*) leads to an impaired vernalization memory and a defective H3K27me3 level at *FLC* upon return to warmth (Hyun et al., 2012). Moreover, also during DNA replication, the incorporation of the H3.1 variant at the replication fork by CAF1 (CHROMATIN ASSEMBLY FACTOR 1) restores H3K27me3 to maintain the memory of silencing (Jiang and Berger, 2017).

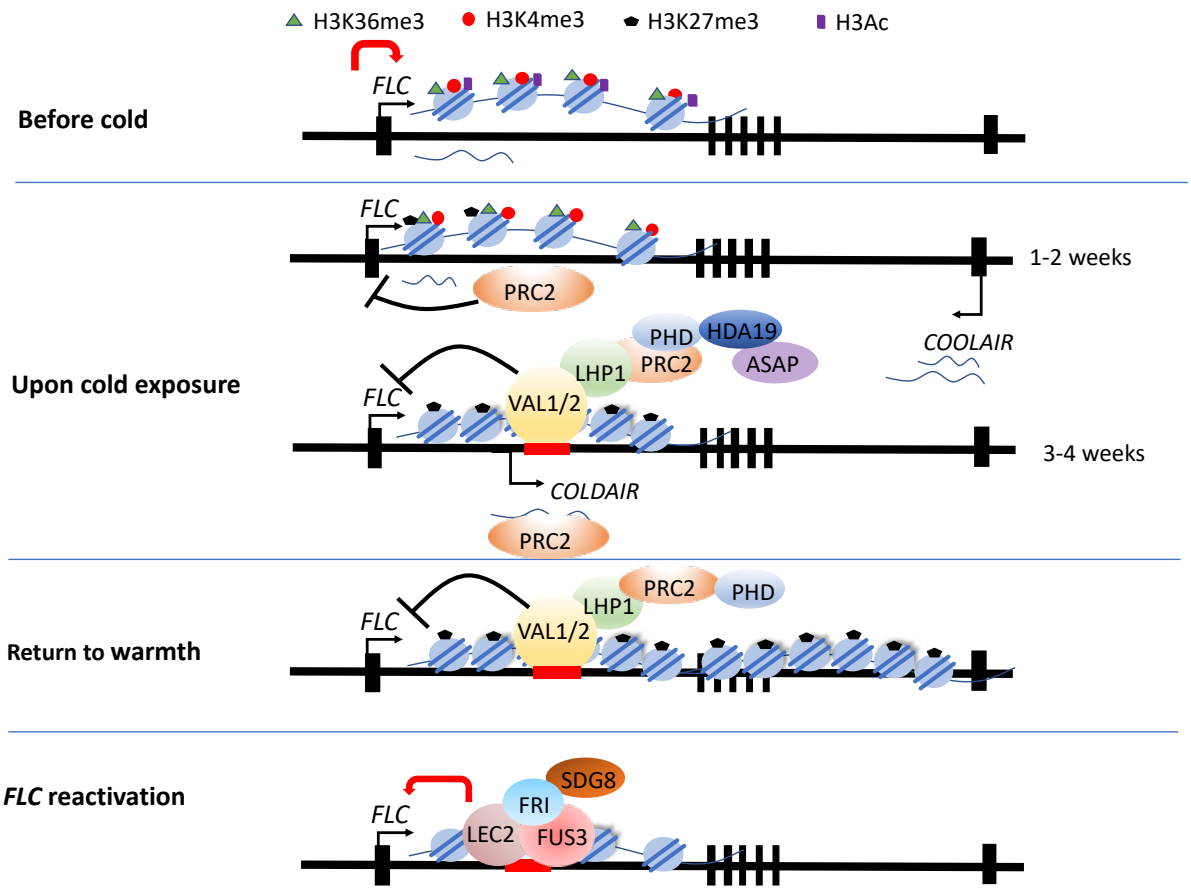

Figure 10: FLC epigenetic silencing in vernalization (before cold, upon cold exposure and return to warmth) and FLC reactivation set up in offspring after vernalization. Before cold exposure, *FLC* sense transcript is highly expressed, and its chromatin nucleation region is deposited by active markers H3K4me3, H3K36me3, H3 acetylation. Upon cold exposure, at 1-2 weeks, *FLC* mRNA expression gradually decreased, accompanying the induced *COOLAIR* and slowly addition of repressive marker H3K27me3 recruited by PRC2 to the nucleation region. At 3-4 weeks, and the recruitment of *COLDAIR*, HDA19 and ASAP to the *FLC* nucleation region and VAL1/2 binding to cold memory element (CME) act redundantly to engage PHD-PRC2 to establish H3K27me3 deposition at nucleation region, ultimately shut down *FLC* sense transcription. Return to warmth, the silenced *FLC* transcription maintains and H3K27me3 spread to cover whole *FLC* locus, and this process still needs VAL1/2 binding to CME. The silenced *FLC* transcription and the H3K27me3 silencing are reset in the next generation. It requires LEC2 and FUS3 binding CME, disrupting PRC2-mediated H3K27me3 silencing, and requires FRIGIDA and SDG8 set up and maintain an active chromatin environment to activate *FLC* transcription.

I.4.2.2.b. *FLC* transcription is antagonistically controlled by FRIGIDA and the autonomous pathway components via histone methylations

While being silenced by vernalization, *FLC* will be later reactivated at embryonic stage (Berry and Dean, 2015). The demethylase ELF6 seems required to remove the H3K27me3 repressive marker at *FLC* chromatin (Pedro et al., 2014). Apart from that,

FRIGIDA (FRI) serves as a scaffold protein recruiting different histone methyltransferases during establishment and maintenance of *FLC* activation (Whittaker and Dean, 2017). Among them, SDG8, ATX1 and SDG25 are involved to establish an active chromatin environment to facilitate *FLC* transcription by increasing H3K4me3 and H3K36me3 (Xu and Chong, 2018).

While FRI activates *FLC*, the autonomous pathway components repress *FLC* expression. So far, all autonomous pathway components regulating *FLC* requires an FLD-dependent removal of H3K4 methylation (Bäurle and Dean, 2008; Liu et al., 2007; Wu et al., 2015). By analyzing the autonomous pathway mutants *fld-4* and *fca-9*, chromatin modifications at *FLC* induced by FCA and FLD, were proposed to coordinately change initiation and elongation to quantitatively regulate the transcriptional output of *FLC* by influencing its antisense transcript *COOLAIR* processing (Wu et al., 2015). Finally, FCA interacts with the PRC2 subunit CLF and binds nascent *COOLAIR* transcripts to allow deposition of H3K27me3 at *FLC* (Tian et al., 2019).

Objectives of Thesis

The objectives of my PhD thesis were to explore the biological function of two

histone methyltransferases in controlling responses to different environmental stimuli in Arabidopsis.

The histone methyltransferase SDG8 was previously reported to play a critical role in plant immunity (Berr et al., 2010; Lee et al., 2016; Palma et al., 2010). Salicylic acid (SA) accumulation and signaling are typically associated with plant defense against biotrophs/hemibiotrophs such as *Pseudomonas syringae* (Pst; Pieterse et al., 2012; Seyfferth and Tsuda, 2014). However, the connection between SA and SDG8 was so far neglected when addressing the higher susceptibility of *sdg8* to bacterial pathogens. To fill this gap, we decided to investigate the contribution of SDG8 to the SA- associated immunity in Arabidopsis. Results are presented in **Chapter II.**

SDG26 is known to positively regulate the transcription of the floral activator *SOC1* via binding its chromatin and depositing H3K4me3 and H3K36me3 (Berr et al., 2015). In addition to the decreased expression of *SOC1* observed in *sdg26*, an increased expression of *FLC*, a repressor of *SOC1,* was also reported (Berr et al., 2015; Liu et al., 2016; Xu et al., 2008). Hence, considering the active role of SDG26 on *SOC1*, a question remains as to how the *SDG26* mutation can result in the up-regulation of *FLC*. On the one side, based on the previously proposed model in which SOC1 would reversely repress *FLC* expression through inhibiting the expression of cold-stress responsive genes such as *CBF* genes (Seo et al., 2009), we supposed SDG26 being involved in this negative feedback loop. Additionally, using the Stress Responsive Transcription Factor Database (STIFDB; Naika et al., 2013), we found two binding sites for stress-responsive WRKY transcription factors in the SDG26 promoter. We therefore investigated the function of SDG26 under cold and other abiotic stresses. Results from this part are presented in **Chapter III**. On the other side, to broaden our knowledge of the SDG26 function in flowering time regulation, we performed a genetic analysis with mutants for essential flowering genes (*flc*, *ft*, *soc1*) together with a large-scale protein-protein interaction approach. Results I obtained so far are presented in **Chapter IV**.

CHAPTER II RESULTS Part I

SDG8-mediated histone methylation potentiates the efficient transcriptional induction of immunity-related genes in Arabidopsis

SDG8-mediated histone methylation potentiates the efficient transcriptional induction of immunity-related genes in Arabidopsis

Xue Zhang[1], Rozenn Ménard[1], Ying Li[2, 3], Gloria M. Coruzzi[3], Thierry Heitz[1], Wen-Hui

Shen[1] and Alexandre Berr[1]*

Affiliations:

[1] Institut de Biologie Moléculaire des Plantes du CNRS, Université de Strasbourg, 12 rue du Général Zimmer, 67084, Strasbourg Cedex, France.

[2] Department of Horticulture and Landscape Architecture, Purdue University, West Lafayette, IN 47907, USA.

[3] Center for Plant Biology, Purdue University, West Lafayette, IN 47907, USA

[4] Department of Biology, Center for Genomics & Systems Biology, New York University, NY NY 10003, USA.

*** Author for correspondence:** Alexandre.Berr@ibmp-cnrs.unistra.fr

Running title: SDG8 potentiates the induction of defense genes

Key words: *Arabidopsis thaliana*, histone, methylation, transcription, RNA polymerase II, biotic stress, salicylic acid, *Pseudomonas syringae*

Abstract (350 words)

Post-translational covalent modifications of histones play important roles in modulating chromatin structure and are involved in the control of multiple developmental processes in plants. Here we provide insight into the contribution of the histone lysine methyltransferase SET DOMAIN GROUP 8 (SDG8), implicated in histone H3 lysine 36 (H3K36) methylation, in connection with RNA polymerase II (RNAPII) to Arabidopsis immunity. We showed that even if the *sdg8-1* mutant, defective in H3K36 methylation of its target genes, displayed a higher sensitivity to different strains of the bacterial pathogen

Pseudomonas syringae, Effector-triggered immunity still operated in the mutant, but less efficiently than in wild-type (WT) plants. In *sdg8-1*, the level of the plant defense hormone salicylic acid (SA) was abnormally high under normal growth conditions and was accumulated similarly to WT at the early stage of pathogen infection but quickly dropped down at later stages. Concomitantly, the transcription of several defense-related genes along the SA signaling pathway was inefficiently induced in the mutant. However, *sdg8-1* retained responsiveness to exogenous SA application. At the level of chromatin, global levels of active and repressive H3 methylation marks were found to be stable following SA treatment in WT, and the SA induction of some defense genes was correlated with an increase in the loading of the RNA polymerase II (RNAPII) and in the enrichment of H3K4 and H3K36 methylation in WT. We show that such changes were impeded in *sdg8-1*. Finally, we demonstrated that SDG8 could physically interact with different phosphorylated and non-phosphorylated forms of the RNAPII C-terminal Domain, supporting the correlation between RNAPII loading and histone methylation increase. Collectively, our results unravel a fundamental role played by SDG8, through its histone methyltransferase activity, in Arabidopsis for providing sustainable immunity *via* the physical coupling between SDG8 and the RNAPII, promoting strong transcriptional induction of defense genes.

II.1. Introduction

Inside eukaryotic nuclei, DNA segments are wrapped around histone octamers (2x(H2A, H2B, H3 and H4)) to form nucleosomes, the basic building block of chromatin (Kornberg, 1974). Besides being structurally important to enable DNA to fit inside the nucleus, chromatin represents an inherent barrier to all processes requiring access to DNA. Thus, mechanisms such as transcription rely notably on dynamic changes in histone/DNA and/or histone/histone contacts inside chromatin, ultimately leading to modifications of DNA accessibility. These changes in the chromatin folding are achieved through different mechanisms and are categorized into different states, ranged from transcriptionally active to poised or constitutively silenced chromatin (Strahl and Allis, 2000).

Protruding from the globular nucleosome, core histone tails may undergo diverse reversible covalent modifications that can either modify the local electrostatic behavior (*e.g.* acetylation) and/or act as specific docking sites for effectors named "readers" (*e.g.* methylation; Rothbart and Strahl, 2014). Distinct modifications can act sequentially or in a combined way to bring about distinct outcomes, thus constituting a histone code that considerably extends the information potential of the genetic code (Jenuwein and Allis, 2001). Among the modifications found in higher plants, histone H3 methylation can occur at different lysine residues through the activity of specific histone lysine methyltransferases (HKMTs). In Arabidopsis, more than 40 genes encoding putative HKMTs have been classified according to their SET domain sequence homology and their domain organization in several groups with different lysine specificity (Springer et al., 2003a). Among them, members of the Trithorax Group (TrxG), known to catalyze H3K4 and/or H3K36 methylation play a pivotal role in promoting RNA polymerase II (RNAPII) transcription, thus controlling key phase transitions and important stages related to plant development (Berr et al., 2016; Fletcher, 2017). In contrast, their contribution to the massive transcriptional reprogramming in defense responses activation to fend off pathogens has been often suggested but comparatively less investigated (Bobadilla and Berr, 2016; Ramirez-Prado et al., 2018).

As sessile organisms, plants are challenged by many pathogens in nature. Beside preformed physical barriers such as cuticle or cell wall and constitutive antimicrobial compounds, plant immunity relies on two layers of defense. Firstly, surface membrane-

anchored receptors named pattern-recognition receptors (PRRs) can perceive conserved pathogen structures called pathogen-associated molecular patterns (PAMPs), thereby activating PAMP-triggered immunity (PTI). To inhibit/interfere with PTI, pathogens secrete effectors or avirulence (Avr) proteins into host cells which in turn can be recognized by cellular plant receptors inducing effector-triggered immunity (ETI), resulting in much stronger defense responses. In contrast to PTI, ETI is accompanied by a rapid and local programmed cell death at the infection site termed the hypersensitive response (HR) and by the activation of systemic acquired resistance (SAR) in distal tissues of the host (Lee et al., 2017). Downstream in PTI and ETI signaling, the crucial role of phytohormone biosynthesis, signaling pathways and interplay is also well-established in pathogen defense (Glazebrook, 2005). Salicylic acid (SA) accumulation and signaling is typically associated with defense against biotrophs/hemibiotrophs while jasmonate (JA) and ethylene (ET) pathways defend plants against necrotrophs (Pieterse et al., 2012).

Four HKMTs, exclusively from the TrxG group (*i.e.* ATX1, SDG8/ASHH2, SDG25/ATXR7 and SDG37/ASHR1), were so far reported to directly or indirectly contribute to the regulation of plant immunity, with their corresponding mutant being more susceptible to different pathogens (Alvarez-Venegas et al., 2007; Palma et al., 2010; Berr et al., 2010; De-La-Peña et al., 2012; Xia et al., 2013; Lee et al., 2016). Among them, SDG8 plays a non-redundant role as it is required for global H3K36me2/me3 deposition (Xu et al., 2008; Li et al., 2015). The *sdg8* mutants show pleiotropic phenotypes and *SDG8* was involved in many biological processes, including the regulation of flowering time, organ growth, ovule and anther development, seed development, carotenoid biosynthesis, brassinosteroid-regulated gene expression and light- and/or carbon-responsive gene expression (Soppe et al., 1999; Zhao et al., 2005; Dong et al., 2008; Cazzonelli et al., 2009; Grini et al., 2009; Tang et al., 2012; Li et al., 2015). Regarding plant immunity, the SDG8-mediated H3K36me3 was reported as being crucial for the transcriptional induction of subsets of JA/ET-inducible genes upon infection by necrotrophic fungi (Berr et al., 2010a). In addition, the *sdg8* mutant was also found more susceptible to hemibiotrophic pathogens and the SDG8 methyltransferase activity was suggested to be required for ETI through the establishment and/or maintenance of a transcription-permissive chromatin state at two *R*-genes (*i.e. RPM1* and *LAZ5*, a RPS4-like R-protein encoding gene; Palma et al., 2010). More recently, *SDG8* together with *SDG25* were proposed to contribute to immunity at least partially through the regulation of *CAROTENOID ISOMERASE2* (*CCR2*) and

ECERIFERUM3 (*CER3*/*WAX2*), two genes encoding enzymes involved in carotenoids and cuticular wax biosynthesis, respectively (Lee et al., 2016).

Despite the essential role played by SA and its accumulation for both local defense and SAR especially against pathogens with a hemibiotrophic lifestyle such as *Pseudomonas syringae* (*Pst*; Seyfferth and Tsuda, 2014), it has been thus far neglected when addressing the higher susceptibility of *sdg8* to bacterial pathogens. To fill this gap, we provide here insight into the contribution of SDG8 and H3K36 methylation in connection with RNAPII to the SA immunity pathway in *Arabidopsis thaliana*. We show that despite of the higher sensitivity of the *sdg8-1* mutant defective in H3K36 methylation to different *Pst* strains, ETI still partially operated in the mutant. We quantified the level of SA and found that it was abnormally high in *sdg8-1* under normal conditions. During infection, SA accumulation was similar to that in wild-type (WT) at early stage, but it quickly dropped down later. In WT, while global histone methylation profiles were unchanged upon SA treatment, the induction of several defense-related genes was correlated with a local increase in RNAPII loading and H3K4 and H3K36 methylation at their chromatin. Further supporting the higher sensitivity of *sdg8-1* to *Pst*, SA-related genes only retained a partial responsiveness to exogenous SA in the mutant and, correspondingly, local chromatin changes observed in WT were impeded in *sdg8-1*. Supporting a direct link between RNAPII loading and histone methylation at defense-related genes, we demonstrate that SDG8 and RNAPII can physically interact. Altogether, our data suggest the fundamental contribution of *SGD8* to plant immunity by potentializing the efficient RNAPII transcriptional of defense-related genes.

II.2. Material and Methods

II.2.1. Plant material

The *Arabidopsis thaliana* ecotype Colombia (Col0) was used as wild-type (WT) plant. The *sdg8-1* mutant (SALK_065480) in the Col0 background has been previously described (Zhao et al., 2005). The *SDG8:FLAG sdg8* (*EFS:FLAG efs*) was kindly provided by Dr. Yoo-Sun Noh (Seoul National University, Korea; (Ko et al., 2010)).

II.2.2. Pathogen assays

Pathogen inoculation assays were performed on 5-week-old Arabidopsis plants grown on soil in a growth chamber with a 12 h photoperiod and a day/night temperature regime of 22 °C / 18 °C. Bacterial pathogens *Pseudomonas syringae pv. tomato* DC3000 (*Pst* DC3000) harboring an empty vector and *Pst* DC3000 carrying a plasmid-borne *avrRpm1* gene (*Pst avrRpm1*) were used. Bacterial strains were inoculated with a needleless 1 ml syringe as previously described (Camera et al., 2005) and bacterial growth was determined by counting colony forming units (cfu) as previously described (Katagiri et al., 2002). For RNA extraction, at least 6 leaves from 10 individual plants were harvested at 0, 1 and 3 days post inoculation (dpi), pooled and flash-frozen in liquid nitrogen until use.

II.2.3. SA quantification and treatments

For analysis of free salicylic acid (SA), inoculated leaves were harvested at 0, 1, 2 and 3 dpi and free SA measurement was performed by ultra-performance liquid chromatography coupled to tandem mass spectrometry (UPLC-MS) on methanolic extracts as previously described using gentisic acid as an internal standard and a 137>93 mass transition in negative mode (Aubert et al., 2015).

SA treatment was performed by spraying an aqueous solution of 1 mM SA (S5922, Sigma-Aldrich) onto 10-day-old Arabidopsis plants grown on soil under mid-day length conditions (12 h light / 12 h dark) in a growth chamber. Before (0 h), 8, 24 and 48 h after treatment, plantlets were quickly dried and flash-frozen in liquid nitrogen and stored until RNA extraction. For chromatin immunoprecipitation (ChIP), plantlets before and 24 h

after treatment were directly fixed in formaldehyde before chromatin extraction.

II.2.4. Gene expression analyses

Total RNA was extracted using the Nucleospin RNA Plant kit (Macherey-Nagel). First strand cDNA was synthesized using Oligo-dT primer and SuperScript® III Reverse Transcriptase (Invitrogen) according to manufacturer's instructions. The relative transcript abundance was determined in triplicates using gene-specific primers listed in Supplementary Table 1 on a LightCycler 480 instrument (Roche) in a final volume of 10 µL of SYBR Green Master mix (Roche). At4g26410 (*EXPRESSED PROTEIN*, *EXP*) At1g13440 (*GLYCERALDEHYDE 3-PHOSPHATE DEHYDROGENASE*, *GAPDH*) and At4g34270 (*TIP41*) were selected as internal reference genes based on their stability under our experimental condition using geNorm (Vandesompele et al., 2002) and Norm Finder (Andersen et al., 2004). Relative expression values were calculated using the comparative cycle threshold method $2^{-\Delta\Delta Ct}$.

II.2.5. Western blotting and chromatin immunoprecipitation

Western-blot analysis was performed on histones extracts prepared from 1-week-old seedlings as described previously (Xu et al., 2008). Protein were separated by 15% SDS-PAGE and transferred onto Immobilon-P membranes (Millipore) using a Trans-Blot semi-dry transfer cell (Bio-Rad). Intensity of individual bands was quantified using ImageJ densitometry software (NIH).

Chromatin immunoprecipitation (ChIP) assays were performed according to the previously described method (Liu et al., 2016). Antibodies used to precipitate chromatin were anti-H3 (05-499; Millipore), anti-trimethyl-H3K4 (07-473; Millipore), anti-trimethyl-H3K36 (ab9050; Abcam) and anti-total RNA polymerase II (RNAPII) CTD repeat antibody (ab817, Abcam), together with protein A magnetic beads (Magna-ChIP, Millipore). DNA was purified with the NucleoSpin Gel and PCR Clean-up kit (Macherey-Nagel, Düren, Germany) and analyzed by real-time PCR (LightCycler 480II; Roche in conjunction with the SYBR Green Master mix) using gene-specific primers listed in Supplementary Table 1. Data were analyzed as described in Zhao et al., 2019 for H3K4me3 and H3K36me3 and in Yang et al., 2016 for RNAPII.

II.2.6. Co-immunoprecipitation Assays

Coimmunoprecipitation assays of SDG8 and the RNAPII proteins were performed using the Arabidopsis *SDG8:FLAG sdg8* transgenic line (Ko et al., 2010). Total proteins were extracted as previously described (Yang et al., 2016). In brief, 10 g of 10-day-old seedlings grown on ½ MS-agar plate was grinded in liquid nitrogen and thawed in lysis buffer: 100 mM Tris-HCl, pH 8, 150 mM of NaCl, 2 mM EDTA pH 8, 1 mM $MgCl_2$, 1% Nonidet P-40 (74385, Sigma-Aldrich) and 1 mM AEBSF (A8456, Sigma-Aldrich) supplemented with cOmplete™, EDTA-free Protease Inhibitor Cocktail (5056489001, Roche). Lysates were incubated with 0.5 µL/mL of the nonspecific endonuclease Benzonase (E1014, Sigma-Aldrich) to degrade DNA and RNA during 1h at 4°C on a rotating wheel. After incubation, homogenates were cleared by centrifugation. Immunoprecipitation was performed on supernatants using the µMACS DYKDDDDK (FLAG) isolation kit according to the manufacturer's instructions (130-101-591, Miltenyi Biotec). Proteins bound to magnetic beads were resolved by electrophoresis on 6% SDS-polyacrylamide gel and detected using either monoclonal antibodies against the FLAG tag (F3165, Sigma-Aldrich), against total RNAPII CTD repeat (ab817; Abcam) or against the phosphorylated serine 5 (Ser5P) or Ser2P forms of the RNAPII CTD repeat (C15200007 and C15200005, respectively; Diagenode), followed by a goat anti-mouse-HRP-conjugated antibody (G-21040, Invitrogen).

II.2.7. Yeast Two-Hybrid Assays

The pGBD-CTD-Kin28, pGBD-CTD-mKin28, and pGBD-Kin28 were kindly provided by Dr. Hisashi Koiwa (Guo et al., 2004). In order to use this tethered system in our yeast two-hybrid system, inserts were amplified by PCR and subcloned into the Gateway donor vector pDONR207 (Stratagene). The SDG8 cDNA was also amplified by PCR and cloned in pDONR207. Next, inserts were fused to the GAL4 binding domain or activation domain using the destination Gateway-compatible pGBT9 (Ghent plasmids collection) or pGADT7 vectors (Clontech), respectively. Plasmids were co-transformed pairwise into the yeast strain AH109 (Clontech) according to the Clontech small-scale LiAc yeast transformation procedure.

The phosphorylation of the CTD was analyzed by western blot using the pGADT7

recombinant constructs containing a hemagglutinin (HA) epitope tag. Indeed, pGBT9 contains a truncated 410 bp ADH1 promoter leading to low expression level making fusion protein hardly detectable by western blot (Van Criekinge and Beyaert, 1999). Protein extracts from yeasts were prepared using the Urea/SDS method described in the Yeast Protocols Handbook (Clontech). Proteins were separated by SDS-polyacrylamide gel electrophoresis (15% SDS-PAGE) and transferred onto Immobilon-P membranes (Millipore). Monoclonal antibodies against the HA tag (H9658; Sigma-Aldrich), against RNAPII (ab817; Abcam) or against Ser5P or Ser2P CTD (C15200007 and C15200005, respectively; Diagenode) were used followed by a goat anti-mouse-HRP-conjugated antibody (G-21040, Invitrogen).

Weak and strong interactions were assayed on synthetic complete medium lacking Leu, Trp and His and containing 25 mM 3-amino-1,2,4-triazole (SD-LWH+3AT) and lacking Leu, Trp, Ade, His (SD-LWAH), allowing growth for 4 days at 30 °C. The synthetic complete medium lacking Leu and Trp (SD-LW) was used as control.

II.2.8. Statistical methods

Statistical analyses were performed in R (http://www.r-project.org/) using a Student's *t*-test with Benjamini–Hochberg FDR correction.

II.3. Results

II.3.1. SDG8 mutation increases susceptibility to Pseudomonas infection

Hemibiotrophic pathogens such as the bacterial pathogen *Pseudomonas syringae pv. tomato* DC3000 (*Pst*) are known to stimulate salicylic acid (SA) accumulation and to induce the expression of SA-related defense genes (Seyfferth and Tsuda, 2014). We therefore decided to use the *Pseudomonas*-Arabidopsis pathosystem to explore the impact of the *sdg8* mutation on the SA-related immunity. Firstly, the susceptibility of the *sdg8-1* mutant to *Pst* was investigated by syringe-inoculated *Pst* expressing or not the effector gene *avrRpm1* (*Pst avrRpm1* or *Pst* DC300, respectively) on leaves of 5-week-old WT and *sdg8-1* plants. After 3 days of infection, we observed more severe symptoms with characteristic tissue necrosis and chlorosis in *sdg8-1* mutants than in WT plants (Figure 11A). Moreover, *sdg8-1* supported significantly higher avirulent bacterial multiplication compared to WT plants (Figure 11B). These results are consistent with those previously reported in *sdg8-2*, another *sdg8* mutant allele (Palma et al., 2010), and together demonstrate the involvement of *SDG8* in ETI (also called gene-for-gene resistance) triggered by *Pst*. Interestingly, we also detected in *sdg8-1* an increased susceptibility and bacterial growth 3 days after inoculation when the virulent strain *Pst* DC3000 was used (Figure 11A and B), supporting similar data reported with the allelic mutant lines *sdg8-4* (De-La-Peña et al., 2012) and *sdg8-2* (Lee et al., 2016). Noteworthy, based on bacterial titers, *sdg8-1* still supported higher growth of the virulent than avirulent *Pst* strain (Figure 11B), suggesting that ETI is still operating in the mutant, but less efficiently than in WT plants. Probably because both PTI and ETI rely on similar transcriptional processes, these results together indicate that in addition to ETI, *SDG8* might also regulate processes important for PTI, leading to basal resistance against *Pst* infection.

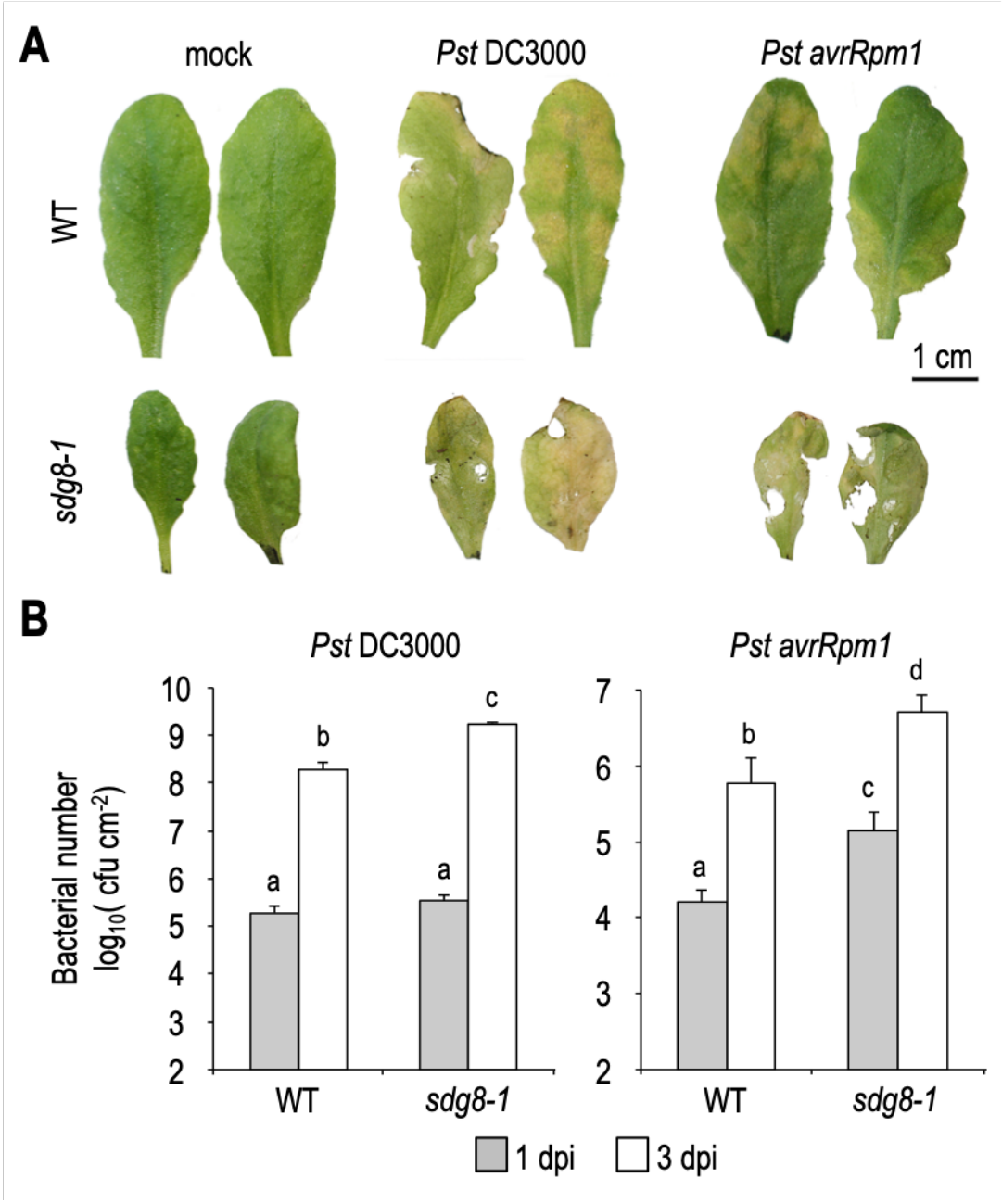

Figure 11: Pathogen-responsive phenotypes in WT and *sdg8-1* mutant plants upon *Pseudomonas syringae* infection. (A) Representative leaves of 5-week-old Arabidopsis WT and *sdg8-1* mutant plants showing disease symptoms after infiltration with *Pst* DC3000 or *Pst avrRpm1* at 5.10^5 colony-forming units (cfu/ml). The control treatment (mock) was inoculated with 10 mM $MgCl_2$. Photographs were taken at 3 days post-inoculation (dpi). **(B)** Growth of virulent *Pst* DC3000 (left) or avirulent *Pst* DC3000 expressing *avrRpm1* (right) at 1 and 3 dpi in WT and *sdg8-1* leaves of 5-week-old plants. Log transformed data shown are means ± SD (n=12). Letters indicate significant differences among sample in Student's *t*-test followed by Benjamini-Hochberg FDR correction ($P < 0.05$)

II.3.2. Infection-induced salicylic acid accumulation is compromised in *sdg8-1*

Next, we quantified by UPLC-MS the levels of the bioactive free SA in WT and *sdg8-1* mutant plants before and after inoculation with *Pst* DC3000 and *Pst avrRpm1*. Before pathogen infiltration, the steady-state level of free SA was below the limit of detection in WT, but significantly elevated levels (118.25 ± 39.6 ng/g FW^{-1}) were detected in *sdg8-1*. Upon infection, WT accumulated SA in response to both *Pst* strains, with a progressive increase in the course of infection. As expected from the known difference in defense intensity between PTI and ETI, the level of free SA was higher after inoculation with *Pst avrRpm1* than with *Pst* DC3000 in WT. Such a lower accumulation of free SA in response to virulent compared to avirulent *Pst* was previously reported and the progressive suppression of the PTI-associated SA accumulation by the virulent strain through the production of *Pst* phytotoxin coronatine was proposed as an explanation (Carviel et al., 2014). In *sdg8-1*, the SA accumulation at early stage of infection (*i.e.* 1 and 2 dpi upon infection with *Pst* DC3000 and 1 dpi upon infection with *Pst avrRpm1*) was similar in magnitude to that of WT (Figure 12A). Also, and similarly to WT, *sdg8-1* mutant plants accumulated SA more rapidly upon infection with the avirulent strain than with the virulent one, further confirming that defense mechanisms triggered by ETI are partially functional in the mutant. Strikingly, contrary to WT that further increased SA levels, the early SA increase detected in *sdg8-1* upon infection with both *Pst* strains vanished at 3 dpi. Together, these results indicate that *SDG8* participates in the negative control of basal SA levels prior to stimulation and promotes SA production/accumulation upon stimulation.

II.3.3. *SDG8* is a positive regulator of salicylic acid pathway genes

SA triggers the induction of a plethora of defense genes and is a major regulator of SAR (Seyfferth and Tsuda, 2014), through a signaling pathway that has been extensively characterized (Janda and Ruelland, 2015). The pathogenesis-related (*PR*) defense genes *PR1* and *PR2* encode antimicrobial proteins and are typical markers of the SA-mediated defense system. Their transcriptional induction in response to infection by (hemi)biotrophic pathogens or SA requires the coactivator NONEXPRESSOR OF PATHOGENESIS-RELATED GENES 1 (NPR1). *NPR1* is constitutively expressed and is

weakly responding to exogenous SA treatment (Cao et al., 1998). *SDG8* was previously involved in ETI using avirulent *Pst* strains (Lee et al., 2016; Palma et al., 2010), we hereafter focus on basal resistance against *Pst* DC3000. Because SDG8 is likely acting in transcriptional regulation, we performed quantitative real-time PCR (qRT-PCR) analyses on leaf tissue harvested before and after infection for the above-mentioned selected genes. In uninoculated plants, steady-state expression levels of the SA-responsive *PR1* and *PR2* genes were slightly but significantly elevated in *sdg8-1* compared to their levels in WT (Figure 12C, far right panels), while the steady-state level of *NPR1* transcript was slightly decreased (Figure 12C). In agreement with the increased susceptibility of the *sdg8-1* mutant to *Pst* DC3000, qRT-PCR analyses revealed that higher bacterial titers in *sdg8-1* mutant plants were correlated with severely reduced induction of *PR* genes, while *NPR1* was not induced at all (Figure 12C).

Previously, we demonstrated the crucial role played by *SDG8* in plant defense against necrotrophic fungal pathogens by regulating a subset of genes within the jasmonic acid (JA)/ethylene (ET)-signaling pathway (Berr et al., 2010). *WRKY70* encodes an important transcription factor regulating cross-talk between SA and JA signaling pathways and its expression is induced by SA, in both NPR1-dependent and NPR1-independent manners (Li et al., 2014). Before inoculation, *WRKY70* transcript level was slightly higher in *sdg8-1* mutant than in WT (Figure 12C), consistent with the higher basal SA level and *PR* genes expression. Upon pathogen infection, *WRKY70* was similarly induced in WT and *sdg8-1* mutant plants, highlighting its NPR1-independent transcriptional induction.

Since *sdg8-1* mutant plants accumulated less SA compared to WT plants, we wondered whether the expression of genes functioning upstream of SA was affected. Three of them were analyzed by qRT-PCR during the infection: *ISOCHORISMATE SYNTHASE1* (*ICS1*, also known as *SID2*) which plays a major role in SA biosynthesis (Garcion et al., 2008; Huang et al., 2010), while more upstream *ENHANCED DISEASE SUSCEPTIBILITY1* (*EDS1*) and *PHYTOALEXIN DEFICIENT 4* (*PAD4*) were reported as being important for plant immunity through a SA-dependent and a SA-independent pathways (Bartsch et al., 2006; Cui et al., 2017). The mRNA level of *ICS1* was higher in non-inoculated *sdg8-1* plants and only slightly increased upon infection compared to the WT control. *EDS1* and its co-regulator *PAD4* were found basally downregulated and not

efficiently induced upon infection in *sdg8-1* (Supplementary Figure 1).

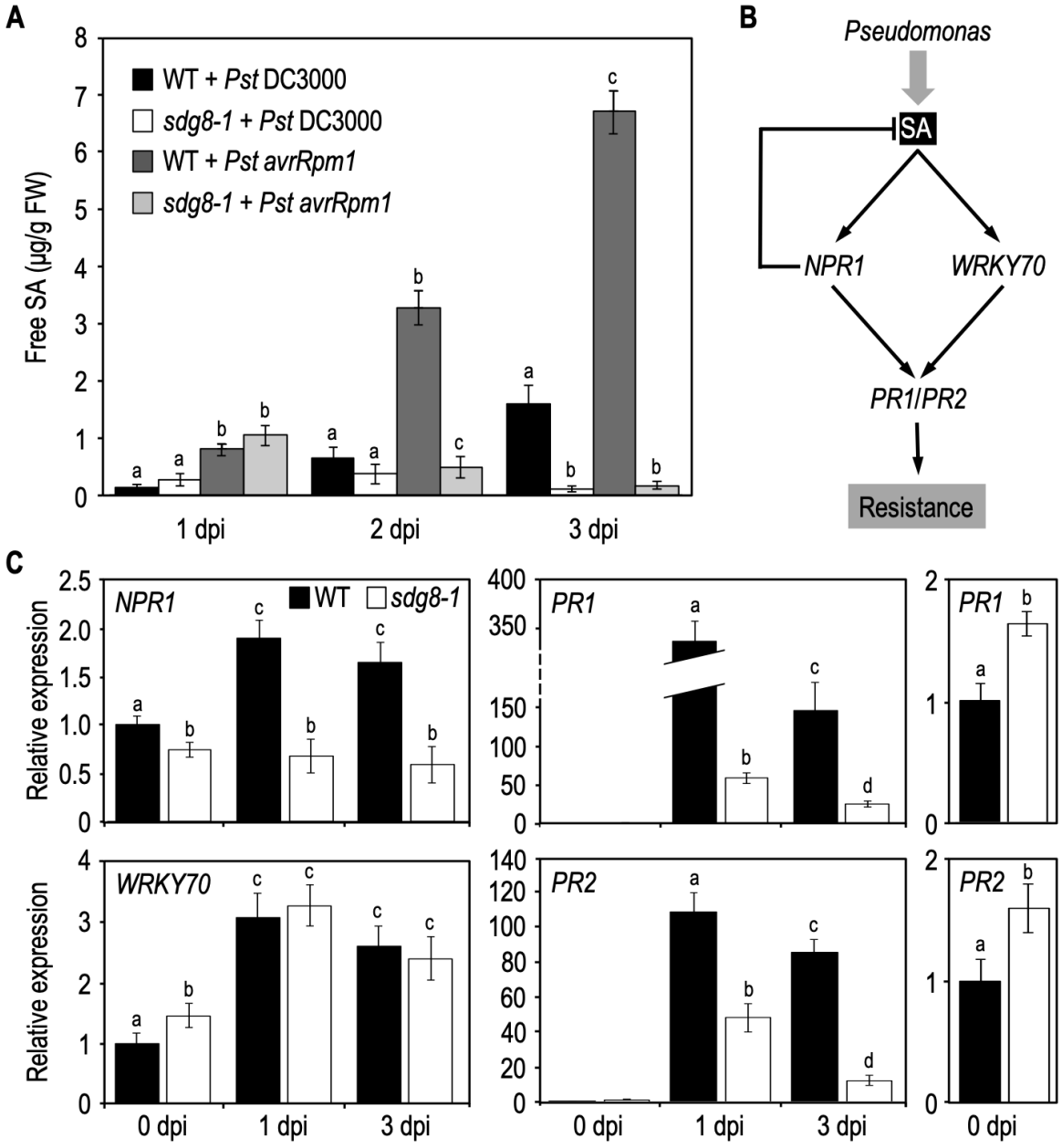

Figure 12: SA accumulation and expression levels of SA pathway-associated genes in WT and *sdg8-1* mutant plants upon *Pseudomonas syringae* infection. (A) Quantification of free SA concentrations at the indicated time points in WT and *sdg8-1* leaves of 5-week-old plants after *Pst* DC3000 or *Pst avrRpm1* inoculation. (**B)** Simplified model for the SA signaling network in *Arabidopsis thaliana* depicting genes (in *italic*) analyzed in the present study. (**C)** Expression levels of SA pathway-associated genes quantified by qRT-PCR in WT (black) and *sdg8-1* (white) mutant 5-week-old plants in response to *Pst* DC3000 inoculation. Expression values for each gene are presented relative to the corresponding WT level at 0 dpi (set as 1) as means ± SD (n=3). Inserts on the right are highlighting differential basal expressions observed between WT and *sdg8-1* for *PR1* and *PR2*. Letters indicate significant differences among sample in Student's *t*-test followed by Benjamini-Hochberg FDR correction ($P < 0.05$).

To determine if the disability of *sdg8-1* mutant plants to properly accumulate SA in response to *Pst* DC3000 is, at least partly, causing the defective transcriptional induction

of SA downstream genes, we tested the effects of the exogenous application of SA. To do so, SA was applied as a foliar spray on 10-day-old Arabidopsis plants, a stage where *sdg8-1* mutant plants are phenotypically indistinguishable from WT plants. As reported in Figure 3, *NPR1* was slightly induced by exogenous SA in WT, but stayed uninduced upon treatment in *sdg8-1* plants. While *WRKY70* was similarly up-regulated in *sdg8-1* and WT upon hormonal treatment, *PR* genes were comparatively much less induced in *sdg8-1* than in WT (Figure 13). In summary, *SDG8* appeared to be involved at different levels to regulate some targets of SA signaling. Before stress, *SDG8* controls the resting-state expression of several defense-related genes, whereas upon stimulation, *SDG8* is required for their efficient transcriptional induction.

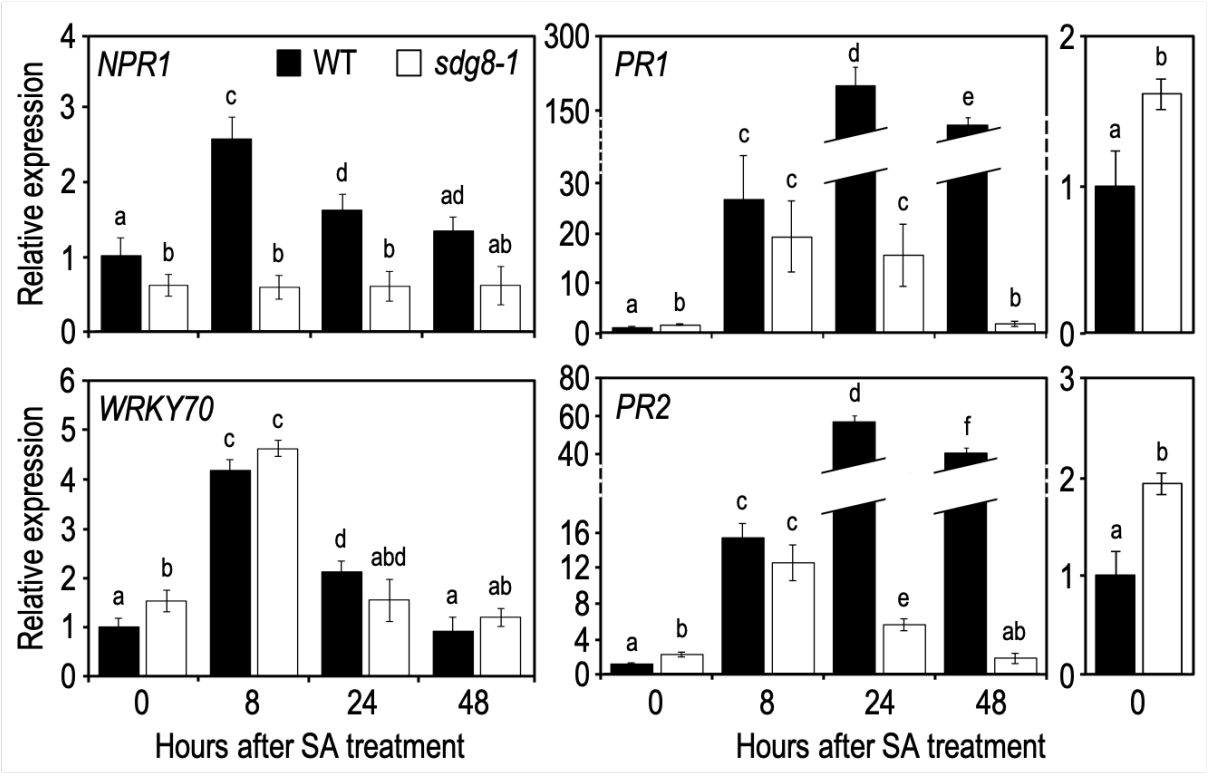

Figure 13: Expression levels of SA pathway-associated genes in WT and *sdg8-1* mutant plants in response to exogenous SA treatment. Expression levels of SA pathway-associated genes in WT (black) and *sdg8-1* (white) mutant 10-day-old seedlings grown in soil and sprayed with 1 mM of SA. Expression values for each gene are presented relative to the WT level at time point 0 (*i.e.* just before spraying) as means ± SD (n=3). Inserts on the right are highlighting differential basal expressions observed between *WT* and *sdg8-1* for *PR1* and *PR2*. Letters indicate significant differences among sample in Student's *t*-test followed by Benjamini-Hochberg FDR correction ($P < 0.05$).

II.3.4. H3K36me3 deposition by SDG8 is required for efficient *PR* genes transcriptional induction

In Arabidopsis, like in other eukaryotes, a strong positive correlation exists between gene expression and the level of active histone modifications marks (i.e. H3K4me3 and H3K36me3), while expression levels correlate negatively with H3K27me3 (Roudier et al., 2011; Sequeira-Mendes et al., 2014). Because Arabidopsis infection with *Pst* or treatment with exogenous SA triggers massive changes in gene expression (Maleck et al., 2000; Schenk et al., 2000; Uknes et al., 1992), we decided to compare the global level of various histone methylation marks by western blot analysis of nuclear protein extract from WT plants before and after SA treatment. Interestingly, despite the massive transcriptional changes previously described, global H3K4me3, H3K36me3 and H3K27me3 levels remained unchanged before and after exogenous SA application (Figure 14A and B).

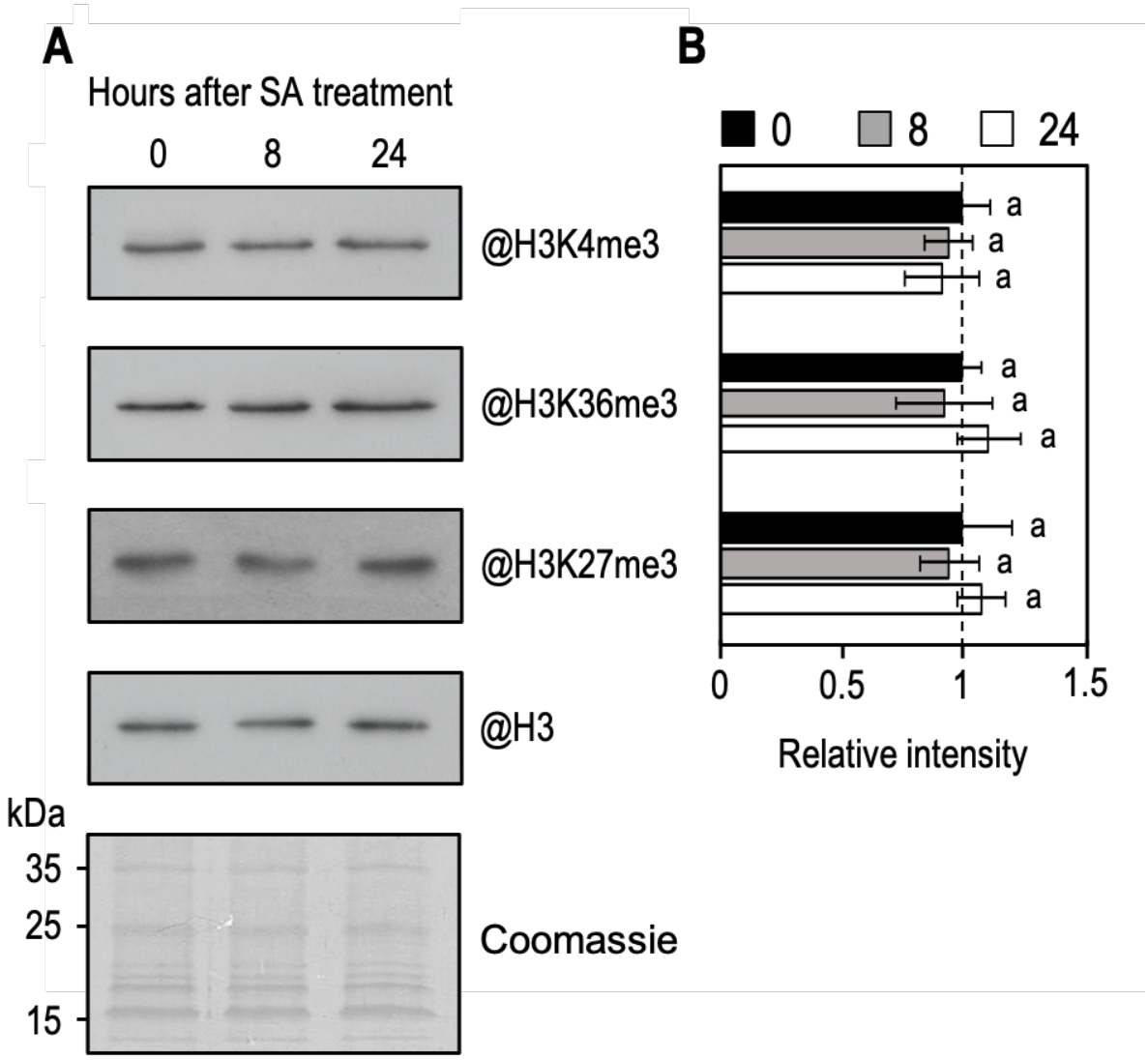

Figure 14: Western-blot analysis of global H3K4me3, H3K36me3 and H3K27me3 in WT plants in response to exogenous SA treatment. (A) Amounts of H3K4me3, H3K36me3 and H3K27me3 were determined on nuclear protein enriched fractions extracted from WT 10-day-old seedlings during exogenous SA exposure using indicated antibodies. Histone H3 total protein and coomassie staining were used as a loading control. **(B)** Mean densitometry values ± SEM for H3K4me3, H3K36me3 and H3K27me3 were calculated from at least 3 independent experiments, normalized to H3 and presented relative to WT. Letters indicate significant differences among sample in Student's *t*-test followed by Benjamini-Hochberg FDR correction ($P < 0.05$).

To further understand molecular mechanisms underlying the impaired transcriptional induction of SA-related genes in *sdg8-1*, we decided to focus on two active histone marks and total RNAPII by analyzing their levels at specific loci using chromatin immunoprecipitation (ChIP). To this end, chromatin was extracted from WT and *sdg8-1* mutant plants before and 24 h after stimulation with exogenous SA and, after

immunoprecipitation with specific antibodies, DNA was used for quantitative PCR with primers spanning the genic region of several SA-related genes (Figure 15 and Supplementary Figure 2). Consistent with SDG8 being primarily involved in H3K36 methylation (Zhao et al., 2005; Xu et al., 2008; Yang et al., 2014; Li et al., 2015), H3K36me3 was generally decreased at all examined genes in *sdg8-1*, whereas H3K4me3 was not significantly changed. In addition, basal levels of RNAPII along the genes we examined were largely similar between WT and *sdg8-1* mutant plants despite the above reported differences in basal transcription. Upon SA stimulation of WT plants, both H3K4me3 and H3K36me3 levels were strongly increased at the two examined SA-inducible *PR* genes (Figure 15), whereas this increase was less pronounced at the upstream genes *NPR1* and *WRKY70* (Supplementary Figure 2). Concomitantly to this increase in active histone methylation marks, a significantly increased loading of RNAPII was observed at all examined genes, except for *NPR1* where, despite an upward trend, almost no statistically significant differences were observed between non-treated and treated wild-type plants (Figure 15 and Supplementary Figure 2). Considering the stronger increase observed at *PR* genes compared to *WRKY70*, these differences should be related to the stronger transcriptional induction measured for *PR* genes relative to *WRKY70* or *NPR1* upon SA exposure (Figure 13). Also, while we observed generally a peak of H3K4me3 around the transcription start site, H3K36me3 appeared more dispersed along the entire gene. In *sdg8-1*, the level of H3K36me3 remained unchangeably low upon stimulation, while H3K4me3 was increased, albeit at a lower level than in stimulated WT plants. Despite the SA treatment, the RNAPII loading was stable between treated and untreated *sdg8-1* mutant plants at *NPR1* and *WRKY70*, while a slight but significant increase was detected at *PR* genes. Further reflecting the less effective transcriptional induction of *PR* genes upon stimulation in *sdg8-1*, this increase was significantly less pronounced than in WT stimulated plants (Figure 16). Thus, basal and induced H3K36me3 established by SDG8 at *PR* genes appear important to potentiate their efficient transcription upon stimulation.

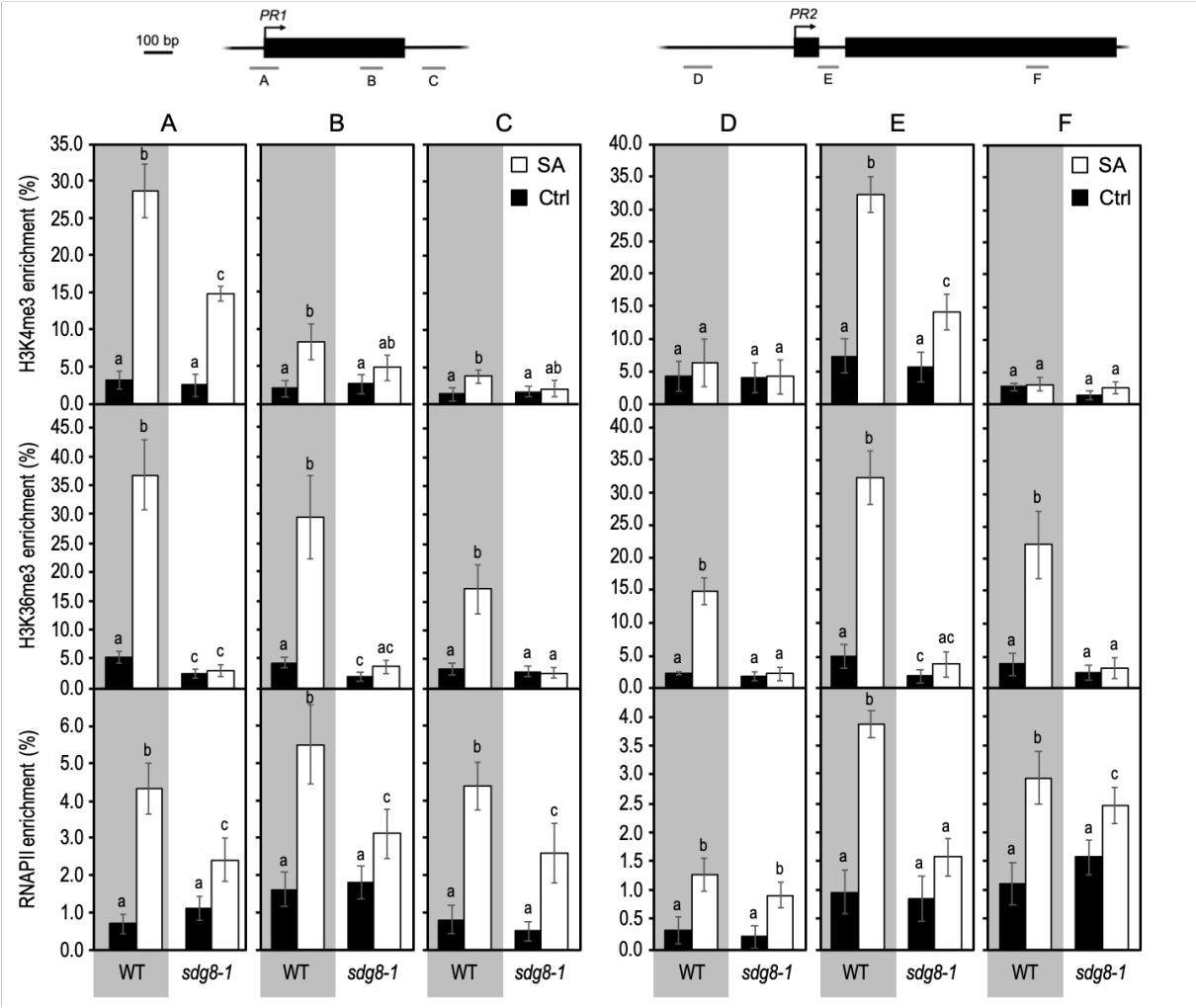

Figure 15: Chromatin immunoprecipitation analyses of H3K4me3, H3K36me3 and total RNAPII at *PR* genes in WT and *sdg8-1* mutant plants in response to exogenous SA treatment. ChIP analyses were used to determine relative levels of H3K4me3, H3K36me3 and total RNAPII during treatment with exogenous SA of 10-day-old WT (grey background) and *sdg8-1* mutant (white background) seedlings at the indicated regions of *PR1* (regions A, B and and C) and *PR2* (regions D, E and F). Genomic structures of the 2 genes and regions analysed by ChIP assays are indicated. Black boxes represent exons, arrows indicate TSS and bars labeled from A to F represent regions amplified. The anti-histone H3 was used to normalize H3K4me3 and H3K36me3 levels to nucleosome occupancy. For total RNAPII, the DNA enrichment was calculated relative to the input DNA. Mean values ± SD are presented based on results from two biological replicates. Letters indicate significant differences among sample in Student's *t*-test followed by Benjamini-Hochberg FDR correction ($P < 0.05$).

II.3.5. SDG8 interacts with both phosphorylated and non-phosphorylated RNAPII CTD

In eukaryotic cells, RNAPII carries out the transcription of all protein-encoding

genes into messenger RNAs. Among its various subunits, RNAPII contains a unique carboxyl-terminal domain (CTD) consisting of a large array of heptapeptide repeats in which Serine residues at position two and five are targets of CTD kinases and phosphatases (Dahmus, 1996). Phosphorylation/dephosphorylation events constitute the canonical "phospho-CTD cycle" with Ser5P at initiation, Ser5P and Ser2P during elongation and Ser2P only to terminate transcription (Buratowski, 2009). Because H3K36me3 is associated with active RNAPII transcription and because SDG8 is the main non-redundant H3K36 methyltransferase in Arabidopsis, we tested whether both proteins can interact. Co-immunoprecipitation (Co-IP) experiments were conducted using a rescued *sdg8* mutant line expressing a SDG8-FLAG fusion protein under the control of its own promoter (*efs-3 EFS-FLAG*; Ko et al., 2010). As shown in Figure 16A, SDG8 coprecipitated with total RNAPII as well as with both phosphorylated forms.

In animal and yeast, SDG8 orthologs were shown to bind preferably the phospho-CTD of the elongating RNAPII (Li et al., 2005; Kizer et al., 2005). To examine whether SDG8 also interacts specifically with the CTD, we carried out a tethered yeast two-hybrid system in which copies of the CTD were fused to the protein kinase Kin28, ensuring the CTD phosphorylation (CTD-Kin28), or to the catalytically inactive Kin28 (CTD-mKin28; Guo et al., 2004). Firstly, we confirmed by western blot analyses that the Kin28 indeed phosphorylates the fused CTD, while the mutated version does not (Figure 16B). Then, we tested the interaction between SDG8 and the CTD by yeast two-hybrid assays. An interaction between SDG8 and both the phosphorylated and non-phosphorylated forms of the CTD, but not with the Kin28 alone was detected (Figure 16C). Finally, because SDG8 and SDG26 are closely related to the yeast sole H3K36-methyltransferase SET2 and to the animal H3K36-methyltransferases ASH1 and HYPB/SETD2 (Xu et al., 2008), we also tested the binding of SDG26 to the CTD and found interaction with neither of these baits (Figure 16C). Together, these results supported an interaction between SDG8 and the phosphorylated and non-phosphorylated forms of the RNAPII CTD.

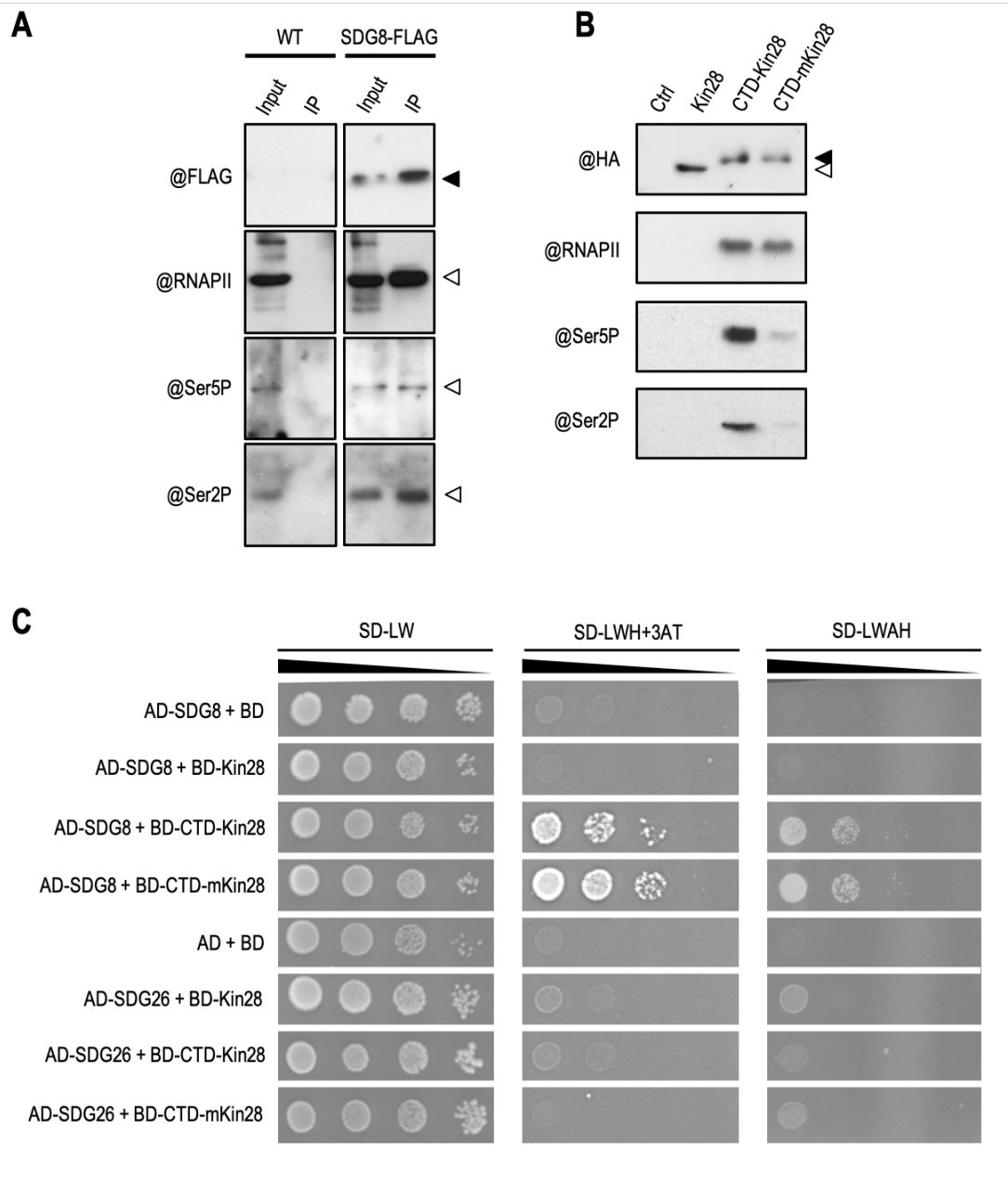

Figure 16: Protein interaction between SDG8 and different phosphorylated forms of RNAPII. (A) Proteins were extracted from wild-type (WT) and plants expressing a functional FLAG-tagged SDG8 protein in a *sdg8* mutant background (SDG8-FLAG). An anti-FLAG antibody was used to detect the tagged SDG8 protein (black arrowhead) in the input and after immunoprecipitation using anti-FLAG beads (IP). Total RNAPII (@RNAPII), the Ser5P form of the CTD of RNAPII (@Ser5P) or the Ser2P form of the CTD of RNAPII (@Ser2P) in input and after IP are indicated by white arrowheads. **(B)** The two-hybrid system used to identify protein-protein interactions requiring post-translational modifications was tested for the phosphorylation of the CTD. An anti-HA antibody was used to detect fusion protein in untransformed yeast (Ctrl) and in yeast transformed with the protein kinase Kin28 alone (white arrowhead) or with the CTD fused to either Kin28 (CTD-Kin28) or the inactive Kin28 (CTD-mKin28). Phosphorylation of the CTD detected by antibodies against the Ser5P form of the CTD (@Ser5P) or the Ser2P form of the CTD (@Ser2P) occurs mainly with the tethered wild-type Kin28 but not with the mutated one. **(C)** Yeast two-hybrid analysis of the interaction between SDG8 and the phosphorylated or non-phosphorylated form of the RNAPII CTD. Full-length SDG8 and SDG26 were separately fused to the Gal4 Activation domain (AD), while Kin28, CTD-Kin28 and CTD-mKin28 were fused to the Gal4 DNA Binding domain (BD). Yeast cells co-transformed with the different recombinant vectors were spotted though a series of tenfold dilutions onto control (SD-LW) and selection media of increasing stringency (SD-LWH+3-AT and SD-LWAH).

II.4. Discussion

In this study, we used the *sdg8-1* mutant (SALK_065480) and found that, like other *sdg8* alleles such as *sdg8-2* (SALK_026442; Palma et al., 2010; Lee et al., 2016) and *sdg8-4* (SALK_014569; De-La-Peña et al., 2012), *sdg8-1* is more sensitive to *Pst* infection (Figure 1). Because the SA-dependent defense have a strong impact on *Pst* growth and plant resistance (Seyfferth and Tsuda, 2014), we addressed for the first time the question of the role of *SDG8* in the SA-mediated defense signaling pathway, with a special emphasis on the behavior of H3K4 and H3K36 methylation and RNAPII loading. We therefore quantified SA before and during infection in *sdg8-1* in comparison to WT and focused our analyses on SA-related genes. Under non-stressful conditions, we observed an abnormally high basal level of SA in *sdg8-1*, together with a significant decrease of *NPR1* basal transcription and increase of *ICS1* (Figures 2 and 3). *ICS1* plays a major role in SA biosynthesis (Garcion et al., 2008; Huang et al., 2010), its increased basal expression in *sdg8-1* may explain the abnormal accumulation of SA under unstimulated conditions and the resulting elevated transcriptional steady states of *PR1*, *PR2* and *WRKY70* genes. Given the existence of a negative feedback loop of NPR1 on SA accumulation through the repression of *ICS1* expression (Zhang et al., 2010), our observations suggest that *sdg8-1* has probably lost this retor-control. However, because loss-of-function mutants for *NPR1* do not constitutively accumulate SA (Genger et al., 2008), SDG8 might also regulate expression levels of other genes important to control basal SA level.

When inoculated with virulent or avirulent strains of *Pst*, the *sdg8-1* mutant shows severe disease symptoms, correlated with enhanced bacterial growth and very low SA accumulation (Figure 1 and 2). Analyses of bacterial titers and SA accumulation upon infection further suggest that ETI is still functional in the *sdg8-1* mutant, but less efficient. Also, despite the low SA accumulation observed in the *sdg8-1* mutant upon infection, all analyzed genes were induced, except *NPR1* and *ICS1* which stayed downregulated or not significantly induced, respectively. Supporting the higher susceptibility of the mutant, inductions were substantially lower in *sdg8-1* for *PAD4* and *EDS1*, two genes functioning upstream of SA, as well as for downstream *PR* genes. This last result put into perspective with the WT-like induction of *WRKY70*, known to induce *PR* genes expression (Li et al., 2004), clearly suggest the involvement of *SDG8* at different levels along the SA-

dependent signaling pathway to support the efficient transcriptional induction of SA-related genes upon stimulation. This involvement at different levels was further confirmed using exogenous SA as a stimulus, since the non-induction of *NPR1*, as well as the inefficient induction of *PR* genes still remained in *sdg8-1*, while *WRKY70* was similarly induced as in WT (Figure 3). NPR1 is known as a central transcriptional regulator critical for transducing the SA signal into activation of most SA-dependent genes (Wang et al., 2005), but the maintenance of an ETI and the incomplete loss of *PR* genes expression in *npr1* mutants suggest that certain SA-related responses could be NPR1-independent (Rairdan and Delaney, 2002; Shah et al., 2001). The reproducibly low induction of *PR* genes, and the normal induction of *WRKY70* we observed in *sdg8-1* upon infection further suggest that a NPR1-independent signaling pathway still operates in *sdg8-1*, but is not sufficient to provide the mutant with an effective response against the pathogen. Supporting the idea of a NPR1-independent signaling pathway, a core EDS1/PAD4 pathway working in parallel with the ICS1-generated SA was recently proposed to maintain important SA-related resistance programs, thereby increasing robustness of the innate immune system (Cui et al., 2017).

Using exogenous SA, we also demonstrated that levels of H3K4me3, H3K36me3 and H3K27me3 were globally unchanged in hormonally treated WT plants. Previously, global changes in histone methylation, especially H3K4me3 and H3K36me3, were observed in WT plants after infection with virulent and avirulent strains of *Pst* (De-La-Peña et al., 2012; Lee et al., 2016). Even if these observations deserve further analysis, especially regarding the origin and purposes of these changes, global variations in some histone methylation marks occur upon *Pst* infection in Arabidopsis, while it is not the case using exogenous SA as a stimulus. These results suggest the existence of a yet unknown mechanism/effector, probably produced by the bacterial pathogen, enabling *Pst* to modify some histone methylation marks, certainly to promote host susceptibility. Supporting this hypothesis, two examples of histone modifying enzyme inhibitors produced by plant pathogens were reported so far, all functioning as potential histone deacetylase (HDACs) inhibitor: *i*) the HC-toxin, produced by the maize pathogen *Cochliobolus carbonum* and required for its pathogenicity (Brosch et al., 1995; Ransom and Walton, 1997) ; and *ii*) the depudecin, produced by *Alternaria brassicicola* and required for virulence in *Brassica oleracea* but not in Arabidopsis (Wight et al., 2009).

In parallel, we addressed the question of local histone methylation levels at the chromatin of several SA-related genes. In non-treated plants, the level of H3K36me3 at all examined genes was substantially decreased in *sdg8-1* compared to WT (Figure 5 and Supplementary Figure 2). In agreement with H3K36me3 and H3K4me3 being deposited largely independently in Arabidopsis (Shafiq et al., 2014; Li et al., 2015; Zhao et al., 2019), the level of H3K4me3 was found unchanged in our analyses. In addition, RNAPII levels were also globally stable between WT and *sdg8-1* plants, except at NPR1 were the loading was slightly decreased in the mutant. Since *NPR1* is among the list of the SDG8-bound genes published by Li and colleagues (Li et al., 2015), its downregulation in *sdg8-1* suggests a direct role for SDG8 and H3K36me3 in controlling *NPR1* basal expression. Interestingly, such role was previously proposed for several other biotic stress-related genes (Berr et al., 2010; Palma et al., 2010; Lee et al., 2016) and might be extended to others since 20.7% of the 121 genes known to function in the host response to pathogen challenge in Arabidopsis (Bhardwaj et al., 2011) were among the expanded list of SDG8 bound genes from Li et al., 2015 (list in Supplementary Table 2 and Supplementary Table 3). Such a role for SDG8 is in agreement with the positive correlation previously described between levels of H3K36me3 and gene expression (Li et al., 2015). However, while 26% of the H3K36me3 hypomethylated genes were downregulated in the deletion mutant *sdg8-5* under normal growth conditions, 5% were upregulated and the remaining 69% were unchanged (Li et al., 2015). In our present study, *WRKY70*, *PR1* and *PR2* were all basally upregulated despite the decreased level of H3K36me3 at their chromatin (Figure 3). In another *sdg8* allele (*ashh2-5*; SALK_036941), Wang and colleagues also reported about the increased *PR2* expression and the corresponding decreased level of H3K36me3 (Wang et al., 2014). Because *WRKY70* and *PR* genes are SA-inducible, we believe that the abnormal accumulation of SA detected in *sdg8-1* and resulting from the *NPR1* downregulation may bypass the low H3K36me3 level, thus leading to their increased basal expression.

Next, we used exogenous SA treatment to follow chromatin changes at several SA-related genes. Previously, treatment with stress related phytohormone (i.e. methyl jasmonate, abscisic acid, indole-3-acetic acid and zeatin) were all reported to provoke changes in histone methylation at some specific hormone responsive genes (Berr et al., 2010; Kim et al., 2013). In our work, we found that both H3K4 and H3K36 methylation were increased upon treatment in WT plants at all SA-related genes we analyzed. As

previously described during some developmental transitions, a strong quantitative correlation exists between histone methylation and gene expression upon stimulation (Brusslan et al., 2015; Engelhorn et al., 2017; You et al., 2017). In agreement with this, *PR1* and *PR2* experienced in our work both the strongest H3K4 and H3K36 methylation increase and transcriptional induction. Compare to WT, the level of H3K36me3 was almost unchanged in *sdg8-1* upon SA stimulation at all analyzed genes, while a H3K4me3 increase occurred but at a lower range compare to WT. In conjunction with the less efficient transcriptional induction of *PR* genes and the correspondingly lower RNAPII loading observed in *sdg8-1*, these results suggest that SDG8, through its H3K36 methyltransferase activity, may establish a chromatin context not necessary for the initial transcriptional induction but latter required to reinforce and further potentiate the initial induction, especially at strongly SA-responding genes. Regarding *NPR1*, the chromatin changes we detected are in agreement with the above proposed hypothesis that SDG8 regulates directly *NPR1* expression. For *WRKY70*, the H3K4me3 increase observed in the mutant after SA treatment seems sufficient to promote its induction despite the stably low H3K36me3. Previously, the H3K4 tri-methyltransferase ARABIDOPSIS TRITHORAX1 (ATX1) was positively involved in the activation of the *WRKY70* expression (Alvarez-Venegas et al., 2007). Together, these data suggest that H3K4me3, compared with H3K36me3, may play a more decisive role in the final *WRKY70* transcriptional outcome. Since histone methylation was involved in gene priming at several *WRKY* genes (Jaskiewicz et al., 2011), it is reasonable to speculate that the H3K36me3 increase observed in WT plants upon SA treatment may serve as a memory mark, thus providing the plant with a life-long protection.

In Arabidopsis, all known histone methyltransferases have a so-called SET catalytic domain, but only SDG8 has in addition a CW domain (Pontvianne et al., 2010). The CW domain found in a small number of chromatin-related proteins in animals and plants is thought to be a “reader” domain that can bind methylated H3K4 and the one found in SDG8 has preference for H3K4me1/me2 peptides (Hoppmann et al., 2011; Liu and Huang, 2018). SDG8 therefore combines an H3K4 methylation-reading module together with an H3K36me3 writing module, making it the only reader and writer of histone methylation. In animals and yeast, the SDG8 orthologs co-purify with RNAPII and binds directly to the CTD, with a weak binding to singly phosphorylated S2P or S5P CTD repeats, and a strong one to CTD repeats simultaneously phosphorylated on both serines (Tanny, 2015).

This affinity and the distribution profile of H3K36me3 with an enrichment toward the 3'-end of genes, as shown in Li et al., 2015, spearhead the coupling between H3K36 methylation and transcription elongation. In Arabidopsis, we and others (Yang et al., 2016; Zhong et al., 2019) demonstrate that SDG8 can also bind RNAPII. However, while its orthologs preferentially bind the phosphorylated CTD of elongating RNAPII, we found that SDG8 can physically interact with both phosphorylated and non-phosphorylated forms of CTD (Figure 6), as also found for the H3K4 methyltransferase ATX1 (Ding et al., 2011). Together, Arabidopsis may employ SDG8 and methylated H3K36 in different ways compare to its paradigm usage in animal and yeast, thus explaining the plant specific distribution of H3K36me3 with peaks in the first half of the coding region, compared to the 3'-end enrichment observed in animal and yeast (Roudier et al., 2011). Because plants are sessile organisms, their adaptation/defense against environmental stress must be extremely efficient. It is therefore tempting to imagine that in the course of evolution, plants have hijacked the H3K36me3 mark to build up a plant-specific epigenetic process ensuring the efficiency of the transcriptional induction of stress responding genes.

Plant innate immunity and development are intimately interconnected, and evidence has accumulated supporting the contribution of SA to this interconnection. Indeed, the level of SA in Arabidopsis leaves was found increased by 2-fold during the transition to flowering (Abreu and Munné-Bosch, 2009) and mutants with increased SA level (*e.g. esd4*, *siz1, acd6*), in addition to be dwarf, show accelerated flowering (Jin et al., 2008; Wang et al., 2011; Villajuana-Bonequi et al., 2014), while SA-deficient mutants (e.g. *nahG*, *sid1/eds5* and *sid2*) exhibit late-flowering phenotypes (Martínez et al., 2004). SA plays also important roles in light-harvesting processes and photoprotection (Janda et al., 2014), since, for example, SA affects carotenoids content (Munné-Bosch et al., 2007). In addition, SA markedly enhances the reinduction of the late maturation program during early stages of germination (Rajjou et al., 2006; Alonso-Ramírez et al., 2009) and interacts with jasmonate/ethylene (Li et al., 2019), as well as with brassinosteroids pathways (Divi et al., 2010). Similarly as other mutants with increased SA level, *sdg8* appears dwarf and affected in the regulation of the flowering time (Kim et al., 2005; Zhao et al., 2005), carotenoid composition (Cazzonelli et al., 2009; Cazzonelli et al., 2010), light responsive genes involved in photosynthesis (Li et al., 2015), seed gene regulation (Tang et al., 2012), brassinosteroid-regulated gene expression (Wang et al., 2014) and JA/ET-mediated responses (Berr et al., 2010; Zhang et al., 2019). Because the stimulation of a given stress-

signaling pathway usually results in the prioritization of defense over growth-related cellular functions, while conserving enough resources for survival and reproduction (Verk et al., 2009), there is a strong need for regulators acting at the junction between defense and development. Together with the evidence presented herein that *SDG8* has a profound impact on the SA-pathway, we raise the hypothesis of its involvement in the controlled balancing between development and immunity for the long-term fitness. How SDG8 is targeted to one or the other process remains unknown, but examples such as the bZIP transcription factors bZIP28 and bZIP60 suggested the involvement of stress-induced transcription factors to recruit histone-modifying complexes at stress responsive genes (Song et al., 2015). Because SDG8 orthologs exist in other plant species (Huang et al., 2011; Liu et al., 2016), it is tempting to speculate that such connection might be conserved in the plant kingdom.

II.5. Supportive information

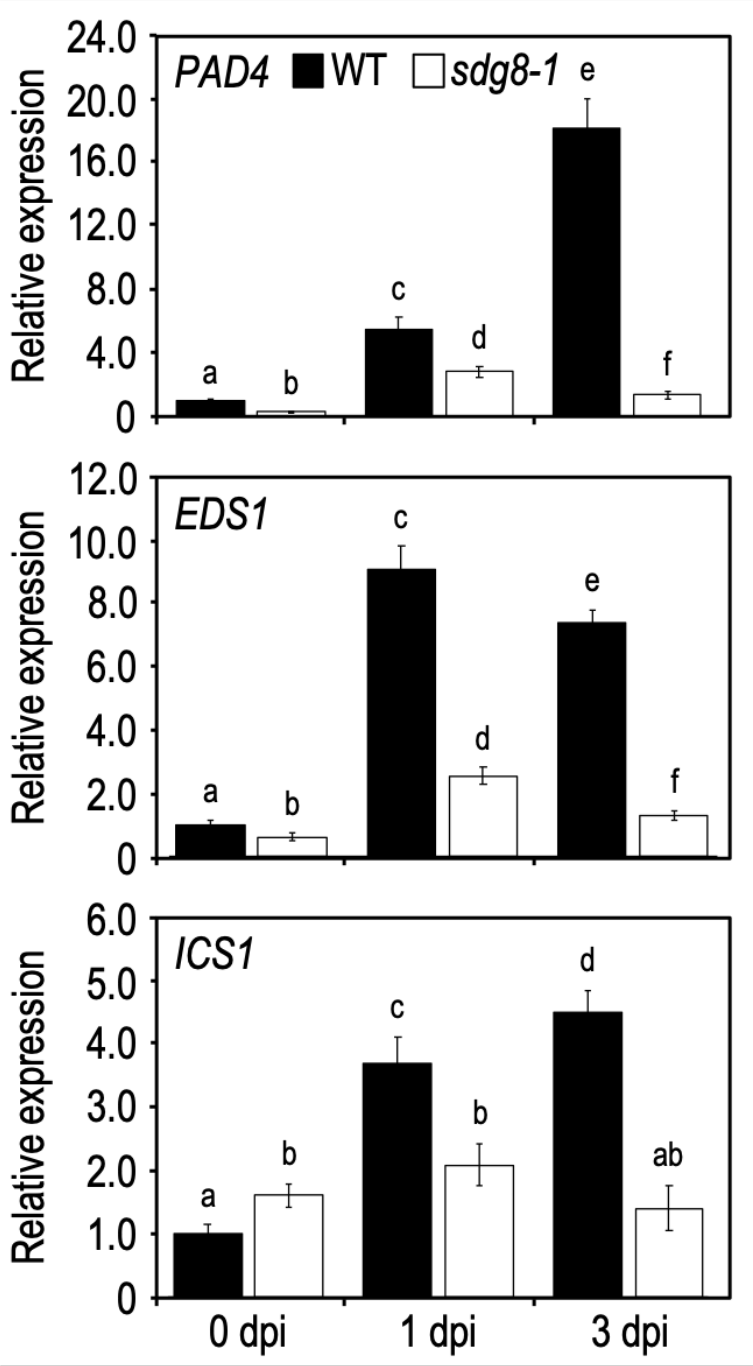

Supplementary Figure 1: Expression levels of genes functioning upstream of SA in WT and *sdg8-1* mutant plants upon *Pseudomonas syringae* infection. Expression levels of *PAD4*, *EDS1* and *ICS1* were quantified by qRT-PCR in WT (black) and *sdg8-1* (white) mutant 5-week-old plants in response to *Pst* DC3000 inoculation. Expression values for each gene are presented relative to the corresponding WT level at 0 dpi (set as 1) as means ± SD (n=3). Letters indicate significant differences among sample in Student's *t*-test followed by Benjamini-Hochberg FDR correction ($P < 0.05$).

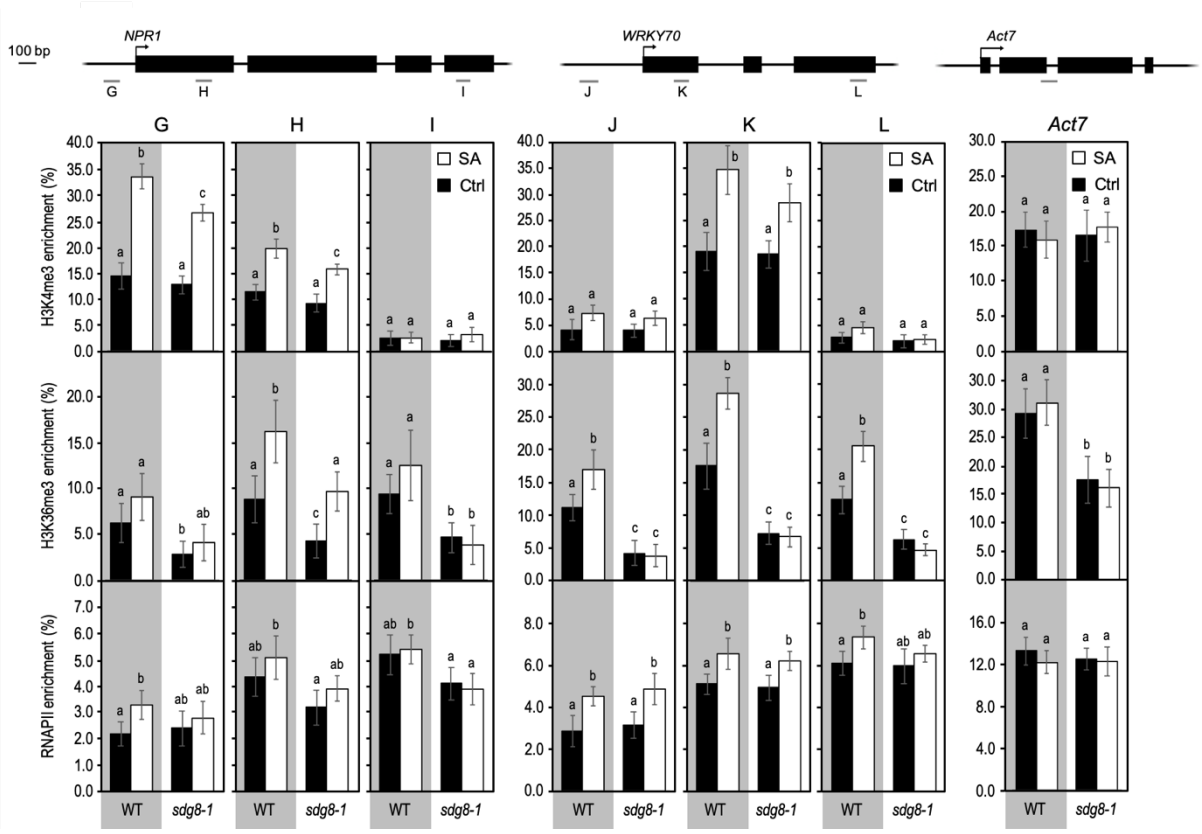

Supplementary Figure 2: Chromatin immunoprecipitation analyses of H3K4me3, H3K36me3 and total RNAPII at *NPR1* and *WRKY70* in WT and *sdg8-1* mutant plants in response to exogenous SA treatment. ChIP analyses were used to determine relative levels of H3K4me3, H3K36me3 and total RNAPII during treatment with exogenous SA of 10-day-old WT (grey background) and *sdg8-1* mutant (white background) seedlings at the indicated regions of *NPR1* (regions G, H and I) and *WRKY70* (regions J, K and L). Genomic structures of the 2 genes and regions analysed by ChIP assays are indicated. Black boxes represent exons, arrows indicate TSS and bars labeled from G to L represent regions amplified. The anti-histone H3 was used to normalize H3K4me3 and H3K36me3 levels to nucleosome occupancy. For total RNAPII, the DNA enrichment was calculated relative to the input DNA. Mean values ± SD are presented based on results from two biological replicates. *ACT2* was used as a control since its transcription is unchanged in *sdg8-1* compare to wild-type and not induced by exogenous SA (data not shown). Letters indicate significant differences among sample in Student's *t*-test followed by Benjamini-Hochberg FDR correction ($P < 0.05$).

Table S1: Primers used in this work

Primers pairs used for qRT-PCR:

Gene	Sequence (5' to 3')
ICS1 (AT1G74710)	CATTGATCTATGCGGGGACAG
	TGGACAAAAGCTCGTACCTGAG
EDS1 (AT3G48090)	AAGCATGATCCGCACTCG
	CGAAGACACAGGGCCGTA
PAD4 (AT3G52430)	GGTTCTGTTCGTCTGATGTTT
	GTTCCTCGGTGTTTTGAGTT
NPR1 (AT1G64280)	AGGCACTTGACTCGGATGATATTG
	CTTCACATTGCAATATGCAACAGC
WRKY70 (AT3G56400)	AGGAGATGGGTTCGAAGGTA
	TCGTTGAAGGCCATGACTTA
PR1 (AT2G14610)	TTCTTCCCTCGAAAGCTCAA
	AAGGCCCACCAGAGTGTATG
PR2 (AT3G57260)	CGATCCAGGGTACTCATACCA
	CTCCGACACCACGATTTCCA
Reference Genes	
GAPDH (AT1G13440)	TTGGTGACAACAGGTCAAGCA
	AAACTTGTCGCTCAATGCAATC
EXP (AT4G26410)	GAGCTGAAGTGGCTTCAATGAC
	GGTCCGACATACCCATGATCC
TIP41 (AT4G34270)	GTGAAAACTGTTGGAGAGAAGCAA
	TCAACTGGATACCCTTTCGCA

Primers pairs used for quantifying qChIP enrichment:

Gene		Sequence (5' to 3')
ACT7 (AT5G09810)		CCCTCGTAGATTGGCACAGT
		GGCCGTTCTTTCTCTCTATGC
PR1 (AT2G14610)	A	CGTCTTTGTAGCTCTTGTAGGTG
		TGAACCCTTAGATAATCTTGTGGGC
	B	TGCAATGGAGTTTGTGGT
		CACCTCACTTTGGCACATCCGA
	C	ATTTCAATAAGGAGCATCATATGCAGG
		GATTCTCGTAATCTCAGCTCTTATTTGT
PR2 (AT3G57260)	D	CGGCCAATATTACCATGATCCAACC
		ATGAATCGCCCAAACCAATTTGGT
	E	TTAGCCTCACCACCAATGTTGATG
		AACCTGTGTGGTTGAAGAAGGA
	F	CCTATTCGACGCAAATCTCGACTC
		GACACCACGATTTCCAACGATCC
NPR1 (AT1G64280)	G	ATGTAAACCGTGGGACGAGG
		GATCGAAGATAACCATTGACGAGCAG
	H	GGAGATTGCCAAGGATTACGAAGT
		CCTTTAGGCGGCGGTCTCA
	I	GTGCTCGACCAGATTATGAACTGTG
		TTTGTAGTCGTTTCTCAGCAGTGT
WRKY70 (AT3G56400)	J	AGGACCCTAAGTTTGGATTTCAGCA
		ATGGTGAGCTTGACGTAAGCTCAAA
	K	CCCATCTCCTCCTCCTCATCCCTCG
		CCGGAATCTTCAAACTTGCCGTCGT
	L	CATCAGGCCAGTTACGTCAATGGGA
		ACTCGAAATCGCCGCCACCTC

Table S2: List of genes bounded by SDG8 among 121 genes known to function in the host response to pathogen challenge in Arabidopsis.

Gene ID	Gene name	Function(s) related to stress	Reference
AT1G64280	NON-EXPRESSER OF PR GENES 1 (NPR1)	Key regulator of SA-mediated signaling	Fan, W, Dong, X (2002) In vivo interaction between NPR1 and transcription factor TGA2 leads to salicylic acid-mediated gene activation in Arabidopsis. Plant Cell 14: 1377-1389.
AT3G53260	PHENYALANINE AMMONIA-LYASE 2 (PAL2)	phenylpropanoid biosynthesis, SA biosynthesis	Wanner, LA, Li, G, Ware, D, Somssich, IE, Davis, KR (1995) The phenylalanine ammonia-lyase gene family in Arabidopsis thaliana. Plant Mol Biol 27: 327-338.
AT5G04230	PAL3	as PAL2	Huang, J, et al. (2010) Functional analysis of the Arabidopsis PAL gene family in plant growth, development, and response to environmental stress. Plant Physiol 153: 1526-1538.
AT2G31880	SUPPRESSOR OF BIR1 (SOBIR1)	leucine rich repeat transmembrane protein that is expressed in response to Pseudomonas syringae. positive regulation of defense response	Gao M, et al. (2009) Regulation of cell death and innate immunity by two receptor-like kinases in Arabidopsis. Cell Host Microbe 6: 34-44.
AT1G59870	PENETRATION3 (PEN3)	plasma membrane ABC transporter, contributes to nonhost resistance to inappropriate pathogens that enter by direct penetration in a salicylic acid–dependent manner. Required for MLO resistance.	Stein, M, et al. (2006) Arabidopsis PEN3/PDR8, an ATP binding cassette transporter, contributes to nonhost resistance to inappropriate pathogens that enter by direct penetration. Plant Cell 18: 731-746.
AT1G01720	ATAF1	putative transcriptional activator with NAC domain. Transcript level increases in response to wounding and abscisic acid.	Collinge M, Boller, T (2001) Differential induction of two potato genes, Stprx2 and StNAC, in response to infection by Phytophthora infestans and to wounding. Plant Mol.Biol 46: 521-529.
AT5G61210	SOLUBLE N-ETHYLMALEIMIDE-SENSITIVE FACTOR ADAPTOR PROTEIN 33 (SNAP33)	Forms part of plasma membrane SNARE PEN1-SNAP33-VAMP721/722 secretory complex that functions in plant defence	Kwon, C et al. (2008) Co-option of a default secretory pathway for plant immune responses. Nature 451: 835-840.
AT5G45250	RESISTANT TO P. SYRINGAE 4 (RPS4)	Toll/interleukin-1 receptor (TIR)-nucleotide binding site (NBS)-LRR class of disease resistance (R) genes. Confers specific resistance to Pseudomonas syringae pv. tomato carrying the avirulence gene AvrRPS4	Wirthmueller, L, Zhang, Y, Jones, JD, Parker, JE (2007) Nuclear accumulation of the Arabidopsis immune receptor RPS4 is necessary for triggering EDS1-dependent defence. Curr Biol 17: 2023-2029.
AT5G13160	avrPphB susceptible 1 (PBS1)	Mutant is defective in perception of Pseudomonas syringae avirulence gene avrPphB. Encodes a putative serine-threonine kinase.	Warren, RF, Merritt, PM, Holub, E, Innes, RW (1999) Identification of three putative signal transduction genes involved in R gene-specified disease resistance in Arabidopsis. Genetics 152: 401-412.
AT5G47910	RESPIRATORY BURST OXIDASE HOMOLOGUE D (RBOHD)	Interacts with AtrbohF gene to fine tune the spatial control of ROI production and hypersensitive response to cell in and around infection site.	Pogany, M et al. (2009) Dual roles of reactive oxygen species and NADPH oxidase rbohD in an Arabidopsis-Alternaria pathosystem Plant Physiol 151: 1459-1475.
AT2G39940	CORONATINE INSENSITIVE 1 (COI1)	Required for wound- and jasmonates-induced transcriptional regulation, defense response to fungus	Xie, DX, Feys, BF, James, S, Nieto-Rostro, M, Turner, JG (1998) COI1: an Arabidopsis gene required for jasmonate-regulated defense and fertility. Science 280: 1091-1094.
AT5G42650	ALLENE OXIDE SYNTHASE (AOS)	JA biosynthetic pathway, defense response	Laudert, D, Pfannschmidt, U, Lottspeich, F, Hollander-Czytko, H, Weiler, EW (1996) Cloning, molecular and functional characterization of Arabidopsis thaliana allene oxide synthase (CYP74), the first enzyme of the octadecanoid pathway to jasmonates. Plant Mol Biol 31: 323-335.
AT2G33150	PEROXISOMAL 3-KETOACYL-COA THIOLASE 3 (PKT3), KAT 2	JA biosynthetic process	Pye, VE, Christensen, CE, Dyer, JH, Arent, S, Henriksen, A (2010) Peroxisomal plant 3-ketoacyl-CoA thiolase structure and activity are regulated by a sensitive redox switch. J Biol Chem. 285: 24078-24088.
AT4G11260	SGT1B	required for defense signaling conferred by several downy mildew resistance genes, JA mediated signaling pathway.	Tor, M, et al. (2002) Arabidopsis SGT1b is required for defense signaling conferred by several downy mildew resistance genes. Plant Cell 14: 993-1003.
AT3G45640	MITOGEN-ACTIVATED PROTEIN KINASE 3 (MPK3)	Functions in MAP kinase cascade involving MEKK1, MKK4/MKK5 and MPK3/MPK6 that functions downstream of the FLS2 fagellin receptor, activation of this MAPK cascade confers resistance to both bacterial and fungal pathogens	Asai, T, et al. (2002) MAP kinase signalling cascade in Arabidopsis innate immunity. Nature 415: 977-983.
AT4G29810	MITOGEN-ACTIVATED PROTEIN KINASE KINASE 2 (MKK2)	Shares functional redundancy with MKK1/2, involved in jasmonate- and salicylate-dependent defense responses	Qiu, JL, et al. (2008) Arabidopsis mitogen-activated protein kinase kinases MKK1 and MKK2 have overlapping functions in defense signaling mediated by MEKK1, MPK4, and MKS1. Plant Physiol 148: 212-222.
AT1G51660	MKK4	Functions in MAP kinase cascade involving MEKK1, MKK4/MKK5 and MPK3/MPK6 that functions downstream of the FLS2 fagellin receptor, activation of this MAPK cascade confers resistance to both bacterial and fungal pathogens	Asai, T, et al. (2002) MAP kinase signalling cascade in Arabidopsis innate immunity. Nature 415: 977-983.
AT1G73500	MKK9	Autophosphorylates and also phosphorylates MPK3 and MPK6. Independently involved in ETH and calmalexin biosynthesis. Induces transcription of ACS2, ACS6, ERF1, ERF2, ERF5, ERF6, CYP79B2, CYP79B3, CYP71A13 and PAD3.	Xu, J, et al. (2008) Activation of MAPK kinase 9 induces ethylene and camalexin biosynthesis and enhances sensitivity to salt stress in Arabidopsis. J Biol Chem 283: 26996-27006.
AT1G10210	MITOGEN-ACTIVATED PROTEIN KINASE 1 (ATMPK1)	Activated by wounding JA	Ortiz-Masia, D, Perez-Amador, MA, Carbonell, J, Marcote, MJ (2007) Diverse stress signals activate the C1 subgroup MAP kinases of Arabidopsis. FEBS Lett 581: 1834-1840.
AT1G32640	MYC2	MYC-related transcriptional activator, regulates diverse JA-dependent functions.	Lorenzo, O, Chico, JM, Sanchez-Serrano, JJ, Solano, R (2004) JASMONATE-INSENSITIVE1 encodes a MYC transcription factor essential to discriminate between different jasmonate- regulated defense responses in Arabidopsis. Plant Cell 16: 1938-1950.
AT3G15210	ETH RESPONSIVE ELEMENT BINDING FACTOR 4 (ERF4)	member of the ERF subfamily of transcription factors, negative regulator of JA-responsive defense gene expression and resistance to the necrotrophic fungal pathogen Fusarium oxysporum and antagonizes JA inhibition of root elongation	McGrath, KC, et al. (2005) Repressor- and activator-type ethylene response factors functioning in jasmonate signaling and disease resistance identified via a genome-wide screen of Arabidopsis transcription factor gene expression. Plant Physiol 139: 949-959.
AT2G38470	WRKY33	Regulates the antagonistic relationship between defense pathways mediating responses to P. syringae and necrotrophic fungal pathogens	Zheng, Z, Qamar, SA, Chen, Z, Mengiste, T (2006) Arabidopsis WRKY33 transcription factor is required for resistance to necrotrophic fungal pathogens. Plant J 48: 592-605.
AT1G80840	WRKY40	Pathogen-induced transcription factor, forms protein complexes with itself and with WRKY40 and WRKY60. WRKY18, -40, and -60 have partially redundant roles in response to the hemibiotrophic bacterial pathogen P. syringae and the necrotrophic fungal pathogen B cinerea, with WRKY18 playing a more important role than the other two.	Chen CH, Chen, ZX (2002) Potentiation of developmentally regulated plant defense response by AtWRKY18, a pathogen-induced Arabidopsis transcription factor. Plant Physiol 129: 706-
AT3G56400	WRKY70	Function as activator of SA-dependent defense genes and a repressor of JA-regulated genes. WRKY70-controlled suppression of JA-signaling is partly executed by NPR1	Li, J, Brader, G, Kariola, T, Palva, ET (2006) WRKY70 modulates the selection of signaling pathways in plant defense. Plant J 46: 477-491.

CHAPTER III RESULTS Part II

The histone methyltransferase SDG26 is involved in the responses to cold stress in Arabidopsis

Xue Zhang, Julie Zumsteg, Mathiu Erhardt, Wen-Hui Shen and Alexandre Berr[1, *]

Affiliations:

[1] Institut de Biologie Moléculaire des Plantes du CNRS, Université de Strasbourg, 12 rue du Général Zimmer, 67084, Strasbourg Cedex, France.

*** Author for correspondence:** Alexandre.Berr@ibmp-cnrs.unistra.fr

III.1. Introduction

In eukaryotes, covalent modifications of histone tails are essential for the proper regulation of gene transcription within the chromatin context (Zentner and Henikoff, 2013). Among these modifications, the specific methylation of particular histone lysine residues is established by histone lysine methyltransferases (HKMTs). In Arabidopsis, all known HKMTs contain a conserved catalytic SET domain and are therefore referred as SET DOMAIN GROUP (SDG) proteins. SDGs can be divided into at least five classes based on their domain architectures and/or enzymatic activity (Pontvianne et al., 2010). Among them, SDGs belonging to the ABSENT, SMALL OR HOMEOTIC DISCS1 (ASH1) and TRITHORAX (TRX) classes form together the Trithorax group (TrxG), which are involved in transcriptional activation through catalysis of H3K4 and/or H3K36 methylation. *SDG26/ASHH1* is one of the 5 SDG genes belonging to the ASH1 subfamily. *SDG26* was involved through a yet unknown mechanism in DNA repair (Campi et al., 2012; Roitinger et al., 2015), but besides this, *SDG26* has been primarily studied regarding the late-flowering phenotype caused by its mutation (Xu et al., 2008). This phenotype is quite unusual because mutations in other ASH1 subfamily members, such as *SDG8*, its closest homolog (Kim et al., 2005; Soppe et al., 1999; Zhao et al., 2005), or *SDG7/ASHH3* (Lee et al., 2015), as well as in TRX class members, such as *ATX1/SDG27* (Pien et al., 2008), *SDG2/ATRX3* (Guo et al., 2010) or *SDG25/ATXR7* (Berr et al., 2009; Tamada et al., 2009) and even in the repressive E(z) family member *CURLY LEAF* (Jiang et al., 2008) result in early-flowering plants. Indeed, *SDG26* promotes flowering through a distinct genetic pathway. It was shown that SDG26 participates in the transcriptional activation of the floral pathway integrator *SUPPRESSOR OF OVEREXPRESSION OF CONSTANS1* (*SOC1*) through binding at *SOC1* promoter region and depositing H3K4me3 and H3K36me3 along its chromatin (Berr et al., 2015). In addition to the decreased expression of *SOC1* observed in *sdg26*, an increased expression of *FLOWERING LOCUS C* (*FLC*) was also detected (Berr et al., 2015; Liu et al., 2016; Xu et al., 2008). It is well known that along the flowering-regulatory network the floral repressor FLC binds and represses *SOC1*. Therefore, considering the active role of SDG26 on *SOC1*, the question remains as to how *FLC* can be up-regulated in *sdg26*. Interestingly, in a previous study about Arabidopsis cold responses, SOC1 was proposed to repress *FLC* expression through the inhibition of cold-inducible genes such as *COLD REGULATED* (*COR*) or *C-REPEAT/DREB BINDING FACTOR* (*CBF*; Seo et al., 2009). An intriguing hypothesis was formulated that the *SOC1* down-regulation in the *sdg26* mutant may cause the *FLC*

up-regulation (Berr et al., 2015). In addition, using the Stress Responsive Transcription Factor Database (STIFDB; Naika et al., 2013), we found that *SDG26* expression may be induced by different abiotic stresses (cold, drought and salt) and a W-box is present at its promoter region with a z-score of 1.89. W-box, with (C/T)TGAC(T/C) as a core sequence, acts as a binding site for WRKY transcription factors that play crucial roles in regulating stress responses under both biotic and abiotic stresses (Phukan et al., 2016). Based on these different observations, we decided to investigate the involvement of *SDG26* in plant abiotic stress responses.

III.2. Results

III.2.1. General features of the SDG26 gene

At first, we decided to better characterize the *SDG26* gene (AT1G76710), starting with general features. Based on the information available in TAIR10, *SDG26* contains 11 introns. While TAIR10 annotates only two representative transcripts (SDG26-a and SDG26-b that give after translation the same protein), AceView predicts four different mRNAs, with three alternatively spliced variants and one unspliced form (Figure 17A). The unspliced form covering 954 base pairs (bp) has a single exon (corresponding to intron 8 and exon 9) and is hypothetically translated in a 115 amino acid (aa) putative protein. The spliced variants SDG26-a (1752 bp) and SDG26-b (1847 bp) differ regarding their 5'UTR region since an alternative promoter was predicted. Despite this difference, their coding sequences (CDS) were identical, producing a unique 492 aa SET-domain protein (about 55 kDa). Interestingly, the third alternatively spliced variant named SDG26-c was so fare omitted from the literature. This variant is the result of the use of an alternative 3' splice junction, also named acceptor site, that change the 5' boundary of the downstream exon. *SDG26-c* results in a 1613 bp mRNA translated in a 253 aa protein (about 29 kDa). SDG26-a/b and SDG26-c proteins contain domains typically found in SET-domains proteins, the conserved SET lysine methyltransferase catalytic domain surrounded on its N-terminal side by the AWS (Associated With SET) motif and on its C-terminal side by the Post-SET domain (Figure 17B). A putative Nuclear Localization Signal (NLS) was also identified.

Because we were not able to detect by neither semi-quantitative RT-PCR nor Real-time quantitative PCR the predicted unspliced mRNA form and because the corresponding predicted protein contains no known protein domain or characteristic motif, we decided to focus our work only on the SDG26-a/b and SDG26-c transcripts.

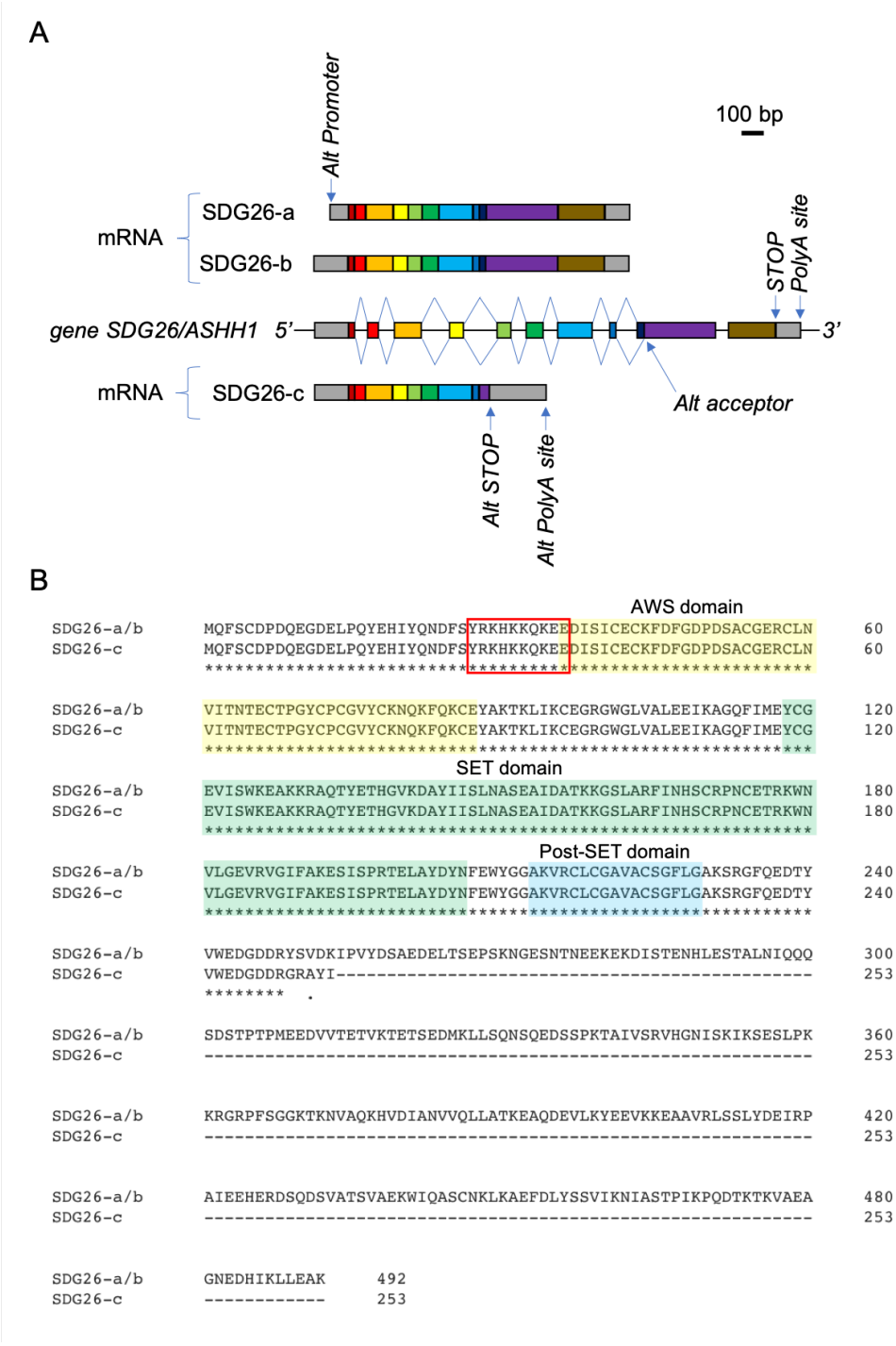

Figure 17: General features of the *SDG26/ASHH1* gene and protein. (A) The SDG26 gene and mRNA (named SDG26-a to c) are presented with exon as colored boxes, 5' and 3' UTR as grey boxes and intron as black lines. The STOP codon (TGA) for mRNA SDG26-a and -b is indicated as well as the corresponding PolyA site. The alternative promoter sequence which cause the SDG26-a variant is indicated, as well as the alternative STOP codon and PolyA site of the SDG26-c variant. (**B)** Proteins corresponding to SDG26-a/b and SDG26-c were aligned using Clustal O (1.2.4). Domains classically found in SET-domain proteins are highlighted in yellow for the AWS domain, in green for the SET domain and in blue for the Post-SET domain. The putative Nuclear Localization Signal (NLS) is framed in red.

III.2.1.1. SDG26-a/b is the main transcript of the *SDG26* gene

RT-qPCR expression analysis was performed using primer pairs specific for the SDG26-a/b and SDG26-c isoforms using cDNA prepared by poly-T reverse transcription on total RNA extracted from different plant tissues and at different day-time points (Figure 18A and B). We observed *SDG26-a/b* being expressed higher in seedlings, roots, stem, rosette leaves, flower buds, mature flowers as well as siliques, and lower in cauline leaves. Compared to *SDG26-a/b*, approximately ten times less *SDG26-c* was expressed in all analyzed tissues (Figure 18C). Moreover, *SDG26-a/b* and *SDG26-c* transcript levels in seedlings were found stably expressed during the day (Figure 18D).

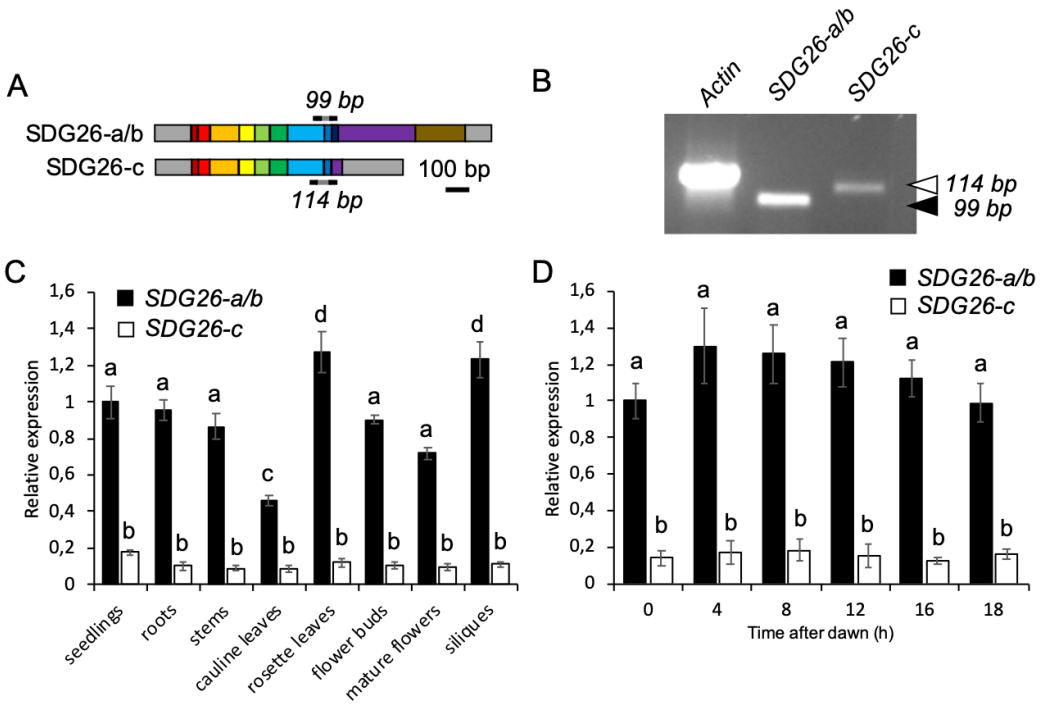

Figure 18: Expression analysis of the *SDG26* isoforms. (A) Primer pairs were designed to specifically quantify the two SDG26 transcripts we were interested in using a reverse primer spanning the junction between exon 8 and 9 for SDG26-a/b and a reverse primer spanning the junction between exon 8 and 10 for SDG26-c. (**B)** Primer pairs were validated by semi-quantitative RT-PCR based on the size of their respective product (99 bp for SDG26a/b and 114 bp for SDG26-c) and the presence of a single band. Real-time quantitative PCR (qPCR) analysis of SDG26 isoforms **(C)** in different tissues of Arabidopsis plants and **(D)** in 10-day-old seedlings grown under LDs (16h light/8 h dark). Transcript levels are expressed relative to the transcript level of SDG26-a/b in seedlings at time 0 h after dawn. Values are the means ±SD of three replicates. *Tip4.*1 and *Exp* were used for normalization. Letters indicate significant differences among sample in Student's *t*-test followed by Benjamini-Hochberg FDR correction ($P < 0.05$).

III.2.1.2. Cellular localization and function of the different SDG26 isoform proteins

To have a better idea of the cellular localization of the SDG26 proteins and because our anti-SDG26 monoclonal antibody can recognize only the protein resulting from the translation of the SDG26-a/b mRNA (either as a result of its high specificity or because the SDG26-c protein is under detection limit; Figure 19A), we generated two different constructs including C-terminal GFP-tagged SDG26-a/b or SDG26-c, all driven by the CaMV35S promoter, and they were named p35S-SDG26-a/b-GFP and p35S-SDG26-c-GFP, respectively.

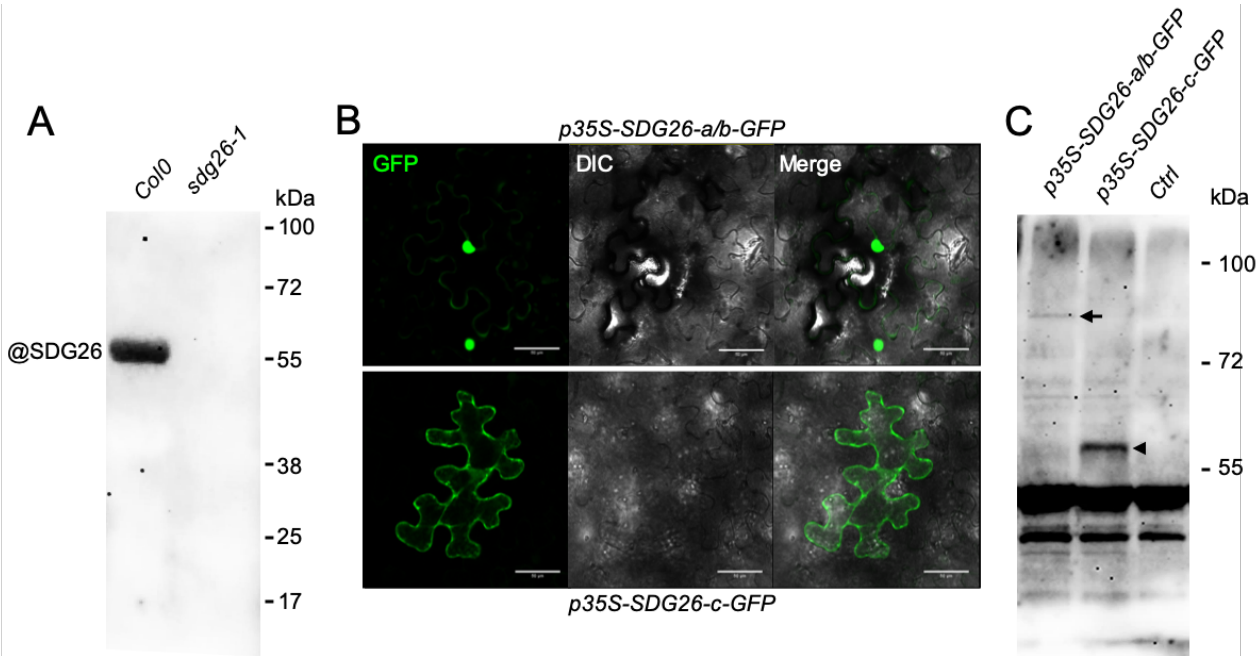

Figure 19: Transient expression of SDG26 protein in tobacco leaves. (A) Western blot analysis using an anti-SDG26 monoclonal antibody on total protein extracts from wild-type Col0 and *sdg26-1* detected SDG26-a/b in Col0 only. **(B)** Cellular localization of SDG26-a/b and SDG26-c fused to GFP and under the control of the 35S promoter transiently expressed in tobacco leaves. Representative images of GFP fluorescent and DIC are shown. Scale bar represents 50 µm. (**C)** Western blot analysis of leaves agroinfiltrated with the different SDG26 constructs compared to not agroinfiltrated one (Ctrl for control). The arrow indicates SDG26-a/b-GFP (82.3 kDa), and the arrow head SDG26-c-GFP (55.8 kDa).

When transiently and heterologously expressed in tobacco epidermal cells after agroinfiltration, SDG26-a/b was detected in the nucleus, while SDG26-c mainly associate with the plasma membrane (Figure 19B). However, SDG26-a/b and SDG26-c share the same putative NLS (Figure 17B) and online tools (NetNES and LocNES) have failed to

identify Nuclear Export Signals (NES). Therefore, the identified NLS is probably functional in SDG26-a/b, while the SDG26-c localization might be due to the conformational structure of this protein that prevents access of the NLS by the nuclear import machinery and/or the presence of a yet unknown motif for membrane association.

Next, constructs for both SDG26-a/b and SDG26-c were separately transformed into the *sdg26* mutant, in which none of the two SDG26 transcripts can be detected (Figure 20B). Transformed *sdg26* T1 progeny from T0 plants were Basta selected on soil and self-pollinated to produce T2 populations. Several T2 plants with 100% herbicide resistance in their progeny were selected and analyzed in detail as exemplified in Figure 20 for a T2 plant expressing C-terminal GFP-tagged either SDG26-a/b or SDG26-c driven by the CaMV35S promoter. As shown in Figure 20, T2 plants expressing *SDG26-a/b* almost entirely rescued the *sdg26* late-flowering phenotype. Nevertheless, for unknown reasons, the number of rosette leaves at bolting was reproducibly slightly higher than in the wild-type control (Figure 20C). The rescued flowering phenotype makes the *sdg26* transgenic plants indistinguishable from wild type plants.

It's known that *sdg26* exhibits a low *SOC1* expression and a high *FLC* expression, which nicely explains its late-flowering phenotype (Berr et al., 2015; Liu et al., 2016; Xu et al., 2008). We then tested in our transgenic lines the expression level of these genes. Further supporting the rescued flowering phenotype of T2 plants expressing *SDG26-a/b*, the expression level of *SOC1* was found back to wild-type level. However, the *FLC* expression was significantly higher than in the wild-type control but still lower than in *sdg26* (Figure 20D). The same was true with other independent T2 transgenic lines displaying higher *SDG26-a/b* expression than the one presented in Figure 20. Also, further confirming the localization observed in the heterologous system, SDG26-a/b-GFP predominantly was found in the nucleus, with a uniform distribution within the nucleoplasm but excluded from the nucleolus. Concerning SDG26-c, T2 transformants with different level of transgene expression were not able to rescue the *sdg26* late-flowering phenotype as exemplified in Figure 20 for one T2 line. Moreover, the SDG26-c-GFP protein was localized at the plasma membrane in Arabidopsis *sdg26* transgenic plants (Figure 20E), which is consistent with the results obtained in transient transformation assay in tobacco epidermal cells (Figure 19B).

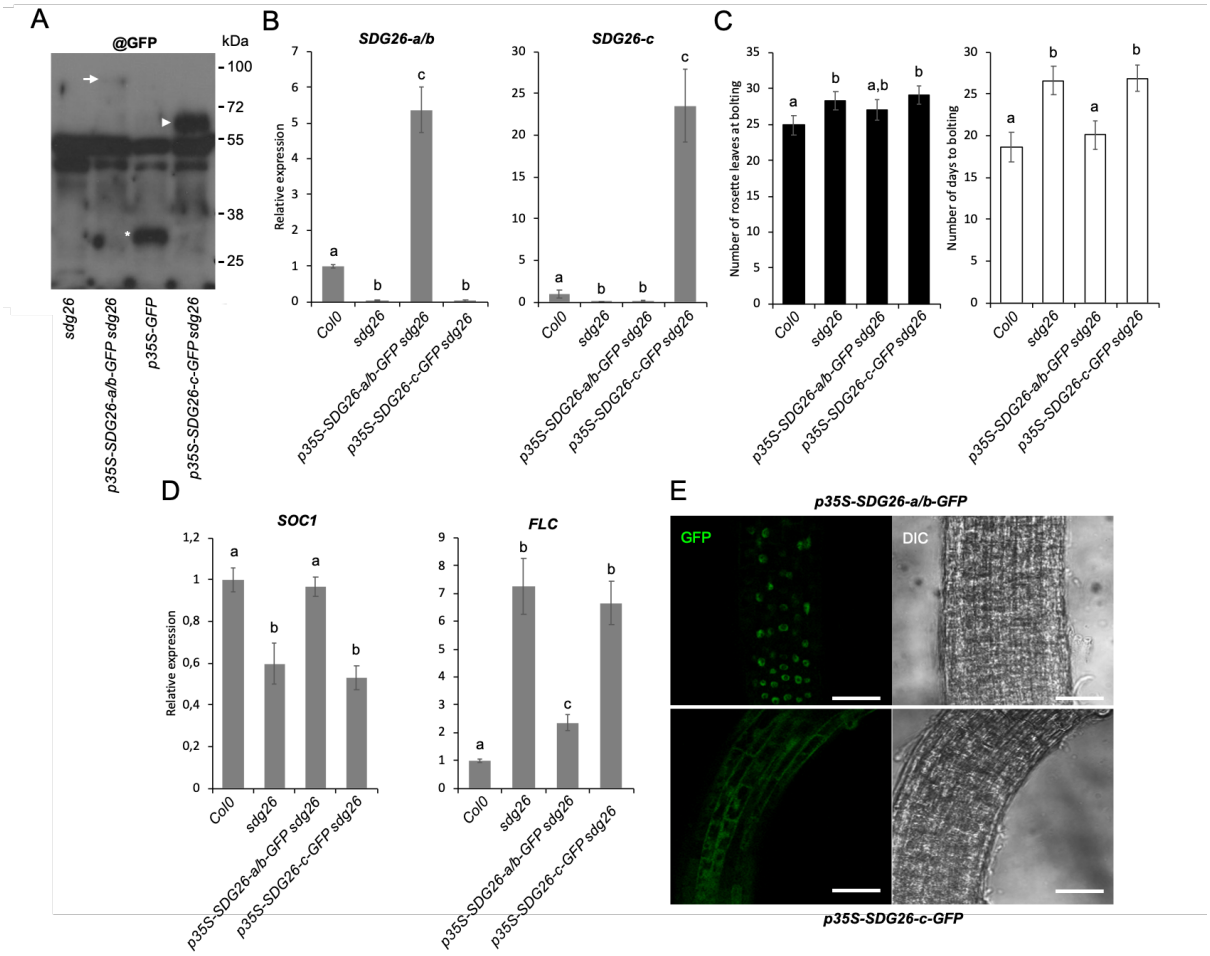

Figure 20: Analyses of two representative T2 plants expressing p35S-*SDG26-a/b-GFP* or p35S-*SDG26-c-GFP*. (A) Western blot analysis of stably expressed *GFP* fused *SDG26-a/b* and *SDG26-c* in *sdg26* transgenic plants detected with anti-GFP antibody on total protein extracts. Untransformed *sdg26* mutants and Col0 plants expressing *p35S-GFP* were used as control. The arrow indicates SDG26-a/b-GFP (83.3 kDa), the arrow head SDG26-c-GFP (55.8 kDa) and the asterisk GFP alone (28.7 kDa). **(B)** SDG26-a/b and SDG26-c transcript levels were quantified by qPCR and compared between transgenic plants, untransformed *sdg26* mutants and wild-type Col0 plants. (**C)** The complementation analysis was conducted in T2 plants by measuring flowering time under long days (LDs; 16 h light/8 h dark). Mean values are shown (± SD) based on two independent biological replicates with each replicate comprising over 20 plants for each genotype. (**D)** The complementation analysis was further conducted by quantifying transcript levels of flowering genes known to be affected in the *sdg26* mutant. Expression analyses in **(B)** and **(D)** were determined in 2-weeks-old plantlets grown under LDs. Mean values of at least three biological replicates (± SD) are presented relative to the Col0 level (set as 1) and were normalized using *EXP* and *TIP4.1* as internal control. (**E)** Cellular localizations of SDG26-a/b and SDG26-c fused to GFP in *sdg26* T2 transformants roots. Representative images of GFP fluorescent and DIC are shown. Scale bar represents 100 µm. Letters indicate significant differences among sample in Student's *t*-test followed by Benjamini-Hochberg FDR correction ($P < 0.05$).

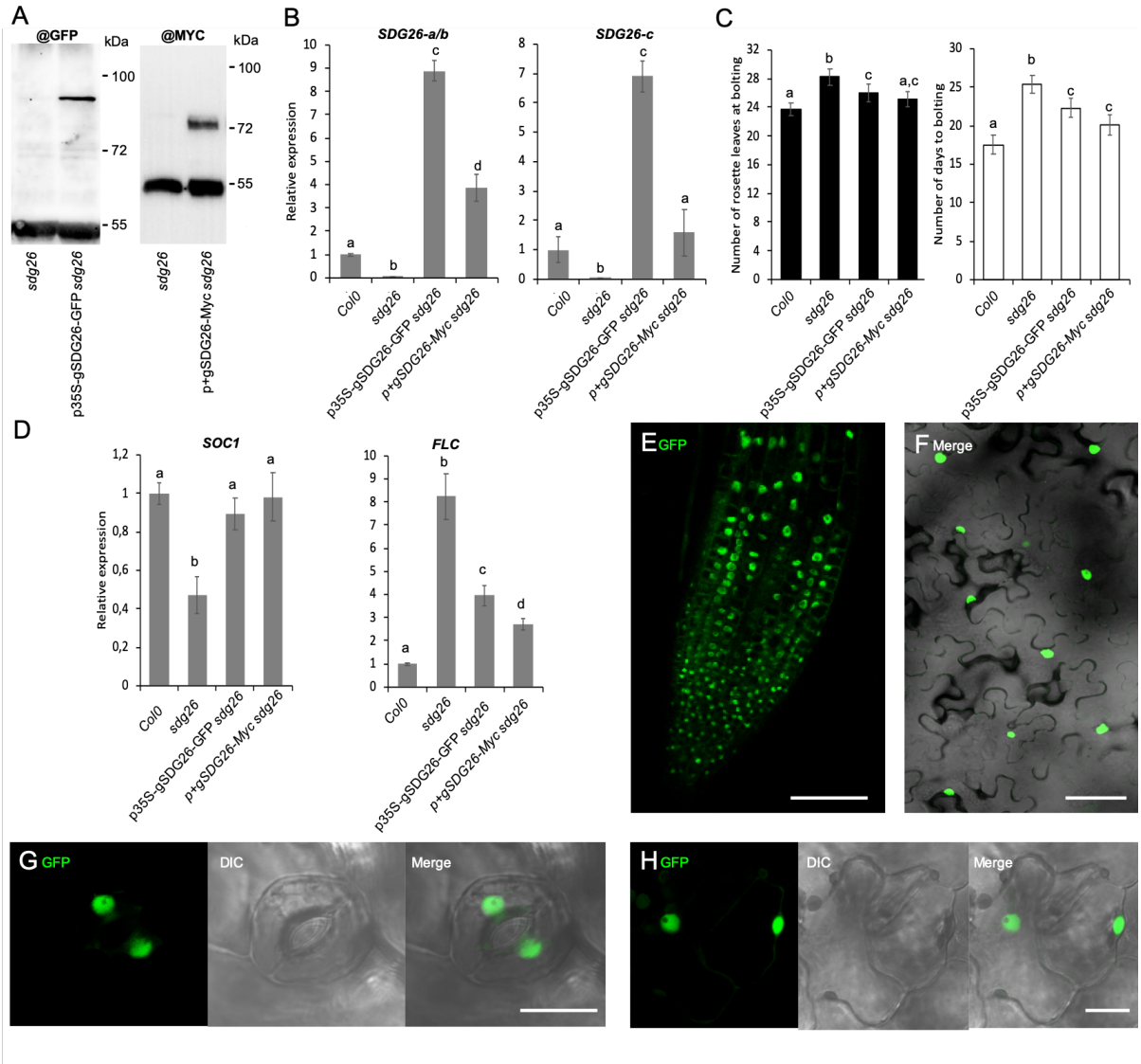

Figure 21: Analyses of *sdg26* transgenic plants expressing *p35S-gSDG26-GFP* or *p+gSDG26-Myc*. (A) The expression of each transgenic SDG26 protein was detected in indicated transgenic lines by western blot using either an anti-GFP or anti-c-Myc antibodies. the sdg26 mutant was used as a negative control. **(B)** The transcript level of each of the two detectable *SDG26* transcripts was quantified by qPCR in different transgenic lines and compared to their respective levels in wild-type Col0 and *sdg26* mutant plants. **(C)** Measures of flowering time, either as the number of rosette leaves or the number of days at bolting, of each transgenic line are presented as mean ± SD. **(D)** Transcript levels of flowering genes affected in *sdg26* were quantified in *sdg26* transgenic lines. Expression analyses in **(B)** and **(D)** were determined in 2-weeks-old plantlets grown under LDs and are presented relative to the Col0 level (set as 1) as mean ± SD of at least three biological replicates. *EXP* and *TIP4.1* were used as internal controls. for normalization Confocal images of transgenic root (**E**), transgenic leaves (**F**), transgenic stomata cells (**G**) and transgenic pavement cells (**H**). Scale bar represents 100 µm in (**E**) and (**F**) or 25 µm in (**G**) and (**H**). Letters indicate significant differences among sample in Student's *t*-test followed by Benjamini-Hochberg FDR correction ($P < 0.05$) ($P < 0.05$).

In addition to *sdg26* transgenic lines expressing cDNA constructs driven by the CaMV35S promoter, we created two other *sdg26* transgenic lines. One carries C-terminal

GFP-tagged the genomic sequence of the *SDG26* gene driven by the CaMV35S promoter (*p35S-gSDG26-GFP*) and the other one carries C-terminal 10xcMyc-tagged the genomic sequence of the *SDG26* gene driven by its native promoter (p+gSDG26-Myc). Based on the molecular weight of the protein detected using an anti-GFP or an anti-Myc antibody and considering the molecular weight of each of the two tags (28.7 kDa for GFP and 12 kDa for 10xcMyc), a single fused protein corresponding to the translation of the SDG26-a/b transcript with tag was detected (Figure 21A). Moreover, like for *sdg26* lines transformed with cDNA constructs, we analyzed T2 plants for their flowering phenotype and the expression of the transgene (Figure 21B, C and D). As T2 plants carrying SDG26-a/b, the ones carrying genomic constructs similarly rescued the sdg26 late-flowering phenotype. Also, the expression level of *SOC1* and *FLC* in T2 plants carrying genomic constructs was found changed like the ones carrying *SDG26-a/b*.

Regarding the localization of the fusion protein, as for transgenic lines expressing only SDG26-a/b, we observed an exclusively nuclear signal in lines expressing genomic constructs (Figure 21E, F, G and H). All these results together with the single protein detected in wild-type Col0 using the monoclonal SDG26 antibody (Figure 19A) suggest that the SDG26-c transcript is most likely not translated in the native *SDG26* or tag-fused genomic *SDG26*.

III.2.1.3. Tissue-specific expression pattern of *SDG26*

RT-PCR analysis demonstrated that *SDG26* is expressed ubiquitously but at varied levels in different organs of Arabidopsis plants (Figure 18C). Using *in situ* hybridization, we investigated in detail the tissue-specific expression pattern of *SDG26*. A pGEM-T Easy plasmid containing a 214 bp fragment including part of the 3′-end and the 3’-untranslated region (UTR) of the SDG26-a/b transcript was used to prepare sense (negative control) and antisense probes. *In situ* hybridization showed that *SDG26-a/b* transcripts are more abundant in young and actively dividing tissues, with hybridization signals (dark brown areas) detected at shoot and floral apical meristem, young embryo, pollen and ovule primordia with a non-uniform distribution in clusters of cells (Figure 22).

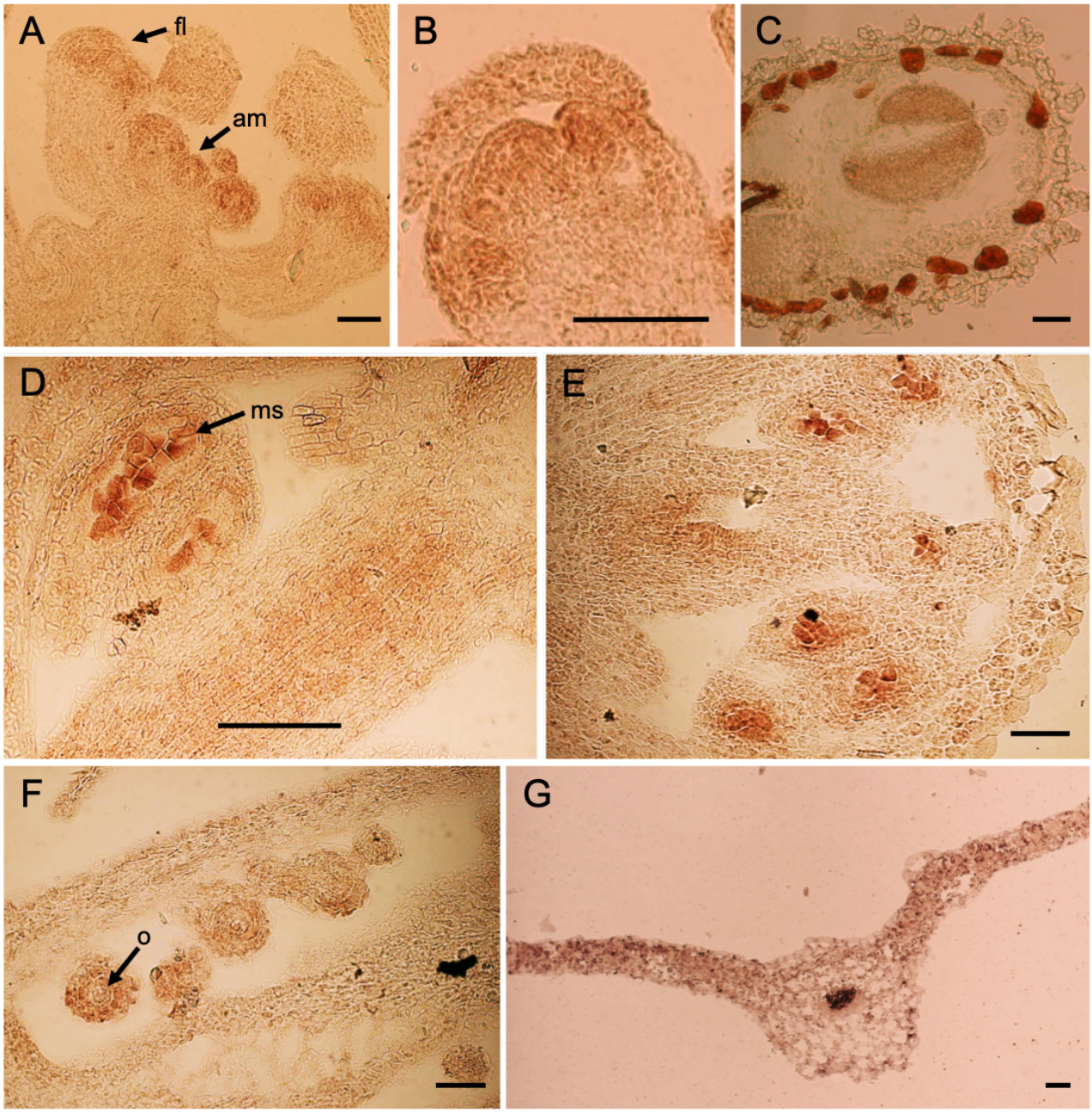

Figure 22: *In situ* hybridization analysis of *SDG26* expression. (A) Longitudinal section through a floral apex with (fl) for flower primordia and (am) for apical meristem. **(B)** Longitudinal section through a vegetative apex with the Shoot Apical Meristem (SAM) in the center. **(C)** Longitudinal section through an embryo at mid-torpedo stage. **(D)** and **(E)** Longitudinal section of anthers at stage 9 with (ms) for microspore. **(F)** Longitudinal section of gynoecium with (o) for ovule. **(G)** Transverse section of a leaf dissected from a 15-day-old seedling with at the center the mid-vein. Bars = 100 µm.

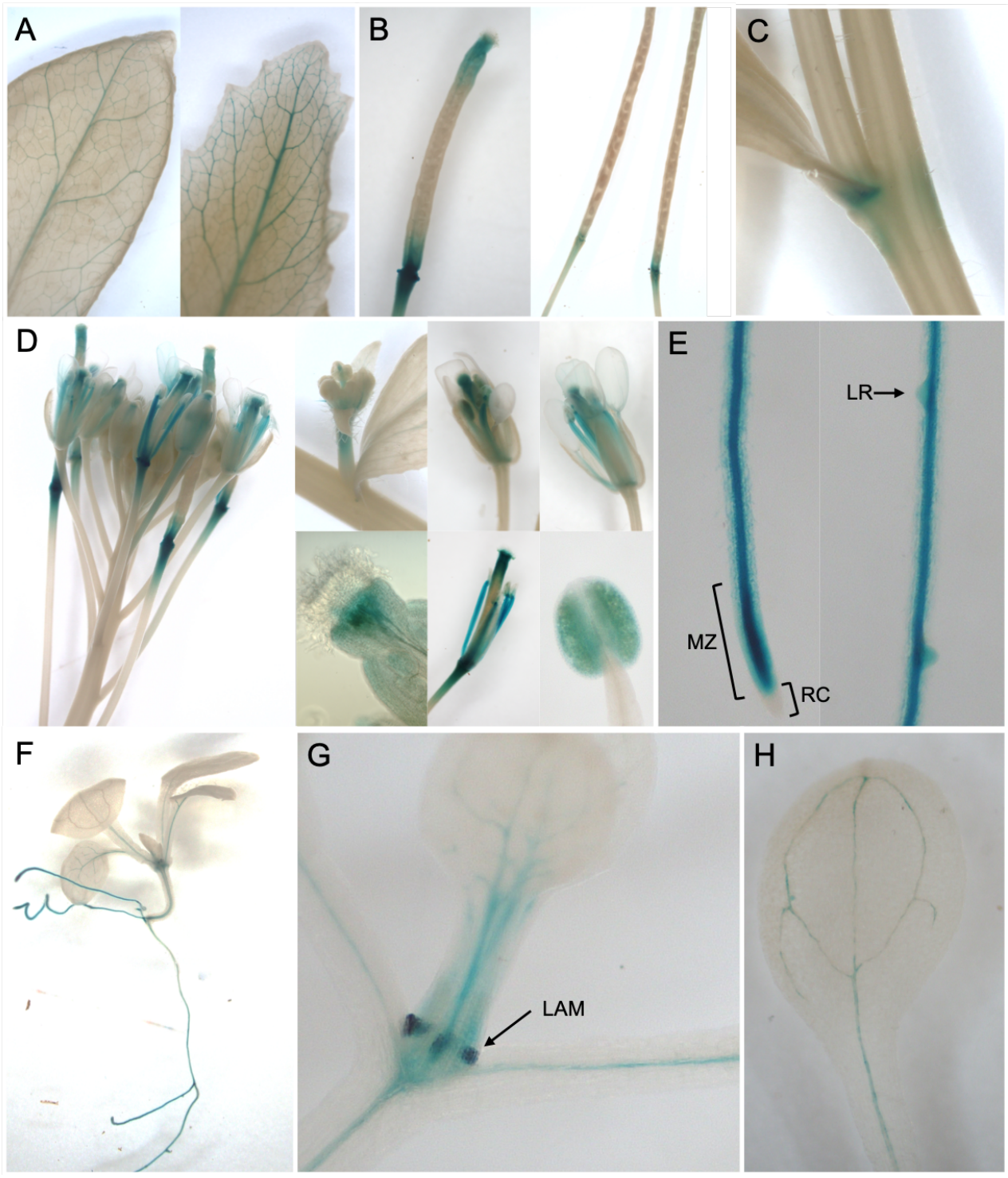

Figure 23: GUS staining in transgenic Arabidopsis plants harboring the pSDG26-GUS construct. (A) Mature (left) and cauline (right) leaves from 6-week-old plants. **(B)** Siliques at different developmental stages, 3 to 4 Days Post Anthesis (DPA; left) and 9 to 11 DPA. **(C)** Base of shoot branches and cauline leaf petiole. **(D)** Total inflorescence and different flower details, from young flower buds (top left), young flower (top middle), open flower (top right), stigma after pollination (bottom left), young silique (bottom middle) and anther (bottom right). **(E)** Root tip with the root cap (RC) and the meristematic zone (MZ; left) and maturation zone with emerging lateral root (LR; right). **(F)** 15-day-old seedling. **(G)** Closeup of the lateral leaf axillary meristem (LAM) of a 10-day-old seedling. **(H)** Cotyledon of a 10-day-old seedling.

Next, we visualized the expression patterns of *SDG26* by using transgenic plants, expressing a *GUS* reporter gene driven by the *SDG26* 1772 bp promoter (pSDG26-GUS). The T2 progeny from six independent homozygous primary transformants was examined for *GUS* expression by histochemical staining. All transgenic lines display a roughly similar expression pattern, and here we show the data from one representative line. GUS staining of plant organs at several developmental stages revealed that the *SDG26* promoter was active in a wide range of plant organs (Figure 23). In adult plants, GUS staining was detected in leaf tissues (*i.e.* in primary, secondary, and tertiary veins; Figure 23A), and in inflorescence and siliques, more especially in cells at organ-stem junctions like at boundaries between peduncle-silique (Figure 23B), stem-petiole (Figure 23C) and peduncle-flower (Figure 23D). At the root, we never detected the GUS activity at the root cap but very strong in the vascular system, pericycle and endodermis at the meristematic zone and in the center of the base region of emergent lateral root primordia (Figure 23E). In seedlings, we also detected GUS activity in the root, leaf and cotyledon vasculatures (Figure 23F and H), as well as at the leaf axillary meristem (Figure 23G). Finally, because SDG26 ubiquitously expressed in both aerial and root part, especially in vascular tissues, we addressed the question of the long-range movement of its protein. Wild-type scions fused onto *sdg26* rootstocks presented a Col0-like flowering phenotype, while *sdg26* scions fused on Col0 rootstocks presented an *sdg26*-like flowering phenotype (Figure 24A). Also, we did not observe fluorescence in *sdg26* scion grafted on transgenic rootstock expressing a GFP tagged version of SDG26 and vice versa (Figure 24B). Therefore, grafting experiments suggested that SDG26 is not capable of long-range movement. Interestingly, *SDG26* GUS staining and *in situ* hybridization present some similarities (*i.e.* at the abscission zone or meristems) with data obtained with *SDG8* (Berr et al., 2010) and *ATX1* (Saleh et al., 2007). These similarities may reflect common functions between these histone methyltransferases, especially because a binding between these proteins was previously detected using a yeast two-hybrid assay (Valencia-Morales et al., 2012).

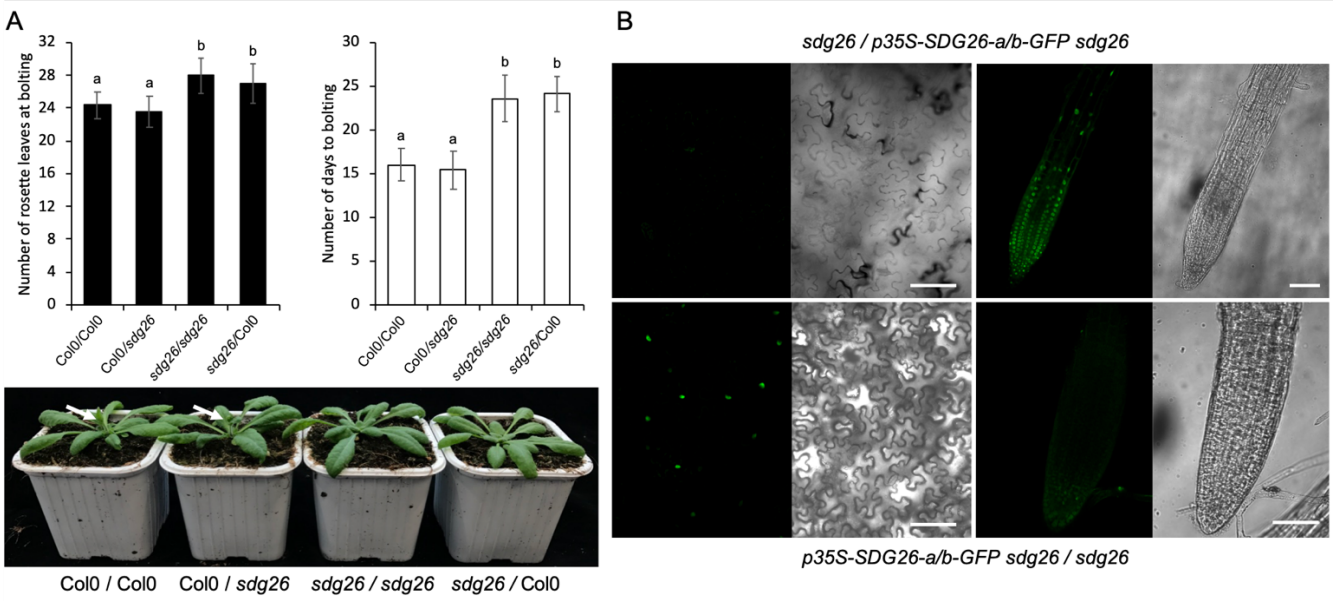

Figure 24: Analyses of the SDG26 protein mobility by different grafting combinations on *sdg26* mutant plants. (A) The flowering phenotypes of Col0 scions grafted on *sdg26* rootstocks (Col0 / *sdg26*) and *vice versa* (*sdg26* / Col0) were compared to Col0 scions grafted on Col0 rootstock (Col0 / Col0) and *sdg26* scions grafted on *sdg26* rootstocks (*sdg26* / *sdg26*). Ten days after grafting, successfully grafted plants were transferred to soil and the flowering time was latter measured on at least 10 plants from each grafting combination grown under MDs. Representative plants of each of the four grafting combinations are presented with emerging inflorescence indicated with a white arrow. Mean (± SD) are presented and letters indicate significant differences among sample in Student's *t*-test followed by Benjamini-Hochberg FDR correction ($P < 0.05$). **(B)** Detection of SDG26-GFP fluorescent signals by confocal microscopy in leaf (left) or root (right) from *sdg26* scion grafted on *p35S-SDG26-a/b-GFP sdg26* transgenic rootstock (top) or *p35S-SDG26-a/b-GFP sdg26* scion grafted on *sdg26* rootstock. Scale bar represents 100 µm.

III.2.2. *SDG26* expression is induced by abiotic stresses

Based on our *in-silico* analyses, *SDG26* could be involved in plant abiotic stress responses. We subsequently decided to test the inducibility of *SDG26* expression in response to different treatments. Abiotic stresses such as cold, drought, or salt treatments cause a slight but significant transient increase in the transcript level of *SDG26* (Figure 25A to C).

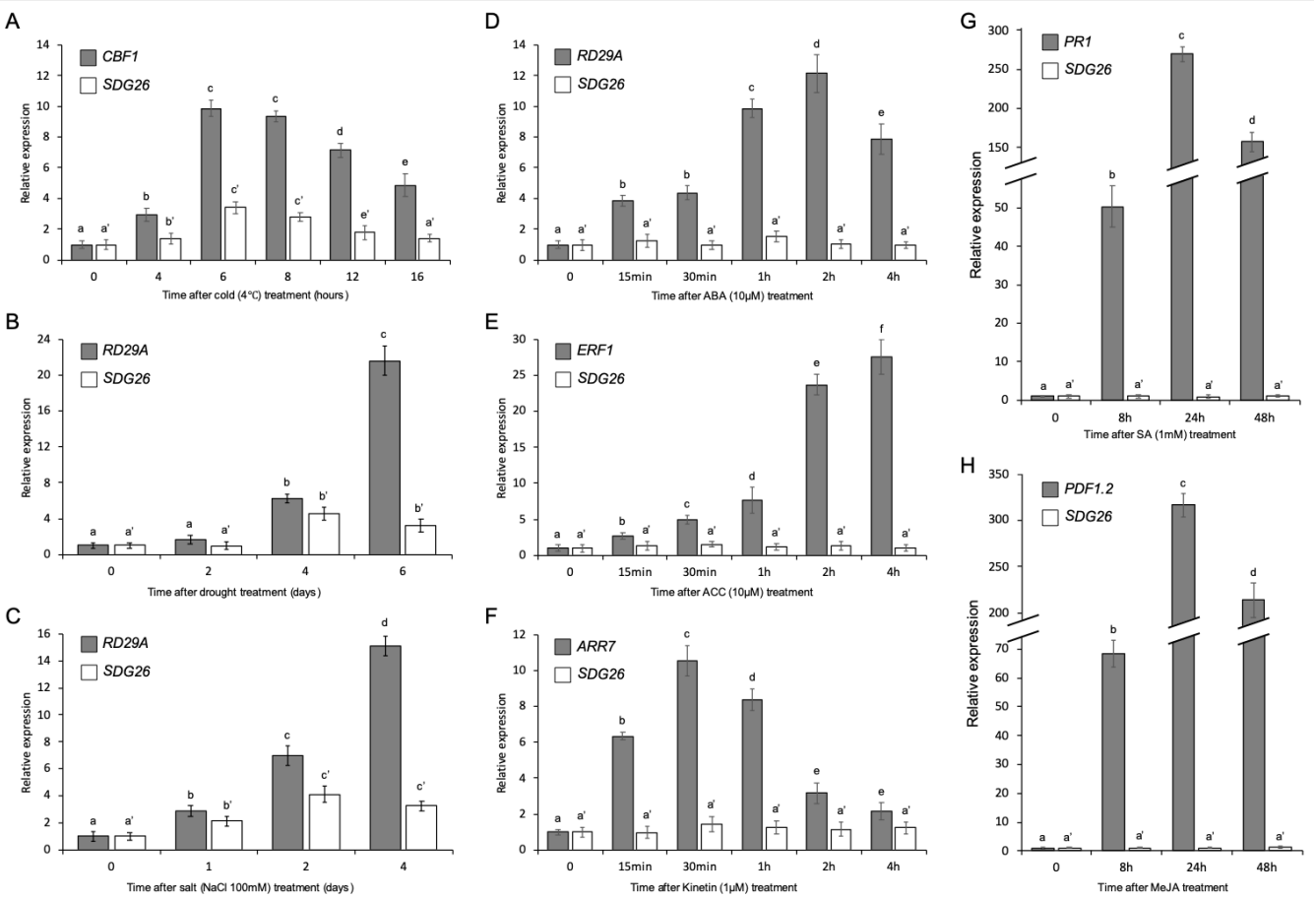

Figure 25: Analyses of the SDG26 expression during different abiotic stresses and in response to stress-related phytohormones. (A to H) The *SDG26* transcript (SDG26-a/b) level was quantified in 2-weeks-old plantlets Col0 plants grown at 21°C under LDs and transferred to 4°C (**A**), not watered (**B**), watered with a salt solution (**C**; NaCl 100mM) or treated with different stress-related-phytohormones (**D**) ABA, (**E**) ACC, (**F**) Kinetin, (**G**) SA or (**H**) MeJA. For each condition, a reference gene known to be transcriptionally induced was used as a control. The expression levels of each gene are presented relative to their level before treatment (set as 1) as mean ± SD of at least three biological replicates. *EXP* and *TIP4.1* were used as internal controls. Letters indicate significant differences among sample in Student's *t*-test followed by Benjamini-Hochberg FDR correction ($P < 0.05$). Not shown here, the level of the SDG26-c transcript was unchanged in all tested conditions.

While the response to abiotic stresses relies on various factors, phytohormones are considered as the essential endogenous substances for modulating physiological and molecular responses (for review see Wani et al., 2016). We next tested the induction of *SDG26* transcription in response to several signaling molecules known to be involved in the adaptive response of plants to abiotic stresses: abscisic acid (ABA), the ethylene precursor 1-aminocyclopropane-1-carboxylic acid (ACC), the synthetic cytokinin kinetin,

the volatile derivative of jasmonic acid methyl jasmonate (MeJA) and the phenolic compound salicylic acid (SA). Interestingly, while hormone application resulted in the strong induction of known responding genes (*e.g. RD29A* for ABA), the *SDG26* transcription was unchanged (Figure 25D to H). Taken together, *SDG26* appeared to be induced by stress but not by phytohormones, indicating that *SDG26* is probably not part of a particular hormone signaling pathway in plant defense response. Supporting the transcriptional induction of *SDG26* by different stresses, an increased GUS staining was observed after a cold treatment using the pSDG26-GUS transgenic lines above described (Figure 26A). In parallel to the increased transcription of *SDG26* detected upon stress exposure, we also observed a gradual increase of the SDG26 protein quantity (Figure 26B). Also, using our *sdg26* p35S-gSDG26-GFP transgenic line, we found that the cellular localization of SDG26 was unchanged in the stressed plants, with an exclusively nuclear localization signal (Figure 26C).

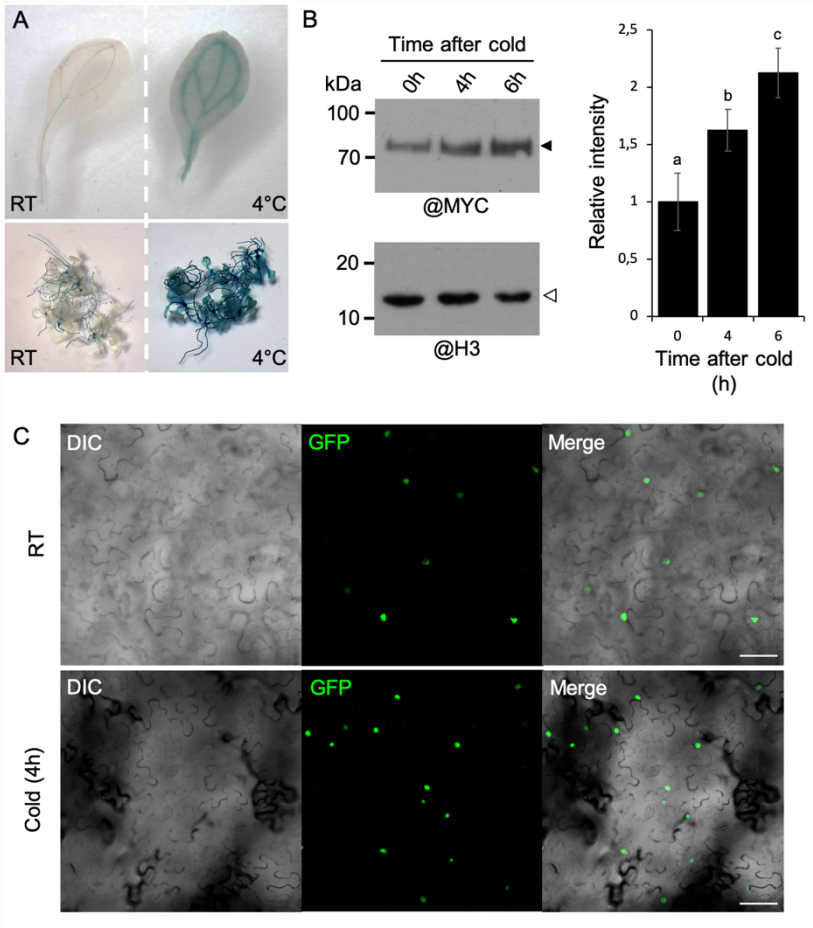

Figure 26: The SDG26 expression increases in response to cold. A) Two-weeks-old plantlets expressing a *GUS* reporter gene driven by the *SDG26* promoter (pSDG26-GUS) were exposed to a 4°C stress during 4h. Stressed and non-stressed (RT for Room Temperature) transgenic lines were similarly fixed in 80% acetone and stained at 37°C for 6h. **B)** The level of the SDG26-Myc transgenic protein was measured by Western blot in the *sdg26* transgenic line p+gSDG26-Myc above described before and after cold stress exposure using an anti-Myc antibody. Histone H3 was used as a loading control. Densitometry values ± SD were normalized to H3 and shown relative to time 0 (set as 1). Letters indicate significant differences among sample in Student's *t*-test followed by Benjamini-Hochberg FDR correction ($P < 0.05$). **C)** Using confocal microscopy, the nuclear localization of the florescent SDG26-GFP transgenic protein was compared between *sdg26* p35S-gSDG26-GFP transgenic lines grown at room temperature (RT = 21°C) and treated or not with a 4h cold stress at 4°C.

III.2.2.1. *SDG26* is involved in the regulation of cold-related genes

SOC1 was previously proposed to be involved in a crosstalk between flowering-time regulation and cold response (Seo et al., 2009). Because SDG26 binds *SOC1* chromatin and is required for H3K4me3 and H3K36me3 at this locus (Berr et al., 2015), we decided to examine the *SOC1* expression in wild-type plants (Col0) and *sdg26* during

a cold stress, as well as in *soc1* and in the double homozygous mutant *sdg26 soc1* obtained by crossing *sdg26* with *soc1* single mutants (Figure 27A). While in untreated plants *SOC1* was stably expressed, we observed a progressive increase of *SOC1* expression in Col0 and *sdg26* plants upon cold treatment. Interestingly, despite the basally lower *SOC1* expression level detected in *sdg26* at room temperature (RT), the induction of *SOC1* was weaker in cold treated *sdg26* compare to cold treated Col0 plants. Because FLC is a *SOC1* repressor, we also addressed its expression under cold stress. As shown in Figure 27A, *FLC* was stably high in *sdg26* and *sdg26 soc1* with or without cold treatment. Surprisingly and despite the *SOC1* increase observed upon cold stress, *FLC* was reproducibly slightly increased in Col0 and *soc1* cold-treated plants. Next, we addressed the level of some active chromatin marks at these two genes using chromatin immunoprecipitation coupled with q-PCR with gene-specific primers (Figure 27 B to D). In untreated plants, we observed both decreased H3K36me3 and H3K4me3 levels at *SOC1* chromatin in *sdg26* compared to Col0. Upon cold exposure, the level of H3K4me3 was increased in Col0 but also in *sdg26*, which correlate nicely with the transcriptional induction above described, while H3K36me3 was unchanged. In addition, using either our SDG26 monoclonal antibody in Col0 and *sdg26* chromatin extracts or an MYC antibody in chromatin extracts from non-transformed Col0 plants and our *p+gSDG26-Myc* transgenic line (Figure 27 E and F), we found an enrichment of SDG26 at *SOC1* chromatin that was unaffected by cold treatment. Together, SDG26 seems to act as a cofactor necessary for the induction of *SOC1* transcription in response to cold.

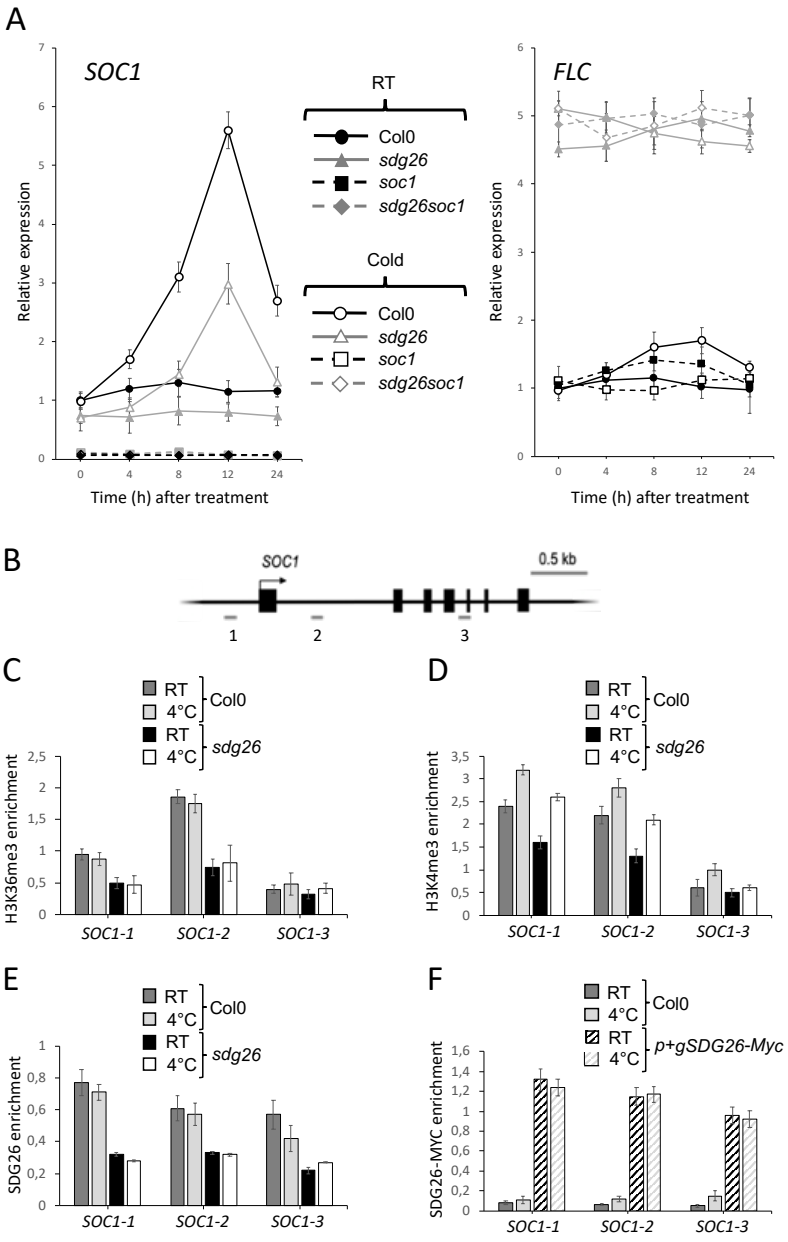

Figure 27: Expression and histone methylation levels of *SOC1* and *FLC* in response to cold stress. (A) The dynamic expression analyses were determined in 2-weeks-old plantlets grown on MS under LDs and treated (Cold) or not (RT for Room Temperature) with a cold stress at 4°C. Data are presented relative to the non-treated Col0 level (set as 1) as mean ± SD of at least three biological replicates. *EXP* and *TIP4.1* were used as internal controls for normalization **(B)** Schematic structure of *SOC1* represented as black boxes for exons and black lines for promoter and introns, with an arrow for the transcription start site. Amplified regions are indicated below by grey lines. **(C** and **D)** Levels of H3K36me3 and H3K4me3 along different regions of *SOC1* were measured by ChIP using 2-weeks-old plantlets grown on MS under MD photoperiod conditions and treated (Cold) or not (RT) with a cold stress at 4°C. **(E** and **F)** ChIP analysis of SDG26 enrichment at the *SOC1* loci using an anti-SDG26 monoclonal antibody or a transgenic *sdg26* line expressing SDG26-MYC and an anti-MYC antibody. Data are presented as the ratio of H3K36me3, H3K4me3, SDG26 and SDG26-MYC for each primer. Mean values ± SD are presented based on results from two biological replicates.

Previously, using a *SOC1* over-expressing line, SOC1 was shown as involved in the negative regulation of several cold response genes along the CBF-COR pathway, including *CBF1*, *CBF2*, and *CBF3* (for CRT/DRE binding factors) and their respective downstream cold-responsive (*COR*) gene-targets *RD29A*, *COR15A*, *KIN1* and *KIN2* (Seo et al., 2009). Because SDG26 regulates *SOC1* and is important for *SOC1* transcriptional induction upon cold stress, we next decided to analyze the expression of several cold response genes (Figure 28 and Supplementary Figure 3). *CBF1*, *CBF2* and *CBF3*, as well as CBF-target COR genes (*RD29A*, *COR15A*, *KIN1* and *KIN2*) were all upregulated in *soc1* compared to Col0 (Figure 28). Interestingly, we also observed that their basal transcript level was abnormally high in *soc1* under normal conditions (Supplementary Figure 3).

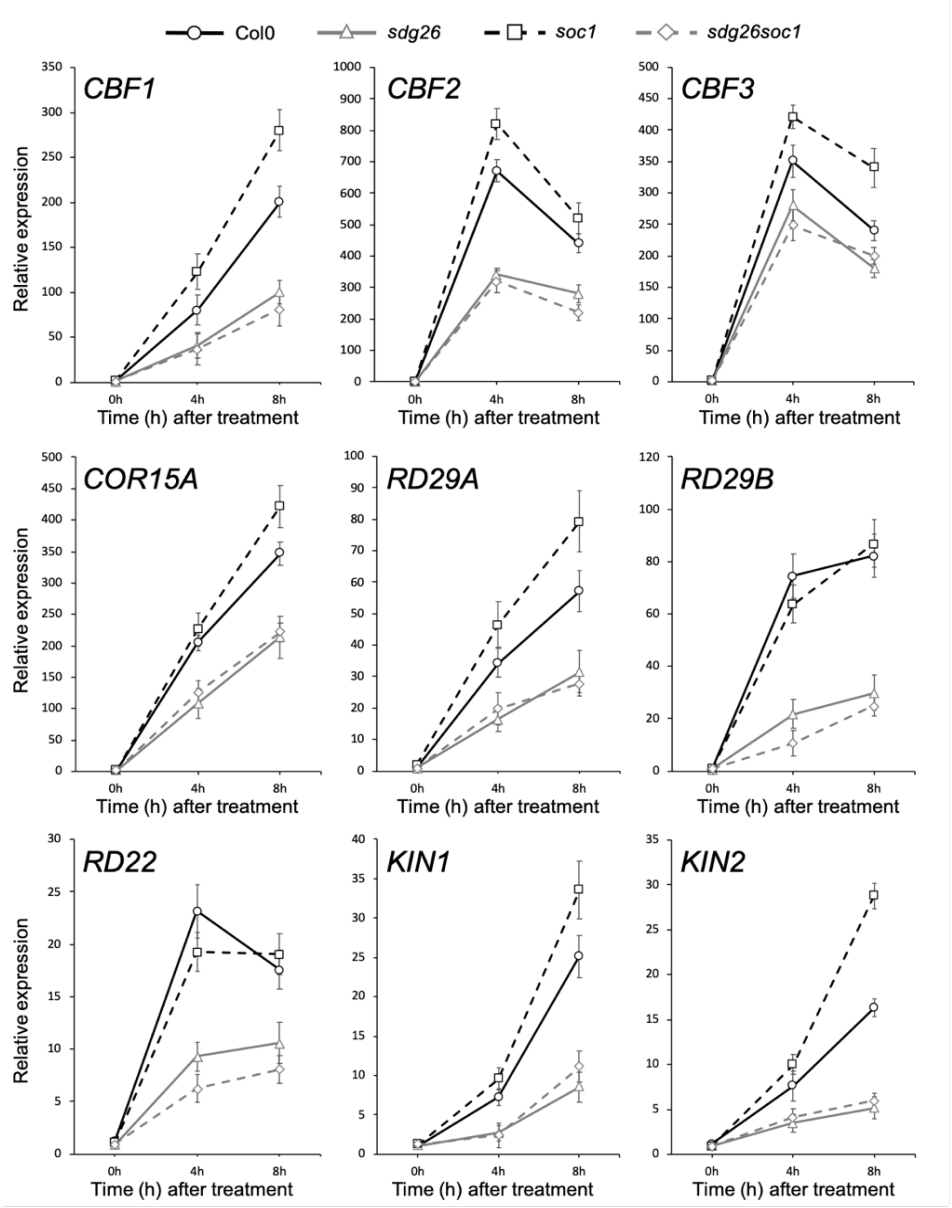

Figure 28: Expression analyses of cold-inducible genes in wild-type Col0, and *sdg26*, *soc1* and *sdg26 soc1* mutant plants in response to cold. The dynamic expression analyses were determined in 2-weeks-old plantlets grown on MS under LDs and treated with a cold stress at 4°C for 4 and 8 hours (h). Data are presented relative to the non-treated Col0 level at 0h (set as 1) as mean ± SD of at least three biological replicates. *EXP* and *TIP4.1* were used as internal controls for normalization.

Surprisingly, we found less induced *CBF1*, *CBF2* and *CBF3* in both *sdg26* single and *sdg26 soc1* double mutant plants upon cold exposure. This result indicates that the downregulation of *SOC1* detected in the *sdg26* mutant is not sufficient to provoke an increase in the transcription of CBF-COR pathway-related genes and suggests a direct

effect of SDG26 on these genes. Resulting from the less efficient transcriptional induction of *CBF* genes, *RD29A*, *COR15A*, *KIN1*, and *KIN2* accordingly appeared less induced in *sdg26* and *sdg26 soc1* than in Col0. Also, in contrast to genes along the CBF-COR pathway, the ABA-dependent but CBF independent genes *RD29B* and *RD22* were unchanged in *soc1*, while they were downregulated in *sdg26* and *sdg26 soc1* compared to Col0. Further supporting a direct role of SDG26 on the transcriptional regulation of *CBF* genes, our ChIP analysis revealed an enrichment of SDG26 at *CBF1*, *CBF2* and *CBF3* chromatin, which was further increased upon cold exposure (Figure 29A, B and C). Concomitantly, the level of H3K36me3 at *CBF1* chromatin was higher in Col0 plants compared to *sdg26* mutants. And this chromatin file was enhanced upon cold exposure (Figure 29D). Together, SDG26 seems to promote the efficient transcriptional induction of both *SOC1* and *CBF* genes upon cold-exposure. Considering the negative effect of SOC1 over *CBF* genes, SDG26 is thus regulating both the repressor and its targets.

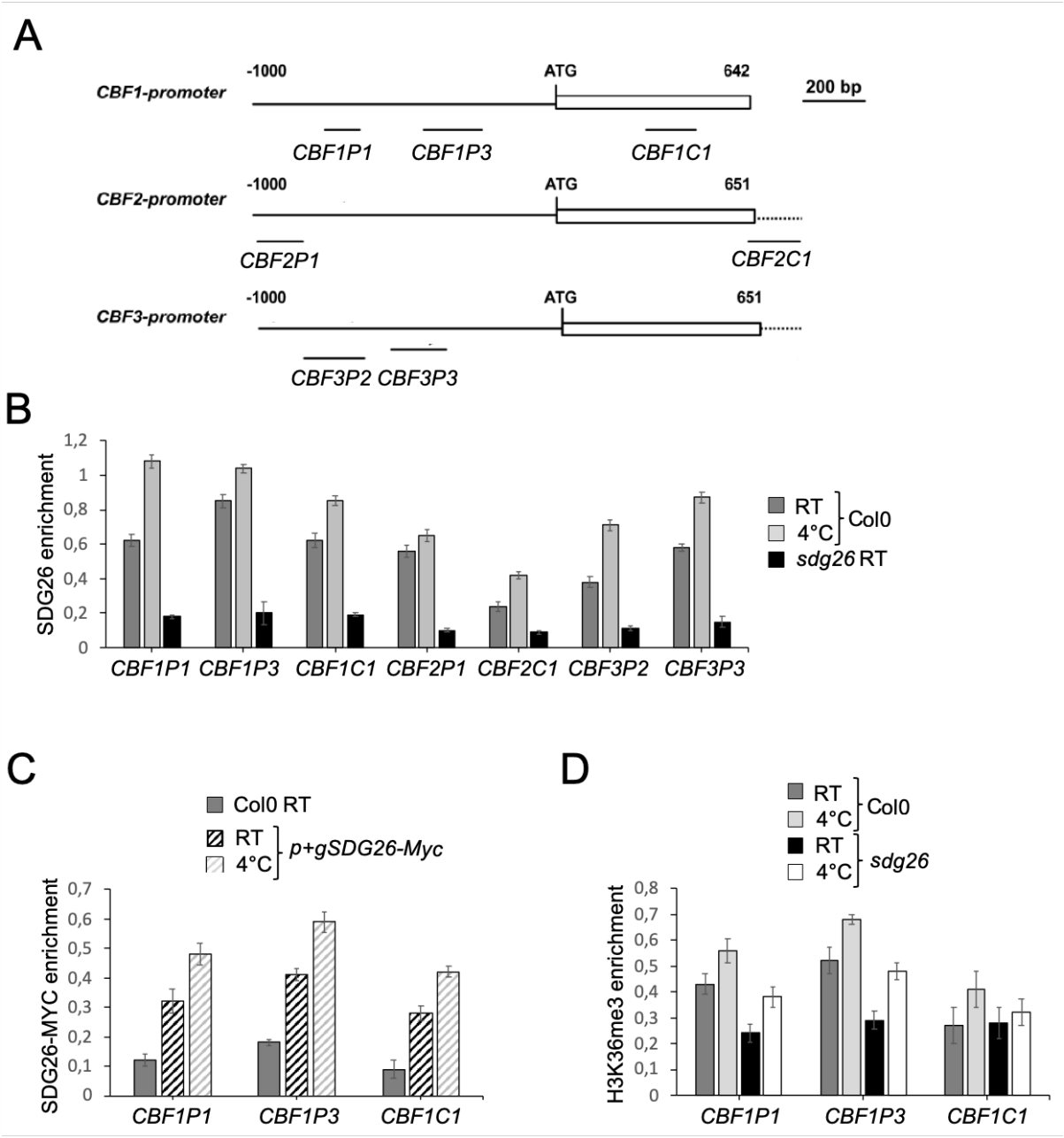

Figure 29: ChIP analyses of SDG26 enrichment and H3K36me3 at *CBF* genes. (A) Schematic diagrams adapted from Shi et al., 2012 showing the promoter structures of the *CBF1*, *CBF2* and *CBF3*. The 1.0-kb upstream regions and coding regions are shown, with the translational start site (ATG) at position +1. P1, P2, P3 and C1 present the fragments used in qChIP. **(B)** ChIP analysis of SDG26 enrichment at *CBF* genes using an anti-SDG26 monoclonal antibody. **(C)** ChIP analysis of SDG26 enrichment at *CBF1* using a transgenic sdg26 line expressing SDG26-MYC and an anti-MYC antibody. **(D)** The level of H3K36me3 along different regions of CBF1 was measured by ChIP using 2-weeks-old plantlets grown on MS under LDs and treated (Cold) or not (RT) with a cold stress at 4°C. Data are presented as the ratio of SDG26, SDG26-MYC and H3K36me3 / H3 for each primer. Mean values ± SD are presented based on results from two biological replicates.

III.2.2.2. *SDG26* is involved in ABA homeostasis

The ABA-dependent but CBF independent genes *RD29B* and *RD22* were downregulated in *sdg26* and *sdg26 soc1* compared to Col0. Hence, to address whether *sdg26* is defective in ABA biosynthesis, we measured ABA levels before and during cold stress. The phytohormone jasmonate (JA) involved in the regulation of cold stress response (Hu et al., 2017) was also quantified in our analysis.

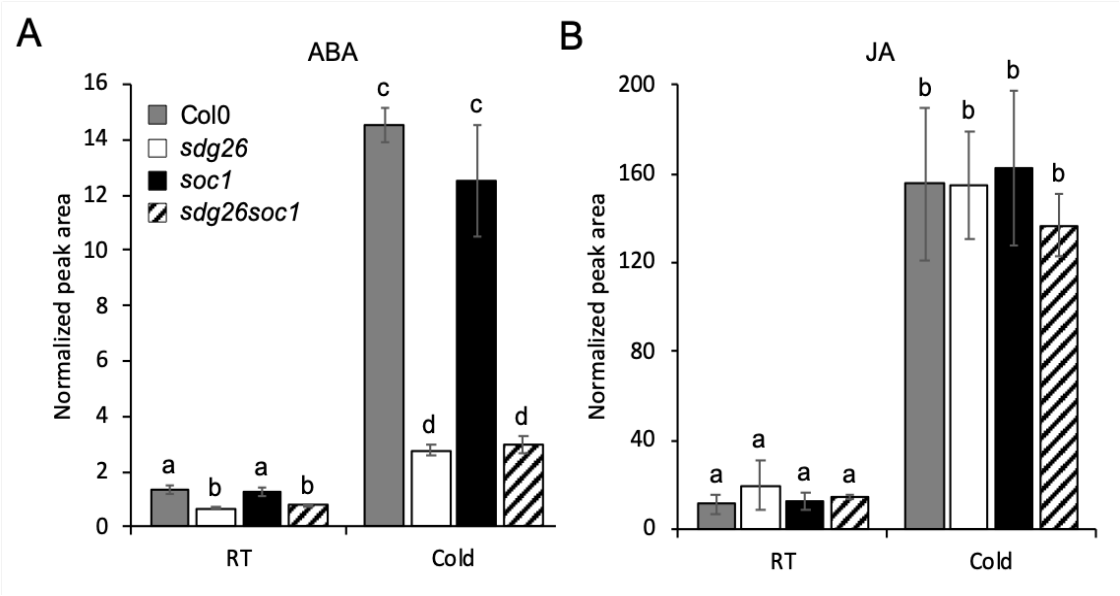

Figure 30: Endogenous levels of phytohormones related to cold stress in wild-type Col0, and *sdg26*, *soc1* and *sdg26 soc1* mutant plants in response to cold. The content of ABA (**A**) and JA (**B**) was determined using UHPLC-MS/MS on methanolic extracts prepared from 2-weeks-old wild-type Col0, *sdg26*, *soc1* and *sdg26 soc1* plants grown on MS under LDs and treated (Cold) or not (RT) with a cold stress at 4°C. Hormonal content is expressed as area of the peaks obtained by UHPLC-MS/MS analysis. Error bars represent SD. ABA, abscisic acid; SA, salicylic acid; JA, jasmonic acid. Letters indicate significant differences among sample in Student's *t*-test followed by Benjamini-Hochberg FDR correction ($P < 0.05$)

As depicted in Figure 30A, B and C, the content of ABA and JA was increased in wild-type Col0 plants under cold stress. Their levels were comparable between *soc1* and Col0 under normal conditions or upon cold stress exposure. In contrast, we detected a lower ABA level in *sdg26* and *sdg26 soc1* compared to Col0 both before and after stress (Figure 30), suggesting a less ABA abundance in *sdg26* plants. Moreover, this result nicely explained the low induction of *RD29B* and *RD22* detected in *sdg26* and *sdg26 soc1* mutants after cold treatment (Figure 29).

De novo synthesis and transport of ABA is of primary importance for increasing

ABA levels in response to abiotic stress, and several studies have led to the identification of genes involved in ABA biosynthesis and metabolism, as well as transport (Baron et al., 2012). Based on previously published microarray analysis searching for mis-regulated genes in *sdg26* (Liu et al., 2016), we identified several key genes involved in the regulation of ABA homeostasis in *Arabidopsis thaliana* (Figure 31A), of which the basal expression was either down- or up-regulated in the mutant. Using qRT-PCR, we further confirmed their basal mis-regulation and also found that other genes involved in the ABA metabolism and homeostasis were mis-regulated in *sdg26* (Figure 31B; only genes mis-regulated in *sdg26* are shown). In particular, biosynthetic genes (*ABA1*, *ABA4*, *NCED5*, *NCED6*, *ABA2* and *AAO3*) were down-regulated in *sdg26* further supporting the lower accumulation of ABA above described. As a response to the decreased ABA biosynthesis, we found the decreased transcript of the ABA exporter encoding gene *ABCG25* in *sdg26*. Also, we detected the up-regulation of the ABA importer encoding gene *ABCG40* and *AtBG1*, which encodes an ABA-specific β-glucosidase involved in the production of bioactive ABA from the inactive pool of glucose-conjugated ABA. As previously reported (Baron et al., 2012), indicating the importance of intracellular ABA homeostasis. Lastly, catabolic genes were also found induced under cold stress in Col0 plants. Among the four members of the CYP707A subfamily encoding ABA 8'-hydrolases playing a critical role for ABA degradation, *CYP707A3* and *CYP707A4* were found upregulated in *sdg26*, especially in non-stressed plants. Together, our results indicate that *SDG26* is involved in controlling ABA homeostasis through the transcriptional regulation of several key genes.

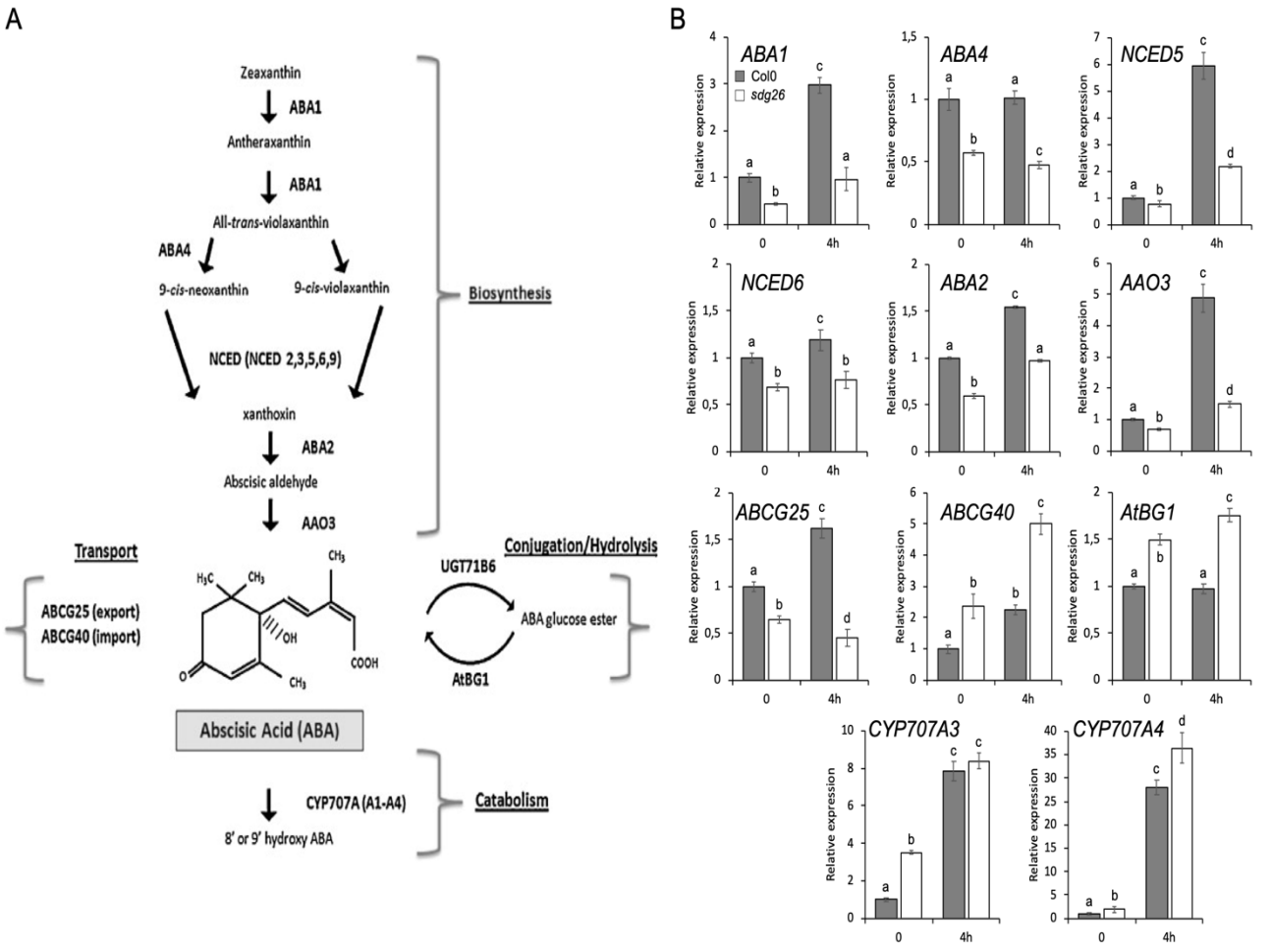

Figure 31: Expression analyses of key genes involved in regulation of ABA homeostasis in wild-type Col0 and *sdg26* plants in response to cold. A) Schematic representation of key genes involved in regulation of ABA homeostasis in *Arabidopsis thaliana* adapted from Baron et al., 2012. **B)** Expression analyses were determined in 2-weeks-old plantlets grown on MS under LDs before (0h) and during (4h) a cold stress at 4°C. Data are presented relative to Col0 level at 0h (set as 1) as mean ± SD of at least three biological replicates. *EXP* and *TIP4.1* were used as internal controls for normalization. Letters indicate significant differences among sample in Student's *t*-test followed by Benjamini-Hochberg FDR correction ($P < 0.05$)

III.2.2.2.1. *sdg26* is affected in several ABA related phenotypes

ABA is produced by plants under cold and drought stress conditions and plays a vital role in mediating plant adaptation to environmental stress (Cutler et al., 2010; Finkelstein et al., 2002; Xiong and Zhu, 2003). Next, we tested whether *sdg26* is affected in phenotypes related to ABA. Firstly, to test if SDG26 functions in modulating plant cold stress response, we performed electrolyte leakage analysis in leaves. Electrolyte leakage

analysis is a standard test to understand the response of plants to cold stress and Arabidopsis plants with increased cold resistance typically show resistance to electrolyte leakage (Uemura and Joseph, 1995). The comparative analyses of electrolyte leakage in wild-type Col0, *sdg26*, *soc1* and *sdg26 soc1* show distinct response patterns (Figure 32A). Electrolyte leakage was increased rapidly in wild-type plants during exposure to stress. Consistent with its known cold resistance (Seo et al., 2009), *soc1* appeared less susceptible to ion leakage. Surprisingly, despite the lower induction of cold stress-related genes and the decreased accumulation of ABA in response to cold, *sdg26* showed the same response as *soc1*, with less ion leakage at 4°C suggesting an enhanced tolerance to cold stress (Figure 32A). Moreover, the double mutant *sdg26 soc1* presented a similar profile as the individual single mutant.

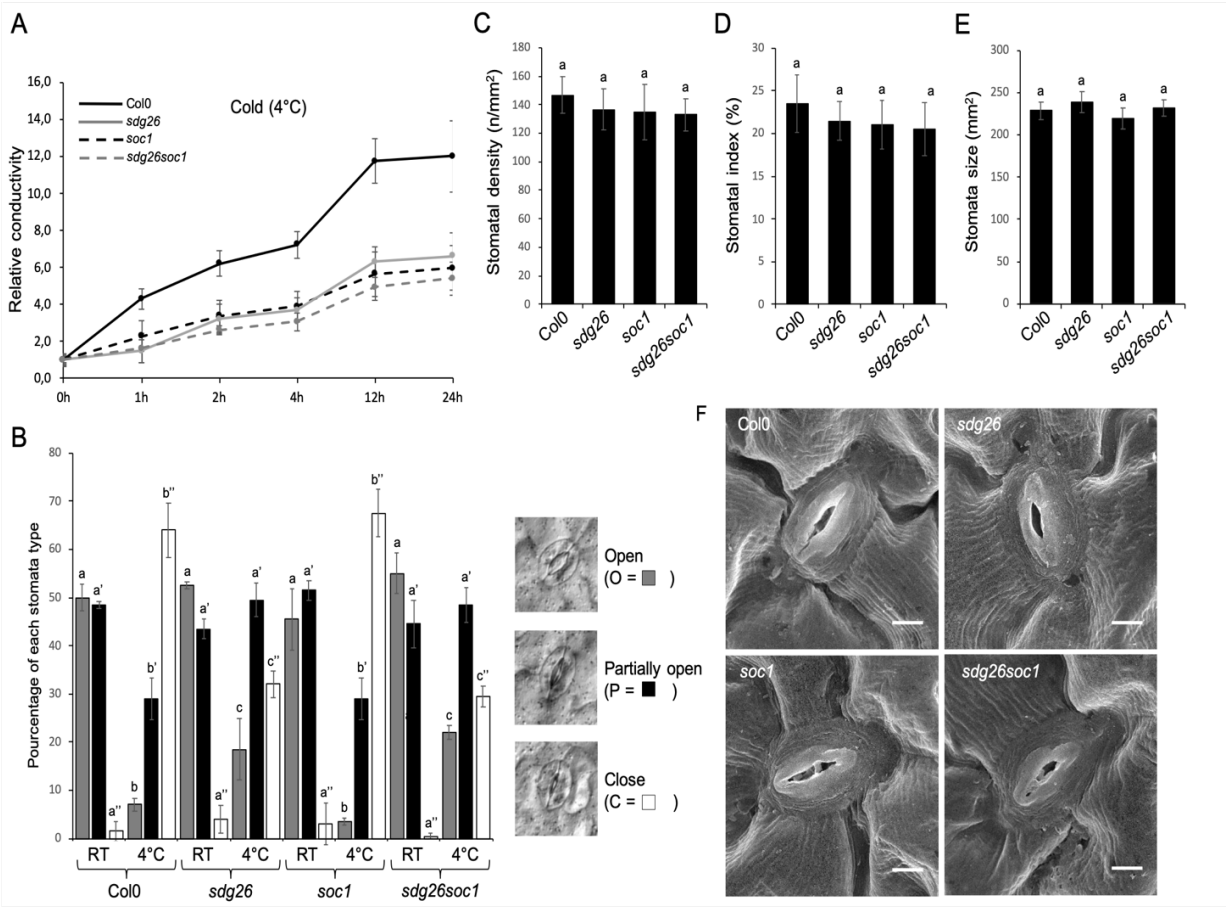

Figure 32: Electrolyte leakage and stomatal characteristics in wild-type Col0 plants and *sdg26*, *soc1* and *sdg26 soc1* mutants. A) Electrolyte leakage was assessed on at least 10 leaves from two-week-old plants during chilling treatment at 4°C. This experiment was repeated three time with similar results. **B)** Stomatal closure was estimated by counting the number of stomata falling into each of the three categories (Open, Partially open and Close) before (RT) and during a chilling treatment at 4°C. This experiment was repeated twice with similar results. **C)** to **E)** Stomatal density (the number of stomata per area), stomatal index (the number of stomata per total epidermal cells), stomata size was analyzed in the leaf abaxial

epidermal layers from wild-type Col0 and *sdg26*, *soc1* and *sdg26 soc1* mutant plants grown on MS under LDs. Data are the mean ± SEM of 2 leaves from at least five individual plants. **F)** Representative scanning electron microscopy images of stomata from wild-type Col0 and *sdg26*, *soc1* and *sdg26 soc1* mutant plants grown on MS under LDs. Bars = 5 µm. Letters indicate significant differences among sample in Student's *t*-test followed by Benjamini-Hochberg FDR correction ($P < 0.05$)

Chilling temperatures (0~10°C) also led to stomatal closure in many cold-tolerant plants such as Arabidopsis, thus limiting leaf dehydration when the water supply from the roots is restricted at low temperature (Allen, 2000; Rohde et al., 2004). We subsequently explored stomatal characteristics in our mutants upon cold stress exposure (Figure 32B). Despite the positive effect of *SOC1* on the light-induced stomatal opening previously reported (Kimura et al., 2015), we were not able to detect any significant difference between Col0 and *soc1* plants grown at 21°C under normal conditions (RT; Figure 32B). Also, while proportions of each of the three stomata categories were roughly similar between Col0, *sdg26*, *soc1* and *sdg26 soc1* at room temperature (RT), we observed a significant decrease in the proportion of "Close" and "Partially close" stomata in favor of "Open" ones in *sdg26* and *sdg26 soc1* upon cold stress treatment. Besides this, we did not observe significant differences between Col0 and our single and double mutants regarding stomatal characteristics (Figure 32C to F). These results suggest that the *sdg26* mutant shows reduced cold-induced stomatal closing without affecting stomatal morphology and development.

Furthermore, soil-grown 2-weeks-old plants were subjected to water deficit, and it was found that *sdg26* as well as *sdg26 soc1* mutants appeared more sensitive than wild-type Col0 or *soc1* mutant plants (Figure 33A). Because all plants were grown in the same conditions, they were exposed to similar water withdrawal, our results thus suggest that *sdg26* and *sdg26 soc1* are more sensitive to soil water deficit, probably because of a faster rate of transpiration. To test this hypothesis, we measured the rate of water loss from detached leaves and found that indeed, *sdg26* and *sdg26 soc1* leaves lost water at a faster rate than wild-type Col0 and *soc1* mutant plants (Figure 33B). Also, after ten days of water withdrawal and three days of re-watering, the number of surviving plants was below 20% for *sdg26* and *sdg26 soc1*, while it was around 80% for Col0 and *soc1* (Figure 33C). Altogether, because ABA plays an important role in inducing the cold stress response, in the process of stomatal closure and in drought resistance, the low ABA accumulation detected in *sdg26* and *sdg26 soc1* (Figure 30) could nicely explain the stress phenotypes

displayed by the mutants.

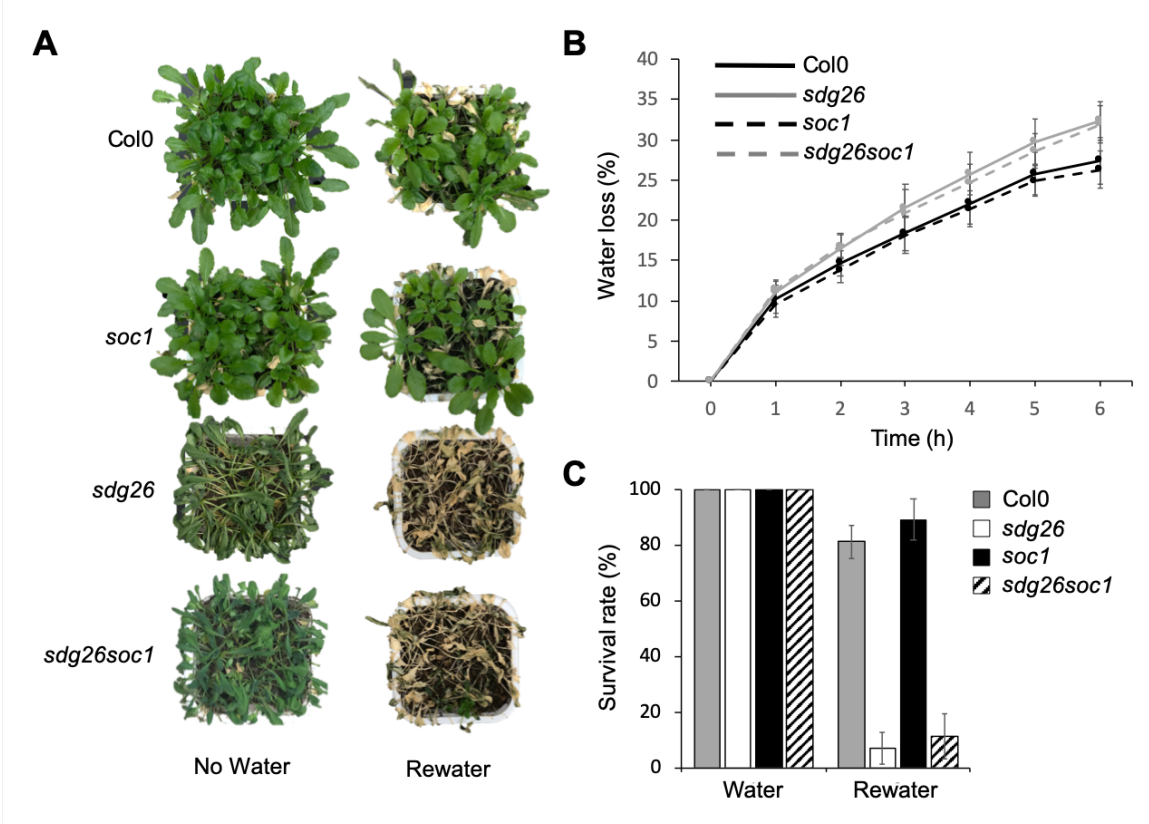

Figure 33: Tolerance of *sdg26* to a drought stress. A) Representative pictures of plants phenotype after a week without water are shown (No Water), as well as following a 3-day re-watering recovery period (Rewater). Wild-type Col0 and *sdg26*, *soc1* and *sdg26 soc1* mutant plants were soil-grown for 10 days under MDs and then subjected to a dehydration stress and latter rewatered. **B)** Water lost was measured every hour for 6h from 5 detached leaves of 3 plants of the indicated genotypes. Data are the mean ± SD. A representative experiment is shown and two other independent experiments have given similar results. **C)** The percentage of survival was measured for the indicated genotypes after 10 days without water followed by 3 days of re-watering. Data are the mean ± SD of 20 plants. Experiments were reproduced three times with similar results.

Cold induces the expression of many genes that are essential to enhance the tolerance of plants to freezing temperature. Lastly, we examined whether *sdg26* exhibits differences in freezing tolerance. The *soc1* mutant was used as a control since *SOC1* was reported to regulate not only flowering but also freezing tolerance (Seo et al., 2009). To address this question, we exposed the plants at -10°C for 2 hours and then transferred to 21°C for recovery (Figure 34). As expected, more *soc1* mutants survived the freezing

treatment compared to wild-type Col0 plants (Figure 34A). Remarkably, *sdg26* appeared to be at least as tolerant as *soc1* (Figure 34A). In contrast, *sdg8* showed less tolerant than wild-type plants to freezing (Figure 34B). Together, our results demonstrated that SDG26 regulates not only flowering but also freezing tolerance. Because the *SDG26* mutation impairs the induction of *CBF*s and *COR* genes while the *soc1* mutant behaves opposite, *SDG26* and *SOC1* might interfere with freezing tolerance through distinct mechanisms.

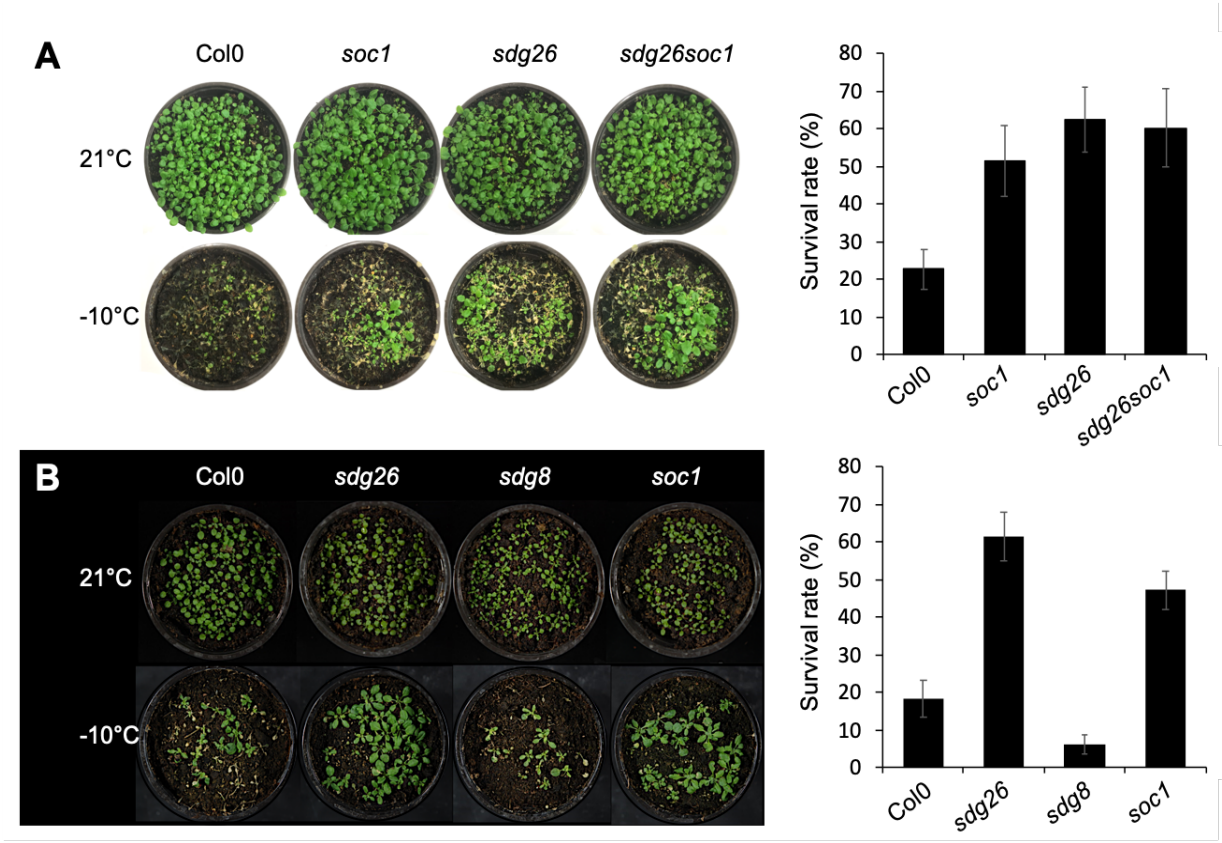

Figure 34: Tolerance of *sdg26* to freezing. (A) and **(B)** Representative pictures showing plants subjected to freezing tolerance assays. The percentage of plants that survived after freezing (survival rate) was calculated by counting the number of living plants before and after 2h at -10°C. Data are the mean ± SEM of three experiments.

III.3. Discussion

In this study, we provide a profound characterization of the *SDG26* gene and its involvement in response to abiotic stresses, with a particular focus on cold response. We identified two alternatively spliced mRNA transcribed from *SDG26* (SDG26-a/b and SDG26-c), which are both ubiquitously detected at a relatively stable rate during the day (Figure 17 and 18). Interestingly, using transgenic Arabidopsis lines, we demonstrated that the shorter transcript (*i.e.* SDG26-c) resulting from the use of an alternative 3′ splice site in exon 10 is most likely not translated, while the other is (Figure 19 and 20). Moreover, SDG26-a/b can complement the late-flowering phenotype of the *sdg26* mutant, while SDG26-c cannot (Figure 20). In addition, the transcription of SDG26-a/b was induced by different abiotic stress treatments, while the level of SDG26-c was unchanged (Figure 25). Together, the function of the SDG26-c alternative transcript remains as yet unknown. Currently, it is estimated that more than 60% of multi-exon plant genes produce alternatively spliced variants under different developmental or environmental conditions, with many alternatively spliced events resulting from the appearance of premature termination codons (Reddy et al., 2013). Some of these truncated mRNA molecules are subjected to non-sense-mediated mRNA decay (NMD), an RNA surveillance mechanism that subjects targeted transcripts for degradation during the first round of translation (Reddy et al., 2013). According to Aceview and because it presents a premature termination codon, SDG26-c was a predicted target of NMD. Interestingly, the vast majority of NMD-targeted transcripts are associated with response to pathogens (Rayson et al., 2012), and NMD represents a physiological gene regulatory mechanism contributing to plant innate immunity by controlling the threshold for activation of certain resistance pathways (Gloggnitzer et al., 2014). Because SDG26 (ASHH1) was found induced early following infection with *Pseudomonas syringae* (Lewis et al., 2015), it would be of interest to determine the function of both transcripts during pathogen infection.

Based on phylogenetic analyses, *SDG26* belong to the TrxG family, which regroup

12 SET domain proteins (Springer et al., 2003). Like other members of this TrxG family that have been analyzed so far, such as ATX1 to ATX5, SDG2, SDG25 or SDG8 (Berr et al., 2009, 2010; Chen et al., 2017; Puig et al., 2007; Zhao et al., 2005), SDG26 localized in the nuclei, which is in accordance with its presumed chromatin function (Figure 19, 20 and 21). Also, like other members of this TrxG family, *SDG26* is ubiquitously expressed in different organs of Arabidopsis plants (Figure 18). However, *in situ* hybridization showed that the *SDG26* transcript was more abundant in young tissues as well as in sporogenous/gametophytic cells in anthers and ovules (Figure 22). Interestingly, similar expression profiles were previously reported for *SDG8* and *SDG2* (Berr et al., 2010; Zhao et al., 2005). Using a promoter-GUS fusion approach, we observed more nuanced similarities between the expression patterns of TrxG family members. Indeed, like *ATX1* to *5* (Chen et al., 2017; Hayot et al., 2012; Saleh et al., 2007), an intense GUS staining was observed in vascular tissues with the *SDG26* promoter (Figure 23A and H), while such staining was absent when using the *SDG7* (Lee et al., 2015) or the *SDG8* promoters (Berr et al., 2010; Kim et al., 2005). Also, a strong GUS signal was detected in root tip for *ATX1*, *ATX2*, *SDG7*, *SDG8* and *SDG26* (Berr et al., 2010; Lee et al., 2015; Saleh et al., 2007; Figure 23E), but not with *ATX3* to *5* (Chen et al., 2017). Finally, GUS staining patterns in flowers were roughly similar between *ATX1* to *5*, *SDG8* and *SDG26* (Berr et al., 2010; Cazzonelli et al., 2009; Chen et al., 2017; Hayot et al., 2012; Saleh et al., 2007; Figure 23D). It is also interesting to point out that some specificities were also reported, with a GUS staining in hydathodes at the leaf margin for *SDG8* (Berr et al., 2010) or in trichomes for *ATX3* to *5* (Chen et al., 2017). These results indicated that Arabidopsis TrxG proteins exhibit few unique but many similar expression patterns, thus suggesting some functional redundancies. In line with this assumption, some protein interactions were reported to occur between TrxG proteins, such as between SDG26 and ATX1 or SDG26 and SDG8 (Valencia-Morales et al., 2012). Taken together, our expression analysis suggests that SDG26 may have, in connection or not with its function in flowering time regulation, additional roles that will require further exploration.

In this work, we demonstrated that *SDG26* is induced by different abiotic stresses (cold, drought and osmotic stresses), but not by stress-related phytohormones (ABA, ACC, Kinetin, SA and MeJA; Figure 25). Such differences in induction implicate that SDG26 may act upstream of phytohormone along the abiotic stress signaling pathway. This stress-induction was further confirmed at the protein level and also using a promoter-GUS fusion

approach (Figure 26). Interestingly, among the up-regulated 3237 probe sets (*i.e.* out of 61,251 probe sets) in winter/dormancy stems over summer/active-growth stems in *Populus trichocarpa* trees, the *SDG26* ortholog was found up-regulated more than thousand times (Ko et al., 2011). Together, these results suggest that the response to cold at the chromatin level might be a broadly conserved process in plants.

Additionally, the nuclear localization of SDG26 was found to be stable even after cold stress. Indeed, we were not able to detect any long-distance movement, as well as changes in cellular subcompartment localization upon stress treatment (Figure 24 and 26). Previously *SDG26* was proposed to regulate *SOC1* in the course of flowering time regulation (Berr et al., 2015; Liu et al., 2016) and *SOC1* was found to mediate crosstalk between cold sensing and flowering (Seo et al., 2009). In the model proposed by Seo et al (2009), *SOC1* expression is supposed to be repressed by cold stress. However, such repression was not experimentally tested so far. Here, we found that while *FLC* was stably expressed, cold stress resulted in the rapid induction of *SOC1* in wild-type Col0 plants (Figure 27A). In parallel, the loading of SDG26 and the level of H3K36me3 at *SOC1* chromatin were unchanged upon cold stress, while H3K4me3 was increased (Figure 27 B to F). In *sdg26*, we found *SOC1* less transcriptionally induced upon cold stress, which nicely correlates with the lower level of the two analyzed active histone marks detected at *SOC1* chromatin in the mutant (Figure 27 B, C and D). Together, our results suggested that SDG26 play a role in the induction of *SOC1* upon cold stress to promote flowering, thus enabling plants to complete their life cycles under stress condition rapidly.

ABA is an important stress hormone in plants, that has been demonstrated to be involved in the cold stress response (Shi and Yang, 2014). And, supporting our results, *SOC1* was very recently found to be induced by ABA through the activity of the ABA-responsive element (ABRE)-binding factors ABF3 and ABF4 (Hwang et al., 2019). Still based on the model proposed by Seo et al., (2009), *SOC1* was assumed to be a repressor of *CBF-COR* genes. Here, we found that despite the lower induction of *SOC1* observed in the *sdg26* mutant, *CBF-COR* genes were less induced upon cold treatment (Figure 28). In parallel, we demonstrated that SDG26 also bind some CBF genes and that this binding was enhanced upon cold stress (Figure 29). Similarly, as for *SOC1*, the level of H3K36me3 decreased in *sdg26* compared to wild-type Col0 plants. Because SOC1 directly binds to the promoters of *CBF* genes *in vivo* to repress their expression (Seo et

al., 2009), it would be interesting to test if SOC1 and SDG26 competitively bind these genes, possibly through similar cis-regulatory modules. Together, our results indicate that SDG26 is acting at the junction between flowering time regulation (*i.e.* through *SOC1*) and cold response (*i.e.* through *CBF-COR* genes). Such an astride positioning is not new for a histone methyltransferase since SDG8 and ATX1 were also involved in the regulation of flowering time and stress responses (Ramirez-Prado et al., 2018) and it may represent an advantage in controlling the precise balance between development and stress response to maximize chances of survival and/or progeny establishment.

Finally, because sdg26 mutant presented down-regulated ABA-dependent but CBF-independent genes, we tested the level of endogenous ABA and found it reduced in the mutant before and after stress treatment (Figure 30). In parallel, several genes encoding key enzymes involved in ABA homeostasis were found mis-regulated in *sdg26*, and typical ABA-related phenotype such as the stomatal aperture or the drought sensitivity were found also affected in the mutant (Figure 31 to 33). Among the down-regulated genes we detected in the *sdg26* mutant, ABA1 and ABA2 were proposed to promote flowering since their ABA-deficient mutants flowered later than control plants (Riboni et al., 2016). Therefore, the decisive role of ABA in accelerating flowering suggests that the late-flowering phenotype of *sdg26* might be partially due to its low endogenous ABA level. The functional link between ABA and SDG26 we described here may be relevant to future studies in other organisms, especially because ABA also promotes early flowering in rice (Du et al., 2018) and because the rice SDG26-homologue SDG708 is also involved in promoting plant flowering (Sui et al., 2013). A similarly impaired production of ABA was also reported for the histone methyltransferase mutant *atx1*, which also behaved a decreased drought tolerance and stomatal closure upon stress (Ding et al., 2011). However, despite its decreased level of ABA, *atx1* is known to flower earlier than wild type plants (Alvarez-Venegas et al., 2003). The discrepancy between *sdg26* and *atx1* regarding the ABA level and the flowering time may reflect the broader impact of the *ATX1* mutation on the whole genome expression compared to the *SDG26* one (Shafiq et al., 2014c). Also, while the subcellular localization of SDG26 was unchanged in response to stress (Figure 26), ATX1 shifts its localization from the nucleus to the cytoplasm (Alvarez-Venegas et al., 2006; Ndamukong et al., 2010). Together with the protein interaction detected between ATX1 and SDG26 (Valencia-Morales et al., 2012), a functional link may exist between these histone methyltransferases in regulating ABA homeostasis and abiotic stress

response, but it awaits future clarification.

In conclusion, our data show the importance of *SDG26* during the abiotic stress response. Other studies of mutants for histone methylation have also proven how histone methyltransferase can be considered as the central regulator of transcription under stress conditions (Berr et al., 2012; Bobadilla and Berr, 2016; Ramirez-Prado et al., 2018). However, research is still limited for correlating transcription and histone methylation at few responsive genes during stress, unfortunately, which is not exhaustive. Identifying essential histone methyltransferases together with genome-wide approaches are indispensable, especially to define whether histone methylations are a cause or a consequence of the transcriptional changes triggered by stress.

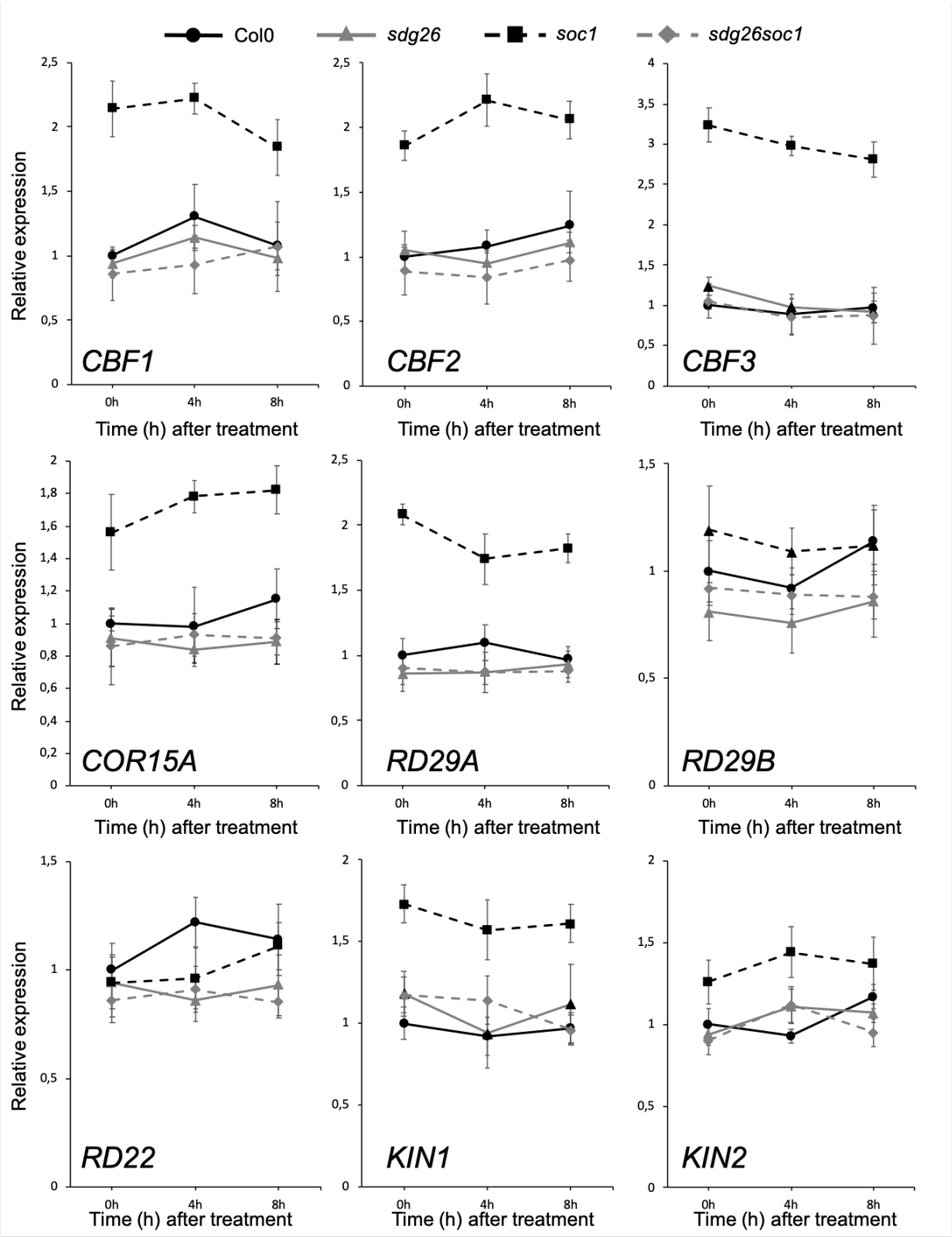

Supplementary Figure 3: Dynamic expression of cold-inducible genes in wild-type Col0, and *sdg26*, *soc1* and *sdg26 soc1* mutant plants under normal growth conditions. The dynamic expression analyses were determined in 2-weeks-old plantlets grown on MS under MDs. Data are presented relative to Col0 level at 0h (set as 1) as mean ± SD of at least three biological replicates. *EXP* and *TIP4.1* were used as internal controls for normalization. Letters indicate significant differences among sample in Student's *t*-test followed by Benjamini-Hochberg FDR correction ($P < 0.05$)

CHAPTER IV RESULTS Part III

The histone methyltransferase SDG26 forms a multiprotein complex involved in the autonomous pathway to regulate *FLC* and *SOC1* expression in Arabidopsis

The histone methyltransferase SDG26 forms a multiprotein complex involved in the autonomous pathway to regulate *FLC* and *SOC1* expression in Arabidopsis

Xue Zhang[1], Dominique Eeckhout[2,3], Geert De Jaeger[2,3], Wen-Hui Shen[1], Alexandre Berr[1]*

Affiliations:

[1] Institut de Biologie Moléculaire des Plantes du CNRS, Université de Strasbourg, 12 rue du Général Zimmer, 67084, Strasbourg Cedex, France.

[2] Ghent University, Department of Plant Biotechnology and Bioinformatics, Technologiepark 71, 9052 Ghent University, Ghent, Belgium

[3] VIB Center for Plant Systems Biology, Technologiepark 71, 9052 Ghent, Belgium

*** Author for correspondence:** Alexandre.Berr@ibmp-cnrs.unistra.fr

Keywords: SDG26, histone modifications, autonomous pathway, transcriptional regulation, *FLOWERING LOCUS C (FLC), SUPPRESSOR OF OVEREXPRESSION OF CO 1(SOC1)*

Abstract

Histone methyltransferases are known to play crucial roles in flowering time

regulation. Previously, the histone methyltransferase SDG26 was reported to promote flowering *via* a distinctive genetic pathway. Indeed, SDG26 was found required for histone H3 lysine 4 trimethylation (H3K4me3) and H3 lysine 36 trimethylation (H3K36me3) at the critical flowering integrator *SUPPRESSOR OF OVEREXPRESSION OF CONSTANS 1*/*AGAMOUS-LIKE 20* (*SOC1*/*AGL20*), thus explaining the downregulation of *SOC1* in the loss-of-function mutant *sdg26*. By contrast, the critical flowering repressor *FLOWERING LOCUS C* (*FLC*) was found upregulated in *sdg26*. Because FLC is known to repress *SOC1* expression directly, the reason of its upregulation in *sdg26* is still not clear. Using a genetic approach, we here demonstrate that *SDG26* is involved in flowering time regulation, specifically through the autonomous pathway, since the mutation of *FLC* suppressed the late flowering and the downregulation of *SOC1* in *sdg26*. Also, a new complex containing the homeobox domain transcription factor LUMINIDEPENDEN (LD), the H3K4 demethylase FLOWERING LOCUS D (FLD), the putative COMPASS subunit APRF1 and SDG26 was characterized. Our protein and genetic interaction analyses indicated that LD might recruit FLD, APRF1, and SDG26 at *FLC* chromatin and coordinate COOLAIR processing to establish a repressive chromatin landscape necessary for *FLC* repression. Meanwhile, this LD complex acts also in the transcriptional activation of *SOC1*. Together, our results indicate that an LD complex containing SDG26 may serve to balance the transcriptional regulation between *FLC* and *SOC1* to regulate flowering timely.

IV.1. Introduction

A precise control of the floral transition, the phase transition from vegetative to reproductive development, ensures the reproductive success of seed-propagated plants (Mylne et al., 2004). Flowering time control in *Arabidopsis thaliana* is finely tuned through different sophisticated genetic networks in response or not to environmental changes. Among these networks, some, such as the aging, gibberellin, and autonomous pathways, are responding to internal cues, while others, such as the photoperiod, circadian clock, ambient temperature, and vernalization pathways, are responding to exogenous signals (Fornara et al., 2010; Ó'Maoiléidigh et al., 2014). All these six pathways converge to regulate the expression of a small set of floral pathway integrator genes to govern flowering (Fornara et al., 2010; Simpson and Dean, 2002).

FLOWERING LOCUS T(FT) and *SUPPRESSOR OF OVEREXPRESSION OF CONSTANS 1 (SOC1)*, commonly known as floral integrators, and the floral repressor *FLOWERING LOCUS C (FLC)* plays essential roles in flowering time control in Arabidopsis (Kardailsky et al., 1999; Lee et al., 2000; Michaels and Amasino, 1999). *FT* encodes a mobile florigen, synthesized in the phloem and able to promote flowering by moving to the shoot apical meristem (SAM) under inductive day length conditions (He, 2009; Shim et al., 2016; Wagner, 2017). FT physically associates with the bZIP transcription factor FD to promote floral initiation by inducing downstream flowering identity genes such as *LEAFY(LFY)*, *APETALA 1(AP1)*, *SEPALLATA3 (SEP3)* and *FRUITFULL (FUL)* either directly, or through the induction of *SOC1* (Abe et al., 2005; Jang et al., 2009; Teper-Bamnolker, 2005; Yoo, 2005). Both *FT* and *SOC1* are repressed by the MADS-box transcription factor FLC, which regulates their expression by binding the first intron of *FT* and the CArG-motif of *SOC1* (Helliwell et al., 2006). Apart from this, the *FLC* homologs named *MAF1 to MAF5* act more or less redundantly in Arabidopsis to regulate flowering time. Indeed; it has been shown that FLC and its homologs MAFs interact with SHORT VEGETATIVE PHASE (SVP) to repress *SOC1* and *FT* (Gu et al., 2013; Lee et al., 2013; Li et al., 2008; Mateos et al., 2015; Posé et al., 2013; Sureshkumar et al., 2016).

Analysis of mutants with late-flowering phenotype under both long-days (LDs) and short-days (SDs) has previously helped to define the autonomous pathway (Koornneef et

al., 1998). These mutants produce a high level of *FLC* mRNA, and their late-flowering phenotype is reverted either when combined with *FLC* mutation or after vernalization treatment (Michaels, 2001; Simpson et al., 2002). So far, many components of the autonomous pathway have been identified, defining an epistatic group: *FLOWERING CONTROL LOCUS A (FCA), FLOWERING LOCUS Y (FY), cleavage stimulation factor 64* (*CstF64*)*, CstF77, Pcf11p-similar protein 4* (*PCFS4*)*, pre-mRNA processing protein 8* (*PRP8*)*, cyclin-dependent kinase C;2* (*CDKC;2*)*, FLOWERING LOCUS PA (FPA), FLOWERING LATE KH MOTIF(FLK), TBP-associated factor 15b* (*TAF15b*)*, LUMINIDEPENDEN (LD), MULTIPLE SUPPRESSOR OF IRA14/FLOWERING LOCUS VE (MSI4/FVE), FLOWERING LOCUS D* (*FLD*; Ausín et al., 2004; Eom et al., 2018; Liu et al., 2010; Koornneef et al., 1998; Lee et al., 1994; Lim, 2004; Liu et al., 2007; Marquardt et al., 2014; Quesada et al., 2003; Wang et al., 2014; Xing et al., 2008). The RNA recognition motif (RRM) proteins FCA and FPA, the RNA cleavage and polyadenylation factors FY, CstF64 and CstF77, the core spliceosome component PRP8, and the P-TEFb transcription elongation factor CDKC;2 trigger *FLC* sense strand transcriptional silencing by affecting the formation of a *FLC* antisense transcript *COOLAIR (cod long non-coding RNA)*, which is produced from the 3'-end of the *FLC* gene (Henderson, 2005; Manzano et al., 2009; Marquardt et al., 2006; Quesada et al., 2003; Simpson et al., 2003; Swiezewski et al., 2009). FY, CstF64, CstF77, PCFS4, PRP8 and CDKC;2 regulate *FLC* expression in a FCA-dependent manner, although FPA acts independently from FCA in the repression of *FLC* (Bäurle and Dean, 2008; Liu et al., 2010; Manzano et al., 2009; Marquardt et al., 2014; Wang et al., 2014).

FLD profound function in the autonomous pathway has been extensively studied in the past years. FLOWERING LOCUS D (FLD) shares high identity with the human H3K4 demethylase LSD1 (LYSINE-SPECIFIC HISTONE DEMETHYLASE), which contains a SWIRM (SWI3p, Rsc8p, Moira) domain, commonly found in enzymes involved in chromatin remodeling (He et al., 2003; Simpson, 2004). FLD represses *FLC* through direct binding at *FLC* intron 1, altering the chromatin environment at *FLC,* as well as association with long non-coding RNAs processing (He et al., 2003; Jin et al., 2008; Liu et al., 2007; Wu et al., 2015; Yu et al., 2011). Both FCA-dependent and FPA-dependent *FLC* transcriptional silencing require FLD-mediated H3K4me2 removal across *FLC* gene body (Bäurle and Dean, 2008; Liu et al., 2007; Wu et al., 2015). Further analyzing *fld-3* and *fca-9* mutants suggest that FLD and FCA repress *FLC* expression through reduced

transcriptional initiation, attenuated RNAPII elongation, as well as promoted antisense transcript processing (Wu et al., 2015). In addition to the increased level of H3K4 methylation, H3 and H4 acetylation was also found increased at *FLC* chromatin in *fld-3* mutant (He et al., 2003; Wu et al., 2015). Such link between demethylation and deacetylation at *FLC* chromatin was later explained by the identification of a complex including FLD, the histone deacetylase (HDAC) HDA6 and FVE (Yu et al., 2016). *FVE* is one of the five Arabidopsis MSI1-like genes, a homolog of the mammalian retinoblastoma associated protein and a homolog of yeast protein MSI (multicopy suppressor of IRA1). FVE is often found in histone deacetylase (HDAC) complex participating in transcription repression (Ausín et al., 2004; Jeon and Kim, 2011; Simpson, 2004). Also, the Polycomb Repressive Complex 2 (PRC2) subunit CLF was reported to repress *FLC* through H3K27me3 deposition at *FLC* chromatin in the absence of vernalization (Jiang et al., 2008; Pazhouhandeh et al., 2011; Tian et al., 2019). Moreover, Tian et al. found FCA binding at *COOLAIR* directly CLF to deposit H3K27me3 along *FLC* chromatin, creating a link between the PRC2-mediated *FLC* silencing and the autonomous pathway components-mediated *FLC* transcriptional silencing. All results together suggest COOLAIR processing, the FLD-dependent histone H3K4 demethylation, the histone deacetylation, and the CLF-dependent histone H3K27 tri-methylation maintain *FLC* transcript at the low level, thus ultimately promoting flowering. As a classical autonomous pathway component, LD encodes a homeobox domain transcription factor which localizes in the nucleus (Lee et al., 2007). LD transcriptionally repress *FLC* through association with H3K4 demethylation, H3 deacetylation, as well as H3K27 tri-methylation (Domagalska et al., 2007; Doyle and Amasino, 2009). Also, LD was found to physically interact with the zinc-finger-containing transcription factor SUPPRESSOR of FRI 4 (SUF4), thus probably limiting its ability to bind *FLC* promoter (Kim et al., 2006). However, how LD function as a transcriptional repressor of *FLC* requires further investigation.

Histone modifications play a profound role in flowering time regulation. Previously, *in vitro* histone methyltransferase assay demonstrated that SDG26 was able to methylate Histone H3 and H4. SDG26 shares high identity limited to the catalytic SET domain and the AWS domain with SDG8, the major histone H3K36 methyltransferase in Arabidopsis. Nevertheless, while the mutation of *SDG8* leads to the specific global loss of H3K36me2 and H3K36me3 in Arabidopsis seedlings, the mutation of *SDG26* did not alter the global

level of any histone methylation marks (Xu et al., 2008). *sdg26* mutant plants present a late flowering phenotype, while mutants for other SET-domain histone methyltransferases, such as *sdg8*, or *clf* are early flowering (Berr et al., 2009; Scott et al., 2002; Zhao et al., 2005). Using a genetic approach by combining *sdg26* with other histone methylation enzyme mutants, including *atx1*, *sdg25*, *clf* and *sdg8*, as well as the demethylase double mutant *lsd1-like1 lsd1-like2* (*ldl1 ldl2*), it was found that *sdg25*, *atx1*, and *clf* interact antagonistically with *sdg26*, *ldl1 ldl2* synergistically and *sdg8* epistatically (Berr et al., 2015; Liu et al., 2016). In addition, the molecular analysis of the *sdg26* late-flowering phenotype led to suppose that SDG26 promotes flowering by binding *SOC1* promoter and enriching H3K4me3 and H3K36me3 at its chromatin, thus explaining the downregulation of *SOC1* in *sdg26* (Berr et al., 2015). However, the reason for the significant upregulation of *FLC* in *sdg26* remained still unclear and highly hypothetic.

Using a genetic and a proteomic approach, combined with molecular analyses, we here decided to better understand SDG26 functions in flowering time control, especially at *FLC*. Firstly, we clarified the genetic position of SDG26 in the autonomous pathway by crossing *sdg26* with *flc*, *ft* and *soc1* mutants. We next found that SDG26 physically interacts with LD, FLD and a putative COMPASS component APRF1/S2La to repress *FLC* and activate *SOC1*. This complex seems to be recruited at both *FLC* and *SOC1* chromatin, to repress *FLC* by association with transcription initiation as well as *COOLAIR* processing and to induce *SOC1*. Although, how the complex activates *SOC1* transcription is not clear yet, we presume this complex may serve to balance the transcriptional regulation between *FLC* and *SOC1* to properly regulate flowering time.

IV.2. Results

IV.2.1. *soc1* and *ft* mutations are additive to *sdg26* whereas *flc* is epistatic to *sdg26*

To better understand the genetic positioning of *SDG26* along the flowering time pathways, we crossed *sdg26*, and also *sdg8* and *sdg25*, with the late-flowering mutants *soc1-2* and *ft-10*, as well as with the *flc-3* null mutant (hereafter shortened as *soc1*, *ft*, and *flc*, respectively). Flowering time analyses by counting the rosette leaves number or days to bolting under long days (LDs), medium days (MDs) or short days (SDs) were conducted for all mutants (Figure 35 and Supplementary Figure S4). Because *FLC* is weakly expressed in rapid-cycling accession Columbia (Gan et al., 2014), the flowering time of *flc* was almost indistinguishable from that of wild-type (Col0) plants, except under LDs where we observed a weak early flowering phenotype. Previously, SDG8 and SDG25 were proposed to repress flowering by activating the transcription of *FLC* (Berr et al., 2009; Zhao et al., 2005). In agreement, both *flc sdg8* and *flc sdg25* double mutants showed a similarly early-flowering phenotype as *sdg8* and *sdg25* single mutants, respectively, under all photoperiod conditions (Figure 35). These results are consistent with an epistasy of *SDG8* and *SDG25* over *FLC* concerning the early-flowering phenotype.

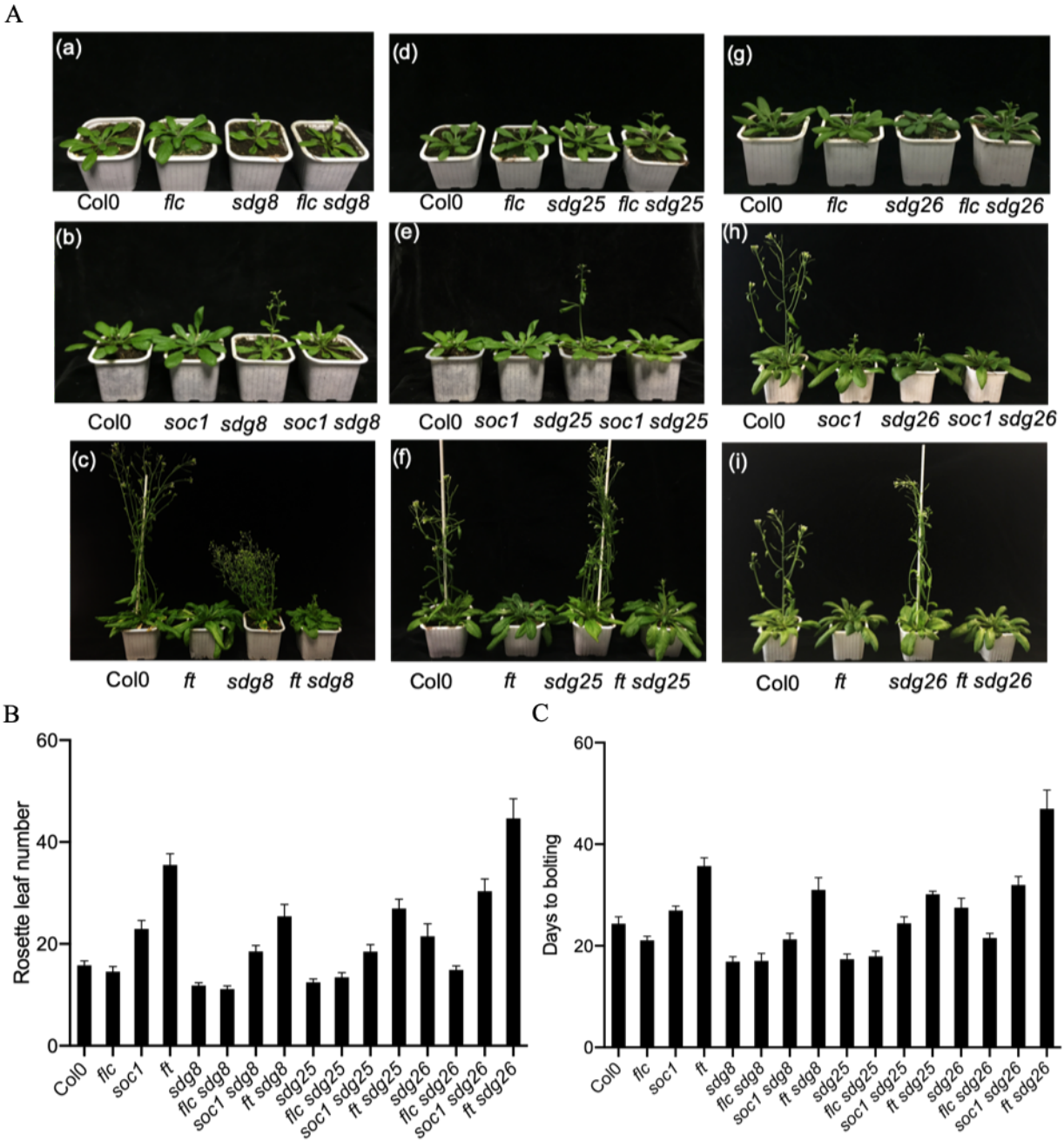

Figure 35: Flowering time analyses of various histone methyltransferase mutants (*sdg8, sdg25* and *sdg26*) alone or in combination with flowering mutant *flc*, *soc1*, *ft*. (A) Representative wild-type plants (Col0) and single or double mutants grown under long days (LDs; 16 h light: 8 h dark). **(B** and **C**) Flowering time analysis presented as rosette leaf number and days to bolting in wild-type plants and single or double mutants grown under LDs. Values are means ± SD of three biological replicates. At least 20 plants were analyzed for each biological experiment.

Introgressing the early flowering mutants *sdg8* or *sdg25* in the late flowering backgrounds *soc1* or *ft* resulted in double mutants with intermediate flowering phenotypes (*i.e.* at the time of thesis writing, results for the *ft sdg8* double mutant under MDs and SDs

were not available). Indeed, independently of photoperiods, the *soc1 sdg8* and *soc1 sdg25* double mutants flowered later than *sdg8* and *sdg25* but earlier than *soc1*, respectively. Then, when crossed with *sdg8* or *sdg25*, the strong mutant *ft* flowered earlier, but later than the *sdg8* or *sdg25* single mutants, respectively. Interestingly, under SDs, although *FT* does not play a major role under these conditions (Corbesier et al., 2007; Yanovsky and Kay, 2002), an intermediate flowering phenotype was also observed in the double mutant *ft sdg25* (Supplementary Figure S4). Together, the intermediate flowering phenotypes compared to single mutants observed with the double mutants *soc1 sdg8*, *ft sdg8* or *soc1 sdg25* and *ft sdg25* are likely due to the direct regulation of *SDG8* and *SDG25* on *FLC*. Also, the relative effect of the mutation of *SOC1* or *FT* was similar in the *sdg8* or *sdg25* mutant backgrounds, but the introduction of *sdg8* or *sdg25* mutations produced additive early flowering in each line commensurate with the extent of late flowering in every single mutant. We conclude from these results that *SDG8* and *SDG25* act as *bona fide* floral repressors that delay flowering in Arabidopsis under both inductive and non-inductive photoperiods.

The *sdg26* mutant was known to flower later than Col0 in both LDs and SDs, and it also showed a response to vernalization, which is characteristic of autonomous-pathway mutants (Berr et al., 2015; Xu et al., 2008). Interestingly, when crossed with the early-flowering mutant *flc*, the late-flowering phenotype of *sdg26* was offset entirely, and the *flc sdg26* double mutant displayed a flowering phenotype similar to that of the *flc* single mutant (Figure 35 and Supplementary Figure S4). This observation indicates that the mutation of *FLC* is epistatic to the mutation of *SDG26*, suggesting that *SDG26* acts in the same genetic pathway as *FLC*. Flowering time analyses of double mutants between *sdg26* and *soc1* or *ft* demonstrated that these mutations have additive effects, resulting in an aggravation of late- flowering phenotypes. Further supporting the complexity of the genetic interactions between flowering genes, the delay in flowering time in the *ft soc1* double mutant was also reported to be additive (Yoo et al., 2005), despite the known function of FT as a major activator of *SOC1*. It is also worth noting that this was true except with *ft* under SD where *FT* does not play a significant role under this non-inductive photoperiod.

Together, our results further confirmed that *SDG26* belongs to the autonomous pathway. Previously, *SDG26* was proposed to promote the transcription of *SOC1* directly (Berr et al., 2015). Here, our results with the *sdg26 soc1* double mutant (Figure 35 and

Supplementary Figure S4) showed that *SDG26* and *SOC1* do not act in a simple linear way because the double mutant showed an additive delay of flowering phenotype. Because SDG26 also bound *FLC* and was also involved in the H3K36 mono-methylation at *FLC* chromatin (Berr et al., 2015; Liu et al., 2016), it points to the multiple regulatory functions of SDG26 on various flowering genes, including at least *SOC1* and *FLC*, which ultimately determine plant flowering time.

IV.2.1.1. Analysis of expression of flowering genes in different mutant combinations including *sdg26* with *soc1*, *ft* or *flc*

To explore the molecular basis of different mutant flowering phenotypes, the transcript level of several flowering genes, including *FLC*, *FT*, and *SOC1,* was analyzed by qRT-PCR (Figure 36). Because the *ft sdg8* double mutant was only recently obtained, it had not been included in our qRT-PCR analysis performed earlier during my thesis work. Besides the expression of *FLC,* which was logically low in *flc*, only the expression level of *FT* was moderately increased, which is in agreement with the weak early flowering phenotype of *flc*. Also, the subtle effect of the mutation of *FLC* on its targets may be due to the redundant function of its paralogs, namely FLM/MAF1, MAF4 and MAF5 as repressors of *FT* and *SOC1* (Gu et al., 2013). Supporting the identical flowering phenotype observed between *sdg8* and *flc sdg8* or between *sdg25* and *flc sdg25*, we detected the similar changed expression levels of *FLC*, *FT*, and *SOC1* between *sdg8* and *flc sdg8*, and between *sdg25* and *flc sdg25* (Figure 36). In agreement with the positive effect of high expression of *SOC1* on the expression level of *FT* previously reported (Searle et al., 2006), we observed in the *soc1* mutant, besides the decreased expression of *SOC1*, reduced expression of *FT*. In *soc1 sdg8*, contributions of both *soc1* (*i.e.* regarding the decreased expression of *SOC1*) and *sdg8* (*i.e.* regarding the increased expression of *FT* and the decreased expression of *FLC*) were detectable. The intermediate flowering phenotype of *soc1 sdg8*, later than *sdg8* but earlier than *soc1*, underline the importance of the slight *SOC1* up-regulation in determining the early flowering phenotype of *sdg8*. Additionally, we found that the increased *FT* expression in *soc1 sdg8,* despite the negative contribution of the *soc1* mutation, might be due to the decreased expression of its repressors, thus suggesting the dominant impact on the regulation of the *FT* transcription level. Nicely explaining its early flowering phenotype, we discovered the up-regulated expression of both *SOC1* and *FT* while down-regulated expression of *FLC* in the *sdg25* single mutant

(*i.e.* similarly as in *sdg8*; Figure 36). Likewise, as for *soc1 sdg8*, the contribution of both mutations was visible in the *soc1 sdg25* double mutant, with transcript levels being decreased for *SOC1* like in *soc1* and increased for *FLC* like in *sdg25*. Supporting the above-mentioned positive effect of *SOC1* on *FT* transcription, *FT* transcript level was attenuated in the *soc1 sdg25* double mutant compared to the *sdg25* single mutant. The difference observed between *soc1 sdg8* and *soc1 sdg25* regarding the level of *FT* up-regulation may reflect the broader impact of the *SDG8* mutation on *FT* repressors (*i.e.* in addition to *FLC*, *MAF4* and *MAF5* were found down-regulated in *sdg25*, while *MAF1*, *MAF4* and *MAF5* were reported down-regulated in *sdg8*; Berr et al., 2015; Shafiq et al., 2014). In *ft sdg25*, we observed *FT* and *SOC1* were down-regulated like in *ft*, supporting the crucial role of *FT* as *SOC1* inducer, while *FLC* was downregulated like in *sdg25* (Figure 36). Together, our results reinforced the positioning of *SDG8* and *SDG25* as *FLC* transcriptional inducers.

In *sdg26* single mutant, as previously published, *SOC1* was downregulated, *FT* unchanged and *FLC* up-regulated, which nicely explains the late-flowering phenotype of *sgd26* (Figure 35 and 36; Berr et al., 2015; Liu et al., 2016). When combining *sdg26* with *flc*, *FLC* appeared logically down-regulated, while *SOC1* was not anymore down-regulated as in *sdg26* (Figure 36). This result confirmed that the *FLC* mutation is epistatic to the *sdg26* mutant. It also further indicates that a decrease in *FLC* expression is enough to increase the transcript level of *SOC1* resulting from the *sdg26* mutation, thus reinforcing the multiple regulatory functions of SDG26 on *SOC1* and *FLC* loci. Regarding the enhanced late-flowering phenotype in *ft sdg26* and *soc1 sdg26* double mutants compared to single mutants, we observed the contribution of *sdg26* regarding the up-regulation of *FLC*, while *FT* and *SOC1* were down-regulated similarly as in *ft* and *soc1*, respectively (Figure 36). These results reinforce a mutual of transcription enhancement between *FT* and *SOC1*. Furthermore, the unchanged *FT* expression detected in *sdg26* despite the *SOC1* downregulation and the stronger effect of the *FT* mutation on *SOC1* expression than the *SOC1* mutation on *FT* expression points to a powerful balance in this mutual stimulation, with *FT* being stronger than *SOC1*, which also nicely correlate with *ft* being more late flowering than *soc1*, especially under LDs (Figure 35).

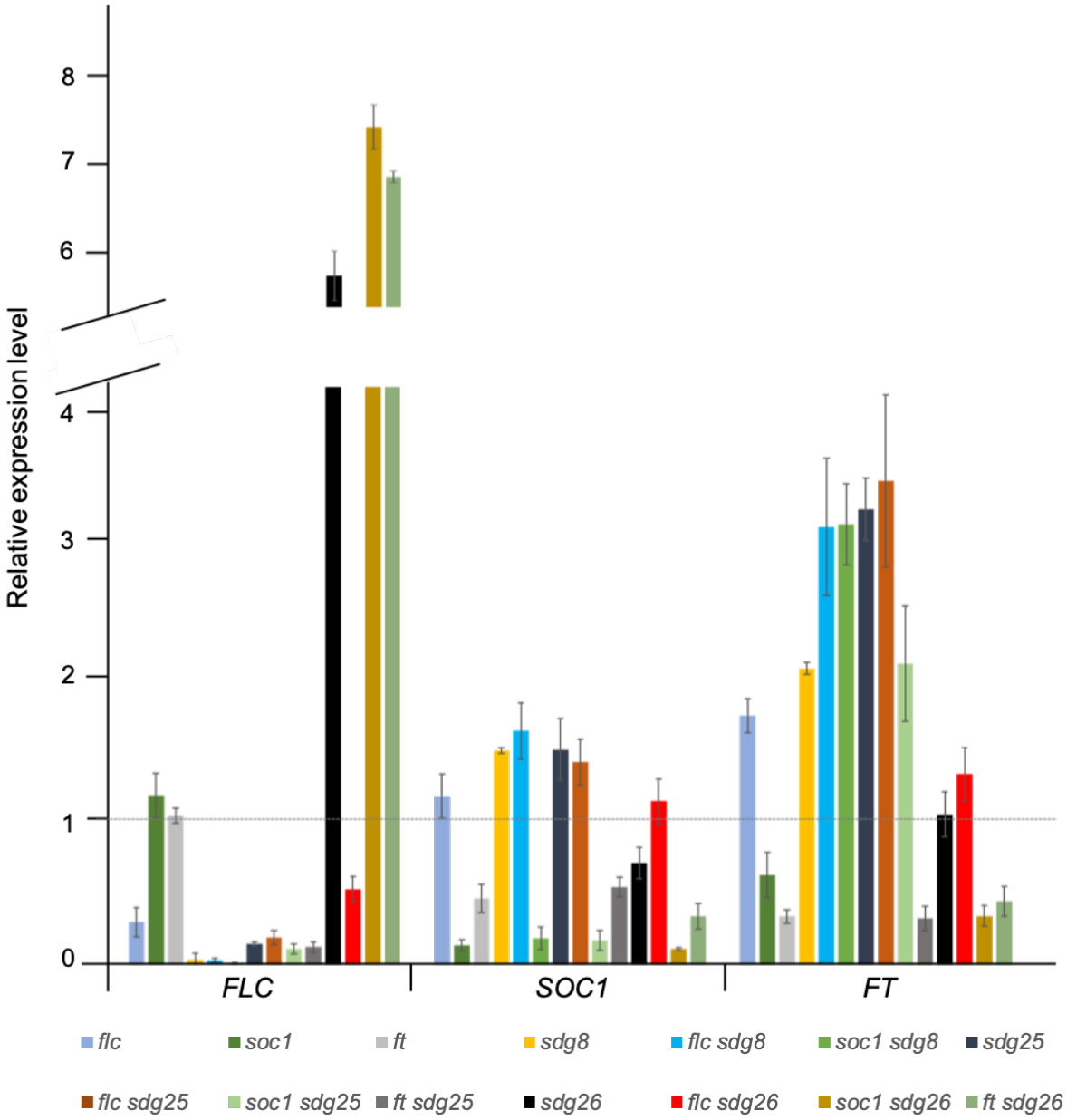

Figure 36: Relative expression analysis of flowering time regulatory genes in various histone methyltransferase mutants (*sdg8, sdg25* and *sdg26*) alone or in combination with flowering mutant *flc*, *soc1*, *ft*. Relative expression levels were measured by qRT-PCR using 2-week-old seedlings grown on MS under LDs. Data were normalized to reference genes *EXP* and *Tip 4.1* and relative values were obtained by setting expression level in Col0 as 1. Mean values are shown together with standard deviation bars based on value of three biological replicates.

IV.2.1.2. Analysis of H3 methylation at flowering genes in different mutant combinations between *sdg26* and *soc1*, *ft* and *flc*

To better understand the role of SDG26 in regulating flowering genes, we next

investigated histone methylation levels at *FLC*, *SOC1*, and *FT* in the *sdg26* mutant combinations (Figure 37). Two active marks (*i.e.* H3K4me3 and H3K36me3) and a repressive one (*i.e.* H3K27me3) were analyzed using chromatin immunoprecipitation (ChIP) assay at four regions of *FLC* (*FLC-1*, *FLC-2*, *FLC-3*, and *FLC-4*), three of *SOC1* (*SOC1-1*, *SOC1-2* and *SOC1-3*) and three of *FT* (*FT-1*, *FT-2* and *FT-3*).

In agreement with its unchanged expression, no clear and apparent variations in levels of H3K4me3, H3K36me3, and H3K27me3 were detected at *FLC* chromatin in *soc1* and *ft* compared to WT. Interestingly, we detected a decrease of H3K27me3 at *FLC* in *sdg26*, which correlate nicely with its increased expression level and suggest a functional link between H3K27me3 at *FLC* and SDG26. However, despite the similarly increased expression of *FLC* detected in *sdg26*, *ft sdg26* or *soc1 sdg26*, the decrease of H3K27me3 was not detected in the double mutants (Figure 37), a result currently without explanation.

In agreement with the repressive role of FLC on *SOC1* and with the increased *SOC1* expression detected in *flc* (Figure 36), we observed a decreased level of H3K27me3, together with increased levels of H3K4me3 and H3K36me3 at *SOC1* in *flc*. Similar antagonism between active and repressive histone methylation marks was previously reported at some flowering genes using different histone methyltransferase mutants (Buzas et al., 2011; Schmitges et al., 2011; Shafiq et al., 2014; Tamada et al., 2009; Yun et al., 2012; Zhao et al., 2019). Moreover, consistent with the positive effect of FT on the expression of *SOC1* and with the decreased *SOC1* transcript level detected in the *ft* mutant, the active histone marks were enriched at *SOC1* chromatin in *ft*, while the repressive mark was reduced. As previously published, we found that decreased active histone marks while increased repressive mark at *SOC1* in *sdg26*, which nicely explain up-regulation of *SOC1* in the mutant (Berr et al., 2015). Interestingly, even if *flc* appeared epistatic to *sdg26* in our flowering phenotype and qRT-PCR analyses, histone mark changes at *SOC1* were largely similar between *sdg26* and *flc sdg26* (Figure 36). Thus, the increased level of active marks detected at *SOC1* in *flc* might be related to the SDG26 methyltransferase activity, which further supports a direct regulatory role of SDG26 on *SOC1* and also indicates that FLC may limit the SDG26 accessibility to *SOC1* chromatin. Finally, consistent with the absence of additive effect between *ft* and *sdg26* regarding the down-regulation of *SOC1* (Figure 36), H3K4me3 and H3K36me3 appeared decreased and H3K27me3 increased at *SOC1* in the *ft sdg26* double mutant similarly as in the *ft* and *sdg26* single mutants.

Like *SOC1*, *FT* transcription is also known as being directly repressed by *FLC* (Helliwell et al., 2006; Searle et al., 2006). However, *SOC1* and *FT* chromatins were found differently affected by the mutation of *FLC*. Indeed, while H3K27me3 was decreased at both *SOC1* and *FT* chromatin in *flc*, the active histone marks were enriched at *SOC1* but largely unchanged at *FT* (Figure 37). Also, in agreement with the positive effect of *SOC1* on *FT* expression previously reported (Searle et al., 2006) and supporting the downregulation of *FT* we detected in the *soc1* mutant, levels of active histone marks were reduced at *FT* in *soc1*. Together with the above-reported impact of the mutation of *FT* on the chromatin and the transcription of *SOC1*, our results underpin the existence of a positive reciprocal regulation between *FT* and *SOC1* in the course of flowering time regulation that involves the deposition of active histone methylation marks at both genes. Finally, in *sdg26* and *flc sdg26*, no significant changes were detected at *FT*, while H3K4me3, H3K36me3 and H3K27me3 levels were similar between *soc1* and *soc1 sdg26* (Figure 37). Taken together, our data further highlighted the complexity of the regulation of flowering genes and supported the regulatory roles of SGD26 at the interface between *SOC1* and *FLC*.

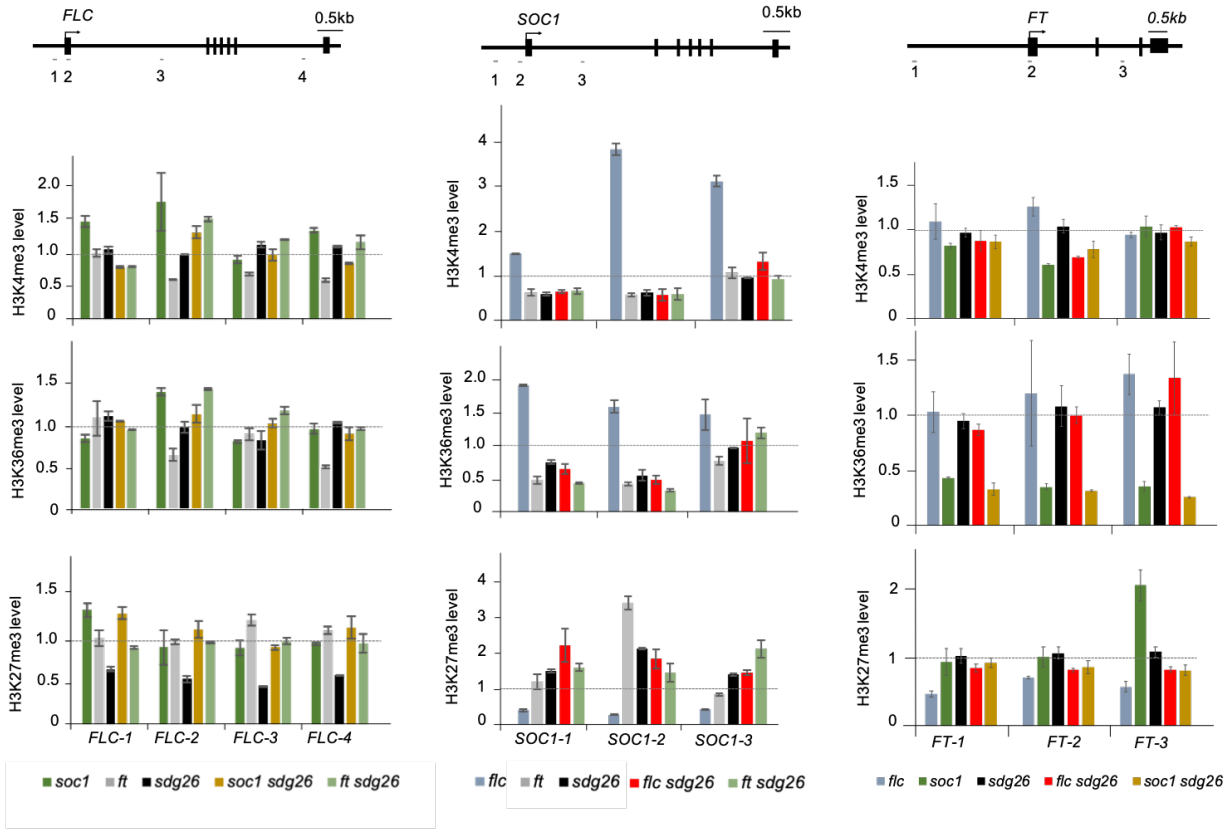

Figure 37: Chromatin immunoprecipitation (ChIP) analysis of H3K4me3, H3K36me3 and H3K27me3 levels at *FLC*, *SOC1* and *FT* in various histone methyltransferase mutants (*sdg8, sdg25* and *sdg26*) alone or in combination with flowering mutant *flc*, *soc1*, *ft*. Schematic diagram of *FLC*, *SOC1* and *FT* with black boxes for exons; black lines for promoters and introns; arrows for transcription start sites. Grey bars beneath the gene indicate DNA regions amplified by q-PCR. Chromatin was extracted from 2-week-old seedlings grown on MS plates under LDs. Data were normalized to Tub2 and presented relative to the value of Col0 at each amplified region. Means values ± SD from two biological replicates are presented.

IV.2.2. SDG26 forms a protein complex with LD, FLD and APRF1/S2La

To identify protein partners of SDG26, tandem affinity purification combined with mass spectrometry method (TAP-MS) was used in GS-tagged SDG26 Arabidopsis cell cultures. Among the different peptides identified, several ones were corresponding to the transcription factor LD, the H3K4 demethylase FLD and the putative COMPASS component APRF1/S2La (Table 1 & Supplementary Figure S5). In another independent assay, we conducted immunoprecipitation (IP) followed by LC-MS/MS with 2-week-old Arabidopsis seedlings expressing a C-terminal FLAG-tagged APRF1 driven by 35S promoter (Kapolas et al., 2016) and a C-terminal FLAG-tagged FLD driven by its native promoter. Peptides corresponding to LD, FLD, and APRF1 were detected using each

transgenic line, while peptides corresponding to SDG26 were only detected using the FLAG-tagged *FLD* line (Table1). The difference we observed may suggest a much more labile interaction between SDG26 and APRF1.

Bait	Detected peptides			
	SDG26 (AT1G76710)	APRF1 (AT5G14530)	LD (AT4G02560)	FLD (AT3G10390)
SDG26-GS	30/28	9/9	28/27	21/24
FLD-FLAG	11	3	27	32
APRF1-FLAG	0	104	4	1

Table1: Summary of several proteins identified by MS in TAP eluates of Arabidopsis cell cultures with GS tagged SDG26 or by LC-MS/MS in 2-week-old Arabidopsis transgenic seedlings expressing a FLAG tagged FLD or APRF1 proteins. Numbers indicate the number of corresponding peptides detected in each experiment.

Next, we investigated whether SDG26 colocalizes with its putative partners. Firstly, the following gene fusions *p35S-gSDG26-GFP*, *p35S-FLD-EGFP*, and *p35S-APRF1-EGFP* were constructed and separately expressed in *Nicotiana benthamiana* (tobacco) leaves. As depicted in Figure 38A, all fusion proteins were found predominantly localized in the cell nucleus. Then, SDG26-RFP was co-expressed with either FLD-EGFP or APRF1-EGFP in tobacco leaves. As exemplified in Figure 4B, SDG26 colocalized with FLD and APRF1, suggesting that they may coordinately function in the nucleus (Figure 38B).

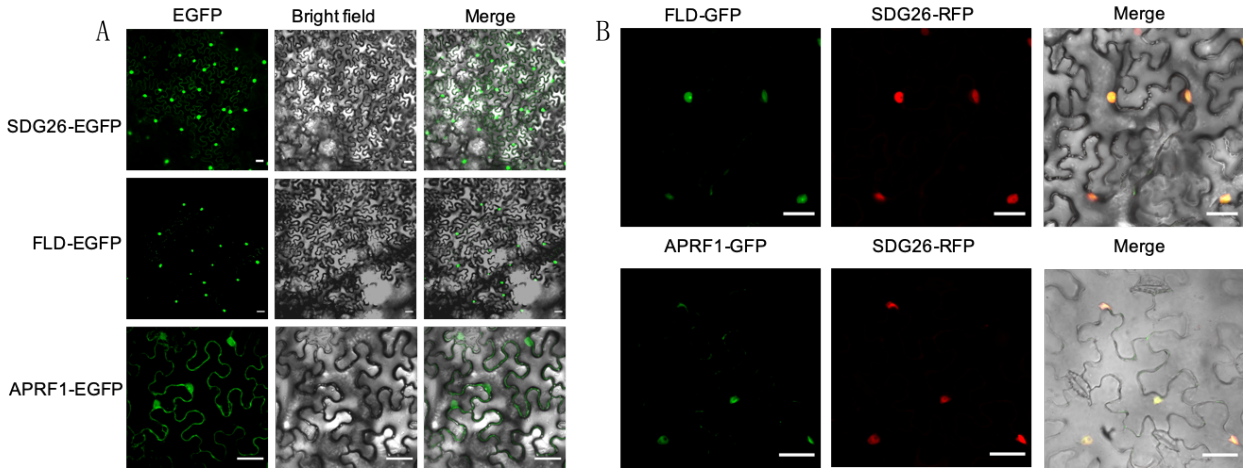

Figure 38: Subcellular localization of SDG26, FLD and APRF1 in tobacco epidermal leaves. (A) Transient expression of *SDG26-EGFP*, *FLD-EGFP*, *APRF1-EGFP* in 3-week-old tobacco leaves. **(B)** Nuclear colocalization between *FLD-EGFP* and *SDG26-RFP* and between *ARPF1-EGFP* and *SDG26-RFP* in 3-week-old tobacco leaves. Two days after infiltration, epidermal leaves were used to observe fluorescence signal under microscope. Scale bars = 40 µm.

To further validate the interactions obtained from TAP-MS and IP/LC-MS/MS experiments, co-immunoprecipitation assays were performed in Arabidopsis using 2-week-old seedlings of wild-type (WT) as negative control and of transgenic plants bearing the functional FLAG-tagged FLD. After immunoprecipitation using a FLAG antibody, SDG26 was detected using a monoclonal SDG26 antibody (Berr et al., 2015) , thus confirming the FLD and SDG26 interaction in vivo (Figure 39A). Analogously, the in vivo interaction between APRF1 and SDG26 was also observed (Figure 39A). Also, we confirmed the interaction between LD and SDG26 by transient co-expression in tobacco and also found that APRF1 and FLD can also interact with LD (Figure 39A). In contrast, interaction between SDG26 and FLD or APRF1 was not detected using this assay. By using the yeast two-hybrid assay, we were able to detect an interaction between LD and APRF1, FLD, or SDG26, and again no direct interaction was detected between SDG26 and APRF1 or FLD, or between FLD and APRF1 (Figure 39B). Furthermore, a direct interaction was confirmed using biomolecular inflorescence complementation (BiFC) assay between SDG26 and LD (Figure 39C). Taken together, our data indicate that LD is a central element to bring APRF1 and/or FLD and/or SDG26 together in multiprotein complex formation. Our qRT-PCR analysis revealed that the transcript levels of *SDG26*, *LD*, *FLD* and *APRF1* were unchanged in their reciprocal mutants (Supplementary Figure S6), indicating that the SDG26-LD/FLD/ARF1 complex is not involved in transcription regulation of these genes.

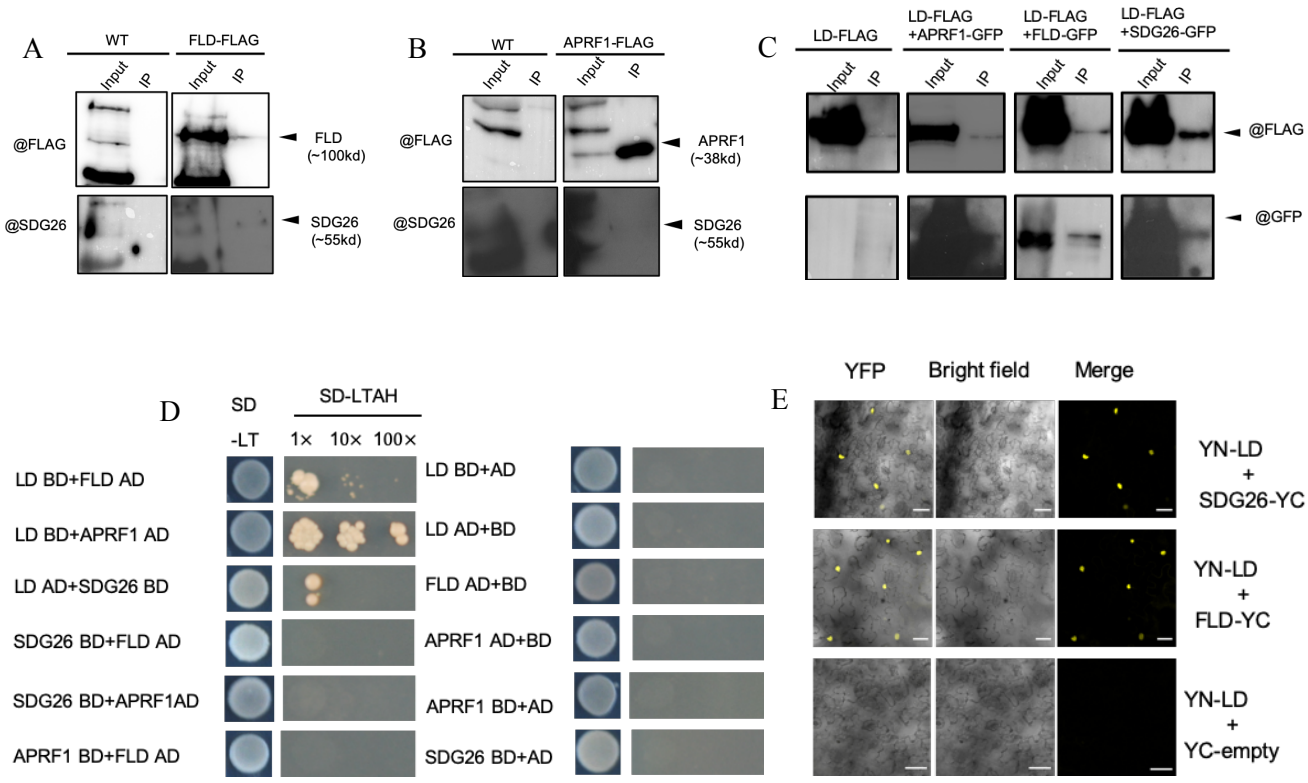

Figure 39: LD, FLD and APRF1 proteins interact with SDG26. (A and B) Protein extracts were immune-precipitated from 2-week-old wild-type plants (Col-0), FLAG tagged FLD transgenic lines or FLAG tagged APRF1 transgenic lines with anti-FLAG beads. Immunoprecipitated samples (IP) were then analyzed using anti-SDG26 or anti-FLAG antibodies by western-blot. **(C)** A FLAG-LD transgene was transiently expressed alone or co-expressed with either a GFP-APRF1, GFP-SDG26 or a GFP-FLD transgene in tobacco leaves. Two days after infiltration, proteins were extracted and immunoprecipitated using anti-FLAG Miltenyi beads. Input and immunoprecipitation (IP) samples were then analyzed with anti-FLAG and anti-GFP antibodies separately by western-blot. **(D)** Yeast two-hybrid assays between LD, FLD, APRF1 and SDG26. AD is for the GAL4 activation domain fusion and BD for the GAL4 DNA-binding domain fusion. **(E)** Biomolecular fluorescence complementation (BiFC) analysis between LD and FLD or SDG26. From left to right: YFP channel, bright field channel and merge of YFP and bright field channel. Scar bars=40 µm.

IV.2.2.1. Interplay of *sdg26* with *ld*, *fld* and *aprf1* in the regulation of flowering time and expression of flowering genes

Because SDG26 physically interacts, either directly or indirectly, with LD, FLD, and APRF1, we decided to test the genetic interactions between corresponding mutants. The T-DNA insertion lines *ld-1* (Kim et al., 2006), *fld*-6 (Liu et al., 2007) and *aprf1-7* and *aprf1-9* (Kapolas et al., 2016) were obtained and separately crossed with *sdg26*. Then,

flowering time was analyzed under LDs and MDs for each double mutant and compared to single ones (Figure 40; at the time of writing my thesis the flowering time analyses for *ld sdg26* were not yet finalized). LD and FLD are "classic" autonomous-pathway genes, and their corresponding mutants are known to be late-flowering (He et al., 2003; Lee et al., 1994). Also, in agreement with previously published data, bolting was found delayed in *aprf1* under both LDs and MDs (Kapolas et al., 2016). However, under MDs, we observed that both *aprf1-7* and *aprf1-9* mutants presented a later flowering phenotype than *sdg26*, while under LDs, both *arpf1* and *sdg26* mutants flowered similarly late. These observations suggest that a stronger photoperiod response happened in *aprf1* mutants compared to *sdg26*. When combined with *sdg26*, *aprf1* mutants flowered even later than the corresponding single mutants, suggesting an additive or even synergistic effects between both mutations. When combined with *fld*, *sdg26* exhibited a late flowering phenotype similar to the *fld* single mutant, suggesting the epistatic grouping of these genes in the autonomous pathway.

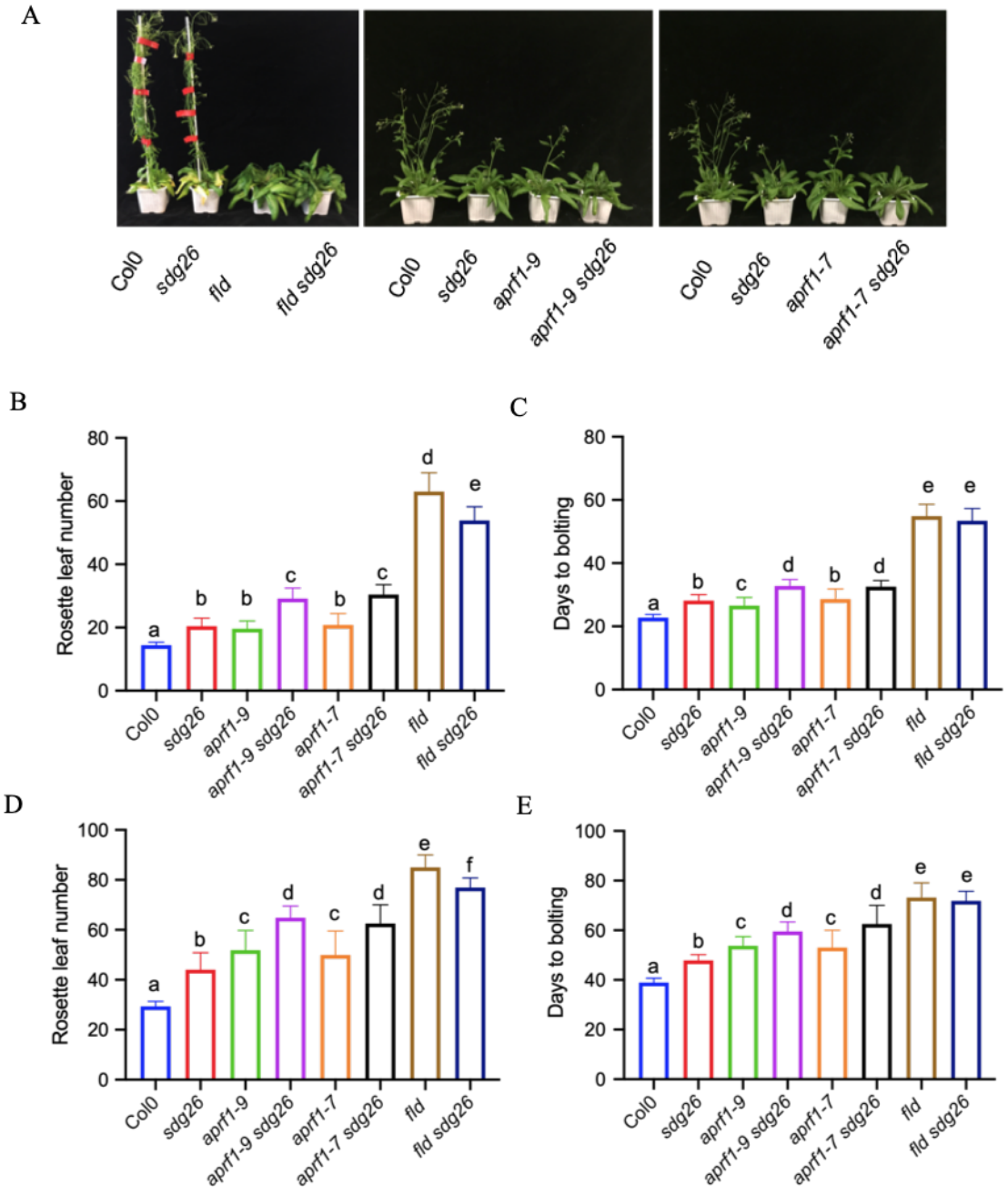

Figure 40: Flowering time analysis in *sdg26* in combination or not with different late-flowering mutants. (A) Representative flowering phenotype of plants grown under LDs. Flowering time measured as the number of rosette leaves and days at bolting under LDs **(B and C)** or under MDs **(D and E)**. The mean values ± SD from two biological experiments are shown. At least 15 plants were analyzed in each experiment. Letters indicate significant differences among sample in Student's *t*-test followed by Benjamini-Hochberg FDR correction ($P < 0.01$).

To go further in characterizing these genetic interactions, expression levels of *FLC*, *MAF4* and *MAF5*, *SOC1* and *FT* were analyzed by qRT-PCR in 2-week-old seedlings grown on MS medium under LDs (Figure 41). In all single mutants, we observed the

increased levels of *FLC*, *MAF4*, and *MAF5*. In agreement with FLC and MAF4/MAF5 in repressing the expression of the floral integrators *FT* and *SOC1* (Gu et al., 2013), transcript levels of *FT* and *SOC1* were inversely decreased. Supporting the later flowering phenotype of the *aprf1 sdg26* double mutant compared to the single mutants, we detected a synergistic increase of *FLC* expression. For *MAF4* and *MAF5*, the results were less clear since these genes were not similarly up-regulated in the two *aprf1* allelic mutants, despite their similarly late-flowering phenotypes.

Interestingly, the *SOC1* expression in *aprf1-9 sdg26* and *aprf1-7 sdg26* was similar as in *aprf1-9* and *aprf1-7*, respectively, while a synergistically decreased *FT* expression was detected in *aprf1 sdg26*. Thus, we suggest that SDG26 and APRF1 may redundantly inhibit *FLC* transcription. Regarding the genetic interaction between *sdg26* and *fld*, transcript levels of all tested genes in *fld sdg26* were similarly affected as in the *fld* single mutant. This result indicates that FLD strongly dominates the autonomous pathway and further support the epistatic effect of its mutation over *sdg26*. Future analysis of *ld sdg26* will further help to evaluate the importance of LD in this complex as a potential central element in flowering time control.

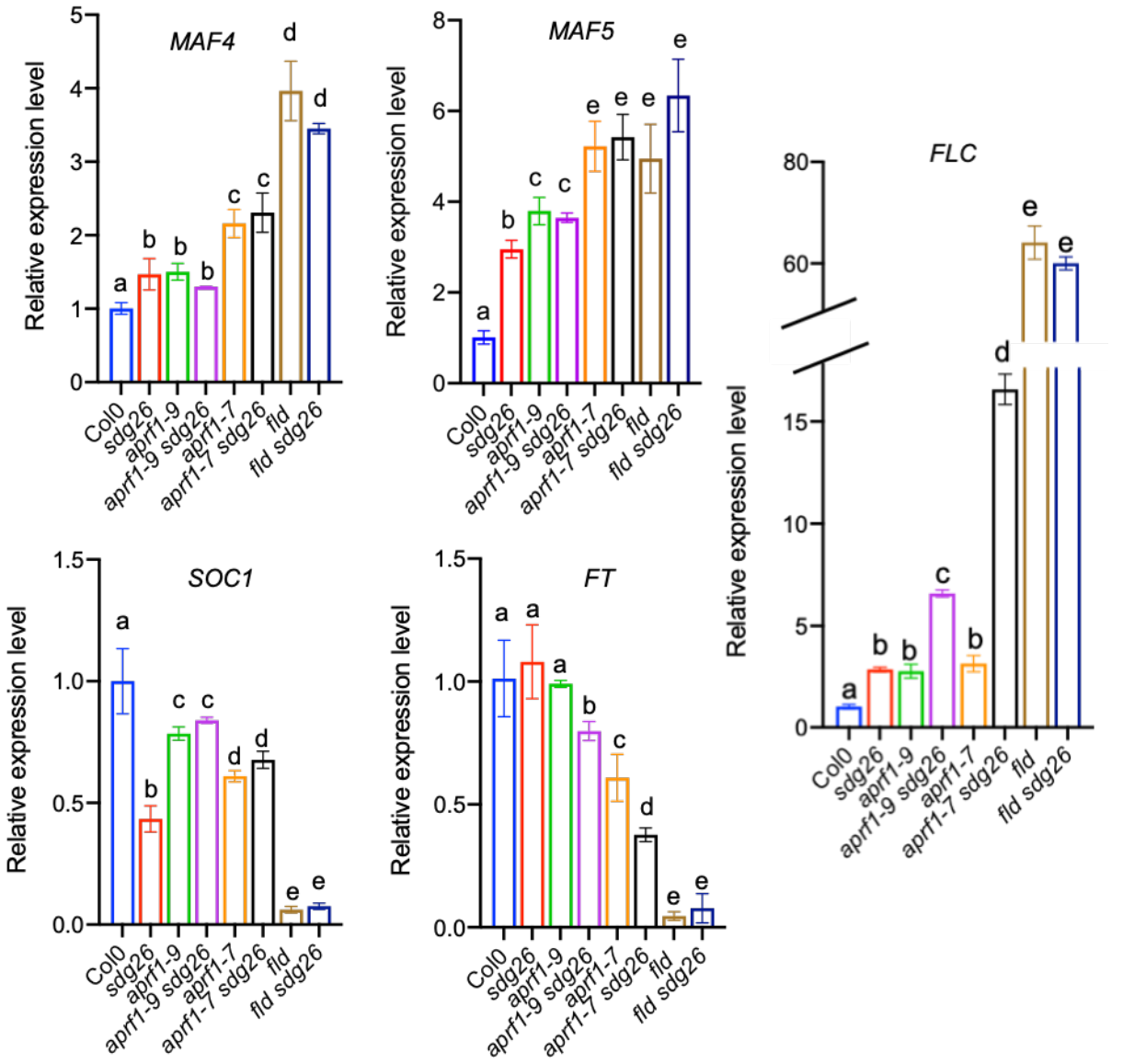

Figure 41: Expression analysis of flowering-time related genes in *sdg26* in combination or not with different late-flowering mutants. Relative expression levels of *FLC*, *MAF4* and *MAF5*, *SOC1* and *FT* were quantified by qRT-PCR using two-week-old seedlings grown on MS under LDs and presented relative to Col0 (set as 1). Letters indicate significant differences among sample in Student's *t*-test followed by Benjamini-Hochberg FDR correction ($P < 0.01$).

IV.2.2.2.a Histone marks at *FLC* are affected differently in the *sdg26*, *aprf1*, *fld*, *ld*, and combined mutants

Because FLD and LD were previously related to changes in histone marks at *FLC* chromatin (Domagalska et al., 2007; Jiang et al., 2008) and because SDG26 interacts with both FLD and LD, we next investigated the chromatin state of *FLC* in our different single

and double mutants. First, we tested SDG26 binding at *FLC* in our different mutant combinations. Chromatin extracts from wild-type Col0 plants and *sdg26*, *aprf1-9*, *fld*, and *ld* mutants were separately immunoprecipitated using an SDG26 monoclonal antibody (Berr et al., 2015). After recovery, DNA was used for qRT-PCR experiments with primers covering the *FLC* chromatin. Confirming the binding of SDG26 to *FLC*, we observed a significant enrichment of SDG26 at *FLC* in Col0 compared to *sdg26*. Interestingly, SDG26 enrichment was drastically reduced in the *aprf1-9*, *fld* and *ld* mutants (Figure 42A), suggesting that the SDG26 binding at *FLC* requires APRF1, FLD, and LD.

Next, we evaluated the levels of two active histone marks (H3K4me3 and H3 acetylation) and a repressive histone mark (H3K27me3) in all single and double mutants (Figure 42B, C and D; at the time of writing my thesis ChIP data for H3K36me3 at *FLC* were only available in *fld*, *ld* mutants and Col0 plants, see Supplementary Figure S7). In agreement with previously published data (Wu et al., 2015), *FLD* mutation caused increased levels of H3K4me3, H3K36me3 and H3 acetylation while decreased H3K27me3 at *FLC* chromatin. The mutation of LD also resulted in similar chromatin alterations. Because H3K4me3, H3K36me3, and H3 acetylation positively and H3K27me3 negatively correlate with transcription (Roudier et al., 2011; Sequeira-Mendes et al., 2014), the chromatin profiles we obtained in *fld* and *ld* nicely explained the transcriptional up-regulation of *FLC*. Compared to *fld* and *ld*, the mutation of *SDG26* did not cause any change in H3K4me3, H3K36me3 or H3 acetylation levels, since their levels remained similar as in wild-type Col0 plants. However, we detected a significant reduction in the level of H3K27me3. Then, mutation of the putative COMPASS component *APRF1* caused an increase in H3K4me3 and H3 acetylation, especially towards the 3'-end of *FLC*, combined with a decrease in H3K27 me3 across the whole gene body. Confirming the epistatic effect of *fld* over *sdg26* as to the flowering phenotype, we found the same chromatin profiles in *fld sdg26* as in *fld*. Finally, chromatin profiles were identical between the *aprf1-9* single mutant and the *aprf1-9 sdg26* double one. Overall, our chromatin analyses indicate that at *FLC* chromatin *APRF1* and *FLD* override *SDG26*.

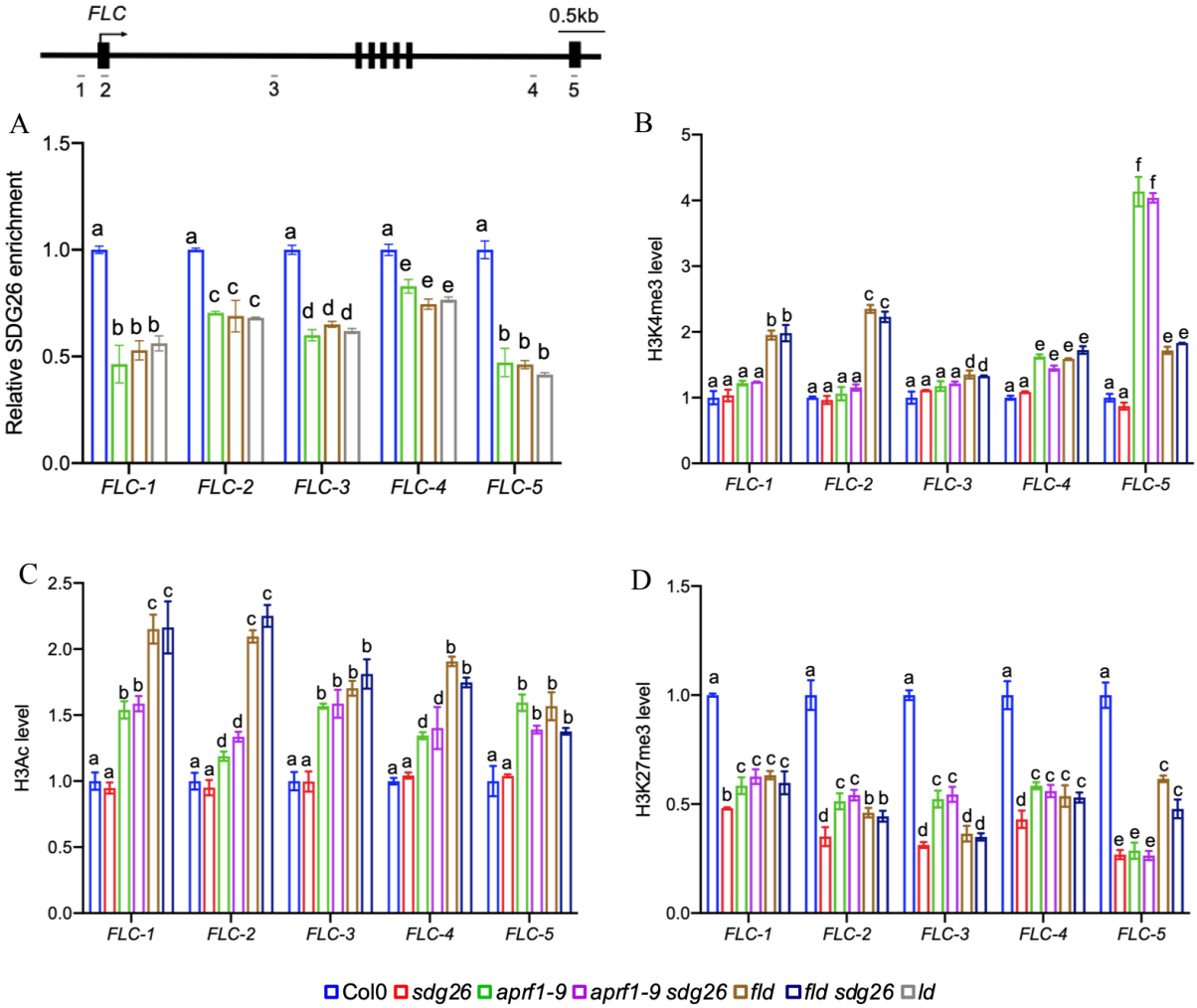

Figure 42: ChIP analysis at *FLC* chromatin in *sdg26* in combination or not with different late-flowering mutants. On top is a schematic diagram of *FLC* with black boxes for exons; black lines for promoters and introns; arrows for transcription start sites. Grey bars beneath the gene indicate DNA regions amplified by q-PCR. Chromatin was extracted from 2-week-old seedlings grown on MS plates under LDs. **(A)** ChIP analysis of SDG26 enrichment at the *FLC* chromatin using an anti-SDG26 monoclonal antibody. **(B to D)** Relative H3K4me3, H3 acetylation and H3K27m3 enrichment. Means value ± SD from two biological replicates are presented Letters indicate significant differences among sample in Student's *t*-test followed by Benjamini-Hochberg FDR correction ($P < 0.01$).

IV.2.2.2.b. Ratio of *COOLAIR* isoforms is affected in *sdg26* similarly as in *fld*

The *COOLAIR* is a set of non-coding antisense RNAs transcribed from the 3'-end of *FLC* and involved in the *FLC* transcriptional repression (Swiezewski et al., 2009). In addition, the FLD activity was found coupled with *COOLAIR* splicing and polyadenylation for *FLC* sense transcription regulation (Marquardt et al., 2014). Interestingly, in our ChIP analyses, the histone mark changes were spread from the *FLC* transcriptional start site to the 3'-end downstream region where the promoter of *COOLAIR*

is located. These distributions urged us to measure *COOLAIR* transcripts in our mutants using qRT-PCR with specific primers (Figure 43A). Consistent with the positive correlation previously described between total *FLC* and total *COOLAIR* production (Swiezewski et al., 2009), we observed an increased level of total *COOLAIR* in *sdg26.* To further understand roles of *SDG26* in *COOLAIR* regulation, we undertook a thorough analysis of the accumulation of COOLAIR isoforms, termed *COOLAIR* class I, when the proximal polyadenylation (poly(A)) site is used, and class II, when the distal poly(A) site is used, and the ratio between class I and class II helps stabilize inactive or active chromatin states (Liu et al., 2007; Swiezewski et al., 2007). Loss of any of the autonomous pathway components, like with the *fld* mutant, reduces usage of the proximal poly(A) site, thus resulting in a higher ratio of class II to class I which positively correlated with higher *FLC* transcription and higher level of active histone marks at *FLC* chromatin (Liu et al., 2007; Marquardt et al., 2014). Interestingly, we detected a similar ratio as *fld* in the *sdg26* mutant, with a similarly high level of class II between *sdg26*, *fld* and *fld sdg26* (Figure 43B and 43C). Overall, our analyses indicate that, within the autonomous pathway, SDG26 might participate together with FLD to coordinate the *COOLAIR* poly(A) site decision necessary for the transcriptional regulation of *FLC*.

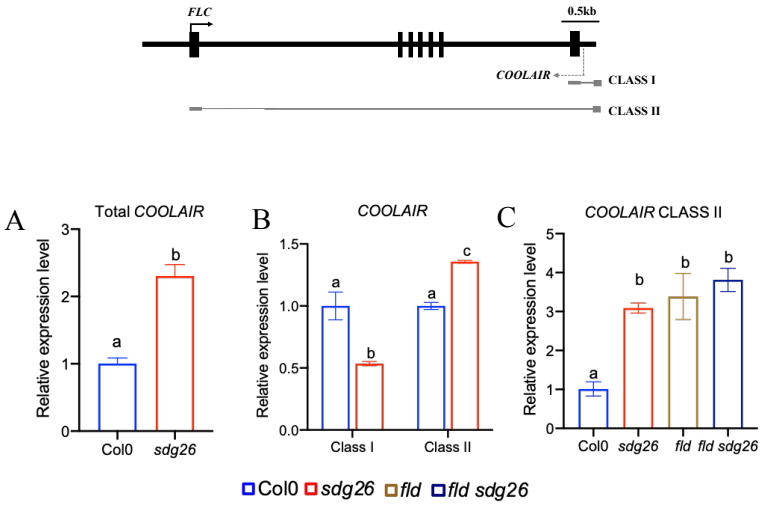

Figure 43: Expression analysis of *COOLAIR* in WT and the indicated mutants. On top is a schematic diagram of the *FLC*; the broken line with the arrow indicates the TSS of *COOLAIR*, Class I and II *COOLAIR* transcripts are diagrammatically illustrated. **(A**, **B** and **C)** *COOLAIR* analysis in indicated flowering mutants. *COOLAIR* analysis is performed by qRT-PCR using 10-day-old seedlings grown on MS under LDs. The transcript of *COOLAIR* Class I and Class II are representative as relative to total *COOLAIR* and normalized to Tub2. Letters indicate significant differences among sample in Student's *t*-test followed by Benjamini-Hochberg FDR correction ($p<0.01$).

IV.2.2.3. *SOC1* chromatin inversely behave as *FLC* chromatin in late-flowering mutants

SDG26 was previously demonstrated to activate the transcription of the floral integrator *SOC1* by directly binding its chromatin and depositing H3K4me3 and H3K36me3 (Berr et al., 2015). We then investigated if the function of SDG26 at *SOC1* require one or other of the SDG26 protein partners we identified by extending our chromatin analyses to *aprf1*, *fld* and *ld* mutants. Due to the enrichment of SDG26 was decreased in *aprf1*, *fld*, and *ld*, we concluded that the SDG26 binding at *SOC1* chromatin requires FLD, LD, and APRF1, thus further reinforcing their interaction (Figure 44A). Next, we analyzed the chromatin state of *SOC1* similarly as we did for *FLC*. In contrast to *FLC* chromatin where active marks were found increased, all mutants displayed decreased levels of H3K4me3 and H3 acetylation at *SOC1* chromatin (Figure 44B & 44C &Supplementary Figure S8). Nicely correlated with the most dramatic *SOC1* downregulation observed in *fld*, the decrease in H3K4me3 was found to be more severe in *fld* compared to other single mutants. Owing to the mutual exclusion between active and repressive histone marks, the sharpest increase in H3K27me3 was found in *fld* and *fld sdg26* (Figure 44D). Because FLD was identified as a H3K4 demethylase involved in *FLC* repression (Liu et al., 2007) and because FLC represses directly *SOC1*, this result indicates that the repression of *SOC1* by FLC may occur through the loading of repressive histone marks and the removal of active ones at *SOC1* chromatin. Also, further supporting that *FLD* overrides *SDG26*, the decreases in H3K4me3 and H3 acetylation, as well as the increase in H3K27me3 were similar between *fld* and *fld sdg26*. In general chromatin changes were similar between *sdg26* and *aprf1* single mutants. Active marks were found decreased in *sdg26* and *aprf1-9*, and the repressive one increased, but at lower levels compared to *fld*. Even if the level of H3K36me3 was only measured in *fld* and *ld* single mutants, a similar tendency as that of H3K4me3 was observed (Supplementary Figure S8). Also, changes in *aprf1 sdg26* were similar as in *sdg26* or *aprf1* single mutants. To conclude, our observations of histone marks at *SOC1* chromatin further support the downregulation of *SOC1* in all our late-flowering mutants.

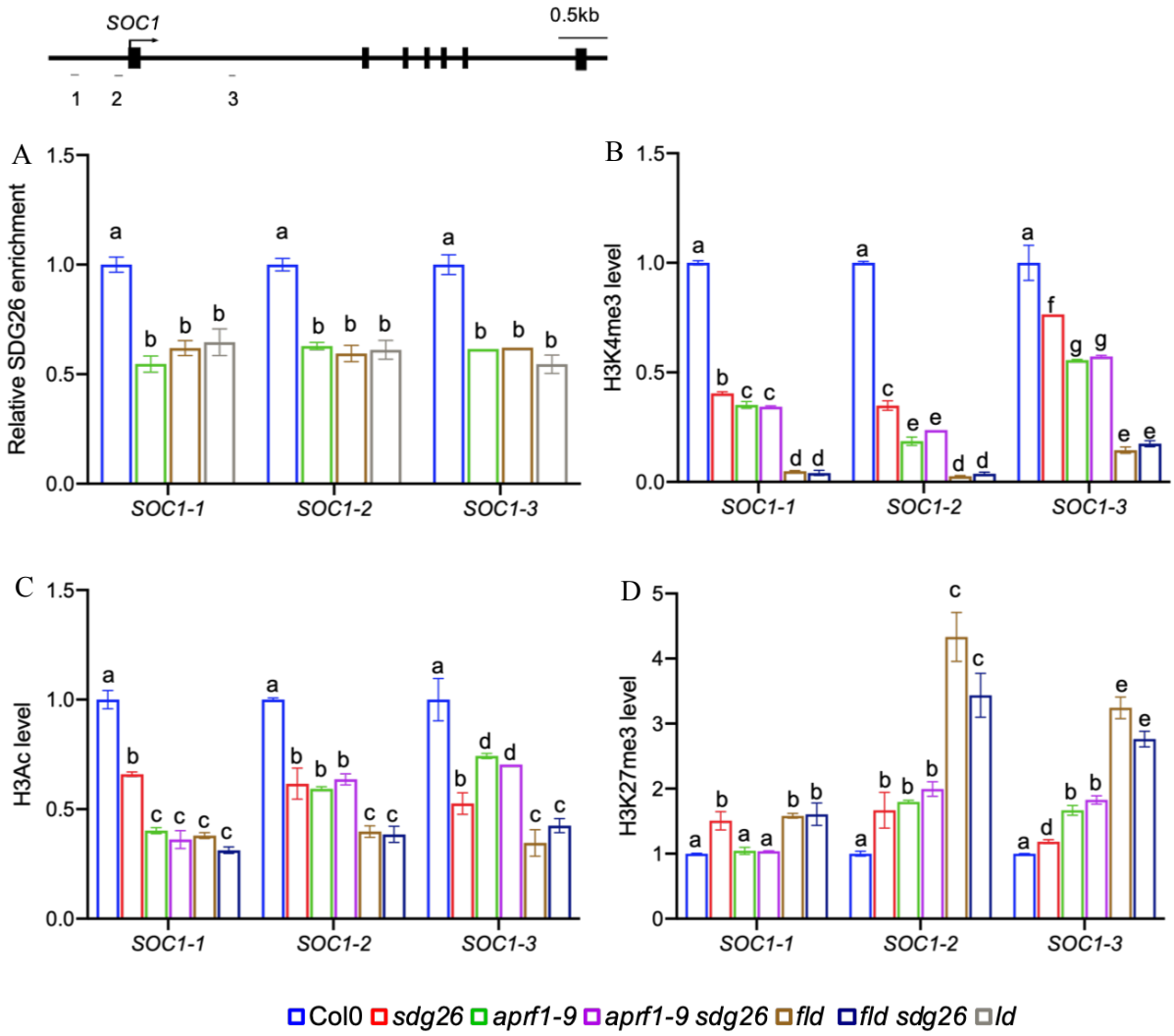

Figure 44: ChIP analysis at *SOC1* chromatin in *sdg26* in combination or not with different late-flowering mutants. On top is a schematic diagram of *SOC1* with black boxes for exons; black lines for promoters and introns; arrows for transcription start sites. Grey bars beneath the gene indicate DNA regions amplified by q-PCR. Chromatin was extracted from 2-week-old seedlings grown on MS plates under LDs. **(A)** ChIP analysis of SDG26 enrichment at the *SOC1* chromatin using an anti-SDG26 monoclonal antibody. **(B to D)** Relative H3K4me3, H3 acetylation and H3K27m3 enrichment. Means value ± SD from two biological replicates are presented. Letters indicate significant differences among sample in Student's *t*-test followed by Benjamini-Hochberg FDR correction ($P < 0.01$).

IV.3. Discussion

In this study, we investigated the function of *SDG26* in regulating flowering genes using various approaches. To have a better idea about the positioning of *SDG26* along the flowering pathways, we firstly undertook genetic crosses between the late-flowering *sdg26* mutant and mutants of key flowering genes, including the weak early-flowering mutant *flc* and the late-lowering ones *soc1* and *ft*. We compared double mutants with single ones regarding their flowering phenotype, the expression of critical flowering genes, as well as the level of histone methylation marks known to be essential for regulating these flowering genes. Crosses with the two early flowering histone methyltransferase mutants *sdg8* and *sdg25* were used as genetic interaction benchmarks. Results obtained with *sdg8* and *sdg25* were consistent with previous reports and confirmed their role as *FLC* inducers and flowering repressors under both inductive and non-inductive photoperiods (Berr et al., 2010; Dong et al., 2008; Grini et al., 2009; Shafiq et al., 2014; Zhao et al., 2005).

Regarding the *sdg26* mutant combinations, our analyses revealed that *flc* is epistatic to *sdg26* and that *sdg26* and *ft* or *soc1* presented an additive effect. Using this approach, we also confirmed *SDG26* being an autonomous pathway member (Berr et al., 2015; Xu et al., 2008). Moreover, the absence of a simple linear relationship between *sdg26* and other mutants suggested the involvement of *SDG26* in regulating several gene targets. Besides this, we observed that the repression of FLC on *FT* and *SOC1* was H3K27me3-dependent. Our data also confirmed the existence of a mutual transcriptional stimulation between *FT* and *SOC1* involving the deposition of active histone marks. Indeed, FT was previously reported to directly activate *SOC1* expression by binding its promoter region (Helliwell et al., 2006), while in the leaf vasculature, high expression of *SOC1* can enhance the expression levels of *FT* in a CO-independent manner (Searle et al., 2006). Together, our genetic approach further underlines the complexity of the regulatory network controlling the floral transition

Gene transcription is the result of the combined effects of multiple actors including the RNA polymerase II (RNAPII), several transcription factors, DNA methylation, histone structure and remodeling, histone modifications and long non-coding RNA (Chen et al., 2017; Durairaj et al., 2017). The transcriptional regulation of *FLC* does not escape this rule since it was reported to be under the control of several histone modifications, histone

remodeling, transcription factor, RNA processing factors and the antisense transcript *COOLAIR* (Berry and Dean, 2015; Bloomer and Dean, 2017; Wang and Chekanova, 2017). Here, we identified several protein-protein interactions involving SDG26, giving rise to a possible new protein complex comprising the homeobox-domain transcription factor LD, the histone methyltransferase SDG26, the histone demethylase FLD and a putative COMPASS component APRF1/S2La. Using mutants for the different protein partners, we have undertaken a genetic interaction analysis and revealed that *FLD* is epistatic to *SDG26* in the regulation of flowering, while *SDG26* and *APRF1* act redundantly/synergistically. Still under progress, the analysis of the genetic interaction between *ld* and *sdg26* will soon further help to gain insight into the functional role of these interactions in regulating flowering time. Additionally, we confirmed that SDG26 binds *FLC* chromatin (Berr et al., 2015), and we found that this binding requires the protein partners we identified, namely LD, FLD, and APRF1. *LD* was characterized as an autonomous pathway component (Lee et al., 1994), which mutation resulted in alteration of histone modifications along *FLC* chromatin (Domagalska et al., 2007; Doyle and Amasino, 2009). Based on our results, we proposed that LD may work as a scaffold protein recruiting several protein partners. Among them, *FLD* was also previously identified as an autonomous pathway member broadly investigated in the past years (He et al., 2003; Jiang et al., 2007; Jin et al., 2008; Liu et al., 2007; Wu et al., 2015; Yu et al., 2016). Beside its H3K4 demethylase activity, especially at *FLC* chromatin, FLD lacks DNA-binding domains, suggesting that it may require other factors to enable its association with *FLC* DNA/chromatin. Here, we found that FLD is interacting directly with the transcription factor LD (*i.e.* and most likely indirectly with SDG26) for the regulation of *FLC* transcription. Hence, we believe that this interaction may contribute to the FLD binding on DNA.

We also demonstrate that APRF1, an Arabidopsis homolog of the yeast Swd2 COMPASS-associated subunit, was involved in the regulation of *FLC* transcription through the autonomous pathway. In yeast, animal, and plants, the COMPASS complex is conservatively responsible for H3K4 methylation (Miller et al., 2001; Roguev et al., 2001). H3K4 methylation is highly enriched at gene promoter and TSS and positively correlates with transcription initiation (Chandrasekharan et al., 2010; Worden and Wolberger, 2019). Recently, the paralog of APRF1/S2La, S2Lb was identified as a COMPASS complex component in Arabidopsis since it co-purifies with the main COMPASS subunit WDR5a . The mutation of *S2Lb* resulted in the global loss of H3K4me2/me3 and caused pleiotropic

phenotypes, including small leaf size, shorter roots, decreased fertility, deficient dormancy, and early flowering. On the contrary to *s2lb* mutant, the *aprf1*/*s2la* mutant we analyzed here presented subtle phenotypic changes, including an inversely late-flowering phenotype, and no drastic changes in global H3K4 methylation level (Fiorucci et al., 2019; Kapolas et al., 2016). Despite the absence of global changes, we found in our chip analyses that H3K4me3 and H3 acetylation were enriched towards the coding region and 3'-end of *FLC* in the *aprf1-9* mutant (Figure 42B & 42C). Together, whether APRF1 is also working as a COMPASS component will require further investigation, but in any case, APRF1 functions differentially then its paralog S2Lb. In yeast, Swd2 is a component of two very different complexes: the COMPASS complex and also the cleavage and polyadenylation factor (CPF), suggesting a role not only in H3K4 methylation, but also during transcription termination for the cleavage and subsequent polyadenylation during 3' processing of messenger RNA precursors (Cheng et al., 2004; Dichtl et al., 2004; Lee et al., 2007; Vitaliano-Prunier et al., 2008). Whether APRF1 function like Swd2 as a component of CPF remains an open question in Arabidopsis.

COOLAIR, a group of long antisense RNAs expressed from the *FLC* locus, has a vital role in mediating *FLC* expression in non-vernalized plants (Liu et al., 2010; Marquardt et al., 2014; Wang et al., 2014). Interestingly, in addition to the enrichment of active marks observed around the TSS, we also detected an enrichment of active marks (*i.e.* especially of H3K4me3) close to the transcription termination site (TTS) of *FLC*, nearby the *COOLAIR* promoter. Also, *COOLAIR* transcript analyses in *sdg26*, *fld* and *fld sdg26* further indicate the involvement of SDG26, similarly as FLD, in coordinating the COOLAIR poly(A) decision necessary for the transcriptional regulation of *FLC*. Together, in addition to being involved in the repression of *FLC* sense transcription by promoting H3K27me3, we proposed SDG26 and FLD being involved, probably inside a complex with LD, in regulating the usage of proximal *COOLAIR* CLASS I transcript. Involving LD in this process will require further experiments, including the measurement of *COOLAIR* transcript and *COOLAIR* splicing in the *ld* mutant in combination or not with *sdg26* and *fld*.

The *sdg26* mutant displayed a decrease in H3K27me3 at *FLC* chromatin, which is in line with the decrease observed in most autonomous pathway mutants (Doyle and Amasino, 2009; Tian et al., 2019; Wu et al., 2015; Yu and Michaels, 2010). The H3K27 methyltransferase CLF was recently found to interact with the autonomous pathway

protein FCA to deposit H3K27me3 along *FLC* chromatin, further supporting PRC2 and autonomous pathway components acting together for the repression of *FLC* transcription (Tian et al., 2019). Also related to the autonomous pathway, the late-flowering phenotype resulting from the mutation of *FLD* was found suppressed when combined with the *clf-59* mutant (Doyle and Amasino, 2009). Likewise, introgressing *clf-59* into *ld-3* or *fca* also suppressed the late-flowering phenotype of *ld-3* or *fca* (Jiang et al., 2008; Doyle and Amasino, 2009). ChIP analyses further showed that the mutation of *FLD* partially hinder the enrichment of CLF at *FLC* chromatin mutant (Doyle and Amasino, 2009) and similarly as for *clf fca*, *clf fld* or *clf ld*, *FLC* was found synergistically increased in *sdg26-1 clf-29* (Berr et al., 2015). Because we found that FLD and SDG26 genetically and molecularly contribute together with LD to repress *FLC* transcription, all these data suggest that the complex we identify, including at least LD, FLD, and SDG26, may cooperatively regulate *FLC* together with the PRC2 methyltransferase CLF.

In conclusion, our work provides pivotal information about the role of SDG26 together with other autonomous pathway components in regulating *FLC* transcription via *COOLAIR*. Based on our results we propose that LD, as a potential central scaffolding protein, may recruit FLD, SDG26, as well as APRF1, to coordinate *COOLAIR* processing and establish a repressive chromatin environment at the *FLC* locus, thus promoting the flowering transition. Surprisingly, the binding of SDG26 to *SOC1* was also found, like the binding of SDG26 to *FLC*, to be dependent on APRF1 and FLD. Furthermore, this dependence was correlated with changes in histone marks at *SOC1*, with a decrease in active marks observed in the different mutant combination between *sdg26*, *aprf1*, *fld*, and *ld*, while the H3K27me3 repressive mark was enriched. Even if further work will be required to determine whether APRF1, FLD and LD bind *SOC1* chromatin, our work emphasizes that SDG26, together with its protein partners regulates both *FLC* and *SOC1* transcription. The positioning of the LD complex we identified in between two genes playing opposite roles on flowering may serve to properly balance the transcriptional regulation between them in order to precisely control flowering time.

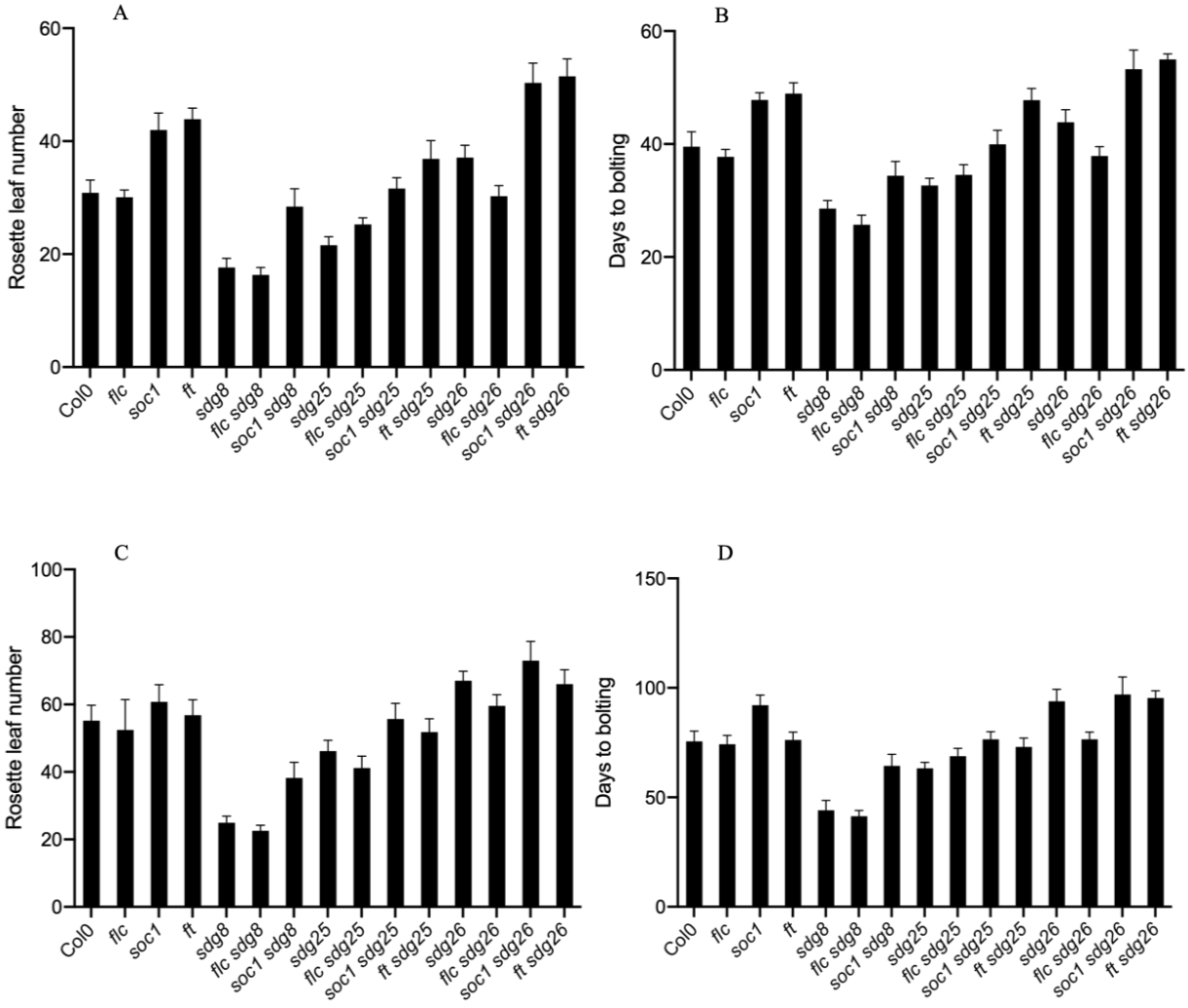

Figure S4: Flowering time analyses of various histone methyltransferase mutants (sdg8, sdg25 and sdg26) alone or in combination with flowering mutant flc, soc1, ft. Flowering time analysis presented as rosette leaf number and days to bolting in wild-type plants and single or double mutants grown under medium-days (MDs) and short-days (SDs). (A-B) MDs, (C-D) SDs. Values are means ± SD of three biological replicates. At least 20 plants were analyzed for each biological experiment.

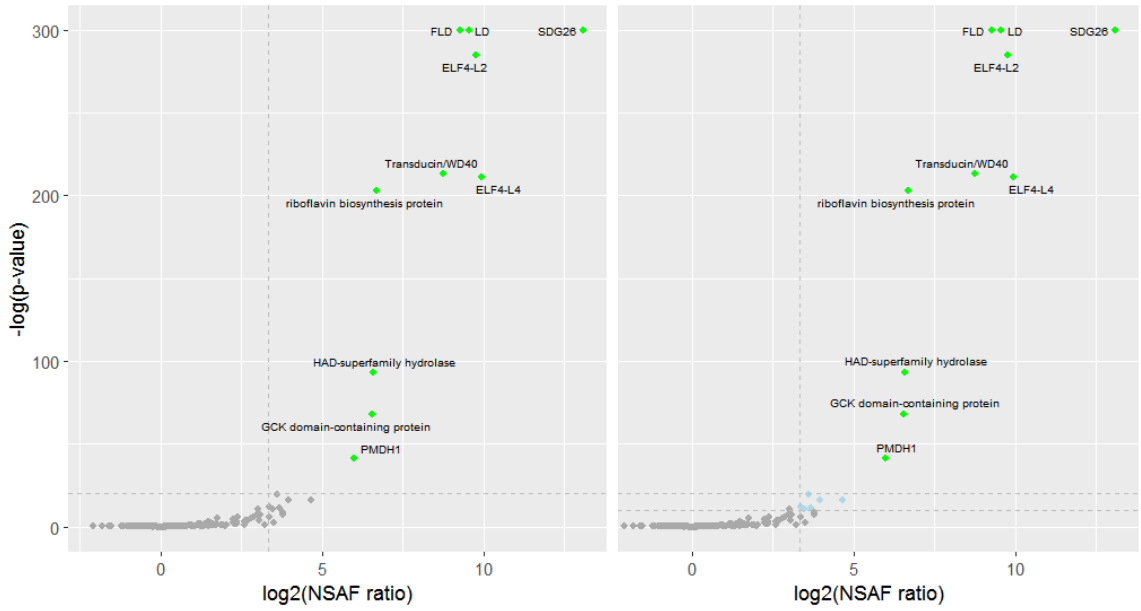

Figure S5: Volcano plot of the observed protein abundance changes quantified by NSAF. The data represents two independent experiments. The proteins significantly enriched with the bait SDG26 are marked by green dots.

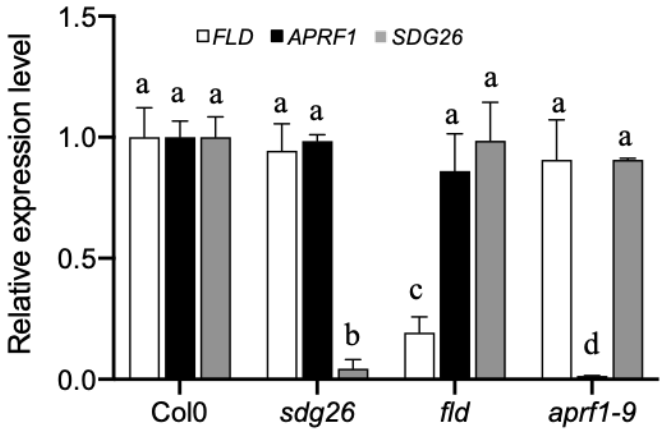

Figure S5: *FLD*, *APRF1* and *SDG26* transcript level in WT, *sdg26*, *fld* and *aprf1-9* mutant plants. The transcript level of FLD, APRF1 and SDG26 were measured by qRT-PCR with 2-week-old seedlings of all genotypes grown on MS medium under long days. The representative mean values ± standard deviation from two biological experiments were normalized to reference genes EXP and Tip 4.1 and relative to Col0 (set as 1). Letters indicate significant differences among sample in Student's *t*-test followed by Benjamini-Hochberg FDR correction ($P < 0.01$).

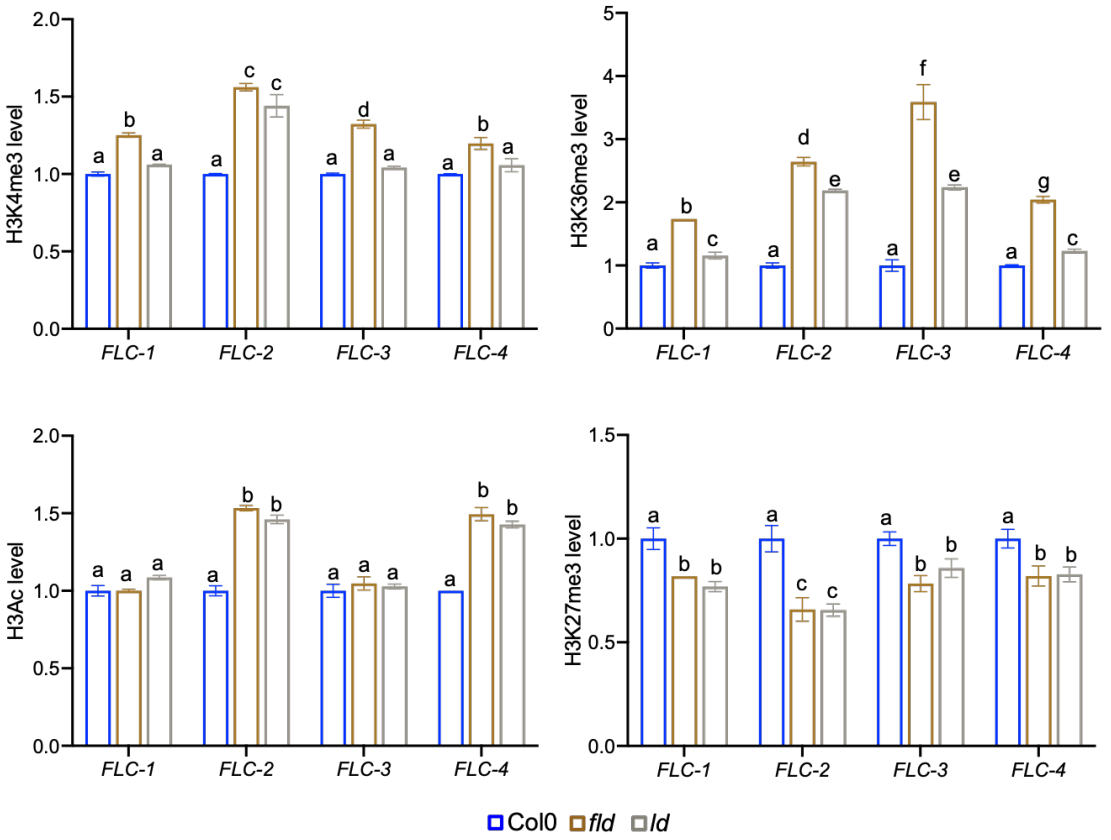

Figure S7: ChIP analysis of H3K4me3, H3K36me3, H3 acetylation and H3K27me3 levels at *FLC* chromatin in WT, *fld*, *ld* plants. Chromatin was extracted from 2-week-old seedlings grown on MS plates under LDs. Data were normalized to Tub2 and presented relative to the value of Col0 at each amplified region. Means value ± SD from two biological replicates are presented. Letters indicate significant differences among sample in Student's *t*-test followed by Benjamini-Hochberg FDR correction ($P < 0.01$).

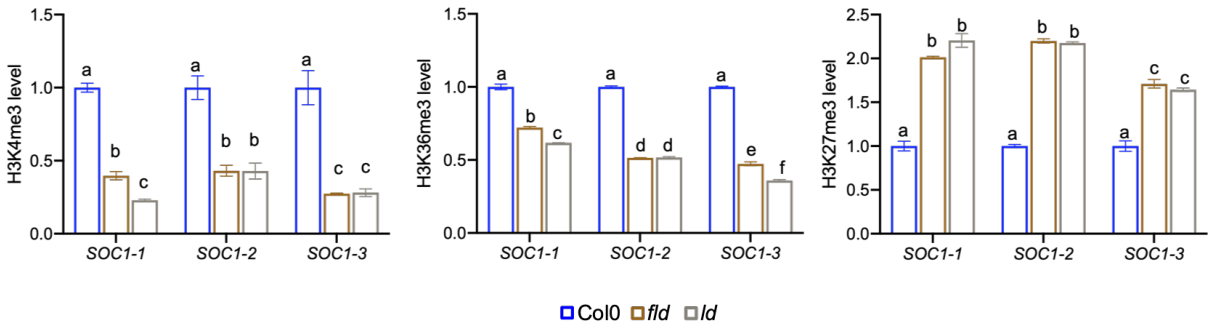

Figure S8: ChIP analysis of H3K4me3, H3 acetylation and H3K27me3 levels at *SOC1* chromatin in WT, *fld*, *ld* plants. Chromatin was extracted from 2-week-old seedlings grown on MS plates under LDs. Data were normalized to Tub2 and presented relative to the value of Col0 at each amplified region. Means value ± SD from two biological replicates are presented. Letters indicate significant differences among sample in Student's *t*-test followed by Benjamini-Hochberg FDR correction ($P < 0.01$).

CHAPTER V

GENERAL CONCLUSIONS AND PERSPECTIVES

During my PhD, I discovered the critical contribution of two TrxG family members

(SDG8 and SDG26) to gene transcription regulation in response to developmental and environmental cues in Arabidopsis.

Firstly, by discovering the hypersensitivity to the hemibiotrophic pathogen *Pseudomonas syringae* and the changes in salicylic acid (SA) accumulation in *sdg8* mutant, we further characterized the involvement of the H3K36-methyltransferase SDG8 in the SA-mediated defense pathway. We demonstrated that SDG8, through its methyltransferase activity, positively control the transcript level of *NPR1*, a central player in the SA-related signaling pathways, and cooperates with the RNAPII to enable the efficient transcriptional induction of the defense genes *PR1* and *PR2* upon stimulation. However, whether H3K36me3 serves as an epigenetic memory mark in immune priming requires more investigations in future. SDG8 is known to regulate multiple developmental processes, such as flowering time (Zhao et al., 2005) and the endogenous SA level was reported to affect flowering time (Jin et al., 2008; Wang et al., 2011; Villajuana-Bonequi et al., 2014). Given the abnormally high basal endogenous SA level and the mis-regulation of several SA related-genes in *sdg8*, we speculate that SDG8 might be involved in controlling the balancing between development and immunity for the long-term fitness. However, how SDG8 is specifically targeted to one or another process remains so far unknown and may constitute a future investigation point.

Secondly, we have focused on SDG26, another methyltransferase grouped by phylogenetic analysis in a clade together with the H3K36-specific histone-methyltransferases so far found in fungi and mammals (Xu et al., 2008). Using Arabidopsis, we found that SDG26 is involved in response to abiotic stresses such as cold, drought, or salt, again highlighting the contributions of histone methyltransferases in response to stresses in plants. By focusing on cold stress, we discovered that SDG26 regulates the cold stress response by directly activating the transcription of *SOC1* and *CBF* genes through binding their chromatin and depositing H3K36me3. We also found that SDG26 controls the accumulation of ABA by regulating the expression of ABA homeostasis-related genes. Cold acclimation has been extensively investigated and can result in increased freezing tolerance in Arabidopsis. Surprisingly, while SDG26 seems to regulate the cold stress response positively, we found that the *sdg26* mutant was more tolerant to freezing. This finding indicates a decoupling between these two processes in the *sdg26* mutant. Because several metabolites (including polyamines, polyols, and soluble sugars) are known to contribute to freezing tolerance (Krasensky and Jonak, 2012;

Tarkowski and Van den Ende, 2015), it would be interesting to analyze the *sdg26* metabolome. SOC1 was previously proposed to act as a repressor of *CBF* genes in cold stress (Seo et al., 2009). In this part, we found that SDG26 can bind at both *SOC1* and *CBFs* chromatin. Interestingly, in the third part of my thesis, SDG26 was also found to be able to bind the chromatin of the floral repressor *FLC*, which is known to repress the transcription of *SOC1* directly. Together, these results may reflect a more complex regulatory process than the simple linear interaction between a repressor and its gene targets. Hence, it would be highly informative to investigate the genome-wide targets of SDG26 with or without stress. Finally, the phytohormone ABA is known to mediate the adaptation to environmental stress in plants, and ABA was reported to accelerate flowering (Hwang et al., 2019; Sah et al., 2016). Thus, the low abundance of ABA in *sdg26* and the positive function of SDG26 on flowering may indicate the involvement of SDG26 at the junction between abiotic stress and flowering.

Lastly, using a genetic approach, we confirmed SDG26 as a component of the autonomous pathway. Using different protein-protein interaction approaches, together with genetic and molecular analysis in different flowering mutants, we demonstrated the involvement of SDG26 in a multi-protein complex including the histone demethylase FLD (known as a classical autonomous pathway component), the homeobox-domain transcription factor LD (also known as a classical autonomous pathway component), as well as a putative COMPASS component APRF1. This complex was proposed to coordinate the *COOLAIR* processing to establish a repressive chromatin environment necessary for the transcriptional repression of the central flowering repressor *FLC*. Apart from regulating *FLC* transcription, SDG26 is known to directly regulate the transcription of floral activator *SOC1,* a downstream target of FLC, by binding its chromatin and deposit H3K4me3 and H3K36me3 (Berr et al., 2015). Surprisingly, we found that the SDG26 enrichment at *SOC1* chromatin requires the same protein partners as for its enrichment at the *FLC* chromatin. However, whether the transcription of *SOC1* is controlled mostly through SDG26 or the whole complex is not clear yet and further ChIP analyses will be required to test the binding of LD, FLD and APRF1 at *SOC1* chromatin. Based on our data available, we propose that SDG26 may control the transcription of both *FLC* and *SOC1* to precisely regulate the floral transition.

Through my PhD, I got useful insights about the contribution of two different histone methyltransferases at the junction between stress and flowering time regulation.

This work thus perfectly illustrates the position of histone methyltransferases at the junction between stress response and developmental transition to control the balance between these ‘external’ and ‘internal’ processes for the long-term fitness of the plant.

CHAPTER VI

MATERIALS AND METHODS

VI.1. Materials

VI.1.1. Plant Materials and growth conditions

All Arabidopsis seeds I used in my study are from Columbia ecotype background. Mutants *sdg26-1* (Xu et al., 2008), *sdg25-1* (Berr et al., 2009), *sdg8-1*(Xu et al., 2008), *soc1-2* (Lee, 2000) and *clf-29* (Xu et al., 2008) have been described previously, and *ft-10* (GK-290E08) is ordered from the Arabidopsis Biological Resource Center (ABRC, http://www.Arabidopsis.org). Kosmas Haralampidis (Molecular Plant Development, National and Kapodistrian University of Athens) kindly provided *aprf1-7*, *aprf1-9*, and the *35S:APRF1- FLAG* transgene line. *fld-6* is a T-DNA insertion line, kindly provided by Keqiang Wu (Institute of plant biology, National Taiwan University), and the *FLD:FLD-FLAG* transgene line kindly provided by Yuehui He (Temasek Life Sciences Laboratory, Singapore). *ld-1* is a point mutation line, kindly provided by Ilha Lee (School of Biological Sciences, Seoul National University), And *flc-3* kindly provided by Patrick Achard (IBMP, Strasbourg university). All other genotypes described in this thesis are generated by genetic crosses or Agrobacterium-mediated transformation, and homozygotes were characterized by antibiotic resistance selection and/or PCR-based genotyping using specific primers.

VI.1.2. Bacterial strains

Escherichia coli strain TOP10 was used for plasmid construction and *Agrobacterium tumefaciens* strain GV3101 was used for plant transformation.

VI.1.3. Vectors and plasmid constructs

The vectors used in this thesis are listed in Table 1-3-1 and different transgenes cloned in the entry vector are listed in Table 1-3-2. The cloning was performed by following the instructions from the GATEWAY® cloning system (Invitrogen™).

Table 1-3-1 List of empty vectors

Name	Selection in bacteria	Application
Entry vectors		
pDONR_207	Gentamycin	Gateway cloning
pDONR_221	Kanamycin	Gateway cloning
pDONR/Zeo	Zeocin	Gateway cloning
Destination vectors		
pGWB21	Kanamycin	Gateway cloning
pGWB29	Kanamycin	Gateway cloning
pGWB11	Kanamycin	Gateway cloning
pGWB14	Kanamycin	Gateway cloning
pGWB604	Spectinomycin	Gateway cloning
pGWB619	Spectinomycin	Gateway cloning
pB7FWG2.0	Spectinomycin	Gateway cloning
pB7RWG2.0	Spectinomycin	Gateway cloning
pEarleygate 302	Kanamycin	Gateway cloning
pEarleygate 203	Kanamycin	Gateway cloning
pGADT7	Ampicillin	Gateway cloning
pGBKT7	Kanamycin	Gateway cloning

Table 1-3-2 List of created entry clones in this study

Name
35S promoter and SDG26-genomic DNA in pDONR_207/ pDONR/Zeo
35S promoter and SDG26 cDNA with/without stop codon in pDONR 221/ pDONR_207
35S promoter and alternative SDG26 cDNA without stop codon in pDONR 221/ pDONR_207
35S promoter and FLD cDNA with/ without stop codon in pDONR_207

35S promoter and LD cDNA with/without stop codon in pDONR_207
35S promoter and APRF1 cDNA with/without stop codon in pDONR_207
35S promoter and ELF4like4 cDNA with/without stop codon in pDONR_207
35S promoter and ELF4like2 cDNA with/without stop codon in pDONR_207

VI.1.4. Transgenes and transgenic plant selection

Tag-fused *SDG26* transgenes, transgenic plant selection marks and antibiotics are listed in Table 1-4.

Table 1-4 List of created transgenic lines

Name	Selection in medium/soil	Description
35S:gSDG26-GFP	hygromycin	transgenic lines with GFP tag
SDG26:gSDG26-10MYC	hygromycin	transgenic lines with MYC tag
35S:cSDG26-GFP	Basta	transgenic lines with GFP tag
35S:GFP-cSDG26	Basta	transgenic lines with GFP tag
35S:MYC-cSDG26	Basta	transgenic lines with MYC tag

VI.1.5. Antibodies

All antibodies used in this thesis are listed in Table1-5.

Table 1-5 Antibodies

Name	Company (Cat. #)	Purpose
Primary antibodies		
anti-H3	Abcam (ab12079)	WB, ChIP
anti-H3K36me3	Abcam (ab9050)	WB, ChIP

anti-H3K36me1	Abcam (ab9048)	WB, ChIP
anti-H3K4me3	Merck Millipore (07-473)	WB, ChIP
anti-H3K27me3	Merck Millipore (07-449)	WB, ChIP
anti-FLAG	Sigma-Aldrich (3165)	WB, ChIP
anti-H3 acetylation	EMD Millipore (06-599)	WB, ChIP
anti-MYC	Sigma-Aldrich (C3956)	WB, ChIP
anti-GFP	Abcam (ab290)	WB, ChIP
anti-GFP	Sigma-Aldrich (11120)	WB, ChIP
Secondary antibodies		
anti-rabbit-HRP	Sigma-Aldrich (A9169)	WB
anti-mouse-HRP	Thermofisher (62-6520)	WB

VI.1.6. Primers

Sequences of primers used for genotyping are listed as follows, those for quantitative RT-PCR in **Table 1-6-1**, those for Chromatin Immunoprecipitation (ChIP) in **Table 1-6-2**, and those for in situ hybridization in **Table 1-6-3**.

Table 1-6-1

Name	**Sequence**
SDG26.1-LP	5'-TTTACATGCTTTGCCGGTTAC-3'
SDG26.1-RP	5'-CTTTCTCGCAAGATCCATGAC -3'
SDG8.1-LP	5'-CCTTCATCGCAATCGTAAATC-3'
SDG8.1-RP	5'-TTTTGCGCTAAACTAGTTGGG-3'
SDG25.1-LP	5'-TCTTGTGACAGGTGCAACTTG -3'
SDG25.1-RP	5'-AAACAAAGCTAGGCACAAGGC-3'
SDG8.2-LP	5'-GCTGGGGGTTTATGTAGGAAG-3'

SDG8.2-RP	5'- CACTGTCCAGTAAAAGCTGGC-3'
FRIGIDA-F	5'-TGATAAGGATGAGTGGTTCGAATG-3'
FRIGIDA-R	5'- CAACAAAAGGAACCACCTTTGC-3'
FLC3-F	5'-GGCGGAGACGACGAGAAGAGC-3'
FLC3-R	5'-GTTCAATCCGTATCGTAGGGGAGG-3'
SOC1-2537	5'-GGATCCATGGTGAGGGGCAAAACTC-3'
SOC1-2538	5'-CTGAAACATCTGATCAAAAGCTG -3'
SOC1-2539	5'-TTGGGTTCACGTAGTGGGCCATCG-3'
FT-JH2295	5'-TAAGCTCAATGATATTCCCGTACA-3'
FT-JH2296	5'-CAGGTTCAAAACAAGCCAAGA-3'
FT-JH2297	5'- CCCATTTGACGTGAATGTAGACAC -3'
CLF-LP	5'- AAGAAACTTGCTAGTTCCGCC -3'
CLF-RP	5'- GAGGCATTGACTTTGATTTGC -3'
FLD-LP	5'- ACTGAGGATCCGAACTATCG-3'
FLD-RP	5'- ATGCATGGTTGCAGGGTATC-3'
LD-F	5'-GCTGGGTAGCTTTCATCAATGCCA-3'
LD-R	5'-GAATATCTTCCTGTTACGACACG-3'
APRF1.7-LP	5'- AGTTGCGTATGACCAACAAGG-3'
APRF1.7-RP	5'-TAAGGCCCAATATGCTCATTG-3'
APRF1.9-LP	5'-GTTTTTCGAGCAAAGGGAAAG-3'
APRF1.9-RP	5'-ACAGGGTACACCCATAGAGGC-3'
LBb1.3	5'- ATTTTGCCGATTTCGGAAC-3'

Table 1-6-2

Name	**Sequence**
SDG26-F	5'-AGTGCGTTGTCTCTGTGGTG-3'
SDG26-R	5'-TCGTCACCATCCTCCCATAC-3'

SDG26 splicing variant-F	5'-AGTGCGTTGTCTCTGTGGTG-3'
SDG26 splicing variant-R	5'-TAAGCTCGTCCTCGATCGTC-3'
FLD-F	5'-CGAGCGAACTGGTCGCAAGC -3'
FLD-R	5'-TGCTTCAGCGGCAACGGTCC-3'
APRF1-F	5'-GCCACCTTCACACCAGATG-3'
APRF1-R	5'-CAGCAACGAACATGGCTCTA-3'
LD-F	5'-GTCTCTCAAATGGAAAGTCAGAG-3'
LD-R	5'-CCTGCGTTCTTTGTTATACGATG-3'
MAF1 -F	5'-GGAAAGAATACGTTGCTGGCAACA-3'
MAF1 -R	5'-CCGTTGATGATGGTGGCTAATTGA-3'
MAF2-F	5'-GGCTCCGGAAAACTCTACAA-3'
MAF2-R	5'-TTCTGCAAGATCTAAGGCTTCA-3'
MAF3 -F	5'-ACAGAACTAATGATGGAGGATATGAA-3'
MAF3-R	5'-CTTCTTCCCCACCTGGCTA-3'
MAF4-F	5′-TGGCCAAGATCCTCAGTCGTTATGA-3′
MAF4-R	5′-GCTGCTCTTCCAGGGACTTTAGACA-3′
MAF5-F	5′-GATGGAGCTTGTGAAGAACCTTCAGG-3′
MAF5-R	5′-CAGCCGTTGATGATTGGTGGTTACTTG-3′
FLC-F	5'-CTAGCCAGATGGAGAATAATCATCATG-3'
FLC-R	5'-TTAAGGTGGCTAATTAAGTAGTGGGAG-3'
FT-F	5'-CTTGGCAGGCAAACAGTGTATGCAC-3'
FT-R	5'-GCCACTCTCCCTCTGACAATTGTAGA-3'
SOC1-F	5'-AGCTGCAGAAAACGAGAAGCTCTCTG-3'
SOC1-R	5'- AAGAACGTACTTGGAGCTGGC-3'
ELF4-F	5'-CGACAATCACCAATCGAGAA-3'
ELF4-R	5'-CAAAGCAACGTTCTTCGACA-3'
FLC Proximal-F	5'-TTTTTTTTTTTTTTACTGCTTCCA-3'

FLC Proximal-R	5'-CACACCACCAAATAACAACCA-3'
FLC Distal-F	5'-TTTTTTTTTTTTTTTGCGGTACAC-3'
FLC Distal-R	5'-GGGGTAAACGAGAGTGATGC-3'
Total COOLAIR-F	5'-TGTATGTGTTCTTCACTTCTGTCAA-3'
Total COOLAIR-R	5'-GCCGTAGGCTTCTTCACTGT-3'
Int1-RT	5'- CTGCTGGACAAATCTCCGACAATC -3'
Int1_unspliced_LP	5'-CGACAATCTTCCGGTGACTCT-3'
Int1_unspliced_RP	5'-TACAAACGCTCGCCCTTATC-3'
Int1_spliced_LP	5'-GACAAATCTCCGACAATCTTCC-3'
Int1_spliced_RP	5'-CTCACACGAATAAGGTGGCTAAT-3'
Class II unspliced F	5'-TCGCTCTTCTCGTCGTCTC-3'
Class II-1_LP	5'-CTCCTCCGGCGATAAGTA-3'
Class II-1_RP	5'-CTCACACGAATAAGAAAAGTAAAA-3'
Class II-2_LP	5'-CTCCTCCGGCGATAAGTA-3'
Class II-2_RP	5'-ACGATAATCATAGAAAAGTAAAAGAGC-3'
Class II unspliced R	5'-AAAACACAAACAAACACAGAACC-3'
UBC-F	5'-CTGCGACTCAGGGAATCTTCTAA-3'
UBC-R	5'-TTGTGCCATTGAATTGAACCC-3'
Tip4.1-F	5'-GTGAAAACTGTTGGAGAGAAGCAA-3'
Tip4.1- R	5'-TCAACTGGATACCCTTTCGCA-3'
GAPDH -F	5'-TTGGTGACAACAGGTCAAGCA-3'
GAPDH-R	5'-AAACTTGTCGCTCAATGCAATC-3'
TUB2.2-F	5'-GACATCCCACCTACTGGTCTGAA-3'
TUB2.2-R	5'-CTCGCCTGAACATCTCTTGGA-3'
CYP707A1-F	5'-TTGTTTCTCACTCTCTTCGCCGGA-3'
CYP707A1-R	5'-AAGTTTCTCCGACGTAAGGCCAAC-3'
CYP707A2-F	5-TCCTCCAAACCCTTTCCTCTTGGA-3'

CYP707A2-R	5'-CTTTGAAAGAAGTGAGGCCCGCAA-3'
CYP707A3-F	5'-GGCGGCTCTGTTTCTCTGTTTACT-3'
CYP707A3-R	5'-TTGGAATGTTTCGCCGACGTAAGG-3'
CYP707A4-F	5’-TCGAGCACATTGCCCTTTCTTCCT-3'
CYP707A4-R	5’-CCACATCAAAGGCGAACTGCAAGA-3'
NCED2-F	5’-GCGTGCATTAATCTCACACGAGCA-3’
NCED2-R	5’-ATGCAGTCAGGGATTGTTCCTTCG-3’
NCED3-F	5’-GGAATCCGGTGAACTCTTCGCTTT-3’
NCED3-R	5’-AAACGACTTGCTGGTCAGGTACGA-3’
NCED5-F	5’-TTCGCCGTCATCCTCCGTTAGTTT-3’
NCED5-R	5’- AGGGTTCCAACGGGAAGTGTCTTT-3’
NCED6-F	5’-GGCTACGATGCTCGACAAGATTGA-3’
NCED6-R	5’-AACCGGACATTCATTAACCGGAGC-3'
NCED9-F	5’-TCTCCGACATTCAAACCACCGTCT-3’
NCED9-R	5’-GCTCGTGTGAGATCATGGCGTTT-3
ABA1-F	5'-TGGGTGCAGATGGCATTTGGTCTA-3’
ABA1-R	5'-CCACCACCAACATCCGAAGAAACA-3’
ABA2-F	5'-CTCGCTTTGGCTCATTTGC-3'
ABA2-R	5'-CCGTCAGTTCCACCCCTTT-3'
ABA4-F	5'-AATGACTCTTGCTTCTGCTTGGAT-3'
ABA4-R	5'-GCTTTGGTTACGAAATGCGAAACGAT-3'
AAO3-F	5'-TGGAAGTGGACCTTGTGACAGGAA-3’
AAO3-R	5'-AACCCGATGCCTTGAACAAATGCTCC-3’
BCG25-F	5’-CGCCATGGCTTACTTTGAATCCGT-3’
BCG25-R	5’-TGTATCATAAGCCGTGACCAGCGT-3’
BCG40-F	5’-ATGTTCTGGGACCTTGGAGGCAAA-3’
BCG40-R	5’- AGCATAAGGCATGGCGGAGTACAT-3’

AtBG1-F	5’-ACAAGGCGAGGTTCGGACTTTACT-3’
AtBG1-R	5’-AGTTCTTCCCTCAGCTTGGAGGTT-3’
CBF1-F	5’-TCTCATCTTGAAAAGCCAACG-3’
CBF1-R	5’-AATCCCGGAGTCAACATGC-3’
CBF2-F	5’-GGTCTTGACATGGAGGAGACC-3’
CBF2-R	5’-AAAGGGTTTGCTCCTGGTTT-3’
CBF3-F	5’-TCCACTGTACGGACGGAAG-3’
CBF3-R	5’-TGCCGAGTTTGTTGGCTAAT-3’
COR15A-F	5’-GTTTGCGGCTTCTTTTCCT-3’
COR15A-R	5’-ACCGCAGATACATTGGGTAAA -3’
COR15B-F	5’- ACCTCAACGAAGCCACAAA -3’
COR15B-R	5’-CTTTTGTTTTCTCGCCATCC-3’
KIN1-F	5’-CTCCAGCTCCAGCACCAG-3’
KIN1-R	5’-GCTGGCAAAGCTGAGGAG-3’
KIN2-F	5’-ACTGCCGCATCCGATATACT-3’
KIN2-R	5’-GGCAAAGCTGAGGAGAAGAG-3’
COR29A-F	5’-GAAGATGATGATGATGACGAGC -3’
COR29A-R	5’-TCAGTGGGTTTGGTGTAATCG -3’
COR29B-F	5’-GAGTTGAAGATTCTGGGAACTGAAG -3’
COR29B-R	5’-GTTCACAAACAGAGGCATCATACA-3’
RD22-F	5’-CCGGTAAAAGAACCGACGTA-3’
RD22-R	5’-AAAGGGTTTGCTCCTGGTTT-3’
PR1-F	5’-TTCTTCCCTCGAAAGCTCAA-3’
PR1-R	5’-AAGGCCCACCAGAGTGTATG-3’
PDF1.2-F	5’-CACCCTTATCTTCGCTGCTCTT-3’
PDF1.2-R	5’-TACACTTGTGTGCTGGGAAGAC-3’
ARR7-F	5’-TTGTGGATCGTAAAGTCATCG-3’

ARR7-R	5’-CTATCAAATTCACCTTCAAATCC-3’
COR47-F	5’-GAGCGATGAAGAAGGTGAGG -3’
COR47-R	5’-CGGGATGGTAGTGGAAACTG -3’
BZR1-F	5’-AAATGGGAAGGCTCGTGGTT -3’
BZR1-R	5’-ATGGAGAAGGCTTTGGGCAG -3’
ERF1-F	5’-AAAGCAGCTTGATCGTAGGC-3’
ERF1-R	5’-ATTCGACTAGAAACGGTATTAG-3’
ERF2-F	5’- AACTTCCCGTTTTCAGACGA-3’
ERF2-R	5’-CGGTTCGGATCACGTCTAAG-3’
ZAT10-F	5’-TAGTAGCGTGTCCAACTCCGAAG-3’
ZAT10-R	5’- ATTCAGGGATCGGAGGGATG-3’
SZF2-F	5’-CAGAGAGAGTGAATGAGAGGGTTG -3’
SZF2-R	5’-TCTATATACATTTGCTCTGCCCACG -3’
CML24-F	5’-TCTCGGCGAAAGAGCTTCATT-3’
CML24-R	5’-ACAACCATCACCATCAATATCAACT-3’
AT4G34150-F	5’-CTACCCTCCGATCCCTTCA-3’
AT4G34150-R	5’-GGATATGGACCTTGTGGGTAAT-3’
ERF104-F	5’-CGCCGGAAGAGGAGAAGG -3’
ERF104-R	5’- CCACCGGCTCAACCTCAG -3’
ERF105-F	5’-AACGCCATCAAGTTGGAAG -3’
ERF105-R	5’-TCCAAGAGATGGACAAGGAGATA-3’
WRKY22-F	5’-GGTTAGAGGAATTCGCAGC-3’
WRKY22-R	5’-TAGTGGCGGCACTGTTCA-3’
MYB77-F	5’-AAGGACGTAGAGGTGAGTTTATGAC-3’
MYB77-R	5’-ACGACGAATCCACCACTTG-3’
ERF4-F	5’-CCTGTGACATCGGCGTTT-3’

ERF4-R	5’-AAATCAACGACCGATGACGAAT-3’
SZF1-F	5’-AGATGAGAAGAAGTGTTTCCTTTGG-3’
SZF1-R	5’-TTAACCCATGACACATCTGGCT-3’
CCA1-F	5’-GGTGGACTGAGGAAGAAC-3’
CCA1-R	5’-GGAGAAAAATTTCTGAGCGTGAC-3’
EPF1-F	5’-ATGCCGTCTTGTGATGGTTAG-3’
EPF1-R	5’-TCAAGGGACAGGGTAGGACTT-3’
EPF2-F	5’-CGCCGCGTGTTCTTTGGTCG-3’
EPF2-R	5’-CGGCGTTTTTCTTT TCTCCGCCA-3’
CAMTA3-F	5’-CTGGGCCTTAGAACCAACAATAA-3’
CAMTA3-R	5’-ACCATTTACATCGCGAAAATCA-3’
HOS1-F	5’-GCACAAGGATGCAACCAGAC-3’
HOS1-R	5’-TTGTTTCATCTGACCGCCAT-3’
ZAT12-F	5’-CCTTAGGAGGTCACCGTGC-3’
ZAT12-R	5’-CAAGCCACTCTCTTCCCACT-3’
SIZ1-F	5’-ATAGCGCCTCTGGGAATCAT-3’
SIZ1-R	5’-GCCTTGTCTTGTCTACTGTCATTCATAC-3’
EIN3-F	5’-TGAGATGGGAATGTGTGGAAAC-3’
EIN3-R	5’-GAGCTCTAGACATTTTCTTCCT-3’
BRII-F	5’-CCGTGTACTTTCGATGGCGTTA-3’
BRII-R	5’-GAGAGACAGGAGAGACGAGGAC-3’
ICE1-F	5’-GTTTGCCTTGGATGTTTTCC-3’
ICE1-R	5’-GCTTTGATTTGATCAGGCAGT-3’
MYB15-F	5’-GGATTCGAGGTTTCTTCGATGACACT-3’
MYB15-R	5’-GGATTCCCCGGGCTAGAGCCCGGCTAAGAGATCTTG-3’
BAK1-F	5’-GTCAGAAAGTAGTGTCGCCA-3’

BAK1-R	5’-ACTTGTAGCGTCAGGACAGC-3’

Table 1-6-3

Name	Sequence
FLC1-F	5'-ATTTAGCAACGAAAGTGAAAACTAAGG-3'
FLC1-R	5'-GCCACGTGTACCGCATGAC-3'
FLC2-F	5'-AGAAATCAAGCGAATTGAGAACAA-3'
FLC2-R	5'-CGTTGCGACGTTTGGAGAA-3'
FLC3-F	5'-CCGCCACATCATCATTATCATC-3'
FLC3-R	5'-ACAAGGTTTTTTCCAGCGATAGA-3'
FLC4-F	5'-CATCATGTGGGAGCAGAAGCT-3'
FLC4-R	5'-CGGAAGATTGTCGGAGATTTG-3'
FLC5-F	5'-TTTTTGGGCCTATGTCGGTCA-3'
FLC5-R	5'-GGTCGGTCACGTTAACAGCA-3'
SOC1-1-F	5'-AGCAGAGAGAGAAGAGACG-3'
SOC1-1-R	5'-GAAGTAGCTTTCCTCGTTTCAT-3'
SOC1-2-F	5'-GCATCCTTCAATTAAACCGATAAC-3'
SOC1-2-R	5'-AAGTCAACGAAAGATTAAGTACCC-3'
SOC1-3-F	5'-TGGATTTGATTGGCCTTTTGTGGAA-3'
SOC1-3-R	5'-AGCCCTAATTTTGCAGAAACCAAG-3'
SOC1-4-F	5'-GCAGCTCAAGCAAAAGGTAAAGTAG-3'
SOC1-4-R	5'-GCACAAGAGGCTTACTTACTTGGAA-3'
FT-1-F	5'-GCATGCGAAAATCTAGTGGAAGA-3'
FT-1-R	5'-GTCGCATAATGTTCGCAACCT-3'
FT-2-F	5'-AGAGGGTTCATGCCTATGATAC-3'
FT-2-R	5'-CTTTGATCTTGAACAAACAGGTG-3'
FT-3-F	5'-GCCAGCCTTTAAGATACTCTCTGCTA-3'
FT-3-R	5'-TGAGATAACACAAGAAAGAAGAAGAAAACT-3'
CBF1-P1-F	5'-AGTCCTGTCCTGGTCCATTTACAT-3'
CBF1-P1-R	5'-AATTATCAATTTCGATGGACGGTT-3'
CBF1-P3-F	5'-GTAACAACAGCAGCCAGCCAA-3'
CBF1-P3-R	5'-CACGGAGTTTTTGTCTCTGTGAAT-3'

CBF1-C1-F	5'-GCATGTCTCAACTTCGCTGA-3'
CBF1-C1-R	5'-ATCGTCTCCTCCATGTCCAG-3'
CBF2-P1-F	5'-ACAAACCCTATCTTGTCTCTCACA-3'
CBF2-P1-R	5'-GAGAAATGAGAACACAAGTTGCTT-3'
CBF2-C1-F	5'-TGACGTGTCCTTATGGAGCTA-3'
CBF2-C1-R	5'-CTGCACTCAAAAACATTTGCA-3'
CBF3-P2-F	5'-ATTAGCAGTCTATTTAGGGTTTTC-3'
CBF3-P2-R	5'-ACGTAAGTCACCAAGTAGTTTTG-3'
CBF3-P3-F	5'-AGGATGTGCTATAAGAATGGGAGA-3'
CBF3-P3-R	5'-GTATGAATGTGTGGCTGTTAAGGA-3'

Oligonucleotide probes used for in situ hybridization in Table 1-9 (below)

SDG26cds-F1	5’-AAGGCAGAGTTTGATCTTTACTCTAGT-3’
SDG26cds-R1	5’-CAAACGTGAAAAGTAAACCAAGTTAG-3’
SDG26cds-F2	5’- GGAAGCAGGAAACGAAGACCATATT-3’
SDG26cds-R2	5’- TAAATTTCAACAAAATGTTCTCAT -3’

Hormone and other chemical products used for thesis are listed in Table 1-9 (below)

Name	Company (Cat. #)
ABA	Sigma-Aldrich, A1049
KINETIN	Sigma-Aldrich, K3378
Methyl jasmonate	Sigma-Aldrich, 392707
Salicylic acid	Sigma-Aldrich, S5922
cOmplete™ Protease Inhibitor Cocktail	Roche
PMSF	Thermo Fisher, 36978

VI.2. Methods

VI.2.1. Plant Methods

VI.2.1.1. Seeds sterilization

Arabidopsis seeds were surface-sterilized by steaming with chlorine gas: seeds in the opened 1.5 ml Eppendorf tubes were placed in a desiccator, and a beaker with 200 ml JAVEL was put beside Eppendorf tubes. Next, 5 ml 37% hydrochloric acid was added to the beaker and closed the lid quickly. The closed desiccator was kept in a fume hood for 5 hours.

Alternatively, by submerging with ethanol: seeds in 2 ml Eppendorf tubes were placed on the rotating wheel with 70% ethanol for 10 min, followed by rinsing twice with 96% ethanol. Then, ethanol was removed and seeds were placed in the super clean hood to dry.

VI.2.1.2. Plant growth conditions

Plants were grown in soil under long days (LDs; in 16 h light: 8 h dark), medium days (MDs; 12 h light: 12 h dark) or short days (SDs; 8 h light: 16 h dark) photoperiod conditions in the greenhouse. For in vitro plant growth, seeds were spread on plates containing MS (Murashige and Skoog) medium (MS salts, 1% sucrose, pH5.8, 0.8% agar). After 3 days stratification at 4°C, the plates were transferred to a growth chamber at 22°C under long-day photoperiod conditions.

VI.2.1.3. Seed germination test

About 100 seeds were sown on MS medium plates supplemented with or without indicated hormones, and stratified at 4°C for 3 days. Then the plates were incubated in the LDs growth chamber at 21°C (16 hours light/8 hours dark). Germination rate was tracked by daily counting the number of seeds within radicle protruded beyond the testa. Three replicates were performed.

VI.2.1.4. Root growth test

Seeds were sown on MS medium plates. After stratification at 4°C for 3 days, the plates

were incubated in the LDs growth chamber at 21°C for 3-4 days. Then the seedlings were transferred to new MS medium plates supplemented with or without a particular concentration of ABA, and the root length was marked. Next, the plates were incubated vertically, and the root length was measured 10 days after.

VI.2.1.5. Genetic crossing of Arabidopsis plants

Anthers in the selected flowering buds from a "recipient" plant were removed using forceps. Two days after emasculation, stigmas were pollinated with pollens from a donor plant. Pistils/siliques will become lengthen with successful pollination. Seeds (F1) were harvested after silique dried.

VI.2.1.6. Arabidopsis transformation

The binary vectors were introduced into *Agrobacterium tumefaciens* GV3101, then the bacteria were used to transform *Arabidopsis thaliana* by using a slight modified floral-dip protocol, previously described (Zhang et al., 2006). Briefly, the first bolts of Arabidopsis plants grown under LDs were removed to make more secondary inflorescences. When plants generated several flower buds, they are ready for *Agrobacterium*-mediated transformation. *Agrobacterium* cells were prepared from a single colony inoculated in 4 ml LB containing appropriate antibiotics and grown at 28 °C for two days. The culture was then amplified in 400 ml LB with the same antibiotics and continued the growth at 28°C for 16-24 hours. The bacteria cells were collected by centrifugation at 4000g for 10 min at room temperature. The pellet was resuspended in the inoculation buffer and centrifuge again at 4000g for 10 min. Lastly, the pellet was resuspended in the inoculation buffer and adjusted to an OD600 of 0.8. 2 hours later, plant inflorescences were dipped in the bacteria solution for 15 seconds. The dipping was repeated once more 15 min later. The plants were subsequently placed in an incubator chamber at dark and high humidity for 24 hours. Afterward, plants were grown in the greenhouse under normal growth conditions.

Inoculation buffer: 1/2 MS medium, 5% sucrose, 0.02% Silwet L-77, pH5.8

VI.2.1.7. Genotyping

Small pieces of leaves from individual plants were collected into 96-well plate with 500

ul extraction buffer and metal beads. Then, materials were crushed for (2×1 min, 25 rmp) with tissue lyser machine. After centrifugation for 15 min at 3700 rpm, the supernatants containing genomic DNA were ready to be used as DNA template for PCR.

DNA extraction buffer: 50mM Tris-HCl pH7.5; 300mM NaCl; 300mM sucrose

VI.2.1.8. *In situ* hybridization

Digoxigenin labeling of RNA probes, tissue preparation, and *in situ* hybridization was performed as previously described (Zhao et al., 2005). Tissue sections were 8 μm thick. A fragment containing the 214 bp of the 3′-end and of the 3'-untranslated region (UTR) of *SDG26* was obtained by PCR amplification using specific primers, cloned into the pGEM-T Easy vector (Promega) and used for the preparation of the *SDG26* sense and antisense probes.

VI.2.1.9. GUS staining

The 1772 bp promoter region of *SDG26* was PCR amplified and cloned into the donor vector pDONR207, and subsequently sub-cloned into the Gateway pGWB633 binary vector carrying the GUS gene. The construct was introduced in *Agrobacterium* and transgenic Arabidopsis plants were generated. The T2 progeny from six independent homozygous primary transformants was examined for GUS expression by histochemical staining. Briefly, freshly harvested plant materials were collected and immediately fixed in 80% cold acetone for 20 min on ice. After two washes with sterile water and one with 50 mM sodium phosphate buffer (pH 7.0), the plant materials were placed in the GUS staining solution (Jefferson et al., 1987). Samples were then vacuum infiltrated for 10 min and incubated in the dark at 37°C overnight. Plant material was cleared in 70% ethanol and images were taken with a differential interference contrast (DIC) microscope (Leica).

GUS staining solution

Note: Prepare fresh and keep in the dark.

50 mM sodium phosphate buffer pH 7.0

10 mM EDTA pH 8.0

0.1% Triton X-100

3 mM Potassium Ferrocyanide

3 mM Potassium Ferricyanide

0.5 mg/ml 5-bromo-4-chloro-3-indolyl glucuronide (X-Gluc)

ddH2O to volume.

VI.2.1.10. Plant micrografting

Micrografting between hypocotyls of rootstocks and scions were carried out without collars on 6-day-old seedlings, as previously described (Turnbull et al., 2002). Successful grafts were transferred into MS medium (for root growth analyses) or soil (for shoot growth analyses) and grown under LDs at 22 °C.

VI.2.1.11. Hormone or cold treatment

For hormone treatment: 10-day-old seedlings grown on MS under LDs were pre-incubated in liquid MS medium plate supplement with or without corresponding phytohormones for indicated hours. For cold treatment, 10-day-old seedlings grown on MS under LDs were put at 4°C cold chamber or kept at the growth chamber for indicated hours. The seedlings were then harvested after treatment, frozen by liquid nitrogen and stored at -80°C.

VI.2.1.12. Hormone quantification

Abscisic acid (ABA) and Jasmonate were identified and quantified by UPLC–MS/MS as described previously (Smirnova et al., 2017). Briefly, around 150 mg of fresh plant material was collected, ground in extraction solution (6xV/W; 70% methanol, 29% water, 1% acetic acid) containing internal standards (deuterated ABA or dABA and deuterated hydroxy JA or dh JA), and immediately frozen in liquid nitrogen. Extraction solutions were used with the following MRM transitions: JA (209 > 59, -), JA-Ile (324 > 151, +), ABA (263 > 153, -), dABA 269 > 159, -) with + and - indicating analysis in positive or negative mode, respectively. Quantitative profiles were analyzed using an EVOQ Elite LC-TQ (Bruker) equipped with an electrospray ionization source and coupled to a Dionex UltiMate 3000 UHPLC system (Thermo). Data acquisition was performed with the MS Workstation 8 for the mass spectrometry and the liquid chromatography was piloted with Bruker Compass Hystar 4.1 SR1 software. The data analysis was performed with the MS Data Review software. Absolute quantifications were achieved by comparison of sample

signals with dose-response curves established with pure compounds.

VI.2.1.13. Electrolyte leakage assay

Electrolyte leakage was conducted on detached leaves according to Thalhammer et al., 2014 (Thalhammer et al., 2014) using an electrical conductivity meter (Mettler Toledo Seven Compact equipped with an InLab Sensors). Briefly, rosettes leaves were cut and separately placed in a glass containing ddH2O at room temperature or 4°C in a cooling bath for the duration of the experiment. After inserting the electrodes carefully into the sample tubes, the electrical conductivity of each sample was measured after mixing the solution thoroughly by moving the electrodes up and down. Each sample was measured three times, with swaying in ddH2O between each measure, and the average of the three measures was latterly used. At the end of the experiment, the total electrolyte content was determined by boiling the leaves for 30 min. The percentage of electrolyte leakage was calculated relative to the conductivity of the boiled samples as follow:

%EL=Conductivity (sample) / Conductivity (boiled sample)

VI.2.1.14. Stomata analysis

Epidermal strips from 2-week-old plants were fixed in 1% glutaraldehyde, 10 mM PIPES pH 7.0, 5 mMgCl2 and 5 mM EGTA for 1h. Then samples were cleared overnight in chloral hydrate and stomata were examined under a Nikon Eclipse 800 microscope. Scanning electron microscopy images were taken using a Hitachi S-3400N (Hitachi High-Technologies Europe). All images were processed using ImageJ.

VI.2.1.15. Drought stress analysis

Soil dehydration was conducted on plants grown at 22°C with a 12 h light photoperiod in a growth chamber. After 10 days, plants were grown under the same conditions with or without additional watering for a week. Plants were then re-watered for 3 days and the number of survival plants was counted based on their color and leaf turgidity.

The water loss was estimated on detached leaves from 10-day-old plants by measuring their weight at each time point.

VI.2.1.16. Freezing tolerance test

2-week-old plants grown in soil under LDs at 22^0C were placed in -20^0C freezer for 2 hours or stayed in the growth chamber. After treatment, the plants were grown in the growth chamber for recovery. After one-week incubation, the survival rates were scored.

VI.2.1.17. Arabidopsis total RNA extraction

Step 1: Plant materials were pooled with liquid nitrogen and ground; the crude powder was put to 1.5 ml Safe-lock Eppendorf tubes and 1ml TRI Reagent was immediately added to tubes.

Step 2: Vortex the tubes and incubate at room temperature (RT) for 10 min.

Step 3: Add 0.2 ml chloroform, shake vigorously for 15 seconds and incubate for 3 min at RT.

Step 4: Centrifuge the samples at 4^0C for 15 min with 11000 g and transfer 500 ml of supernatants to new 1.5ml microcentrifuge tubes followed by adding 500ml isopropanol. Incubate for 10 min at RT.

Step 5: Centrifuge the samples at 4°C for 10 min with 11000 g to get pellets.

Step 6: Remove supernatant and wash pellets with 1ml 75% EtOH, vortex once to suspend the pellets and centrifuge at 4°C for 5mins with 7500 g.

Step 7: Remove supernatant and centrifuge again at 4°C for 5mins with 7500 g.

Step 8: Gently discard supernatant with a pipette and dry the pellet in the hood for 10 min.

Step 9: Dissolve pellets in sterilized milli-Q water and measure the concentration with Nanodrop2000.

VI.2.1.18. Reverse transcription

DNase treatment (Promega, http://www.promega.com) was followed by first-strand cDNA synthesis using a reverse transcription kit (Promega) according to the manufacturer's recommendation.

For COOLAIR transcript analysis, first-strand cDNA was synthesized using specific primers or oligo dT primer and the kit from SuperScript® IV Reverse Transcriptase (Invitrogen) according to manufacturer's instructions

VI.2.1.19. Quantitative PCR

Quantitative PCR was performed in 384 wells optical plate in a light cycler 480 II (Roche) machine, according to the manufacturers' instructions. The reaction mixture is made up of 5µl SYBR Green master mix, 2 µl primer mix, 2 µl H2O and 1 µl Template. Each sample was conducted qPCR with three replicates. GAPDH, EXP, Tub2 and Tip4.1 were used as the internal reference controls.

VI.2.1.20. Bimolecular Fluorescence Complementation

To generate the constructs for BiFC, full-length coding sequences of FLD, APRF1, LD, and SDG26 were PCR amplified. The PCR products were sub-cloned into the pDONR207 and then recombined into pYFC43 and pYFN43 vectors (Belda-Palazón et al., 2012). The constructs bearing empty vectors were used as negative controls. The different constructs were introduced in *Agrobacterium* and the resulting strains were used to transform 3- or 4-week-old tobacco leaves by infiltration. After 2 days, leaves were examined for fluorescence signals and imaged by using LSM 780 Confocal Microscope Imaging System.

VI.2.1.21. Total protein extraction

Step 1: Preheat 2×SDS loading buffer with DTT (50 µl DTT/1ml 1×SDS)

Step 2: Use tissue lyser machine to grind Arabidopsis seedlings or tobacco leaves in sate-lock tubes within glass beads (15s×2)

Note: Do not thaw the tissues, before processing 2nd grinding, keep them in liquid nitrogen once after grinding.

Step3: Add hot 2×SDS loading buffer to tubes (200 ul/100 mg tissue), vortex few seconds.

Step4: Heat samples at 95°C for 5min with shaking at 800 rpm.

Step5: Centrifuge for 5 min at RT with maximum speed.

2×SDS loading buffer (20ml)

1M Tris-HCl pH6.8	2ml
10% SDS	8ml

Glycerol 4ml

β-Mercaptoethanol 2.5ml

1% bromophenol blue little

ddH_2O up to 20 ml

2.1.22 SDS (sodium dodecyl sulfate)-polyacrylamide gel electrophoresis (PAGE)

Step 1: Prepare PAGE gel

Step 2: Protein samples (in SDS loading buffer) were heated at 95 °C for 5 min and then centrifuged at maximum speed for 5 min.

Step 3: Load protein samples and pre-stained protein ladder (4 µl) to a PAGE gel.

Step 4: Run the gel in 1x SDS electrophoresis buffer at 70 volt (V) about 10 min until the ladder becomes clearly differentiable.

Step 5: Change to 120V to finish running when the certain protein being separate.

Step 6: Incubate the gel in a Coomassie solution with shaking for 20 min at 25 °C. Remove Coomassie solution and incubate the gel with shaking in the distaining solution until the proteins on the gel can be visualized.

A PAGE gel includes two parts, resolving gel and stacking gel.

Resolving gel: 10-15% Acrylamide/ Bis-acrylamide (29:1); 375 mM Tris-HCl pH 8.8; 0.1% SDS; 0.1% Ammonium persulfate (AP); 0.4 µl/ ml TEMED

Stacking gel: 5% Acrylamide/ Bis-acrylamide (29:1); 125 mM Tris-HCl pH 6.8; 0.1% SDS; 0.1% AP; 1 µl / ml TEMED

1X SDS running buffer: 25 mM Tris pH 8.0; 250 mM glycine; 0.1% SDS

1X SDS loading buffer: 50 mM Tris-HCl pH 6.8; 100 mM DTT; 2% SDS; 0.1% bromophenol blue; 10% glycerol

Coomassie blue solution: 40% methanol; 10% acetic acid; 50% water; 0.1% (w/v) Coomassie brilliant blue R250

Coomassie distaining solution (1L): 400 mL Ethanol 100%; 100 mL Acetic Acid; 500 mL H_2O

VI.2.1.23. Western blot analysis

Step1: Protein samples were separated on 6% or 8% or 10% or 15% percentage gel by SDS-PAGE, and then the gel was equilibrated in transferring buffer for at least 5mins before transference.

Step 2: Proteins on the gel were transferred to the PVDF membrane in transferring buffer at constant 300 milliampere (mA) for 2 hours at 4 °C. PVDF membrane (Roche) was pretreated with absolute methanol for 15 seconds, followed by washing with milli-Q water for 1mins and then the membrane was equilibrated for at least 5 min.

Step 3: Washed the membrane in 1×TTBS (1×TBS buffer with 0.1% Triton-X100) buffer for 10 mins.

Step 4: Blocked the membrane in milk-TTBS (5% non-fat milk in 1×TTBS) buffer for 1 hour

Step 5: Incubated the membrane in the diluted primary antibody at 4 °C overnight.

Step 6: Rinsed the membrane 3 times with the milk-TTBS buffer and each time for 10 min.

Step 7: Incubated the membrane in the diluted secondary antibody (1/2 concentration of primary antibody) for 1 hour at RT.

Step 8: Rinsed the membrane with milk-TTBS buffer for 5mins, followed by 1×TTBS for 3 times and each time for 10 min.

Step 9: Put the membrane in ECL western blot detection reagents for 5 min at RT.

Step 10: Capture WB image on the film.

Transferring buffer: 25 mM Tris pH 8.0; 192 mM glycine; 15% methanol

TBS buffer: 20 mM Tris-HCl pH7.4; 150 mM NaCl

VI.2.1.24. Co-immunoprecipitation

Step 1: 1g plants tissues (2-week-old seedlings of transgenic plants or tobacco leaves) were finely ground in liquid nitrogen in the mortar.

Step 2: Then the tissues were thawed in 3ml lysis buffer A: 50 mM HEPES, pH 7.6, 100 mM of NaCl, 2 mM MgCl2, 1mM DTT, 0.5% Nonidet P-40 (74385, Sigma-Aldrich) and 10% glycerol supplemented with cOmplete™, EDTA-free Protease Inhibitor Cocktail (5056489001, Roche).

Step 3: Lysates were incubated with 0.5 µl/ml of the nonspecific endonuclease Benzonase (E1014, Sigma-Aldrich,1:1000) during 45 min ~1h at 4°C on a rotating wheel.

Step 4: Clear supernatants without pellet were obtained for the subsequent immunoprecipitation after centrifugation for 15 min with 11000×g at 4°C.

Step 5: If not clean, the supernatants should be centrifugated again with 10 min.

Step 6: 1.7ml supernatant was incubated with 50 µl FLAG antibody with magnetic beads at 4°C with moderate speed about 6 rpm. The FLAG antibody with magnetic beads is from the µMACS DYKDDDDK (FLAG) isolation kit according to the manufacturer's instructions (130-101-591, Miltenyi Biotec). And, the left supernatants were added the identical volume of the pre-heated EB buffer from the kit with DTT and incubated 95°C for 5 min. Then centrifuge samples for 5 min at maximum speed and store -20°C.

Step 7: The MACS M columns from Miltenyi Biotec were fixed at the MACS separator and were rinsed with 200 µl lysis buffer provided by the kit once and with two times rinse of 200 µl buffer B: 50 mM HEPES, pH 7.6, 100 mM of NaCl, 2 mM MgCl2

Step 8: After incubation, the lysates were flowed through pre-rinsed M columns with 200 µl per time.

Step 9: Then, wash the columns with 200 µl buffer B for 4 times.

Step 10: Rinse the columns with 100 µl wash buffer from Kit.

Step 11: Take out the separator with columns to room temperature and wash the columns with 20 µl, keep still at RT for 5mins followed by 3×30 µl. Push out the elution to 1.5 safe-lock microcentrifuge tubes with a pump.

Step 12: Incubate samples at 95 °C for 5mins and centrifuge for 5mins with maximum speed followed by storing at -20°C for subsequent Western blot analysis.

VI.2.1.25. Chromatin immunoprecipitation (ChIP)

Day1

Step 1: 2-week-old seedlings grown on MS medium under LDs were immediately frozen in liquid nitrogen and stored at -80 °C.

Step 2: 1-1.5g frozen seedlings were finely ground in liquid nitrogen within a chilled mortar. Transfer fine powders to 20ml Fixation buffer (without formaldehyde) at room

temperature (RT) in a 50 ml Falcon tube. Homogenize samples well with vortex 3×10s and quickly add 540 μl fresh formaldehyde (1% final concentration) and incubate at RT for 7 min on a rotating wheel with 6 rpm. Terminate the crosslinking reaction by adding 1.2 ml 2.5M Glycine (150mM final) and incubate 5 min at RT.

Step 3: Filter the solution through one layer of Miracloth and centrifuge the filtered solution for 20 min at 3000g (with a swing bucket rotor) at 4°C. Gently remove the supernatant without disturbing the pellet and resuspend pellet with pipette in 40 ml of chilled Extraction buffer 1 and incubate for 10 min on a rotating wheel with 12 rpm at 4°C. Following centrifugation for 20 min at 3000 g at 4°C, remove supernatant and resuspend pellet gently with 1ml+0.3ml of chilled Extraction buffer 2.

Step 4: Transfer the solution to 1.5 ml microcentrifuge tube and centrifuge for 10 min at 12000g at 4°C. Discard the supernatant without disturbing the pellet with pipette followed by resuspending pellets in 300 μl of cold nuclei lysis buffer (place on ice right before the step) by gently pipetting the solution up and down. Incubate on ice for 10 min.

Step 5: Using pre-chilled Bioruptor sonicator, sonicate samples for 5×5 min with a 30s ON and 30s OFF cycle at high setting. Centrifuge the sonicated chromatin solution for 10 min at 12000 g at 4°C and transfer the supernatant to a new 2 ml microcentrifuge tube. Take 40 μl for sonication e analysis and keep 10 μl for input control, and others at -80°C.

Day2

Step 6: Add 400 μl of Elution buffer to 40 μl sample after sonication and add 20 μl of NaCl 5 M. Incubate the samples at 65°C with vigorous shaking for 5-6 hours. Then precipitate DNA process is followed: add an equal volume of Phenol: Chloroform (1:1), vortex vigorously for 15s and centrifuge at maximum speed for 5mins. Transfer supernatant to a new tube and add first 1/10 volume of 3M sodium Acetate, 2 volumes of 100% EtOH, place at -20°C for at least 20 min. Centrifuge the mixture at 10000 rpm for 15 min at 4°C. Wash DNA with cold EtOH 70%. Lastly, pellets are resuspended in 30 μl of H_2O. Mix 10μl with 1 μl of RNase, incubate 10mins at RT and lead on an agarose gel.

Step 7: Following the finished sonication analysis, 30 μl chromatin is mixed with 270 μl of a preincubated mixture at 4°C for 1hour, which containing ChIP dilution buffer, 2 μl antibody and magnetic Protein A beads. The prepared mixture is used for immunoprecipitation overnight at 4°C with a rotating wheel at 8rpm. In parallel, chromatin without any antibody was used as a negative control.

Day 3

Step 8: Place IP sample on a magnetic stand for 2mins and remove the supernatant carefully with a pipette. Wash the beads with 500 μl of each wash buffer. For each buffer, incubate beads in the buffer for 10 min at 4°C with a rotating wheel at 12 rpm. Then, place the magnetic stand still for 2 min and discard the supernatant with a pipette, and add the next buffer:

1) Low Salt Wash Buffer

2) High Salt Wash Buffer

3) LiCl Wash Buffer

4) TE Wash Buffer

The whole process is performed at 4°C.

Step 9: Keep the magnetic stand for 2 min at room temperature and remove TE Wash Buffer. Elute samples with 100 μl freshly prepared ChIP elution buffer and add 1 μl Proteinase K. Process a short centrifugation and incubate samples at 65°C 5-6 h with 900 rpm rotation.

Step 10: Cool the samples down to room temperature, separate beads using the magnetic stand and remove supernatant to new 1.5 ml microcentrifuge tubes. Recover DNA by NucleoSpin® Gel and PCR Clean-up kit (MACHEREY-NAGEL, Germany) and Resuspend in 50 μl milli-Q H_2O and stored at -20°C.

Nuclear isolation buffer: 10mM HEPES pH 7.6; 0.5M sucrose; 5mM KCl; 5mM MgCl2; 5mM EDTA (pH 8); Proteinase inhibitor 1 tablet per 50 ml solution.

Fixation buffer for 100ml: nuclear isolation buffer 95ml; 14mM β-mercaptoethanol; 0.6%

Triton X-100; 1% Formaldehyde

Extraction buffer 1: 0.4M sucrose; 10mM Tris-HCl (pH 8); 10mM MgCl2, 5mM β-mercaptoethanol; Proteinase inhibitor 1 tablet per 50 ml solution; 0.1mM PMSF

Extraction buffer 2: 0.25M sucrose; 10mM Tris-HCl (pH 8); 10mM MgCl2, 1%Triton X-100; Proteinase inhibitor 1 tablet per 50 ml solution; 0.1mM PMSF

Nuclei lysis buffer: 50mM Tris-HCl (pH 8); 10mM EDTA; 1%SDS; Proteinase inhibitor

1 tablet per 50 ml solution; 0.1mM PMSF

ChIP dilution buffer: 1.1% Triton X-100; 1.2 mM EDTA (pH 8); 16.7mM Tris-HCl pH 8.0; 167 mM NaCl; Proteinase inhibitor 1 tablet per 50 ml solution; 0.1mM PMSF

Low Salt Wash Buffer: 150 mM NaCl; 0.1% SDS; 1% TritonX-100; 2mM EDTA;20mM Tris-HCl (pH 8)

High Salt Wash Buffer: 500 mM NaCl; 0.1% SDS; 1% TritonX-100; 2mM EDTA;20mM Tris-HCl (pH 8)

LiCl Wash Buffer: 0.25 M LiCl; 1% NP-40;1% sodium deoxycholate; 10 mM Tris-HCl (pH 8)

TE Wash Buffer: 10 mM Tris-HCl (pH 8); 1 mM EDTA (pH 8)

Elution buffer: 1% SDS; 0.1 M NaHCO3;5M NaCl

VI.2.2. Bacterial techniques

VI.2.2.1. Preparation of competent cells for heat shock transformation

A single bacterial colony was inoculated in 1 ml LB medium and incubated with shaking at 37°C overnight. The culture was diluted in 100 ml LB and incubated by shaking at 37°C until OD600 value reaches 0.4-0.6. The cell culture was chilled on ice for 10 min and harvested by centrifugation at 3000 g for 10 min at 4°C. After removing the supernatant, the pellet was resuspended gently in 10 ml of ice-cold 50 mM CaCl2 solution and kept still on ice for 30 min. After centrifugation at 3000 g for 10 min at 4°C, the pellet without supernatants was resuspended gently in 4 ml of ice-cold 50 mM CaCl2 (15% glycerol) on ice. The competent cells were subsequently aliquoted into microcentrifuge tubes with a volume of 50 µl, immediately frozen in liquid nitrogen and stored in -80°C.

LB medium: 10 g/ L Tryptone; 5 g/ L Yeast extract; 10 g/ L NaCl, autoclave for 15 min at 121°C

VI.2.2.2. Preparation of Agrobacterium competent cells for electroporation

A single colony of the Agrobacterium strain was inoculated in 2 ml LB with the antibiotics (rifampicin 40 mg/L, gentamycin 50mg/L) and incubated with shaking at 30°C overnight.

The culture was diluted in 400 ml SOB medium and incubated by shaking at 30°C until OD600 value reaches 0.5 to 1.0. Cells were harvested in ice-cold flask by centrifugation at 3600 rpm for 10 min at 4°C and resuspended in 40 ml ice-cold 10% glycerol, followed by repeating resuspension in 18ml ice-cold 10% glycerol. After centrifugation at 3600 rpm for 10 min at 4°C, cells without supernatants were resuspended gently in 1 ml ice-cold 10% glycerol. The competent cells were then dispensed into 50 µl aliquots and frozen immediately in liquid nitrogen and stored at -80°C.

SOB medium: Tryptone 20 g/L, Yeast extract 5 g/L, NaCl 0.5 g/L, autoclave for 15 min at 121°C.

VI.2.2.3. Heat shock transformation

After 10 min still on ice, a mixture of DNA and 50 µl competent cells were incubated at 42°C for 45 seconds and then kept on ice for 2 min. Following the addition of 0.5ml LB liquid medium and incubation the cells at 37°C for 1 hour with agitation. Spin the cell culture with few seconds of centrifugation. The supernatant was mostly removed with 100 µl left one. Lastly, the resuspended cell culture was spread on LB agar medium with the antibiotics. The inverted plates were then incubated at 37°C overnight.

VI.2.2.4. Transformation of Agrobacterium via electroporation

Agrobacterium GV3101 competent cells were thawed in ice and 0.5 µl (6-10 ng/µl) DNA was added gently. The mixture was placed in the chilled electroporation cuvette, and 2.5 V was stetted using the Gene Pulse (Bio red). Following the pulse, the cells were removed to microcentrifuge tubes and mixed with LB liquid medium. The transformed cells were incubated at 28°C for 1.5-2 hours. 300 µl cell culture was spread on LB agar medium with corresponding antibiotics. The inverted plates were incubated at 28 °C for 2 days.

VI.2.2.5. Yeast two-hybrid (Y2H)

To generate the constructs for Y2H, full-length coding sequences of FLD, APRF1, LD, and SDG26 were PCR amplified. The PCR products were sub-cloned into the pDONR207 and then recombined into pGADT7 and pGBKT7 vectors. The constructs bearing empty vectors were used as negative controls. The different constructs were co-transformed into the yeast strain AH109 (Clontech). Transformants were selected on synthetic (SD)/-Leu/-

Trp (-LW) medium for 3 days at 30°C. Weak and strong interactions were tested by transferring transformants on SD/-Leu/-Trp/-His (-LWH) and SD/-Leu/-Trp/-Ade/-His (-LWAH) media, respectively, allowing growth for 4 days at 30°C.

CHAPTER VII

REFERENCE

Abou-Elwafa, S. F., Büttner, B., Chia, T., Schulze-Buxloh, G., Hohmann, U., Mutasa-Göttgens, E., … Müller, A. E. (2011). Conservation and divergence of autonomous pathway genes in the flowering regulatory network of Beta vulgaris. Journal of Experimental Botany, 62(10), 3359–3374. https://doi.org/10.1093/jxb/erq321

Abreu, M. E., & Munné-Bosch, S. (2009). Salicylic acid deficiency in NahG transgenic lines and sid2 mutants increases seed yield in the annual plant Arabidopsis thaliana. Journal of Experimental Botany, 60(4), 1261–1271. https://doi.org/10.1093/jxb/ern363

Adrian, J., Torti, S., & Turck, F. (2009). From Decision to Commitment: The Molecular Memory of Flowering. Molecular Plant, 2(4), 628–642. https://doi.org/10.1093/mp/ssp031

Allen, G. J. (2000). Alteration of Stimulus-Specific Guard Cell Calcium Oscillations and Stomatal Closing in Arabidopsis det3 Mutant. Science, 289(5488), 2338–2342. https://doi.org/10.1126/science.289.5488.2338

Allison, L. A., & Ingles, C. J. (1989). Mutations in RNA polymerase II enhance or suppress mutations in GAL4. Proceedings of the National Academy of Sciences of the United States of America, 86(8), 2794–2798. https://doi.org/10.1073/pnas.86.8.2794

Allshire, R. C., & Madhani, H. D. (2018). Ten principles of heterochromatin formation and function. Nature Reviews Molecular Cell Biology, 19(4), 229–244. https://doi.org/10.1038/nrm.2017.119

Alonso-Ramírez, A., Rodríguez, D., Reyes, D., Jiménez, J. A., Nicolás, G., López-Climent, M., … Nicolás, C. (2009). Evidence for a role of gibberellins in salicylic acid-modulated early plant responses to abiotic stress in Arabidopsis seeds. Plant Physiology, 150(3), 1335–1344. https://doi.org/10.1104/pp.109.139352

Alvarez-Venegas, R. (2005). Methylation patterns of histone H3 Lys 4, Lys 9 and Lys 27 in transcriptionally active and inactive Arabidopsis genes and in atx1 mutants. Nucleic Acids Research, 33(16), 5199–5207. https://doi.org/10.1093/nar/gki830

Alvarez-Venegas, R., Sadder, M., Hlavacka, A., Baluska, F., Xia, Y., Lu, G., … Avramova, Z. (2006). The Arabidopsis homolog of trithorax, ATX1, binds phosphatidylinositol 5-phosphate, and the two regulate a common set of target genes. Proceedings of the National Academy of Sciences, 103(15), 6049–6054. https://doi.org/10.1073/pnas.0600944103

Alvarez-Venegas, Raúl. (2010). Regulation by Polycomb and Trithorax Group Proteins in Arabidopsis. The Arabidopsis Book, 8, e0128. https://doi.org/10.1199/tab.0128

Alvarez-Venegas, Raul, Abdallat, A. A., Guo, M., Alfano, J. R., & Avramova, Z. (2007). Epigenetic control of a transcription factor at the cross section of two antagonistic pathways. Epigenetics, 2(2), 106–113. https://doi.org/10.4161/epi.2.2.4404

Alvarez-Venegas, Raul, Pien, S., Sadder, M., Witmer, X., Grossniklaus, U., & Avramova, Z. (2003). ATX-1, an Arabidopsis homolog of trithorax, activates flower homeotic genes. Current Biology: CB, 13(8), 627–637.

Andersen, C. L., Jensen, J. L., & Ørntoft, T. F. (2004). Normalization of Real-Time Quantitative Reverse Transcription-PCR Data: A Model-Based Variance Estimation Approach to Identify Genes Suited for Normalization, Applied to Bladder and Colon Cancer Data Sets. Cancer Research, 64(15), 5245–5250.

https://doi.org/10.1158/0008-5472.CAN-04-0496

Andrés, F., & Coupland, G. (2012). The genetic basis of flowering responses to seasonal cues. Nature Reviews Genetics, 13(9), 627–639. https://doi.org/10.1038/nrg3291

Andrés, F., Porri, A., Torti, S., Mateos, J., Romera-Branchat, M., García-Martínez, J. L., … Coupland, G. (2014). SHORT VEGETATIVE PHASE reduces gibberellin biosynthesis at the Arabidopsis shoot apex to regulate the floral transition. Proceedings of the National Academy of Sciences, 111(26), E2760–E2769. https://doi.org/10.1073/pnas.1409567111

Andrews, A. J., & Luger, K. (2011). Nucleosome Structure(s) and Stability: Variations on a Theme. Annual Review of Biophysics, 40(1), 99–117. https://doi.org/10.1146/annurev-biophys-042910-155329

Angel, A., Song, J., Dean, C., & Howard, M. (2011). A Polycomb-based switch underlying quantitative epigenetic memory. Nature, 476(7358), 105–108. https://doi.org/10.1038/nature10241

Antosz, W., Pfab, A., Ehrnsberger, H. F., Holzinger, P., Köllen, K., Mortensen, S. A., … Grasser, K. D. (2017). The Composition of the Arabidopsis RNA Polymerase II Transcript Elongation Complex Reveals the Interplay between Elongation and mRNA Processing Factors. The Plant Cell, 29(4), 854–870. https://doi.org/10.1105/tpc.16.00735

Aranda, S., Mas, G., & Di Croce, L. (2015). Regulation of gene transcription by Polycomb proteins. Science Advances, 1(11), e1500737. https://doi.org/10.1126/sciadv.1500737

Asensi-Fabado, M-A., Amtmann, A., & Perrella, G. (2017). Plant responses to abiotic stress: The chromatin context of transcriptional regulation. Biochimica et Biophysica Acta (BBA)-Gene Regulatory Mechanisms, 1860(1), 106–122. https://doi.org/10.1016/j.bbagrm.2016.07.015

Asselbergh, B., De Vleesschauwer, D., & Höfte, M. (2008). Global Switches and Fine-Tuning—ABA Modulates Plant Pathogen Defense. Molecular Plant-Microbe Interactions, 21(6), 709–719. https://doi.org/10.1094/MPMI-21-6-0709

Atkinson, N. J., & Urwin, P. E. (2012). The interaction of plant biotic and abiotic stresses: From genes to the field. Journal of Experimental Botany, 63(10), 3523–3543. https://doi.org/10.1093/jxb/ers100

Aubert, Y., Widemann, E., Miesch, L., Pinot, F., & Heitz, T. (2015). CYP94-mediated jasmonoyl-isoleucine hormone oxidation shapes jasmonate profiles and attenuates defence responses to Botrytis cinerea infection. Journal of Experimental Botany, 66(13), 3879–3892. https://doi.org/10.1093/jxb/erv190

Auboeuf, D. (2018). Alternative mRNA processing sites decrease genetic variability while increasing functional diversity. Transcription, 9(2), 75–87. https://doi.org/10.1080/21541264.2017.1373891

Audonnet, L., Shen, Y., & Zhou, D-X. (2017). JMJ24 antagonizes histone H3K9 demethylase IBM1/JMJ25 function and interacts with RNAi pathways for gene silencing. Gene Expression Patterns, 25–26, 1–7. https://doi.org/10.1016/j.gep.2017.04.001

Auge, G. A., Blair, L. K., Karediya, A., & Donohue, K. (2018). The autonomous

flowering-time pathway pleiotropically regulates seed germination in Arabidopsis thaliana. Annals of Botany, 121(1), 183–191. https://doi.org/10.1093/aob/mcx132

Aukerman, M. J., Lee, I., Weigel, D., & Amasino, R. M. (1999). The Arabidopsis flowering-time gene LUMINIDEPENDENS is expressed primarily in regions of cell proliferation and encodes a nuclear protein that regulates LEAFY expression. The Plant Journal, 18(2), 195–203. https://doi.org/10.1046/j.1365-313X.1999.00442.x

Ausín, I., Alonso-Blanco, C., Jarillo, J. A., Ruiz-García, L., & Martínez-Zapater, J. M. (2004). Regulation of flowering time by FVE, a retinoblastoma-associated protein. Nature Genetics, 36(2), 162–166. https://doi.org/10.1038/ng1295

Au-Yeung, N., & Horvath, C. M. (2018). Transcriptional and chromatin regulation in interferon and innate antiviral gene expression. Cytokine & Growth Factor Reviews, 44, 11–17. https://doi.org/10.1016/j.cytogfr.2018.10.003

Balasubramanian, S., Sureshkumar, S., Lempe, J., & Weigel, D. (2006). Potent Induction of Arabidopsis thaliana Flowering by Elevated Growth Temperature. PLoS Genetics, 2(7), 10. https://doi.org/10.1371/journal.pgen.0020106

Banerjee, A., Wani, S. H., & Roychoudhury, A. (2017). Epigenetic Control of Plant Cold Responses. Frontiers in Plant Science, 8, 1643. https://doi.org/10.3389/fpls.2017.01643

Bannister, A. J., & Kouzarides, T. (2011). Regulation of chromatin by histone modifications. Cell Research, 21(3), 381–395. https://doi.org/10.1038/cr.2011.22

Bao, S., Hua, C., Huang, G., Cheng, P., Gong, X., Shen, L., & Yu, H. (2019). Molecular Basis of Natural Variation in Photoperiodic Flowering Responses. Developmental Cell, 50(1), 90-101.e3. https://doi.org/10.1016/j.devcel.2019.05.018

Bar, M., & Ori, N. (2014). Leaf development and morphogenesis. Development, 141(22), 4219–4230. https://doi.org/10.1242/dev.106195

Baralle, F. E., & Giudice, J. (2017). Alternative splicing as a regulator of development and tissue identity. Nature Reviews Molecular Cell Biology, 18(7), 437–451. https://doi.org/10.1038/nrm.2017.27

Bari, R., & Jones, J. D. G. (2009). Role of plant hormones in plant defence responses. Plant Molecular Biology, 69(4), 473–488. https://doi.org/10.1007/s11103-008-9435-0

Barnes, C. E., English, D. M., & Cowley, S. M. (2019). Acetylation & Co: An expanding repertoire of histone acylations regulates chromatin and transcription. Essays In Biochemistry, 63(1), 97–107. https://doi.org/10.1042/EBC20180061

Baron, K. N., Schroeder, D. F., & Stasolla, C. (2012). Transcriptional response of abscisic acid (ABA) metabolism and transport to cold and heat stress applied at the reproductive stage of development in Arabidopsis thaliana. Plant Science, 188–189, 48–59. https://doi.org/10.1016/j.plantsci.2012.03.001

Barth, T. K., & Imhof, A. (2010). Fast signals and slow marks: The dynamics of histone modifications. Trends in Biochemical Sciences, 35(11), 618–626. https://doi.org/10.1016/j.tibs.2010.05.006

Bartlett, M. E. (2017). Changing MADS-Box Transcription Factor Protein–Protein Interactions as a Mechanism for Generating Floral Morphological Diversity.

Integrative and Comparative Biology, 57(6), 1312–1321. https://doi.org/10.1093/icb/icx067

Bartsch, M., Gobbato, E., Bednarek, P., Debey, S., Schultze, J. L., Bautor, J., & Parker, J. E. (2006). Salicylic acid-independent ENHANCED DISEASE SUSCEPTIBILITY1 signaling in Arabidopsis immunity and cell death is regulated by the monooxygenase FMO1 and the Nudix hydrolase NUDT7. The Plant Cell, 18(4), 1038–1051. https://doi.org/10.1105/tpc.105.039982

Bäurle, I., & Dean, C. (2008). Differential Interactions of the Autonomous Pathway RRM Proteins and Chromatin Regulators in the Silencing of Arabidopsis Targets. PLoS ONE, 3(7), e2733. https://doi.org/10.1371/journal.pone.0002733

Baurle, I., Smith, L., Baulcombe, D. C., & Dean, C. (2007). Widespread Role for the Flowering-Time Regulators FCA and FPA in RNA-Mediated Chromatin Silencing. Science, 318(5847), 109–112. https://doi.org/10.1126/science.1146565

Beischlag, T. V., Prefontaine, G. G., & Hankinson, O. (2018). ChIP-re-ChIP: Co-occupancy Analysis by Sequential Chromatin Immunoprecipitation. In N. Visa & A. Jordán-Pla (Eds.), Chromatin Immunoprecipitation (Vol. 1689, pp. 103–112). https://doi.org/10.1007/978-1-4939-7380-4_9

Belda-Palazón, B., Ruiz, L., Martí, E., Tárraga, S., Tiburcio, A. F., Culiáñez, F., … Ferrando, A. (2012). Aminopropyltransferases Involved in Polyamine Biosynthesis Localize Preferentially in the Nucleus of Plant Cells. PLoS ONE, 7(10), e46907. https://doi.org/10.1371/journal.pone.0046907

Bemer, M. (2018). Unraveling the Complex Epigenetic Mechanisms that Regulate Gene Activity. In M. Bemer & C. Baroux (Eds.), Plant Chromatin Dynamics (Vol. 1675, pp. 205–231). https://doi.org/10.1007/978-1-4939-7318-7_13

Bentley, D. L. (2014). Coupling mRNA processing with transcription in time and space. Nature Reviews Genetics, 15(3), 163–175. https://doi.org/10.1038/nrg3662

Bentley, G. A., Lewit-Bentley, A., & Roth, M. (1984). Crystal Structure of the Nucleosome Core Particle at 16 A Resolution. J Mol Biol,176(1),55-75. https://doi.org/ 10.1016/0022-2836(84)90382-6

Ben-Yishay, R., & Shav-Tal, Y. (2019). The dynamic lifecycle of mRNA in the nucleus. Current Opinion in Cell Biology, 58, 69–75. https://doi.org/10.1016/j.ceb.2019.02.007

Berger, S. L. (2007). The complex language of chromatin regulation during transcription. Nature, 447(7143), 407–412. https://doi.org/10.1038/nature05915

Berr, A., & Shen, W. H. (2010). Molecular Mechanisms in Epigenetic Regulation of Plant Growth and Development. In E. C. Pua & M. R. Davey (Eds.), Plant Developmental Biology-Biotechnological Perspectives: Volume 2 (pp. 325–344). https://doi.org/10.1007/978-3-642-04670-4_17

Berr, Alexandre, McCallum, E. J., Alioua, A., Heintz, D., Heitz, T., & Shen, W-H. (2010). Arabidopsis histone methyltransferase SET DOMAIN GROUP8 mediates induction of the jasmonate/ethylene pathway genes in plant defense response to necrotrophic fungi. Plant Physiology, 154(3), 1403–1414. https://doi.org/10.1104/pp.110.161497

Berr, Alexandre, Ménard, R., Heitz, T., & Shen, W-H. (2012). Chromatin modification

and remodelling: A regulatory landscape for the control of Arabidopsis defence responses upon pathogen attack. Cellular Microbiology, 14(6), 829–839. https://doi.org/10.1111/j.1462-5822.2012.01785.x

Berr, Alexandre, Shafiq, S., Pinon, V., Dong, A., & Shen, W-H. (2015). The trxG family histone methyltransferase SET DOMAIN GROUP 26 promotes flowering via a distinctive genetic pathway. The Plant Journal, 81(2), 316–328. https://doi.org/10.1111/tpj.12729

Berr, Alexandre, Shafiq, S., & Shen, W-H. (2011). Histone modifications in transcriptional activation during plant development. Biochimica Et Biophysica Acta, 1809(10), 567–576. https://doi.org/10.1016/j.bbagrm.2011.07.001

Berr, Alexandre, Xu, L., Gao, J., Cognat, V., Steinmetz, A., Dong, A., & Shen, W-H. (2009). SET DOMAIN GROUP25 Encodes a Histone Methyltransferase and Is Involved in FLOWERING LOCUS C Activation and Repression of Flowering. Plant Physiology, 151(3), 1476–1485. https://doi.org/10.1104/pp.109.143941

Berr, Alexandre, Zhang, X., & Shen, W-H. (2016). [Reciprocity between active transcription and histone methylation]. Biologie Aujourd'hui, 210(4), 269–282. https://doi.org/10.1051/jbio/2017004

Berry, S., & Dean, C. (2015). Environmental perception and epigenetic memory: Mechanistic insight through FLC. The Plant Journal, 83(1), 133–148. https://doi.org/10.1111/tpj.12869

Berry, S., Rosa, S., Howard, M., Bühler, M., & Dean, C. (2017). Disruption of an RNA-binding hinge region abolishes LHP1-mediated epigenetic repression. Genes & Development, 31(21), 2115–2120. https://doi.org/10.1101/gad.305227.117

Bhardwaj, V., Meier, S., Petersen, L. N., Ingle, R. A., & Roden, L. C. (2011). Defence Responses of Arabidopsis thaliana to Infection by Pseudomonas syringae Are Regulated by the Circadian Clock. PLOS ONE, 6(10), e26968. https://doi.org/10.1371/journal.pone.0026968

Bicocca, V. T., Ormsby, T., Adhvaryu, K. K., Honda, S., & Selker, E. U. (2018). ASH1-catalyzed H3K36 methylation drives gene repression and marks H3K27me2/3-competent chromatin. ELife, 7, e41497. https://doi.org/10.7554/eLife.41497

Binenbaum, J., Weinstain, R., & Shani, E. (2018). Gibberellin Localization and Transport in Plants. Trends in Plant Science, 23(5), 410–421. https://doi.org/10.1016/j.tplants.2018.02.005

Birkenbihl, R. P., Kracher, B., Roccaro, M., & Somssich, I. E. (2017). Induced Genome-Wide Binding of Three Arabidopsis WRKY Transcription Factors during Early MAMP-Triggered Immunity. The Plant Cell, 29(1), 20–38. https://doi.org/10.1105/tpc.16.00681

Blanco, F., Salinas, P., Cecchini, N. M., Jordana, X., Van Hummelen, P., Alvarez, M. E., & Holuigue, L. (2009). Early genomic responses to salicylic acid in Arabidopsis. Plant Molecular Biology, 70(1–2), 79–102. https://doi.org/10.1007/s11103-009-9458-1

Bloomer, R. H., & Dean, C. (2017). Fine-tuning timing: Natural variation informs the mechanistic basis of the switch to flowering in Arabidopsis thaliana. Journal of Experimental Botany, 68(20), 5439–5452. https://doi.org/10.1093/jxb/erx270

Blümel, M., Dally, N., & Jung, C. (2015). Flowering time regulation in crops — what did we learn from Arabidopsis? Current Opinion in Biotechnology, 32, 121–129. https://doi.org/10.1016/j.copbio.2014.11.023

Bobadilla, R., & Berr, A. (2016). Histone Methylation - A Cornerstone for Plant Responses to Environmental Stresses? Abiotic and Biotic Stress in Plants - Recent Advances and Future Perspectives. https://doi.org/10.5772/61733

Boycheva, I., Vassileva, V., & Iantcheva, A. (2014). Histone Acetyltransferases in Plant Development and Plasticity. Current Genomics, 15(1), 28–37. https://doi.org/10.2174/1389202915011403061127 42

Boyes, D. C., Zayed, A. M., Ascenzi, R., McCaskill, A. J., Hoffman, N. E., Davis, K. R., & Görlach, J. (2001). Growth Stage–Based Phenotypic Analysis of Arabidopsis: A Model for High Throughput Functional Genomics in Plants. Plant Cell, 13(7),1499-510. https://doi.org/ 10.1105/tpc.010011

Brosch, G., Ransom, R., Lechner, T., Walton, J. D., & Loidl, P. (1995). Inhibition of maize histone deacetylases by HC toxin, the host-selective toxin of Cochliobolus carbonum. The Plant Cell, 7(11), 1941–1950. https://doi.org/10.1105/tpc.7.11.1941

Brusslan, J. A., Bonora, G., Rus-Canterbury, A. M., Tariq, F., Jaroszewicz, A., & Pellegrini, M. (2015). A Genome-Wide Chronological Study of Gene Expression and Two Histone Modifications, H3K4me3 and H3K9ac, during Developmental Leaf Senescence. Plant Physiology, 168(4), 1246–1261. https://doi.org/10.1104/pp.114.252999

Buratowski, S. (2009). Progression through the RNA polymerase II CTD cycle. Molecular Cell, 36(4), 541–546. https://doi.org/10.1016/j.molcel.2009.10.019

Buzas, D. M. (2017). Capturing Environmental Plant Memories in DNA, with a Little Help from Chromatin. Plant and Cell Physiology, 58(8), 1302–1312. https://doi.org/10.1093/pcp/pcx092

Buzas, D. M., Robertson, M., Finnegan, E. J., & Helliwell, C. A. (2011). Transcription-dependence of histone H3 lysine 27 trimethylation at the Arabidopsis polycomb target gene FLC: Transcription dependence of FLC H3K27me3. The Plant Journal, 65(6), 872–881. https://doi.org/10.1111/j.1365-313X.2010.04471.x

Calixto, C. P. G., Waugh, R., & Brown, J. W. S. (2015). Evolutionary Relationships Among Barley and Arabidopsis Core Circadian Clock and Clock-Associated Genes. Journal of Molecular Evolution, 80(2), 108–119. https://doi.org/10.1007/s00239-015-9665-0

Campi, M., D'Andrea, L., Emiliani, J., & Casati, P. (2012). Participation of Chromatin-Remodeling Proteins in the Repair of Ultraviolet-B-Damaged DNA. Plant Physiology, 158(2), 981–995. https://doi.org/10.1104/pp.111.191452

Campos-Rivero, G., Osorio-Montalvo, P., Sánchez-Borges, R., Us-Camas, R., Duarte-Aké, F., & De-la-Peña, C. (2017). Plant hormone signaling in flowering: An epigenetic point of view. Journal of Plant Physiology, 214, 16–27. https://doi.org/10.1016/j.jplph.2017.03.018

Cao, H., Bowling, S. A., Gordon, A. S., & Dong, X. (1994). Characterization of an Arabidopsis Mutant That Is Nonresponsive to Inducers of Systemic Acquired Resistance. The Plant Cell, 6(11), 1583–1592.

https://doi.org/10.1105/tpc.6.11.1583

Cao, H., Li, X., & Dong, X. (1998). Generation of broad-spectrum disease resistance by overexpression of an essential regulatory gene in systemic acquired resistance. Proceedings of the National Academy of Sciences of the United States of America, 95(11), 6531–6536. https://doi.org/10.1073/pnas.95.11.6531

Cao, Y., Dai, Y., Cui, S., & Ma, L. (2008). Histone H2B Monoubiquitination in the Chromatin of FLOWERING LOCUS C Regulates Flowering Time in Arabidopsis. The Plant Cell, 20(10), 2586–2602. https://doi.org/10.1105/tpc.108.062760

Capovilla, G., Schmid, M., & Pose, D. (2015). Control of flowering by ambient temperature. Journal of Experimental Botany, 66(1), 59–69. https://doi.org/10.1093/jxb/eru416

Carillo, P., Grazia, M., Pontecorvo, G., Fuggi, A., & Woodrow, P. (2011). Salinity Stress and Salt Tolerance. In A. Shanker (Ed.), Abiotic Stress in Plants - Mechanisms and Adaptations. https://doi.org/10.5772/22331

Carter, B., Bishop, B., Ho, K. K., Huang, R., Jia, W., Zhang, H., … Ogas, J. (2018). The Chromatin Remodelers PKL and PIE1 Act in an Epigenetic Pathway That Determines H3K27me3 Homeostasis in Arabidopsis. The Plant Cell, 30(6), 1337–1352. https://doi.org/10.1105/tpc.17.00867

Carviel, J. L., Wilson, D. C., Isaacs, M., Carella, P., Catana, V., Golding, B., … Cameron, R. K. (2014). Investigation of intercellular salicylic acid accumulation during compatible and incompatible Arabidopsis-pseudomonas syringae interactions using a fast neutron-generated mutant allele of EDS5 identified by genetic mapping and whole-genome sequencing. PloS One, 9(3), e88608. https://doi.org/10.1371/journal.pone.0088608

Casañal, A., Kumar, A., Hill, C. H., Easter, A. D., Emsley, P., Degliesposti, G., … Passmore, L. A. (2017). Architecture of eukaryotic mRNA 3′-end processing machinery. Science, 358(6366), 1056–1059. https://doi.org/10.1126/science.aao6535

Castaings, L., Bergonzi, S., Albani, M. C., Kemi, U., Savolainen, O., & Coupland, G. (2014). Evolutionary conservation of cold-induced antisense RNAs of FLOWERING LOCUS C in Arabidopsis thaliana perennial relatives. Nature Communications, 5(1), 4457. https://doi.org/10.1038/ncomms5457

Cazzonelli, Christopher I., Roberts, A. C., Carmody, M. E., & Pogson, B. J. (2010). Transcriptional control of SET DOMAIN GROUP 8 and CAROTENOID ISOMERASE during Arabidopsis development. Molecular Plant, 3(1), 174–191. https://doi.org/10.1093/mp/ssp092

Cazzonelli, Christopher Ian, Yin, K., & Pogson, B. J. (2009). Potential implications for epigenetic regulation of carotenoid biosynthesis during root and shoot development. Plant Signaling & Behavior, 4(4), 339–341. https://doi.org/10.4161/psb.4.4.8193

Chan, S., Choi, E-A., & Shi, Y. (2011). Pre-mRNA 3′-end processing complex assembly and function: Pre-mRNA 3′-end processing complex assembly. Wiley Interdisciplinary Reviews: RNA, 2(3), 321–335. https://doi.org/10.1002/wrna.54

Chandrasekharan, M. B., Huang, F., & Sun, Z-W. (2010). Histone H2B ubiquitination and beyond: Regulation of nucleosome stability, chromatin dynamics and the trans-

histone H3 methylation. Epigenetics, 5(6), 460–468. https://doi.org/10.4161/epi.5.6.12314

Chen, F. X., Smith, E. R., & Shilatifard, A. (2018). Born to run: Control of transcription elongation by RNA polymerase II. Nature Reviews Molecular Cell Biology, 19(7), 464–478. https://doi.org/10.1038/s41580-018-0010-5

Chen, L-Q., Luo, J-H., Cui, Z-H., Xue, M., Wang, L., Zhang, X-Y., … He, Y. (2017). ATX3, ATX4, and ATX5 Encode Putative H3K4 Methyltransferases and Are Critical for Plant Development. Plant Physiology, 174(3), 1795–1806. https://doi.org/10.1104/pp.16.01944

Chen, L-T., Luo, M., Wang, Y-Y., & Wu, K. (2010). Involvement of Arabidopsis histone deacetylase HDA6 in ABA and salt stress response. Journal of Experimental Botany, 61(12), 3345–3353. https://doi.org/10.1093/jxb/erq154

Chen, Xiangbin, Yao, Q., Gao, X., Jiang, C., Harberd, N. P., & Fu, X. (2016). Shoot-to-Root Mobile Transcription Factor HY5 Coordinates Plant Carbon and Nitrogen Acquisition. Current Biology, 26(5), 640–646. https://doi.org/10.1016/j.cub.2015.12.066

Chen, Xiangsong, Hu, Y., & Zhou, D-X. (2011). Epigenetic gene regulation by plant Jumonji group of histone demethylase. Biochimica et Biophysica Acta (BBA) - Gene Regulatory Mechanisms, 1809(8), 421–426. https://doi.org/10.1016/j.bbagrm.2011.03.004

Chen, Z. J., & Tian, L. (2007). Roles of dynamic and reversible histone acetylation in plant development and polyploidy. Biochimica et Biophysica Acta (BBA) - Gene Structure and Expression, 1769(5–6), 295–307. https://doi.org/10.1016/j.bbaexp.2007.04.007

Chen, Z., Li, S., Subramaniam, S., Shyy, J. Y-J., & Chien, S. (2017). Epigenetic Regulation: A New Frontier for Biomedical Engineers. Annual Review of Biomedical Engineering, 19(1), 195–219. https://doi.org/10.1146/annurev-bioeng-071516-044720

Cheng, J-Z., Zhou, Y-P., Lv, T-X., Xie, C-P., & Tian, C-E. (2017). Research progress on the autonomous flowering time pathway in Arabidopsis. Physiology and Molecular Biology of Plants, 23(3), 477–485. https://doi.org/10.1007/s12298-017-0458-3

Cheung, A. C. M., & Cramer, P. (2012). A Movie of RNA Polymerase II Transcription. Cell, 149(7), 1431–1437. https://doi.org/10.1016/j.cell.2012.06.006

Chiang, G. C. K., Barua, D., Kramer, E. M., Amasino, R. M., & Donohue, K. (2009). Major flowering time gene, FLOWERING LOCUS C, regulates seed germination in Arabidopsis thaliana. Proceedings of the National Academy of Sciences, 106(28), 11661–11666. https://doi.org/10.1073/pnas.0901367106

Chinnusamy, V., Zhu, J., & Zhu, J-K. (2007). Cold stress regulation of gene expression in plants. Trends in Plant Science, 12(10), 444–451. https://doi.org/10.1016/j.tplants.2007.07.002

Cho, L-H., Yoon, J., & An, G. (2017). The control of flowering time by environmental factors. The Plant Journal, 90(4), 708–719. https://doi.org/10.1111/tpj.13461

Choi, K., Park, C., Lee, J., Oh, M., Noh, B., & Lee, I. (2007). Arabidopsis homologs of

components of the SWR1 complex regulate flowering and plant development. Development, 134(10), 1931–1941. https://doi.org/10.1242/dev.001891

Choi, Kyuha, Kim, J., Hwang, H-J., Kim, S., Park, C., Kim, S. Y., & Lee, I. (2011). The FRIGIDA Complex Activates Transcription of FLC, a Strong Flowering Repressor in Arabidopsis, by Recruiting Chromatin Modification Factors. The Plant Cell, 23(1), 289–303. https://doi.org/10.1105/tpc.110.075911

Chung, H-R., Xu, C., Fuchs, A., Mund, A., Lange, M., Staege, H., … Kinkley, S. (2016). PHF13 is a molecular reader and transcriptional co-regulator of H3K4me2/3. ELife, 5, e10607. https://doi.org/10.7554/eLife.10607

Collins, B. E., Greer, C. B., Coleman, B. C., & Sweatt, J. D. (2019). Histone H3 lysine K4 methylation and its role in learning and memory. Epigenetics & Chromatin, 12(1), 7. https://doi.org/10.1186/s13072-018-0251-8

Corbesier, L., Vincent, C., Jang, S., Fornara, F., Fan, Q., Searle, I., … Coupland, G. (2007). FT Protein Movement Contributes to Long-Distance Signaling in Floral Induction of Arabidopsis. Science, 316(5827), 1030–1033. https://doi.org/10.1126/science.1141752

Coupland, G. (2019). FLOWERING LOCUS C Isolation and Characterization: Two Articles That Opened Many Doors. The Plant Cell, 31(6), 1190–1191. https://doi.org/10.1105/tpc.19.00325

Cramer, P., Bushnell, D. A., & Kornberg, R. D. (2001). Structural basis of transcription: RNA polymerase II at 2.8 angstrom resolution. Science (New York, N.Y.), 292(5523), 1863–1876. https://doi.org/10.1126/science.1059493

Crevillén, P., & Dean, C. (2011). Regulation of the floral repressor gene FLC: The complexity of transcription in a chromatin context. Current Opinion in Plant Biology, 14(1), 38–44. https://doi.org/10.1016/j.pbi.2010.08.015

Crevillén, P., Sonmez, C., Wu, Z., & Dean, C. (2012). A gene loop containing the floral repressor FLC is disrupted in the early phase of vernalization. The EMBO Journal, 32(1), 140–148. https://doi.org/10.1038/emboj.2012.324

Crevillén, P., Yang, H., Cui, X., Greeff, C., Trick, M., Qiu, Q., … Dean, C. (2014). Epigenetic reprogramming that prevents transgenerational inheritance of the vernalized state. Nature, 515(7528), 587–590. https://doi.org/10.1038/nature13722

Crisucci, E. M., & Arndt, K. M. (2011). The Paf1 complex represses ARG1 transcription in Saccharomyces cerevisiae by promoting histone modifications. Eukaryotic Cell, 10(6), 712–723. https://doi.org/10.1128/EC.05013-11

Csorba, T., Questa, J. I., Sun, Q., & Dean, C. (2014). Antisense COOLAIR mediates the coordinated switching of chromatin states at FLC during vernalization. Proceedings of the National Academy of Sciences, 111(45), 16160–16165. https://doi.org/10.1073/pnas.1419030111

Cui, H., Gobbato, E., Kracher, B., Qiu, J., Bautor, J., & Parker, J. E. (2017). A core function of EDS1 with PAD4 is to protect the salicylic acid defense sector in Arabidopsis immunity. The New Phytologist, 213(4), 1802–1817. https://doi.org/10.1111/nph.14302

Cutler, S. R., Rodriguez, P. L., Finkelstein, R. R., & Abrams, S. R. (2010). Abscisic Acid:

Emergence of a Core Signaling Network. Annual Review of Plant Biology, 61(1), 651–679. https://doi.org/10.1146/annurev-arplant-042809-112122

Czesnick, H., & Lenhard, M. (2016). Antagonistic control of flowering time by functionally specialized poly(A) polymerases in Arabidopsis thaliana. The Plant Journal, 88(4), 570–583. https://doi.org/10.1111/tpj.13280

Dahmus, M. E. (1996). Reversible phosphorylation of the C-terminal domain of RNA polymerase II. The Journal of Biological Chemistry, 271(32), 19009–19012. https://doi.org/10.1074/jbc.271.32.19009

Dalal, C. K., & Johnson, A. D. (2017). How transcription circuits explore alternative architectures while maintaining overall circuit output. Genes & Development, 31(14), 1397–1405. https://doi.org/10.1101/gad.303362.117

Daviere, J-M., & Achard, P. (2013). Gibberellin signaling in plants. Development, 140(6), 1147–1151. https://doi.org/10.1242/dev.087650

de Bossoreille, S., Morel, P., Trehin, C., & Negrutiu, I. (2018). REBELOTE, a regulator of floral determinacy in Arabidopsis thaliana, interacts with both nucleolar and nucleoplasmic proteins. FEBS Open Bio, 8(10), 1636–1648. https://doi.org/10.1002/2211-5463.12504

De Lucia, F., Crevillen, P., Jones, A. M. E., Greb, T., & Dean, C. (2008). A PHD-Polycomb Repressive Complex 2 triggers the epigenetic silencing of FLC during vernalization. Proceedings of the National Academy of Sciences, 105(44), 16831–16836. https://doi.org/10.1073/pnas.0808687105

de Montaigu, A., Giakountis, A., Rubin, M., Tóth, R., Cremer, F., Sokolova, V., … Coupland, G. (2015). Natural diversity in daily rhythms of gene expression contributes to phenotypic variation. Proceedings of the National Academy of Sciences, 112(3), 905–910. https://doi.org/10.1073/pnas.1422242112

Deal, R. B., & Henikoff, S. (2011). Histone variants and modifications in plant gene regulation. Current Opinion in Plant Biology, 14(2), 116–122. https://doi.org/10.1016/j.pbi.2010.11.005

De-La-Peña, C., Rangel-Cano, A., & Alvarez-Venegas, R. (2012). Regulation of disease-responsive genes mediated by epigenetic factors: Interaction of Arabidopsis–Pseudomonas. Molecular Plant Pathology, 13(4), 38-398. https://doi.org/10.1111/j.1364-3703.2011.00757.x

del Olmo, I., López, J. A., Vázquez, J., Raynaud, C., Piñeiro, M., & Jarillo, J. A. (2016). Arabidopsis DNA polymerase ϵ recruits components of Polycomb repressor complex to mediate epigenetic gene silencing. Nucleic Acids Research, 44(12), 5597–5614. https://doi.org/10.1093/nar/gkw156

Deng, S., & Chua, N-H. (2015). Inverted-Repeat RNAs Targeting FT Intronic Regions Promote FT Expression in Arabidopsis. Plant and Cell Physiology, 56(8), 1667–1678. https://doi.org/10.1093/pcp/pcv091

Deng, W., Ying, H., Helliwell, C. A., Taylor, J. M., Peacock, W. J., & Dennis, E. S. (2011). FLOWERING LOCUS C (FLC) regulates development pathways throughout the life cycle of Arabidopsis. Proceedings of the National Academy of Sciences, 108(16), 6680–6685. https://doi.org/10.1073/pnas.1103175108

Deng, Weiwei, Buzas, D. M., Ying, H., Robertson, M., Taylor, J., Peacock, W., …

Helliwell, C. (2013). Arabidopsis Polycomb Repressive Complex 2 binding sites contain putative GAGA factor binding motifs within coding regions of genes. BMC Genomics, 14(1), 593. https://doi.org/10.1186/1471-2164-14-593

Dennis, E. S., & Peacock, W. J. (2007). Epigenetic regulation of flowering. Current Opinion in Plant Biology, 10(5), 520–527. https://doi.org/10.1016/j.pbi.2007.06.009

Derkacheva, M., Steinbach, Y., Wildhaber, T., Mozgová, I., Mahrez, W., Nanni, P., … Hennig, L. (2013). Arabidopsis MSI1 connects LHP1 to PRC2 complexes. The EMBO Journal, 32(14), 2073–2085. https://doi.org/10.1038/emboj.2013.145

Di Giulio, M. (2019). The key role of the elongation factors in the origin of the organization of the genetic code. Biosystems, 181, 20–26. https://doi.org/10.1016/j.biosystems.2019.04.009

Dimitrova, E., Turberfield, A. H., & Klose, R. J. (2015). Histone demethylases in chromatin biology and beyond. EMBO Reports, 16(12), 1620–1639. https://doi.org/10.15252/embr.201541113

Ding, B., & Wang, G-L. (2015). Chromatin versus pathogens: The function of epigenetics in plant immunity. Frontiers in Plant Science, 6. https://doi.org/10.3389/fpls.2015.00675

Ding, L., Kim, S. Y., & Michaels, S. D. (2013). FLOWERING LOCUS C EXPRESSOR Family Proteins Regulate FLOWERING LOCUS C Expression in Both Winter-Annual and Rapid-Cycling Arabidopsis. Plant Physiology, 163(1), 243–252. https://doi.org/10.1104/pp.113.223958

Ding, Yezhang, & Mou, Z. (2015). Elongator and its epigenetic role in plant development and responses to abiotic and biotic stresses. Frontiers in Plant Science, 6. https://doi.org/10.3389/fpls.2015.00296

Ding, Yong, Avramova, Z., & Fromm, M. (2011). The Arabidopsis trithorax-like factor ATX1 functions in dehydration stress responses via ABA-dependent and ABA-independent pathways: ATX1 functions in dehydration stress responses. The Plant Journal, 66(5), 735–744. https://doi.org/10.1111/j.1365-313X.2011.04534.x

Ding, Yong, Fromm, M., & Avramova, Z. (2012). Multiple exposures to drought “train” transcriptional responses in Arabidopsis. Nature Communications, 3, 740. https://doi.org/10.1038/ncomms1732

Ding, Yong, Ndamukong, I., Xu, Z., Lapko, H., Fromm, M., & Avramova, Z. (2012). ATX1-Generated H3K4me3 Is Required for Efficient Elongation of Transcription, Not Initiation, at ATX1-Regulated Genes. PLoS Genetics, 8(12), e1003111. https://doi.org/10.1371/journal.pgen.1003111

Divi, U. K., Rahman, T., & Krishna, P. (2010). Brassinosteroid-mediated stress tolerance in Arabidopsis shows interactions with abscisic acid, ethylene and salicylic acid pathways. BMC Plant Biology, 10, 151. https://doi.org/10.1186/1471-2229-10-151

Domagalska, M. A., Schomburg, F. M., Amasino, R. M., Vierstra, R. D., Nagy, F., & Davis, S. J. (2007). Attenuation of brassinosteroid signaling enhances FLC expression and delays flowering. Development, 134(15), 2841–2850. https://doi.org/10.1242/dev.02866

Dong, G., Ma, D-P., & Li, J. (2008). The histone methyltransferase SDG8 regulates shoot branching in Arabidopsis. Biochemical and Biophysical Research Communications, 373(4), 659–664. https://doi.org/10.1016/j.bbrc.2008.06.096

Dong, J., Chen, C., & Chen, Z. (2003). Expression profiles of the Arabidopsis WRKY gene superfamily during plant defense response. 17.

Doyle, M. R., & Amasino, R. M. (2009). A Single Amino Acid Change in the Enhancer of Zeste Ortholog CURLY LEAF Results in Vernalization-Independent, Rapid Flowering in Arabidopsis. Plant Physiology, 151(3), 1688–1697. https://doi.org/10.1104/pp.109.145581

Du, H., Huang, F., Wu, N., Li, X., Hu, H., & Xiong, L. (2018). Integrative Regulation of Drought Escape through ABA-Dependent and -Independent Pathways in Rice. Molecular Plant, 11(4), 584–597. https://doi.org/10.1016/j.molp.2018.01.004

Duc, C., Sherstnev, A., Cole, C., Barton, G. J., & Simpson, G. G. (2013). Transcription Termination and Chimeric RNA Formation Controlled by Arabidopsis thaliana FPA. PLoS Genetics, 9(10), e1003867. https://doi.org/10.1371/journal.pgen.1003867

Durairaj, G., Malik, S., & Bhaumik, S. R. (2017). Eukaryotic Gene Expression by RNA Polymerase II. In S. S. Mandal (Ed.), Gene Regulation, Epigenetics and Hormone Signaling (pp. 1–28). https://doi.org/10.1002/9783527697274.ch1

Dürr, J., Lolas, I. B., Sørensen, B. B., Schubert, V., Houben, A., Melzer, M., … Grasser, K. D. (2014). The transcript elongation factor SPT4/SPT5 is involved in auxin-related gene expression in Arabidopsis. Nucleic Acids Research, 42(7), 4332–4347. https://doi.org/10.1093/nar/gku096

Dutta, A., Choudhary, P., Caruana, J., & Raina, R. (2017). JMJ27, an Arabidopsis H3K9 histone demethylase, modulates defense against Pseudomonas syringae and flowering time. The Plant Journal, 91(6), 1015–1028. https://doi.org/10.1111/tpj.13623

Eckersley-Maslin, M. A., Alda-Catalinas, C., & Reik, W. (2018). Dynamics of the epigenetic landscape during the maternal-to-zygotic transition. Nature Reviews Molecular Cell Biology, 19(7), 436–450. https://doi.org/10.1038/s41580-018-0008-z

Eissenberg, J. C., & Shilatifard, A. (2010). Histone H3 lysine 4 (H3K4) methylation in development and differentiation. Developmental Biology, 339(2), 240–249. https://doi.org/10.1016/j.ydbio.2009.08.017

Engelhorn, J., Blanvillain, R., Kröner, C., Parrinello, H., Rohmer, M., Posé, D., … Carles, C. (2017). Dynamics of H3K4me3 Chromatin Marks Prevails over H3K27me3 for Gene Regulation during Flower Morphogenesis in Arabidopsis thaliana. Epigenomes, 1(2), 8. https://doi.org/10.3390/epigenomes1020008

Farrona, S., Thorpe, F. L., Engelhorn, J., Adrian, J., Dong, X., Sarid-Krebs, L., … Turck, F. (2011). Tissue-Specific Expression of FLOWERING LOCUS T in Arabidopsis Is Maintained Independently of Polycomb Group Protein Repression. The Plant Cell, 23(9), 3204–3214. https://doi.org/10.1105/tpc.111.087809

Feng, Q., Wang, H., Ng, H. H., Erdjument-Bromage, H., Tempst, P., Struhl, K., & Zhang, Y. (2002). Methylation of H3-lysine 79 is mediated by a new family of HMTases without a SET domain. Current Biology: CB, 12(12), 1052–1058.

Feng, S., & Jacobsen, S. E. (2011). Epigenetic modifications in plants: An evolutionary perspective. Current Opinion in Plant Biology, 14(2), 179–186. https://doi.org/10.1016/j.pbi.2010.12.002

Feng, W., Jacob, Y., Veley, K. M., Ding, L., Yu, X., Choe, G., & Michaels, S. D. (2011). Hypomorphic Alleles Reveal FCA -Independent Roles for FY in the Regulation of FLOWERING LOCUS C. Plant Physiology, 155(3), 1425–1434. https://doi.org/10.1104/pp.110.167817

Feng, W., & Michaels, S. D. (2015). Accessing the Inaccessible: The Organization, Transcription, Replication, and Repair of Heterochromatin in Plants. Annual Review of Genetics, 49(1), 439–459. https://doi.org/10.1146/annurev-genet-112414-055048

Figueiredo, D. D., Batista, R. A., Roszak, P. J., & Köhler, C. (2015). Auxin production couples endosperm development to fertilization. Nature Plants, 1(12), 15184. https://doi.org/10.1038/nplants.2015.184

Fiil, B. K., Qiu, J-L., Petersen, K., Petersen, M., & Mundy, J. (2008). Coimmunoprecipitation (co-IP) of Nuclear Proteins and Chromatin Immunoprecipitation (ChIP) from Arabidopsis. CSH Protocols, 2008, pdb.prot5049. https://doi.org/10.1101/pdb.prot5049

Finkelstein, R. R., Gampala, S. S. L., & Rock, C. D. (2002). Abscisic Acid Signaling in Seeds and Seedlings. The Plant Cell, 14(suppl 1), S15–S45. https://doi.org/10.1105/tpc.010441

Fiorucci, A-S., Bourbousse, C., Concia, L., Rougée, M., Deton-Cabanillas, A.-F., Zabulon, G., … Barneche, F. (2019). Arabidopsis S2Lb links AtCOMPASS-like and SDG2 activity in H3K4me3 independently from histone H2B monoubiquitination. Genome Biology, 20(1), 100. https://doi.org/10.1186/s13059-019-1705-4

Fletcher, J. C. (2017). State of the Art: TrxG Factor Regulation of Post-embryonic Plant Development. Frontiers in Plant Science, 8, 1925. https://doi.org/10.3389/fpls.2017.01925

Fornara, F., de Montaigu, A., & Coupland, G. (2010). SnapShot: Control of Flowering in Arabidopsis. Cell, 141(3), 550-550.e2. https://doi.org/10.1016/j.cell.2010.04.024

Forneris, F., Battaglioli, E., Mattevi, A., & Binda, C. (2009). New roles of flavoproteins in molecular cell biology: Histone demethylase LSD1 and chromatin. FEBS Journal, 276(16), 4304–4312. https://doi.org/10.1111/j.1742-4658.2009.07142.x

Fromm, M., & Avramova, Z. (2014). ATX1/AtCOMPASS and the H3K4me3 marks: How do they activate Arabidopsis genes? Current Opinion in Plant Biology, 21, 75–82. https://doi.org/10.1016/j.pbi.2014.07.004

Fu, Z. Q., & Dong, X. (2013). Systemic acquired resistance: Turning local infection into global defense. Annual Review of Plant Biology, 64, 839–863. https://doi.org/10.1146/annurev-arplant-042811-105606

Fuchs, S. M., Kizer, K. O., Braberg, H., Krogan, N. J., & Strahl, B. D. (2012). RNA Polymerase II Carboxyl-terminal Domain Phosphorylation Regulates Protein Stability of the Set2 Methyltransferase and Histone H3 Di- and Trimethylation at Lysine 36. Journal of Biological Chemistry, 287(5), 3249–3256. https://doi.org/10.1074/jbc.M111.273953

Fujita, M., Fujita, Y., Noutoshi, Y., Takahashi, F., Narusaka, Y., Yamaguchi-Shinozaki, K., & Shinozaki, K. (2006). Crosstalk between abiotic and biotic stress responses: A current view from the points of convergence in the stress signaling networks. Current Opinion in Plant Biology, 9(4), 436–442. https://doi.org/10.1016/j.pbi.2006.05.014

Galvão, V. C., Collani, S., Horrer, D., & Schmid, M. (2015). Gibberellic acid signaling is required for ambient temperature-mediated induction of flowering in Arabidopsis thaliana. The Plant Journal, 84(5), 949–962. https://doi.org/10.1111/tpj.13051

Gan, E-S., Xu, Y., & Ito, T. (2015). Dynamics of H3K27me3 methylation and demethylation in plant development. Plant Signaling & Behavior, 10(9), e1027851. https://doi.org/10.1080/15592324.2015.1027851

Gan, E-S., Xu, Y., Wong, J-Y., Geraldine Goh, J., Sun, B., Wee, W-Y., … Ito, T. (2014). Jumonji demethylases moderate precocious flowering at elevated temperature via regulation of FLC in Arabidopsis. Nature Communications, 5(1), 5098. https://doi.org/10.1038/ncomms6098

Gao, J-P., Chao, D-Y., & Lin, H-X. (2007). Understanding Abiotic Stress Tolerance Mechanisms: Recent Studies on Stress Response in Rice. Journal of Integrative Plant Biology, 49(6), 742–750. https://doi.org/10.1111/j.1744-7909.2007.00495.x

Gao, Y., Yang, S., Yuan, L., Cui, Y., & Wu, K. (2012). Comparative Analysis of SWIRM Domain-Containing Proteins in Plants. Comparative and Functional Genomics, 2012, 1–8. https://doi.org/10.1155/2012/310402

Garcion, C., Lohmann, A., Lamodière, E., Catinot, J., Buchala, A., Doermann, P., & Métraux, J-P. (2008). Characterization and biological function of the ISOCHORISMATE SYNTHASE2 gene of Arabidopsis. Plant Physiology, 147(3), 1279–1287. https://doi.org/10.1104/pp.108.119420

Genger, R. K., Jurkowski, G. I., McDowell, J. M., Lu, H., Jung, H. W., Greenberg, J. T., & Bent, A. F. (2008). Signaling pathways that regulate the enhanced disease resistance of Arabidopsis "defense, no death" mutants. Molecular Plant-Microbe Interactions: MPMI, 21(10), 1285–1296. https://doi.org/10.1094/MPMI-21-10-1285

Glazebrook, J. (2005). Contrasting mechanisms of defense against biotrophic and necrotrophic pathogens. Annual Review of Phytopathology, 43, 205–227. https://doi.org/10.1146/annurev.phyto.43.040204.135923

Glazebrook, J., Chen, W., Estes, B., Chang, H-S., Nawrath, C., Métraux, J-P., … Katagiri, F. (2003). Topology of the network integrating salicylate and jasmonate signal transduction derived from global expression phenotyping. The Plant Journal: For Cell and Molecular Biology, 34(2), 217–228.

Gloggnitzer, J., Akimcheva, S., Srinivasan, A., Kusenda, B., Riehs, N., Stampfl, H., … Riha, K. (2014). Nonsense-Mediated mRNA Decay Modulates Immune Receptor Levels to Regulate Plant Antibacterial Defense. Cell Host & Microbe, 16(3), 376–390. https://doi.org/10.1016/j.chom.2014.08.010

Gnesutta, N., Mantovani, R., & Fornara, F. (2018). Plant Flowering: Imposing DNA Specificity on Histone-Fold Subunits. Trends in Plant Science, 23(4), 293–301. https://doi.org/10.1016/j.tplants.2017.12.005

Golembeski, G. S., & Imaizumi, T. (2015). Photoperiodic Regulation of Florigen Function

in Arabidopsis thaliana. The Arabidopsis Book, 13, e0178. https://doi.org/10.1199/tab.0178

Goralogia, G. S., Liu, T-K., Zhao, L., Panipinto, P. M., Groover, E. D., Bains, Y. S., & Imaizumi, T. (2017). CYCLING DOF FACTOR 1 represses transcription through the TOPLESS co-repressor to control photoperiodic flowering in Arabidopsis. The Plant Journal, 92(2), 244–262. https://doi.org/10.1111/tpj.13649

Grant, M. R., & Jones, J. D. G. (2009). Hormone (Dis)harmony Moulds Plant Health and Disease. Science, 324(5928), 750–752. https://doi.org/10.1126/science.1173771

Grasser, K. D. (2005). Emerging role for transcript elongation in plant development. Trends in Plant Science, 10(10), 484–490. https://doi.org/10.1016/j.tplants.2005.08.004

Greb, T., Mylne, J. S., Crevillen, P., Geraldo, N., An, H., Gendall, A. R., & Dean, C. (2007). The PHD Finger Protein VRN5 Functions in the Epigenetic Silencing of Arabidopsis FLC. Current Biology, 17(1), 73–78. https://doi.org/10.1016/j.cub.2006.11.052

Greenup, A., Peacock, W. J., Dennis, E. S., & Trevaskis, B. (2009). The molecular biology of seasonal flowering-responses in Arabidopsis and the cereals. Annals of Botany, 103(8), 1165–1172. https://doi.org/10.1093/aob/mcp063

Grini, P. E., Thorstensen, T., Alm, V., Vizcay-Barrena, G., Windju, S. S., Jørstad, T. S., … Aalen, R. B. (2009). The ASH1 HOMOLOG 2 (ASHH2) histone H3 methyltransferase is required for ovule and anther development in Arabidopsis. PloS One, 4(11), e7817. https://doi.org/10.1371/journal.pone.0007817

Gruner, K., Griebel, T., Návarová, H., Attaran, E., & Zeier, J. (2013). Reprogramming of plants during systemic acquired resistance. Frontiers in Plant Science, 4. https://doi.org/10.3389/fpls.2013.00252

Gu, X., Jiang, D., Yang, W., Jacob, Y., Michaels, S. D., & He, Y. (2011). Arabidopsis Homologs of Retinoblastoma-Associated Protein 46/48 Associate with a Histone Deacetylase to Act Redundantly in Chromatin Silencing. PLoS Genetics, 7(11), e1002366. https://doi.org/10.1371/journal.pgen.1002366

Gu, X., Wang, Y., & He, Y. (2013). Photoperiodic Regulation of Flowering Time through Periodic Histone Deacetylation of the Florigen Gene FT. PLoS Biology, 11(9), e1001649. https://doi.org/10.1371/journal.pbio.1001649

Guo, C., & Morris, S. A. (2017). Engineering cell identity: Establishing new gene regulatory and chromatin landscapes. Current Opinion in Genetics & Development, 46, 50–57. https://doi.org/10.1016/j.gde.2017.06.011

Guo, D., Hazbun, T. R., Xu, X-J., Ng, S-L., Fields, S., & Kuo, M-H. (2004). A tethered catalysis, two-hybrid system to identify protein-protein interactions requiring post-translational modifications. Nature Biotechnology, 22(7), 888–892. https://doi.org/10.1038/nbt985

Guo, L., Yu, Y., Law, J. A., & Zhang, X. (2010). SET DOMAIN GROUP2 is the major histone H3 lysine 4 trimethyltransferase in Arabidopsis. Proceedings of the National Academy of Sciences, 107(43), 18557–18562. https://doi.org/10.1073/pnas.1010478107

Hacker, K. E., Fahey, C. C., Shinsky, S. A., Chiang, Y-C. J., DiFiore, J. V., Jha, D. K., …

Rathmell, W. K. (2016). Structure/Function Analysis of Recurrent Mutations in SETD2 Protein Reveals a Critical and Conserved Role for a SET Domain Residue in Maintaining Protein Stability and Histone H3 Lys-36 Trimethylation. Journal of Biological Chemistry, 291(40), 21283–21295. https://doi.org/10.1074/jbc.M116.739375

Hajheidari, M., Koncz, C., & Eick, D. (2013). Emerging roles for RNA polymerase II CTD in Arabidopsis. Trends in Plant Science, 18(11), 633–643. https://doi.org/10.1016/j.tplants.2013.07.001

Han, S-K., & Torii, K. U. (2019). Linking cell cycle to stomatal differentiation. Current Opinion in Plant Biology, 51, 66–73. https://doi.org/10.1016/j.pbi.2019.03.010

Hansen, J. C. (2002). Conformational Dynamics of the Chromatin Fiber in Solution: Determinants, Mechanisms, and Functions. Annual Review of Biophysics and Biomolecular Structure, 31(1), 361–392. https://doi.org/10.1146/annurev.biophys.31.101101.140858

Harris, C. J., Scheibe, M., Wongpalee, S. P., Liu, W., Cornett, E. M., Vaughan, R. M., … Jacobsen, S. E. (2018). A DNA methylation reader complex that enhances gene transcription. Science, 362(6419), 1182–1186. https://doi.org/10.1126/science.aar7854

Hartl, M., Füßl, M., Boersema, P. J., Jost, J., Kramer, K., Bakirbas, A., … Finkemeier, I. (2017). Lysine acetylome profiling uncovers novel histone deacetylase substrate proteins in Arabidopsis. Molecular Systems Biology, 13(10), 949. https://doi.org/10.15252/msb.20177819

Hawkes, E. J., Hennelly, S. P., Novikova, I. V., Irwin, J. A., Dean, C., & Sanbonmatsu, K. Y. (2016). COOLAIR Antisense RNAs Form Evolutionarily Conserved Elaborate Secondary Structures. Cell Reports, 16(12), 3087–3096. https://doi.org/10.1016/j.celrep.2016.08.045

Hayot, C. M., Forouzesh, E., Goel, A., Avramova, Z., & Turner, J. A. (2012). Viscoelastic properties of cell walls of single living plant cells determined by dynamic nanoindentation. Journal of Experimental Botany, 63(7), 2525–2540. https://doi.org/10.1093/jxb/err428

He, Y. (2003). Regulation of Flowering Time by Histone Acetylation in Arabidopsis. Science, 302(5651), 1751–1754. https://doi.org/10.1126/science.1091109

He, Y. (2004). PAF1-complex-mediated histone methylation of FLOWERING LOCUS C chromatin is required for the vernalization-responsive, winter-annual habit in Arabidopsis. Genes & Development, 18(22), 2774–2784. https://doi.org/10.1101/gad.1244504

He, Yuehui. (2009). Control of the Transition to Flowering by Chromatin Modifications. Molecular Plant, 2(4), 554–564. https://doi.org/10.1093/mp/ssp005

He, Yuehui. (2012). Chromatin regulation of flowering. Trends in Plant Science, 17(9), 556–562. https://doi.org/10.1016/j.tplants.2012.05.001

He, Yuehui, & Amasino, R. M. (2005). Role of chromatin modification in flowering-time control. Trends in Plant Science, 10(1), 30–35. https://doi.org/10.1016/j.tplants.2004.11.003

He, Yuehui, Doyle, M. R., & Amasino, R. M. (2004). PAF1-complex-mediated histone

methylation of FLOWERING LOCUS C chromatin is required for the vernalization-responsive, winter-annual habit in Arabidopsis. Genes & Development, 18(22), 2774–2784. https://doi.org/10.1101/gad.1244504

He, Yuehui, Michaels, S. D., & Amasino, R. M. (2003). Regulation of Flowering Time by Histone Acetylation in Arabidopsis. Science, New Series, 302(5651), 1751–1754. Retrieved from http://www.jstor.org/stable/3835886

Heidemann, M., Hintermair, C., Voß, K., & Eick, D. (2013). Dynamic phosphorylation patterns of RNA polymerase II CTD during transcription. Biochimica Et Biophysica Acta, 1829(1), 55–62. https://doi.org/10.1016/j.bbagrm.2012.08.013

Helliwell, C. A., Anderssen, R. S., Robertson, M., & Finnegan, E. J. (2015). How is FLC repression initiated by cold? Trends in Plant Science, 20(2), 76–82. https://doi.org/10.1016/j.tplants.2014.12.004

Helliwell, C. A., Robertson, M., Finnegan, E. J., Buzas, D. M., & Dennis, E. S. (2011). Vernalization-Repression of Arabidopsis FLC Requires Promoter Sequences but Not Antisense Transcripts. PLoS ONE, 6(6), e21513. https://doi.org/10.1371/journal.pone.0021513

Henderson, I. R. (2004). Control of Arabidopsis flowering: The chill before the bloom. Development, 131(16), 3829–3838. https://doi.org/10.1242/dev.01294

Henriques, T., Scruggs, B. S., Inouye, M. O., Muse, G. W., Williams, L. H., Burkholder, A. B., … Adelman, K. (2018). Widespread transcriptional pausing and elongation control at enhancers. Genes & Development, 32(1), 26–41. https://doi.org/10.1101/gad.309351.117

Heo, J. B., & Sung, S. (2011). Vernalization-Mediated Epigenetic Silencing by a Long Intronic Noncoding RNA. Science, 331(6013), 76–79. https://doi.org/10.1126/science.1197349

Hepworth, J., & Dean, C. (2015). Flowering Locus C's Lessons: Conserved Chromatin Switches Underpinning Developmental Timing and Adaptation. Plant Physiology, 168(4), 1237–1245. https://doi.org/10.1104/pp.15.00496

Hepworth, S. R. (2002). Antagonistic regulation of flowering-time gene SOC1 by CONSTANS and FLC via separate promoter motifs. The EMBO Journal, 21(16), 4327–4337. https://doi.org/10.1093/emboj/cdf432

Hernandez-Garcia, C. M., & Finer, J. J. (2014). Identification and validation of promoters and cis-acting regulatory elements. Plant Science, 217–218, 109–119. https://doi.org/10.1016/j.plantsci.2013.12.007

Herr, A. J., Molnar, A., Jones, A., & Baulcombe, D. C. (2006). Defective RNA processing enhances RNA silencing and influences flowering of Arabidopsis. Proceedings of the National Academy of Sciences, 103(41), 14994–15001. https://doi.org/10.1073/pnas.0606536103

Herzel, L., Ottoz, D. S. M., Alpert, T., & Neugebauer, K. M. (2017). Splicing and transcription touch base: Co-transcriptional spliceosome assembly and function. Nature Reviews Molecular Cell Biology, 18(10), 637–650. https://doi.org/10.1038/nrm.2017.63

Hollerer, I., Grund, K., Hentze, M. W., & Kulozik, A. E. (2014). mRNA 3′end processing: A tale of the tail reaches the clinic. EMBO Molecular Medicine, 6(1), 16–26.

https://doi.org/10.1002/emmm.201303300

Hong, E-H., Jeong, Y-M., Ryu, J-Y., Amasino, R. M., Noh, B., & Noh, Y-S. (2009). Temporal and spatial expression patterns of nine Arabidopsis genes encoding Jumonji C-domain proteins. Molecules and Cells, 27(4), 481–490. https://doi.org/10.1007/s10059-009-0054-7

Hoppmann, V., Thorstensen, T., Kristiansen, P. E., Veiseth, S. V., Rahman, M. A., Finne, K., … Aasland, R. (2011). The CW domain, a new histone recognition module in chromatin proteins. The EMBO Journal, 30(10), 1939–1952. https://doi.org/10.1038/emboj.2011.108

Hornyik, C., Terzi, L. C., & Simpson, G. G. (2010). The Spen Family Protein FPA Controls Alternative Cleavage and Polyadenylation of RNA. Developmental Cell, 18(2), 203–213. https://doi.org/10.1016/j.devcel.2009.12.009

Hou, X., Zhou, J., Liu, C., Liu, L., Shen, L., & Yu, H. (2014). Nuclear factor Y-mediated H3K27me3 demethylation of the SOC1 locus orchestrates flowering responses of Arabidopsis. Nature Communications, 5(1), 4601. https://doi.org/10.1038/ncomms5601

Hsin, J-P., & Manley, J. L. (2012). The RNA polymerase II CTD coordinates transcription and RNA processing. Genes & Development, 26(19), 2119–2137. https://doi.org/10.1101/gad.200303.112

Hsu, H-T., Chen, H-M., Yang, Z., Wang, J., Lee, N. K., Burger, A., … Mango, S. E. (2015). Recruitment of RNA polymerase II by the pioneer transcription factor PHA-4. Science, 348(6241), 1372–1376. https://doi.org/10.1126/science.aab1223

Hsu, P. L., Li, H., Lau, H-T., Leonen, C., Dhall, A., Ong, S-E., … Zheng, N. (2018). Crystal Structure of the COMPASS H3K4 Methyltransferase Catalytic Module. Cell, 174(5), 1106-1116.e9. https://doi.org/10.1016/j.cell.2018.06.038

Hu, Y., Jiang, Y., Han, X., Wang, H., Pan, J., & Yu, D. (2017). Jasmonate regulates leaf senescence and tolerance to cold stress: Crosstalk with other phytohormones. Journal of Experimental Botany, 68(6), 1361–1369. https://doi.org/10.1093/jxb/erx004

Huang, D., Wu, W., Abrams, S. R., & Cutler, A. J. (2008). The relationship of drought-related gene expression in Arabidopsis thaliana to hormonal and environmental factors. Journal of Experimental Botany, 59(11), 2991–3007. https://doi.org/10.1093/jxb/ern155

Huang, J., Gu, M., Lai, Z., Fan, B., Shi, K., Zhou, Y-H., … Chen, Z. (2010). Functional analysis of the Arabidopsis PAL gene family in plant growth, development, and response to environmental stress. Plant Physiology, 153(4), 1526–1538. https://doi.org/10.1104/pp.110.157370

Huang, Y., Liu, C., Shen, W-H., & Ruan, Y. (2011). Phylogenetic analysis and classification of the Brassica rapa SET-domain protein family. BMC Plant Biology, 11, 175. https://doi.org/10.1186/1471-2229-11-175

Hutagalung, A. H. (2002). The UCS family of myosin chaperones. Journal of Cell Science, 115(21), 3983–3990. https://doi.org/10.1242/jcs.00107

Hwang, K., Susila, H., Nasim, Z., Jung, J-Y., & Ahn, J. H. (2019). Arabidopsis ABF3 and ABF4 Transcription Factors Act with the NF-YC Complex to Regulate SOC1

Expression and Mediate Drought-Accelerated Flowering. Molecular Plant, 12(4), 489–505. https://doi.org/10.1016/j.molp.2019.01.002

Hyun, K., Jeon, J., Park, K., & Kim, J. (2017). Writing, erasing and reading histone lysine methylations. Experimental & Molecular Medicine, 49(4), e324–e324. https://doi.org/10.1038/emm.2017.11

Ietswaart, R., Wu, Z., & Dean, C. (2012). Flowering time control: Another window to the connection between antisense RNA and chromatin. Trends in Genetics, 28(9), 445–453. https://doi.org/10.1016/j.tig.2012.06.002

Immink, R. G. H., Posé, D., Ferrario, S., Ott, F., Kaufmann, K., Valentim, F. L., … Angenent, G. C. (2012). Characterization of SOC1's Central Role in Flowering by the Identification of Its Upstream and Downstream Regulators. Plant Physiology, 160(1), 433–449. https://doi.org/10.1104/pp.112.202614

Ionescu, I. A., Møller, B. L., & Sánchez-Pérez, R. (2016). Chemical control of flowering time. Journal of Experimental Botany, erw427. https://doi.org/10.1093/jxb/erw427

Izban, M. G., & Luse, D. S. (1991). Transcription on nucleosomal templates by RNA polymerase II in vitro: Inhibition of elongation with enhancement of sequence-specific pausing. Genes & Development, 5(4), 683–696. https://doi.org/10.1101/gad.5.4.683

Jabre, I., Reddy, A. S. N., Kalyna, M., Chaudhary, S., Khokhar, W., Byrne, L. J., … Syed, N. H. (2019). Does co-transcriptional regulation of alternative splicing mediate plant stress responses? Nucleic Acids Research, 47(6), 2716–2726. https://doi.org/10.1093/nar/gkz121

Jaeger, K. E., & Wigge, P. A. (2007). FT Protein Acts as a Long-Range Signal in Arabidopsis. Current Biology, 17(12), 1050–1054. https://doi.org/10.1016/j.cub.2007.05.008

Janda, M., & Ruelland, E. (2015). Magical mystery tour: Salicylic acid signalling. Environmental and Experimental Botany, 114, 117–128. https://doi.org/10.1016/j.envexpbot.2014.07.003

Janda, T., Gondor, O. K., Yordanova, R., Szalai, G., & Pál, M. (2014). Salicylic acid and photosynthesis: Signalling and effects. Acta Physiologiae Plantarum, 36(10), 2537–2546. https://doi.org/10.1007/s11738-014-1620-y

Jang, S., Torti, S., & Coupland, G. (2009). Genetic and spatial interactions between FT, TSF and SVP during the early stages of floral induction in Arabidopsis. The Plant Journal, 60(4), 614–625. https://doi.org/10.1111/j.1365-313X.2009.03986.x

Jaskiewicz, M., Conrath, U., & Peterhänsel, C. (2011). Chromatin modification acts as a memory for systemic acquired resistance in the plant stress response. EMBO Reports, 12(1), 50–55. https://doi.org/10.1038/embor.2010.186

Jefferson, R. A., Kavanagh', T. A., & Bevan, M. W. (1987). GUS fusions: B-glucuronidase as a sensitive and versatile gene fusion marker in higher plants. EMBO J, 6(13),3901-7.

Jenuwein, T., & Allis, C. D. (2001). Translating the histone code. Science (New York, N.Y.), 293(5532), 1074–1080. https://doi.org/10.1126/science.1063127

Jeon, J., & Kim, J. (2011). FVE, an Arabidopsis homologue of the retinoblastoma-

associated protein that regulates flowering time and cold response, binds to chromatin as a large multiprotein complex. Molecules and Cells, 32(3), 227–234. https://doi.org/10.1007/s10059-011-1022-6

Jeon, Junhyun, & Lee, Yong-Hwan. (2014). Histone Acetylation in Fungal Pathogens of Plants. The Plant Pathology Journal, 30(1), 1–9. https://doi.org/10.5423/PPJ.RW.01.2014.0003

Jeong, H. J., Yang, J., Yi, J., & An, G. (2015). Controlling flowering time by histone methylation and acetylation in arabidopsis and rice. Journal of Plant Biology, 58(4), 203–210. https://doi.org/10.1007/s12374-015-0219-1

Jiang, D., & Berger, F. (2017). Histone variants in plant transcriptional regulation. Biochimica et Biophysica Acta (BBA) - Gene Regulatory Mechanisms, 1860(1), 123–130. https://doi.org/10.1016/j.bbagrm.2016.07.002

Jiang, D., Gu, X., & He, Y. (2009). Establishment of the Winter-Annual Growth Habit via FRIGIDA -Mediated Histone Methylation at FLOWERING LOCUS C in Arabidopsis. The Plant Cell, 21(6), 1733–1746. https://doi.org/10.1105/tpc.109.067967

Jiang, D., Kong, N. C., Gu, X., Li, Z., & He, Y. (2011). Arabidopsis COMPASS-Like Complexes Mediate Histone H3 Lysine-4 Trimethylation to Control Floral Transition and Plant Development. PLoS Genetics, 7(3), e1001330. https://doi.org/10.1371/journal.pgen.1001330

Jiang, D., Wang, Y., Wang, Y., & He, Y. (2008). Repression of FLOWERING LOCUS C and FLOWERING LOCUS T by the Arabidopsis Polycomb Repressive Complex 2 Components. PLoS ONE, 3(10), e3404. https://doi.org/10.1371/journal.pone.0003404

Jiang, D., Yang, W., He, Y., & Amasino, R. M. (2007). Arabidopsis Relatives of the Human Lysine-Specific Demethylase1 Repress the Expression of FWA and FLOWERING LOCUS C and Thus Promote the Floral Transition. The Plant Cell, 19(10), 2975–2987. https://doi.org/10.1105/tpc.107.052373

Jimeno-González, S., Payán-Bravo, L., Muñoz-Cabello, A. M., Guijo, M., Gutierrez, G., Prado, F., & Reyes, J. C. (2015). Defective histone supply causes changes in RNA polymerase II elongation rate and cotranscriptional pre-mRNA splicing. Proceedings of the National Academy of Sciences, 112(48), 14840–14845. https://doi.org/10.1073/pnas.1506760112

Jin, J. B., Jin, Y. H., Lee, J., Miura, K., Yoo, C. Y., Kim, W-Y., … Hasegawa, P. M. (2007). The SUMO E3 ligase, AtSIZ1, regulates flowering by controlling a salicylic acid-mediated floral promotion pathway and through affects on FLC chromatin structure: Floral repression by the SUMO E3 ligase SIZ1. The Plant Journal, 53(3), 530–540. https://doi.org/10.1111/j.1365-313X.2007.03359.x

Johansson, M., & Staiger, D. (2015). Time to flower: Interplay between photoperiod and the circadian clock. Journal of Experimental Botany, 66(3), 719–730. https://doi.org/10.1093/jxb/eru441

Jones, A. L., & Sung, S. (2014). Mechanisms Underlying Epigenetic Regulation in Arabidopsis thaliana. Integrative and Comparative Biology, 54(1), 61–67. https://doi.org/10.1093/icb/icu030

Jones, A. M. (2016). A new look at stress: Abscisic acid patterns and dynamics at high-

resolution. New Phytologist, 210(1), 38–44. https://doi.org/10.1111/nph.13552

Jones, J. D. G., & Dangl, J. L. (2006). The plant immune system. Nature, 444(7117), 323–329. https://doi.org/10.1038/nature05286

Jung, Jae-Hoon, & Park, C-M. (2013). HOS1-mediated activation of FLC via chromatin remodeling under cold stress. Plant Signaling & Behavior, 8(12), e27342. https://doi.org/10.4161/psb.27342

Jung, J-H., Park, J-H., Lee, S., To, T. K., Kim, J-M., Seki, M., & Park, C.-M. (2013). The Cold Signaling Attenuator HIGH EXPRESSION OF OSMOTICALLY RESPONSIVE GENE1 Activates FLOWERING LOCUS C Transcription via Chromatin Remodeling under Short-Term Cold Stress in Arabidopsis. The Plant Cell, 25(11), 4378–4390. https://doi.org/10.1105/tpc.113.118364

Kang, H., Zhang, C., An, Z., Shen, W., & Zhu, Y. (2019). AtINO80 and AtARP5 physically interact and play common as well as distinct roles in regulating plant growth and development. New Phytologist, 223(1), 336–353. https://doi.org/10.1111/nph.15780

Kapazoglou, A., Ganopoulos, I., Tani, E., & Tsaftaris, A. (2018). Epigenetics, Epigenomics and Crop Improvement. In Advances in Botanical Research (Vol. 86, pp. 287–324). https://doi.org/10.1016/bs.abr.2017.11.007

Kapolas, G., Beris, D., Katsareli, E., Livanos, P., Zografidis, A., Roussis, A., … Haralampidis, K. (2016). APRF1 promotes flowering under long days in Arabidopsis thaliana. Plant Science, 253, 141–153. https://doi.org/10.1016/j.plantsci.2016.09.015

Katagiri, F., Thilmony, R., & He, S. Y. (2002). The Arabidopsis thaliana-pseudomonas syringae interaction. The Arabidopsis Book, 1, e0039. https://doi.org/10.1199/tab.0039

Kaufmann, K., Pajoro, A., & Angenent, G. C. (2010). Regulation of transcription in plants: Mechanisms controlling developmental switches. Nature Reviews Genetics, 11(12), 830–842. https://doi.org/10.1038/nrg2885

Kenzior, A., & Folk, W. R. (2015). Arabidopsis thaliana MSI4/FVE associates with members of a novel family of plant specific PWWP/RRM domain proteins. Plant Molecular Biology, 87(4–5), 329–339. https://doi.org/10.1007/s11103-014-0280-z

Kim, D-H., & Sung, S. (2014). Genetic and Epigenetic Mechanisms Underlying Vernalization. The Arabidopsis Book, 12, e0171. https://doi.org/10.1199/tab.0171

Kim, D-H., Xi, Y., & Sung, S. (2017). Modular function of long noncoding RNA, COLDAIR, in the vernalization response. PLOS Genetics, 13(7), e1006939. https://doi.org/10.1371/journal.pgen.1006939

Kim, Dong-Hwan, & Sung, Sibum. (2014). Polycomb-Mediated Gene Silencing in Arabidopsis thaliana. Molecules and Cells, 37(12), 841–850. https://doi.org/10.14348/MOLCELLS.2014.0249

Kim, H-J., Hyun, Y., Park, J-Y., Park, M-J., Park, M-K., Kim, M. D., … Kim, J. (2004). A genetic link between cold responses and flowering time through FVE in Arabidopsis thaliana. Nature Genetics, 36(2), 167–171. https://doi.org/10.1038/ng1298

Kim, J., Kwon, J., Kim, M., Do, J., Lee, D., & Han, H. (2016a). Low-dielectric-constant polyimide aerogel composite films with low water uptake. Polymer Journal, 48(7), 829–834. https://doi.org/10.1038/pj.2016.37

Kim, J-M., Sasaki, T., Ueda, M., Sako, K., & Seki, M. (2015). Chromatin changes in response to drought, salinity, heat, and cold stresses in plants. Frontiers in Plant Science, 6, 114. https://doi.org/10.3389/fpls.2015.00114

Kim, J-M., To, T. K., Ishida, J., Morosawa, T., Kawashima, M., Matsui, A., … Seki, M. (2008). Alterations of Lysine Modifications on the Histone H3 N-Tail under Drought Stress Conditions in Arabidopsis thaliana. Plant and Cell Physiology, 49(10), 1580–1588. https://doi.org/10.1093/pcp/pcn133

Kim, K., Lee, B., Kim, J., Choi, J., Kim, J-M., Xiong, Y., … An, W. (2013). Linker Histone H1.2 cooperates with Cul4A and PAF1 to drive H4K31 ubiquitylation-mediated transactivation. Cell Reports, 5(6), 1690–1703. https://doi.org/10.1016/j.celrep.2013.11.038

Kim, S., Choi, K., Park, C., Hwang, H-J., & Lee, I. (2006). SUPPRESSOR OF FRIGIDA4 , Encoding a C2H2-Type Zinc Finger Protein, Represses Flowering by Transcriptional Activation of Arabidopsis FLOWERING LOCUS C. The Plant Cell, 18(11), 2985–2998. https://doi.org/10.1105/tpc.106.045179

Kim, S., Lee, J., Yang, J-Y., Jung, C., & Chua, N-H. (2013). Arabidopsis histone methyltransferase SET DOMAIN GROUP2 is required for regulation of various hormone responsive genes. Journal of Plant Biology, 56(1), 39–48. https://doi.org/10.1007/s12374-012-0320-7

Kim, S. Y., He, Y., Jacob, Y., Noh, Y-S., Michaels, S., & Amasino, R. (2005). Establishment of the vernalization-responsive, winter-annual habit in Arabidopsis requires a putative histone H3 methyl transferase. The Plant Cell, 17(12), 3301–3310. https://doi.org/10.1105/tpc.105.034645

Kimura, Y., Aoki, S., Ando, E., Kitatsuji, A., Watanabe, A., Ohnishi, M., … Kinoshita, T. (2015). A Flowering Integrator, SOC1, Affects Stomatal Opening in Arabidopsis thaliana. Plant and Cell Physiology, 56(4), 640–649. https://doi.org/10.1093/pcp/pcu214

Kinoshita, T., & Seki, M. (2014). Epigenetic Memory for Stress Response and Adaptation in Plants. Plant and Cell Physiology, 55(11), 1859–1863. https://doi.org/10.1093/pcp/pcu125

Kizer, K. O., Phatnani, H. P., Shibata, Y., Hall, H., Greenleaf, A. L., & Strahl, B. D. (2005). A Novel Domain in Set2 Mediates RNA Polymerase II Interaction and Couples Histone H3 K36 Methylation with Transcript Elongation. Molecular and Cellular Biology, 25(8), 3305–3316. https://doi.org/10.1128/MCB.25.8.3305-3316.2005

Knezetic, J. A., & Luse, D. S. (1986). The presence of nucleosomes on a DNA template prevents initiation by RNA polymerase II in vitro. Cell, 45(1), 95–104.

Knight, H., Brandt, S., & Knight, M. R. (1998). A history of stress alters drought calcium signalling pathways inArabidopsis: Stress history in Arabidopsis. The Plant Journal, 16(6), 681–687. https://doi.org/10.1046/j.1365-313x.1998.00332.x

Ko, D., & Helariutta, Y. (2017). Shoot–Root Communication in Flowering Plants. Current Biology, 27(17), R973–R978. https://doi.org/10.1016/j.cub.2017.06.054

Ko, Jae-Heung, Prassinos, C., Keathley, D., Han, K-H., & Li, C. (2011). Novel aspects of transcriptional regulation in the winter survival and maintenance mechanism of poplar. Tree Physiology, 31(2), 208–225. https://doi.org/10.1093/treephys/tpq109

Ko, Jong-Hyun, Mitina, I., Tamada, Y., Hyun, Y., Choi, Y., Amasino, R. M., … Noh, Y.-S. (2010). Growth habit determination by the balance of histone methylation activities in Arabidopsis. The EMBO Journal, 29(18), 3208–3215. https://doi.org/10.1038/emboj.2010.198

Kohler, A., Schwindling, S., & Conrath, U. (2002). Benzothiadiazole-Induced Priming for Potentiated Responses to Pathogen Infection, Wounding, and Infiltration of Water into Leaves Requires the NPR1/NIM1 Gene in Arabidopsis. Plant Physiology, 128(3), 1046–1056. https://doi.org/10.1104/pp.010744

Kornberg, R. D. (1974). Chromatin structure: A repeating unit of histones and DNA. Science (New York, N.Y.), 184(4139), 868–871.

Kouzarides, T. (2007). Chromatin modifications and their function. Cell, 128(4), 693–705. https://doi.org/10.1016/j.cell.2007.02.005

Krasensky, J., & Jonak, C. (2012). Drought, salt, and temperature stress-induced metabolic rearrangements and regulatory networks. Journal of Experimental Botany, 63(4), 1593–1608. https://doi.org/10.1093/jxb/err460

Krause, K., & Turck, F. (2018). Plant H3K27me3 has finally found its readers. Nature Genetics, 50(9), 1206–1208. https://doi.org/10.1038/s41588-018-0201-1

Krishnamurthy, S., & Hampsey, M. (2009). Eukaryotic transcription initiation. Current Biology, 19(4), R153–R156. https://doi.org/10.1016/j.cub.2008.11.052

Krogan, N. J., Kim, M., Tong, A., Golshani, A., Cagney, G., Canadien, V., … Greenblatt, J. (2003). Methylation of Histone H3 by Set2 in Saccharomyces cerevisiae Is Linked to Transcriptional Elongation by RNA Polymerase II. Molecular and Cellular Biology, 23(12), 4207–4218. https://doi.org/10.1128/MCB.23.12.4207-4218.2003

Kumar, S. (2018a). Epigenomics of Plant Responses to Environmental Stress. Epigenomes, 2(1), 6. https://doi.org/10.3390/epigenomes2010006

Kumar, S. V., Lucyshyn, D., Jaeger, K. E., Alós, E., Alvey, E., Harberd, N. P., & Wigge, P. A. (2012). Transcription factor PIF4 controls the thermosensory activation of flowering. Nature, 484(7393), 242–245. https://doi.org/10.1038/nature10928

Kumpf, R., Thorstensen, T., Rahman, M. A., Heyman, J., Nenseth, H. Z., Lammens, T., … Aalen, R. B. (2014). The ASH1-RELATED3 SET-Domain Protein Controls Cell Division Competence of the Meristem and the Quiescent Center of the Arabidopsis Primary Root. PLANT PHYSIOLOGY, 166(2), 632–643. https://doi.org/10.1104/pp.114.244798

Kwon, C. S., Lee, D., Choi, G., & Chung, W-I. (2009). Histone occupancy-dependent and -independent removal of H3K27 trimethylation at cold-responsive genes in Arabidopsis. The Plant Journal, 60(1), 112–121. https://doi.org/10.1111/j.1365-313X.2009.03938.x

Kwon, H. J., Owa, T., Hassig, C. A., Shimada, J., & Schreiber, S. L. (1998). Depudecin induces morphological reversion of transformed fibroblasts via the inhibition of histone deacetylase. Proceedings of the National Academy of Sciences, 95(7),

3356–3361. https://doi.org/10.1073/pnas.95.7.3356

Kwon, Ho Jeong, Kim, J-H., Kim, M., Lee, J-K., Hwang, W-S., & Kim, D-Y. (2003). Anti-parasitic activity of depudecin on Neospora caninum via the inhibition of histone deacetylase. Veterinary Parasitology, 112(4), 269–276.

La Camera, S., Geoffroy, P., Samaha, H., Ndiaye, A., Rahim, G., Legrand, M., & Heitz, T. (2005). A pathogen-inducible patatin-like lipid acyl hydrolase facilitates fungal and bacterial host colonization in Arabidopsis. The Plant Journal: For Cell and Molecular Biology, 44(5), 810–825. https://doi.org/10.1111/j.1365-313X.2005.02578.x

Lai, X., Stigliani, A., Vachon, G., Carles, C., Smaczniak, C., Zubieta, C., … Parcy, F. (2019). Building Transcription Factor Binding Site Models to Understand Gene Regulation in Plants. Molecular Plant, 12(6), 743–763. https://doi.org/10.1016/j.molp.2018.10.010

https://doi.org/10.3390/molecules23081914

Lai, Z., Schluttenhofer, C. M., Bhide, K., Shreve, J., Thimmapuram, J., Lee, S. Y., … Mengiste, T. (2014). MED18 interaction with distinct transcription factors regulates multiple plant functions. Nature Communications, 5(1), 3064. https://doi.org/10.1038/ncomms4064

Lämke, J., Brzezinka, K., & Bäurle, I. (2016). HSFA2 orchestrates transcriptional dynamics after heat stress in Arabidopsis thaliana. Transcription, 7(4), 111–114. https://doi.org/10.1080/21541264.2016.1187550

Landrein, B., Kiss, A., Sassi, M., Chauvet, A., Das, P., Cortizo, M., … Hamant, O. (2015). Mechanical stress contributes to the expression of the STM homeobox gene in Arabidopsis shoot meristems. ELife, 4, e07811. https://doi.org/10.7554/eLife.07811

Laugesen, A., Højfeldt, J. W., & Helin, K. (2019). Molecular Mechanisms Directing PRC2 Recruitment and H3K27 Methylation. Molecular Cell, 74(1), 8–18. https://doi.org/10.1016/j.molcel.2019.03.011

Leavitt, J. M., & Alper, H. S. (2015). Advances and current limitations in transcript-level control of gene expression. Current Opinion in Biotechnology, 34, 98–104. https://doi.org/10.1016/j.copbio.2014.12.015

Lee, H. (2000). The AGAMOUS-LIKE 20 MADS domain protein integrates floral inductive pathways in Arabidopsis. Genes & Development, 14(18), 2366–2376. https://doi.org/10.1101/gad.813600

Lee, H-A., Lee, H-Y., Seo, E., Lee, J., Kim, S-B., Oh, S., … Choi, D. (2017). Current Understandings of Plant Nonhost Resistance. Molecular Plant-Microbe Interactions: MPMI, 30(1), 5–15. https://doi.org/10.1094/MPMI-10-16-0213-CR

Lee, J. H., Ryu, H-S., Chung, K. S., Pose, D., Kim, S., Schmid, M., & Ahn, J. H. (2013). Regulation of Temperature-Responsive Flowering by MADS-Box Transcription Factor Repressors. Science, 342(6158), 628–632. https://doi.org/10.1126/science.1241097

Lee, J., & Lee, I. (2010). Regulation and function of SOC1, a flowering pathway integrator. Journal of Experimental Botany, 61(9), 2247–2254. https://doi.org/10.1093/jxb/erq098

Lee, Joohyun, & Amasino, R. M. (2013). Two FLX family members are non-redundantly required to establish the vernalization requirement in Arabidopsis. Nature Communications, 4(1), 2186. https://doi.org/10.1038/ncomms3186

Lee, Joohyun, Yun, J-Y., Zhao, W., Shen, W-H., & Amasino, R. M. (2015). A methyltransferase required for proper timing of the vernalization response in Arabidopsis. Proceedings of the National Academy of Sciences, 112(7), 2269–2274. https://doi.org/10.1073/pnas.1423585112

Lee, J-S., & Shilatifard, A. (2007). A site to remember: H3K36 methylation a mark for histone deacetylation. Mutation Research/Fundamental and Molecular Mechanisms of Mutagenesis, 618(1–2), 130–134. https://doi.org/10.1016/j.mrfmmm.2006.08.014

Lee, K., Park, O-S., & Seo, P. J. (2017). Arabidopsis ATXR2 deposits H3K36me3 at the promoters of LBD genes to facilitate cellular dedifferentiation. Science Signaling, 10(507), eaan0316. https://doi.org/10.1126/scisignal.aan0316

Lee, K., Park, O-S., & Seo, P. J. (2018). JMJ30-mediated demethylation of H3K9me3 drives tissue identity changes to promote callus formation in Arabidopsis. The Plant Journal, 95(6), 961–975. https://doi.org/10.1111/tpj.14002

Lee, S., Fu, F., Xu, S., Lee, S. Y., Yun, D-J., & Mengiste, T. (2016). Global regulation of plant immunity by histone lysine methyl transferases. The Plant Cell, tpc.00012.2016. https://doi.org/10.1105/tpc.16.00012

Lee, W. Y., Lee, D., Chung, W-I., & Kwon, C. S. (2009). Arabidopsis ING and Alfin1-like protein families localize to the nucleus and bind to H3K4me3/2 via plant homeodomain fingers. The Plant Journal, 58(3), 511–524. https://doi.org/10.1111/j.1365-313X.2009.03795.x

Lewis, C. J. T., Pan, T., & Kalsotra, A. (2017). RNA modifications and structures cooperate to guide RNA–protein interactions. Nature Reviews Molecular Cell Biology, 18(3), 202–210. https://doi.org/10.1038/nrm.2016.163

Lewis, L. A., Polanski, K., de Torres-Zabala, M., Jayaraman, S., Bowden, L., Moore, J., … Grant, M. (2015). Transcriptional Dynamics Driving MAMP-Triggered Immunity and Pathogen Effector-Mediated Immunosuppression in Arabidopsis Leaves Following Infection with Pseudomonas syringae pv tomato DC3000. The Plant Cell, 27(11), 3038–3064. https://doi.org/10.1105/tpc.15.00471

Lfing, V., & Palva, E. T. (n.d.). The expression of a tab-related gene, rabl8, is induced by abscisic acid during the cold acclimation process ofArabidopsis thaliana (L.) Heynh. 12.

Li, D., Liu, C., Shen, L., Wu, Y., Chen, H., Robertson, M., … Yu, H. (2008). A Repressor Complex Governs the Integration of Flowering Signals in Arabidopsis. Developmental Cell, 15(1), 110–120. https://doi.org/10.1016/j.devcel.2008.05.002

Li, F., Cheng, C., Cui, F., de Oliveira, M. V. V., Yu, X., Meng, X., … He, P. (2014). Modulation of RNA polymerase II phosphorylation downstream of pathogen perception orchestrates plant immunity. Cell Host & Microbe, 16(6), 748–758. https://doi.org/10.1016/j.chom.2014.10.018

Li, J., Brader, G., & Palva, E. T. (2004). The WRKY70 transcription factor: A node of convergence for jasmonate-mediated and salicylate-mediated signals in plant

defense. The Plant Cell, 16(2), 319–331. https://doi.org/10.1105/tpc.016980

Li, M., Phatnani, H. P., Guan, Z., Sage, H., Greenleaf, A. L., & Zhou, P. (2005). Solution structure of the Set2-Rpb1 interacting domain of human Set2 and its interaction with the hyperphosphorylated C-terminal domain of Rpb1. Proceedings of the National Academy of Sciences of the United States of America, 102(49), 17636–17641. https://doi.org/10.1073/pnas.0506350102

Li, N., Han, X., Feng, D., Yuan, D., & Huang, L-J. (2019). Signaling Crosstalk between Salicylic Acid and Ethylene/Jasmonate in Plant Defense: Do We Understand What They Are Whispering? International Journal of Molecular Sciences, 20(3). https://doi.org/10.3390/ijms20030671

Li, Yang, Wang, H., Li, X., Liang, G., & Yu, D. (2017). Two DELLA-interacting proteins bHLH48 and bHLH60 regulate flowering under long-day conditions in Arabidopsis thaliana. Journal of Experimental Botany, 68(11), 2757–2767. https://doi.org/10.1093/jxb/erx143

Li, Ying, Mukherjee, I., Thum, K. E., Tanurdzic, M., Katari, M. S., Obertello, M., … Coruzzi, G. M. (2015). The histone methyltransferase SDG8 mediates the epigenetic modification of light and carbon responsive genes in plants. Genome Biology, 16(1), 79. https://doi.org/10.1186/s13059-015-0640-2

Li, Z., Fu, X., Wang, Y., Liu, R., & He, Y. (2018). Polycomb-mediated gene silencing by the BAH–EMF1 complex in plants. Nature Genetics, 50(9), 1254–1261. https://doi.org/10.1038/s41588-018-0190-0

Li, Z., Jiang, D., Fu, X., Luo, X., Liu, R., & He, Y. (2016). Coupling of histone methylation and RNA processing by the nuclear mRNA cap-binding complex. Nature Plants, 2(3), 16015. https://doi.org/10.1038/nplants.2016.15

Li, Z., Jiang, D., & He, Y. (2018). FRIGIDA establishes a local chromosomal environment for FLOWERING LOCUS C mRNA production. Nature Plants, 4(10), 836–846. https://doi.org/10.1038/s41477-018-0250-6

Lim, M-H., Kim, J., Kim, Y-S., Chung, K-S., Seo, Y-H., Lee, I., … Park, C-M. (2004). A New Arabidopsis Gene, FLK, Encodes an RNA Binding Protein with K Homology Motifs and Regulates Flowering Time via FLOWERING LOCUS C. The Plant Cell, 16(3), 731–740. https://doi.org/10.1105/tpc.019331

Liu, Bing, Liu, Y., Wang, B., Luo, Q., Shi, J., Gan, J., … Dong, A. (2019). The transcription factor OsSUF4 interacts with SDG725 in promoting H3K36me3 establishment. Nature Communications, 10(1), 2999. https://doi.org/10.1038/s41467-019-10850-5

Liu, Bing, Wei, G., Shi, J., Jin, J., Shen, T., Ni, T., … Dong, A. (2016). SET DOMAIN GROUP 708, a histone H3 lysine 36-specific methyltransferase, controls flowering time in rice (Oryza sativa). New Phytologist, 210(2), 577–588. https://doi.org/10.1111/nph.13768

Liu, Boyu, Berr, A., Chang, C., Liu, C., Shen, W-H., & Ruan, Y. (2016). Interplay of the histone methyltransferases SDG8 and SDG26 in the regulation of transcription and plant flowering and development. Biochimica Et Biophysica Acta, 1859(4), 581–590. https://doi.org/10.1016/j.bbagrm.2016.02.003

Liu, C., Thong, Z., & Yu, H. (2009). Coming into bloom: The specification of floral meristems. Development, 136(20), 3379–3391.

https://doi.org/10.1242/dev.033076

Liu, Chunyan, Lu, F., Cui, X., & Cao, X. (2010). Histone Methylation in Higher Plants. Annual Review of Plant Biology, 61(1), 395–420. https://doi.org/10.1146/annurev.arplant.043008.091939

Liu, F., Marquardt, S., Lister, C., Swiezewski, S., & Dean, C. (2010). Targeted 3' Processing of Antisense Transcripts Triggers Arabidopsis FLC Chromatin Silencing. Science, 327(5961), 94–97. https://doi.org/10.1126/science.1180278

Liu, Fuquan, Quesada, V., Crevillén, P., Bäurle, I., Swiezewski, S., & Dean, C. (2007). The Arabidopsis RNA-Binding Protein FCA Requires a Lysine-Specific Demethylase 1 Homolog to Downregulate FLC. Molecular Cell, 28(3), 398–407. https://doi.org/10.1016/j.molcel.2007.10.018

Liu, Xia, Luo, M., Zhang, W., Zhao, J., Zhang, J., Wu, K., … Duan, J. (2012). Histone acetyltransferases in rice (Oryza sativa L.): Phylogenetic analysis, subcellular localization and expression. BMC Plant Biology, 12(1), 145. https://doi.org/10.1186/1471-2229-12-145

Liu, Xu, Yang, Y., Hu, Y., Zhou, L., Li, Y., & Hou, X. (2018). Temporal-Specific Interaction of NF-YC and CURLY LEAF during the Floral Transition Regulates Flowering. Plant Physiology, pp.00296.2018. https://doi.org/10.1104/pp.18.00296

Liu, Xuncheng, Yang, S., Zhao, M., Luo, M., Yu, C-W., Chen, C-Y., … Wu, K. (2014). Transcriptional Repression by Histone Deacetylases in Plants. Molecular Plant, 7(5), 764–772. https://doi.org/10.1093/mp/ssu033

Liu, Y., & Min, J. (2016). Structure and function of histone methylation-binding proteins in plants. Biochemical Journal, 473(12), 1663–1680. https://doi.org/10.1042/BCJ20160123

Liu, Yanchao, & Huang, Y. (2018). Uncovering the mechanistic basis for specific recognition of monomethylated H3K4 by the CW domain of Arabidopsis histone methyltransferase SDG8. The Journal of Biological Chemistry, 293(17), 6470–6481. https://doi.org/10.1074/jbc.RA117.001390

Liu, Yawen, Li, X., Ma, D., Chen, Z., Wang, J., & Liu, H. (2018). CIB1 and CO interact to mediate CRY2-dependent regulation of flowering. EMBO Reports, 19(10), e45762. https://doi.org/10.15252/embr.201845762

Liu, Yuanyuan, You, S., Taylor-Teeples, M., Li, W. L., Schuetz, M., Brady, S. M., & Douglas, C. J. (2014). BEL1-LIKE HOMEODOMAIN6 and KNOTTED ARABIDOPSIS THALIANA7 Interact and Regulate Secondary Cell Wall Formation via Repression of REVOLUTA. The Plant Cell, 26(12), 4843–4861. https://doi.org/10.1105/tpc.114.128322

López-González, L., Mouriz, A., Narro-Diego, L., Bustos, R., Martínez-Zapater, J. M., Jarillo, J. A., & Piñeiro, M. (2014). Chromatin-Dependent Repression of the Arabidopsis Floral Integrator Genes Involves Plant Specific PHD-Containing Proteins. The Plant Cell, 26(10), 3922–3938. https://doi.org/10.1105/tpc.114.130781

Lorch, Y., LaPointe, J. W., & Kornberg, R. D. (1987). Nucleosomes inhibit the initiation of transcription but allow chain elongation with the displacement of histones. Cell, 49(2), 203–210. https://doi.org/10.1016/0092-8674(87)90561-7

Lu, F., Cui, X., Zhang, S., Jenuwein, T., & Cao, X. (2011). Arabidopsis REF6 is a histone H3 lysine 27 demethylase. Nature Genetics, 43(7), 715–719. https://doi.org/10.1038/ng.854

Lu, F., Li, G., Cui, X., Liu, C., Wang, X-J., & Cao, X. (2008). Comparative Analysis of JmjC Domain-containing Proteins Reveals the Potential Histone Demethylases in Arabidopsis and Rice. Journal of Integrative Plant Biology, 50(7), 886–896. https://doi.org/10.1111/j.1744-7909.2008.00692.x

Lu, L., Chen, X., Qian, S., & Zhong, X. (2018). The plant-specific histone residue Phe41 is important for genome-wide H3.1 distribution. Nature Communications, 9(1), 630. https://doi.org/10.1038/s41467-018-02976-9

Lu, L., Chen, X., Sanders, D., Qian, S., & Zhong, X. (2015). High-resolution mapping of H4K16 and H3K23 acetylation reveals conserved and unique distribution patterns in Arabidopsis and rice. Epigenetics, 10(11), 1044–1053. https://doi.org/10.1080/15592294.2015.1104446

Lucero, L. E., Manavella, P. A., Gras, D. E., Ariel, F. D., & Gonzalez, D. H. (2017). Class I and Class II TCP Transcription Factors Modulate SOC1-Dependent Flowering at Multiple Levels. Molecular Plant, 10(12), 1571–1574. https://doi.org/10.1016/j.molp.2017.09.001

Luger, K., Mäder, A. W., Richmond, R. K., Sargent, D. F., & Richmond, T. J. (1997). Crystal structure of the nucleosome core particle at 2.8 A resolution. Nature, 389(6648), 251–260. https://doi.org/10.1038/38444

Luo, C., Sidote, D. J., Zhang, Y., Kerstetter, R. A., Michael, T. P., & Lam, E. (2013). Integrative analysis of chromatin states in Arabidopsis identified potential regulatory mechanisms for natural antisense transcript production. The Plant Journal, 73(1), 77–90. https://doi.org/10.1111/tpj.12017

Luo, M., Tai, R., Yu, C-W., Yang, S., Chen, C-Y., Lin, W-D., … Wu, K. (2015). Regulation of flowering time by the histone deacetylase HDA5 in Arabidopsis. The Plant Journal, 82(6), 925–936. https://doi.org/10.1111/tpj.12868

Ma, J. (2011). Transcriptional activators and activation mechanisms. Protein & Cell, 2(11), 879–888. https://doi.org/10.1007/s13238-011-1101-7

Ma, S., Tang, N., Li, X., Xie, Y., Xiang, D., Fu, J., … Xiong, L. (2019). Reversible Histone H2B Monoubiquitination Fine-Tunes Abscisic Acid Signaling and Drought Response in Rice. Molecular Plant, 12(2), 263–277. https://doi.org/10.1016/j.molp.2018.12.005

Mack, K. L., & Nachman, M. W. (2017). Gene Regulation and Speciation. Trends in Genetics, 33(1), 68–80. https://doi.org/10.1016/j.tig.2016.11.003

Mahrez, W., Arellano, M. S. T., Moreno-Romero, J., Nakamura, M., Shu, H., Nanni, P., … Hennig, L. (2016). H3K36ac Is an Evolutionary Conserved Plant Histone Modification That Marks Active Genes. Plant Physiology, 170(3), 1566–1577. https://doi.org/10.1104/pp.15.01744

Mahrez, W., Shin, J., Muñoz-Viana, R., Figueiredo, D. D., Trejo-Arellano, M. S., Exner, V., … Hennig, L. (2016). BRR2a Affects Flowering Time via FLC Splicing. PLOS Genetics, 12(4), e1005924. https://doi.org/10.1371/journal.pgen.1005924

Malapeira, J., Khaitova, L. C., & Mas, P. (2012). Ordered changes in histone

modifications at the core of the Arabidopsis circadian clock. Proceedings of the National Academy of Sciences, 109(52), 21540–21545. https://doi.org/10.1073/pnas.1217022110

Maleck, K., Levine, A., Eulgem, T., Morgan, A., Schmid, J., Lawton, K. A., … Dietrich, R. A. (2000). The transcriptome of Arabidopsis thaliana during systemic acquired resistance. Nature Genetics, 26(4), 403–410. https://doi.org/10.1038/82521

Manzano, D., Marquardt, S., Jones, A. M. E., Baurle, I., Liu, F., & Dean, C. (2009). Altered interactions within FY/AtCPSF complexes required for Arabidopsis FCA-mediated chromatin silencing. Proceedings of the National Academy of Sciences, 106(21), 8772–8777. https://doi.org/10.1073/pnas.0903444106

Marquardt, S, Boss, P., Hadfield, J., & Dean, C. (2006). Additional targets of the Arabidopsis autonomous pathway members, FCA and FY. Journal of Experimental Botany, 57(13), 3379–3386. https://doi.org/10.1093/jxb/erl073

Marquardt, Sebastian, Raitskin, O., Wu, Z., Liu, F., Sun, Q., & Dean, C. (2014). Functional Consequences of Splicing of the Antisense Transcript COOLAIR on FLC Transcription. Molecular Cell, 54(1), 156–165. https://doi.org/10.1016/j.molcel.2014.03.026

Marr, M. T. (2006). Coactivator cross-talk specifies transcriptional output. Genes & Development, 20(11), 1458–1469. https://doi.org/10.1101/gad.1418806

Martínez, C., Pons, E., Prats, G., & León, J. (2004). Salicylic acid regulates flowering time and links defence responses and reproductive development. The Plant Journal: For Cell and Molecular Biology, 37(2), 209–217. https://doi.org/10.1046/j.1365-313X.2003.01954.x

Marvin, B., & Inada, M. (2014). Co-transcriptional mRNA Processing in Eukaryotes. In E. Bell (Ed.), Molecular Life Sciences (pp. 1–10). https://doi.org/10.1007/978-1-4614-6436-5_41-4

Mateos, J. L., Madrigal, P., Tsuda, K., Rawat, V., Richter, R., Romera-Branchat, M., … Coupland, G. (2015). Combinatorial activities of SHORT VEGETATIVE PHASE and FLOWERING LOCUS C define distinct modes of flowering regulation in Arabidopsis. Genome Biology, 16(1), 31. https://doi.org/10.1186/s13059-015-0597-1

Mathieu, J., Warthmann, N., Küttner, F., & Schmid, M. (2007). Export of FT Protein from Phloem Companion Cells Is Sufficient for Floral Induction in Arabidopsis. Current Biology, 17(12), 1055–1060. https://doi.org/10.1016/j.cub.2007.05.009

Matsumoto, M., Matsutani, S., Sugita, K., Yoshida, H., Hayashi, F., Terui, Y., … Matsumoto, K. (1992). Depudecin: A novel compound inducing the flat phenotype of NIH3T3 cells doubly transformed by ras- and src-oncogene, produced by Alternaria brassicicola. The Journal of Antibiotics, 45(6), 879–885.

Mayran, A., & Drouin, J. (2018). Pioneer transcription factors shape the epigenetic landscape. Journal of Biological Chemistry, 293(36), 13795–13804. https://doi.org/10.1074/jbc.R117.001232

Michaels, S. D., Bezerra, I. C., & Amasino, R. M. (2004). FRIGIDA-related genes are required for the winter-annual habit in Arabidopsis. Proceedings of the National Academy of Sciences, 101(9), 3281–3285. https://doi.org/10.1073/pnas.0306778101

Michaels, Scott D, & Amasino, R. M. (2001). Loss of FLOWERING LOCUS C Activity Eliminates the Late-Flowering Phenotype of FRIGIDA and Autonomous Pathway Mutations but Not Responsiveness to Vernalization. Plant Cell. 13(4), 935-41. https://doi.org/10.1105/tpc.13.4.935

Michaels, Scott D., Himelblau, E., Kim, S. Y., Schomburg, F. M., & Amasino, R. M. (2005). Integration of Flowering Signals in Winter-Annual Arabidopsis. Plant Physiology, 137(1), 149–156. https://doi.org/10.1104/pp.104.052811

Milosevich, N., Warmerdam, Z., & Hof, F. (2016). Structural aspects of small-molecule inhibition of methyllysine reader proteins. Future Medicinal Chemistry, 8(13), 1681–1702. https://doi.org/10.4155/fmc-2016-0082

Mischo, H. E., & Proudfoot, N. J. (2013). Disengaging polymerase: Terminating RNA polymerase II transcription in budding yeast. Biochimica et Biophysica Acta (BBA)-Gene Regulatory Mechanisms, 1829(1), 174–185. https://doi.org/10.1016/j.bbagrm.2012.10.003

Mittler, R. (2006). Abiotic stress, the field environment and stress combination. Trends in Plant Science, 11(1), 15–19. https://doi.org/10.1016/j.tplants.2005.11.002

Mockler, T. C., Yu, X., Shalitin, D., Parikh, D., Michael, T. P., Liou, J., … Lin, C. (2004). Regulation of flowering time in Arabidopsis by K homology domain proteins. Proceedings of the National Academy of Sciences, 101(34), 12759–12764. https://doi.org/10.1073/pnas.0404552101

Montavon, T., & Duboule, D. (2013). Chromatin organization and global regulation of Hox gene clusters. Philosophical Transactions of the Royal Society B: Biological Sciences, 368(1620), 20120367–20120367. https://doi.org/10.1098/rstb.2012.0367

Moon, J., Lee, H., Kim, M., & Lee, I. (2005). Analysis of Flowering Pathway Integrators in Arabidopsis. Plant and Cell Physiology, 46(2), 292–299. https://doi.org/10.1093/pcp/pci024

Moore, J. W., Loake, G. J., & Spoel, S. H. (2011). Transcription dynamics in plant immunity. The Plant Cell, 23(8), 2809–2820. https://doi.org/10.1105/tpc.111.087346

Moore, M. J., & Proudfoot, N. J. (2009). Pre-mRNA Processing Reaches Back toTranscription and Ahead to Translation. Cell, 136(4), 688–700. https://doi.org/10.1016/j.cell.2009.02.001

Mosammaparast, N., & Shi, Y. (2010). Reversal of Histone Methylation: Biochemical and Molecular Mechanisms of Histone Demethylases. Annual Review of Biochemistry, 79(1), 155–179. https://doi.org/10.1146/annurev.biochem.78.070907.103946

Mosher, R. A., Durrant, W. E., Wang, D., Song, J., & Dong, X. (2006). A Comprehensive Structure–Function Analysis of Arabidopsis SNI1 Defines Essential Regions and Transcriptional Repressor Activity. The Plant Cell, 18(7), 1750–1765. https://doi.org/10.1105/tpc.105.039677

Mozgova, I., Köhler, C., & Hennig, L. (2015). Keeping the gate closed: Functions of the polycomb repressive complex PRC2 in development. The Plant Journal, 83(1), 121–132. https://doi.org/10.1111/tpj.12828

Mukherjee, K., Brocchieri, L., & Burglin, T. R. (2009). A Comprehensive Classification and Evolutionary Analysis of Plant Homeobox Genes. Molecular Biology and Evolution, 26(12), 2775–2794. https://doi.org/10.1093/molbev/msp201

Mündermann, L., Erasmus, Y., Lane, B., Coen, E., & Prusinkiewicz, P. (2005). Quantitative Modeling of Arabidopsis Development. Plant Physiology, 139(2), 960–968. https://doi.org/10.1104/pp.105.060483

Munné-Bosch, S., Peñuelas, J., & Llusià, J. (2007). A deficiency in salicylic acid alters isoprenoid accumulation in water-stressed NahG transgenic Arabidopsis plants. Plant Science, 172(4), 756–762. https://doi.org/10.1016/j.plantsci.2006.12.005

Musselman, C. A., Lalonde, M-E., Côté, J., & Kutateladze, T. G. (2012). Perceiving the epigenetic landscape through histone readers. Nature Structural & Molecular Biology, 19(12), 1218–1227. https://doi.org/10.1038/nsmb.2436

Mylne, J., Greb, T., Lister, C., & Dean, C. (2004). Epigenetic Regulation in the Control of Flowering. Cold Spring Harbor Symposia on Quantitative Biology, 69(0), 457–464. https://doi.org/10.1101/sqb.2004.69.457

Naika, M., Shameer, K., Mathew, O. K., Gowda, R., & Sowdhamini, R. (2013). STIFDB2: An Updated Version of Plant Stress-Responsive TranscrIption Factor DataBase with Additional Stress Signals, Stress-Responsive Transcription Factor Binding Sites and Stress-Responsive Genes in Arabidopsis and Rice. Plant and Cell Physiology, 54(2), e8–e8. https://doi.org/10.1093/pcp/pcs185

Nakamura, Y., Andrés, F., Kanehara, K., Liu, Y., Dörmann, P., & Coupland, G. (2014). Arabidopsis florigen FT binds to diurnally oscillating phospholipids that accelerate flowering. Nature Communications, 5(1), 3553. https://doi.org/10.1038/ncomms4553

Nakashima, K., Ito, Y., & Yamaguchi-Shinozaki, K. (2009). Transcriptional Regulatory Networks in Response to Abiotic Stresses in Arabidopsis and Grasses: Figure 1. Plant Physiology, 149(1), 88–95. https://doi.org/10.1104/pp.108.129791

Napsucialy-Mendivil, S., Alvarez-Venegas, R., Shishkova, S., & Dubrovsky, J. G. (2014). ARABIDOPSIS HOMOLOG of TRITHORAX1 (ATX1) is required for cell production, patterning, and morphogenesis in root development. Journal of Experimental Botany, 65(22), 6373–6384. https://doi.org/10.1093/jxb/eru355

Ndamukong, I., Jones, D. R., Lapko, H., Divecha, N., & Avramova, Z. (2010). Phosphatidylinositol 5-Phosphate Links Dehydration Stress to the Activity of ARABIDOPSIS TRITHORAX-LIKE Factor ATX1. PLoS ONE, (10), e13396. https://doi.org/10.1371/journal.pone.0013396

Nechaev, S., & Adelman, K. (2011). Pol II waiting in the starting gates: Regulating the transition from transcription initiation into productive elongation. Biochimica et Biophysica Acta (BBA)-

Gene Regulatory Mechanisms, 1809(1), 34–45. https://doi.org/10.1016/j.bbagrm.2010.11.001

Ng, D. W-K., Wang, T., Chandrasekharan, M. B., Aramayo, R., Kertbundit, S., & Hall, T. C. (2007). Plant SET Domain-containing Proteins: Structure, Function and Regulation. Biochimica et Biophysica Acta, 1769(5–6), 316–329. https://doi.org/10.1016/j.bbaexp.2007.04.003

Nicoglou, A., & Merlin, F. (2017). Epigenetics: A way to bridge the gap between biological fields. Studies in History and Philosophy of Science Part C: Studies in History and Philosophy of Biological and Biomedical Sciences, 66, 73–82. https://doi.org/10.1016/j.shpsc.2017.10.002

Nielsen, M., Ard, R., Leng, X., Ivanov, M., Kindgren, P., Pelechano, V., & Marquardt, S. (2019). Transcription-driven chromatin repression of Intragenic transcription start sites. PLOS Genetics, 15(2), e1007969. https://doi.org/10.1371/journal.pgen.1007969

Nonet, M., Scafe, C., Sexton, J., & Young, R. (1987). Eucaryotic RNA polymerase conditional mutant that rapidly ceases mRNA synthesis. Molecular and Cellular Biology, 7(5), 1602–1611. https://doi.org/10.1128/mcb.7.5.1602

Notaguchi, M., Abe, M., Kimura, T., Daimon, Y., Kobayashi, T., Yamaguchi, A., … Araki, T. (2008). Long-Distance, Graft-Transmissible Action of Arabidopsis FLOWERING LOCUS T Protein to Promote Flowering. Plant and Cell Physiology, 49(11), 1645–1658. https://doi.org/10.1093/pcp/pcn154

Oakenfull, R. J., & Davis, S. J. (2017). Shining a light on the Arabidopsis circadian clock. Plant, Cell & Environment, 40(11), 2571–2585. https://doi.org/10.1111/pce.13033

O'Connor, D. L., Elton, S., Ticchiarelli, F., Hsia, M. M., Vogel, J. P., & Leyser, O. (2017). Cross-species functional diversity within the PIN auxin efflux protein family. Elife, 6, e31804. https://doi.org/10.7554/eLife.31804.

Oh, S., Park, S., & van Nocker, S. (2008). Genic and global functions for Paf1C in chromatin modification and gene expression in Arabidopsis. PLoS Genetics, 4(8), e1000077. https://doi.org/10.1371/journal.pgen.1000077

Ohnacker, M., Barabino, S. M. L., Preker, P. J., & Keller, W. (2000). The WD-repeat protein Pfs2p bridges two essential factors within the yeast pre-mRNA 3J-end-processing complex. EMBO J, 19(1),37–47. https://doi.org/10.1093/emboj/19.1.37

Oikawa, T., Onozawa, C., Inose, M., & Sasaki, M. (1995). Depudecin, a microbial metabolite containing two epoxide groups, exhibits anti-angiogenic activity in vivo. Biological & Pharmaceutical Bulletin, 18(9), 1305–1307. https://doi.org/10.1248/bpb.18.1305

Osakabe, Y., Yamaguchi-Shinozaki, K., Shinozaki, K., & Tran, L.-S. P. (2013). Sensing the environment: Key roles of membrane-localized kinases in plant perception and response to abiotic stress. Journal of Experimental Botany, 64(2), 445–458. https://doi.org/10.1093/jxb/ers354

Pajoro, A., Severing, E., Angenent, G. C., & Immink, R. G. H. (2017). Histone H3 lysine 36 methylation affects temperature-induced alternative splicing and flowering in plants. Genome Biology, 18(1), 102. https://doi.org/10.1186/s13059-017-1235-x

Palma, K., Thorgrimsen, S., Malinovsky, F. G., Fiil, B. K., Nielsen, H. B., Brodersen, P., … Mundy, J. (2010). Autoimmunity in Arabidopsis acd11 Is Mediated by Epigenetic Regulation of an Immune Receptor. PLoS Pathogens, 6(10), e1001137. https://doi.org/10.1371/journal.ppat.1001137

Park, H. J., Baek, D., Cha, J-Y., Liao, X., Kang, S-H., McClung, C. R., … Kim, W-Y. (2019). HOS15 Interacts with the Histone Deacetylase HDA9 and the Evening Complex to Epigenetically Regulate the Floral Activator GIGANTEA. The Plant Cell, 31(1), 37–

51. https://doi.org/10.1105/tpc.18.00721

Pazhouhandeh, M., Molinier, J., Berr, A., & Genschik, P. (2011). MSI4/FVE interacts with CUL4-DDB1 and a PRC2-like complex to control epigenetic regulation of flowering time in Arabidopsis. Proceedings of the National Academy of Sciences, 108(8), 3430–3435. https://doi.org/10.1073/pnas.1018242108

Peck, S. A., Hughes, K. D., Victorino, J. F., & Mosley, A. L. (2019). Writing a wrong: Coupled RNA polymerase II transcription and RNA quality control. Wiley Interdisciplinary Reviews: RNA, e1529. https://doi.org/10.1002/wrna.1529

Peng, Y., van Wersch, R., & Zhang, Y. (2018). Convergent and Divergent Signaling in PAMP-Triggered Immunity and Effector-Triggered Immunity. Molecular Plant-Microbe Interactions, 31(4), 403–409. https://doi.org/10.1094/MPMI-06-17-0145-CR

Périlleux, C., Bouché, F., Randoux, M., & Orman-Ligeza, B. (2019). Turning Meristems into Fortresses. Trends in Plant Science, 24(5), 431–442. https://doi.org/10.1016/j.tplants.2019.02.004

Phukan, U. J., Jeena, G. S., & Shukla, R. K. (2016). WRKY Transcription Factors: Molecular Regulation and Stress Responses in Plants. Frontiers in Plant Science, 7. https://doi.org/10.3389/fpls.2016.00760

Pichler, G. (2012). Crosstalk between DNA Methylation and Histone Modifications. 171.

Pien, S., Fleury, D., Mylne, J. S., Crevillen, P., Inzé, D., Avramova, Z., … Grossniklaus, U. (2008). ARABIDOPSIS TRITHORAX1 Dynamically Regulates FLOWERING LOCUS C Activation via Histone 3 Lysine 4 Trimethylation. The Plant Cell, 20(3), 580–588. https://doi.org/10.1105/tpc.108.058172

Pien, S., & Grossniklaus, U. (2007). Polycomb group and trithorax group proteins in Arabidopsis. Biochimica et Biophysica Acta (BBA) - Gene Structure and Expression, 1769(5–6), 375–382. https://doi.org/10.1016/j.bbaexp.2007.01.010

Pieterse, C. M. J. (2013). Induced plant responses to microbes and insects (2013). Frontiers in Plant Science, 4. https://doi.org/10.3389/fpls.2013.00475

Pieterse, C. M. J., Leon-Reyes, A., Van der Ent, S., & Van Wees, S. C. M. (2009). Networking by small-molecule hormones in plant immunity. Nature Chemical Biology, 5(5), 308–316. https://doi.org/10.1038/nchembio.164

Pieterse, C. M. J., Van der Does, D., Zamioudis, C., Leon-Reyes, A., & Van Wees, S. C. M. (2012). Hormonal modulation of plant immunity. Annual Review of Cell and Developmental Biology, 28, 489–521. https://doi.org/10.1146/annurev-cellbio-092910-154055

Pinon, V., Yao, X., Dong, A., & Shen, W-H. (2017). SDG2-Mediated H3K4me3 Is Crucial for Chromatin Condensation and Mitotic Division during Male Gametogenesis in Arabidopsis. Plant Physiology, 174(2), 1205–1215. https://doi.org/10.1104/pp.17.00306

Pisignano, G., Pavlaki, I., & Murrell, A. (2019). Being in a loop: How long non-coding RNAs organise genome architecture. Essays In Biochemistry, 63(1), 177–186. https://doi.org/10.1042/EBC20180057

Pontvianne, F., Blevins, T., & Pikaard, C. S. (2010). Arabidopsis Histone Lysine Methyltransferases. Advances in Botanical Research, 53, 1–22. https://doi.org/10.1016/S0065-2296(10)53001-5

Porri, A., Torti, S., Romera-Branchat, M., & Coupland, G. (2012). Spatially distinct regulatory roles for gibberellins in the promotion of flowering of Arabidopsis under long photoperiods. Development, 139(12), 2198–2209. https://doi.org/10.1242/dev.077164

Porrua, O., Boudvillain, M., & Libri, D. (2016). Transcription Termination: Variations on Common Themes. Trends in Genetics, 32(8), 508–522. https://doi.org/10.1016/j.tig.2016.05.007

Porrua, O., & Libri, D. (2015). Transcription termination and the control of the transcriptome: Why, where and how to stop. Nature Reviews Molecular Cell Biology, 16(3), 190–202. https://doi.org/10.1038/nrm3943

Posé, D., Verhage, L., Ott, F., Yant, L., Mathieu, J., Angenent, G. C., … Schmid, M. (2013). Temperature-dependent regulation of flowering by antagonistic FLM variants. Nature, 503(7476), 414–417. https://doi.org/10.1038/nature12633

Proietti, S., Bertini, L., Timperio, A. M., Zolla, L., Caporale, C., & Caruso, C. (2013). Crosstalk between salicylic acid and jasmonate in Arabidopsis investigated by an integrated proteomic and transcriptomic approach. Molecular BioSystems, 9(6), 1169–1187. https://doi.org/10.1039/c3mb25569g

Proudfoot, N. J. (2016). Transcriptional termination in mammals: Stopping the RNA polymerase II juggernaut. Science, 352(6291), aad9926–aad9926. https://doi.org/10.1126/science.aad9926

Pu, L., Liu, M-S., Kim, S. Y., Chen, L-F. O., Fletcher, J. C., & Sung, Z. R. (2013a). EMBRYONIC FLOWER1 and ULTRAPETALA1 Act Antagonistically on Arabidopsis Development and Stress Response. Plant Physiology, 162(2), 812–830. https://doi.org/10.1104/pp.112.213223

Pu, L., & Sung, Z. R. (2015). PcG and trxG in plants – friends or foes. Trends in Genetics, 31(5), 252–262. https://doi.org/10.1016/j.tig.2015.03.004

Puig, S., Mira, H., Dorcey, E., Sancenón, V., Andrés-Colás, N., Garcia-Molina, A., … Peñarrubia, L. (2007). Higher plants possess two different types of ATX1-like copper chaperones. Biochemical and Biophysical Research Communications, 354(2), 385–390. https://doi.org/10.1016/j.bbrc.2006.12.215

Putterill, J., & Varkonyi-Gasic, E. (2016). FT and florigen long-distance flowering control in plants. Current Opinion in Plant Biology, 33, 77–82. https://doi.org/10.1016/j.pbi.2016.06.008

Qian, S., Lv, X., Scheid, R. N., Lu, L., Yang, Z., Chen, W., … Du, J. (2018). Dual recognition of H3K4me3 and H3K27me3 by a plant histone reader SHL. Nature Communications, 9(1), 2425. https://doi.org/10.1038/s41467-018-04836-y

Qu, A-L., Ding, Y-F., Jiang, Q., & Zhu, C. (2013). Molecular mechanisms of the plant heat stress response. Biochemical and Biophysical Research Communications, 432(2), 203–207. https://doi.org/10.1016/j.bbrc.2013.01.104

Qu, Q., Takahashi, Y., Yang, Y., Hu, H., Zhang, Y., Brunzelle, J. S., … Skiniotis, G. (2018). Structure and Conformational Dynamics of a COMPASS Histone H3K4 Methyltransferase Complex. Cell, 174(5), 1117-1126.e12. https://doi.org/10.1016/j.cell.2018.07.020

Quesada, V. (2003). Autoregulation of FCA pre-mRNA processing controls Arabidopsis flowering time. The EMBO Journal, 22(12), 3142–3152. https://doi.org/10.1093/emboj/cdg305

Qüesta, J. I., Song, J., Geraldo, N., An, H., & Dean, C. (2016). Arabidopsis transcriptional repressor VAL1 triggers Polycomb silencing at FLC during vernalization. Science, 353(6298):485-8. https://doi.org/10.1126/science.aaf7354

Rairdan, G. J., & Delaney, T. P. (2002). Role of salicylic acid and NIM1/NPR1 in race-specific resistance in arabidopsis. Genetics, 161(2), 803–811.

Rajjou, L., Belghazi, M., Huguet, R., Robin, C., Moreau, A., Job, C., & Job, D. (2006). Proteomic investigation of the effect of salicylic acid on Arabidopsis seed germination and establishment of early defense mechanisms. Plant Physiology, 141(3), 910–923. https://doi.org/10.1104/pp.106.082057

Ramirez-Prado, J. S., Piquerez, S. J. M., Bendahmane, A., Hirt, H., Raynaud, C., & Benhamed, M. (2018). Modify the Histone to Win the Battle: Chromatin Dynamics in Plant-Pathogen Interactions. Frontiers in Plant Science, 9, 355. https://doi.org/10.3389/fpls.2018.00355

Rando, O. J., & Chang, H. Y. (2009). Genome-wide views of chromatin structure. Annual Review of Biochemistry, 78, 245–271. https://doi.org/10.1146/annurev.biochem.78.071107.134639

Ransom, R. F., & Walton, J. D. (1997). Histone Hyperacetylation in Maize in Response to Treatment with HC-Toxin or Infection by the Filamentous Fungus Cochliobolus carbonum. Plant Physiology, 115(3), 1021–1027. https://doi.org/10.1104/pp.115.3.1021

Rataj, K., & Simpson, G. G. (2014). Message ends: RNA 3′ processing and flowering time control. Journal of Experimental Botany, 65(2), 353–363. https://doi.org/10.1093/jxb/ert439

Rayson, S., Arciga-Reyes, L., Wootton, L., De Torres Zabala, M., Truman, W., Graham, N., … Davies, B. (2012). A Role for Nonsense-Mediated mRNA Decay in Plants: Pathogen Responses Are Induced in Arabidopsis thaliana NMD Mutants. PLoS ONE, 7(2), e31917. https://doi.org/10.1371/journal.pone.0031917

Reddy, A. S. N., Marquez, Y., Kalyna, M., & Barta, A. (2013). Complexity of the Alternative Splicing Landscape in Plants. The Plant Cell, 25(10), 3657–3683. https://doi.org/10.1105/tpc.113.117523

Ren, C-M., Zhu, Q., Gao, B-D., Ke, S-Y., Yu, W-C., Xie, D-X., & Peng, W. (2008). Transcription Factor WRKY70 Displays Important but No Indispensable Roles in Jasmonate and Salicylic Acid Signaling. Journal of Integrative Plant Biology, 50(5), 630–637. https://doi.org/10.1111/j.1744-7909.2008.00653.x

Riboni, M., Robustelli Test, A., Galbiati, M., Tonelli, C., & Conti, L. (2016). ABA-dependent control of GIGANTEA signalling enables drought escape via up-regulation of FLOWERING LOCUS T in Arabidopsis thaliana. Journal of Experimental Botany, 67(22), 6309–6322. https://doi.org/10.1093/jxb/erw384

Richard, P., & Manley, J. L. (2009). Transcription termination by nuclear RNA polymerases. Genes & Development, 23(11), 1247–1269. https://doi.org/10.1101/gad.1792809

Richter, R., Bastakis, E., & Schwechheimer, C. (2013). Cross-Repressive Interactions between SOC1 and the GATAs GNC and GNL/CGA1 in the Control of Greening, Cold Tolerance, and Flowering Time in Arabidopsis. Plant Physiology, 162(4), 1992–2004. https://doi.org/10.1104/pp.113.219238

Richter, R., Kinoshita, A., Vincent, C., Martinez-Gallegos, R., Gao, H., van Driel, A. D., … Coupland, G. (2019). Floral regulators FLC and SOC1 directly regulate expression of the B3-type transcription factor TARGET OF FLC AND SVP 1 at the Arabidopsis shoot apex via antagonistic chromatin modifications. PLOS Genetics, 15(4), e1008065. https://doi.org/10.1371/journal.pgen.1008065

Riechmann, J. L., & Ratcliffe, O. J. (2000). A genomic perspective on plant transcription factors. Current Opinion in Plant Biology, 3(5), 423–434.

Ripoll, J. J., Rodríguez-Cazorla, E., González-Reig, S., Andújar, A., Alonso-Cantabrana, H., Perez-Amador, M. A., … Vera, A. (2009). Antagonistic interactions between

Arabidopsis K-homology domain genes uncover PEPPER as a positive regulator of the central floral repressor FLOWERING LOCUS C. Developmental Biology, 333(2), 251–262. https://doi.org/10.1016/j.ydbio.2009.06.035

Rivas-San Vicente, M., & Plasencia, J. (2011). Salicylic acid beyond defence: Its role in plant growth and development. Journal of Experimental Botany, 62(10), 3321–3338. https://doi.org/10.1093/jxb/err031

Rohde, P., Hincha, D. K., & Heyer, A. G. (2004). Heterosis in the freezing tolerance of crosses between two Arabidopsis thaliana accessions (Columbia-0 and C24) that show differences in non-acclimated and acclimated freezing tolerance. The Plant Journal, 38(5), 790–799. https://doi.org/10.1111/j.1365-313X.2004.02080.x

Roitinger, E., Hofer, M., Köcher, T., Pichler, P., Novatchkova, M., Yang, J., … Mechtler, K. (2015). Quantitative Phosphoproteomics of the Ataxia Telangiectasia-Mutated (ATM) and Ataxia Telangiectasia-Mutated and Rad3-related (ATR) Dependent DNA Damage Response in Arabidopsis thaliana. Molecular & Cellular Proteomics, 14(3), 556–571. https://doi.org/10.1074/mcp.M114.040352

Romera-Branchat, M., Andrés, F., & Coupland, G. (2014). Flowering responses to seasonal cues: What's new? Current Opinion in Plant Biology, 21, 120–127. https://doi.org/10.1016/j.pbi.2014.07.006

Rosa, S., Duncan, S., & Dean, C. (2016). Mutually exclusive sense–antisense transcription at FLC facilitates environmentally induced gene repression. Nature Communications, 7(1), 13031. https://doi.org/10.1038/ncomms13031

Rothbart, S. B., & Strahl, B. D. (2014). Interpreting the language of histone and DNA modifications. Biochimica Et Biophysica Acta, 1839(8), 627–643. https://doi.org/10.1016/j.bbagrm.2014.03.001

Roudier, F., Ahmed, I., Bérard, C., Sarazin, A., Mary-Huard, T., Cortijo, S., … Colot, V. (2011). Integrative epigenomic mapping defines four main chromatin states in Arabidopsis. The EMBO Journal, 30(10), 1928–1938. https://doi.org/10.1038/emboj.2011.103

Saleh, A., Al-Abdallat, A., Ndamukong, I., Alvarez-Venegas, R., & Avramova, Z. (2007). The Arabidopsis homologs of trithorax (ATX1) and enhancer of zeste (CLF) establish 'bivalent chromatin marks' at the silent AGAMOUS locus. Nucleic Acids Research, 35(18), 6290–6296. https://doi.org/10.1093/nar/gkm464

Samach, A. (2000). Distinct Roles of CONSTANS Target Genes in Reproductive Development of Arabidopsis. Science, 288(5471), 1613–1616. https://doi.org/10.1126/science.288.5471.1613

Sani, E., Herzyk, P., Perrella, G., Colot, V., & Amtmann, A. (2013). Hyperosmotic priming of Arabidopsis seedlings establishes a long-term somatic memory accompanied by specific changes of the epigenome. Genome Biology, 14(6), R59. https://doi.org/10.1186/gb-2013-14-6-r59

Sartorelli, V., & Puri, P. L. (2018). Shaping Gene Expression by Landscaping Chromatin Architecture: Lessons from a Master. Molecular Cell, 71(3), 375–388. https://doi.org/10.1016/j.molcel.2018.04.025

Saze, H., Shiraishi, A., Miura, A., & Kakutani, T. (2008). Control of Genic DNA Methylation by a jmjC Domain–Containing Protein in. 319, 5.

Schenk, P. M., Kazan, K., Wilson, I., Anderson, J. P., Richmond, T., Somerville, S. C., & Manners, J. M. (2000). Coordinated plant defense responses in Arabidopsis revealed

by microarray analysis. Proceedings of the National Academy of Sciences of the United States of America, 97(21), 11655–11660. https://doi.org/10.1073/pnas.97.21.11655

Schmitges, F. W., Prusty, A. B., Faty, M., Stützer, A., Lingaraju, G. M., Aiwazian, J., … Thomä, N. H. (2011). Histone Methylation by PRC2 Is Inhibited by Active Chromatin Marks. Molecular Cell, 42(3), 330–341. https://doi.org/10.1016/j.molcel.2011.03.025

Schmitz, R. J. (2005). FRIGIDA-ESSENTIAL 1 interacts genetically with FRIGIDA and FRIGIDA-LIKE 1 to promote the winter-annual habit of Arabidopsis thaliana. Development, 132(24), 5471–5478. https://doi.org/10.1242/dev.02170

Schomburg, F. M., Patton, D. A., Meinke, D. W., & Amasino, R. M. (2001). FPA, a Gene Involved in Floral Induction in Arabidopsis, Encodes a Protein Containing RNA-Recognition Motifs. Plant Cell, 13(6):1427-36. https://doi.org/ 10.1105/tpc.13.6.1427

Schubert, D. (2019). Evolution of Polycomb-group function in the green lineage. F1000Research, 8, 268. https://doi.org/10.12688/f1000research.16986.1

Schuettengruber, B., Bourbon, H-M., Di Croce, L., & Cavalli, G. (2017). Genome Regulation by Polycomb and Trithorax: 70 Years and Counting. Cell, 171(1), 34–57. https://doi.org/10.1016/j.cell.2017.08.002

Searle, I. (2006). The transcription factor FLC confers a flowering response to vernalization by repressing meristem competence and systemic signaling in Arabidopsis. Genes & Development, 20(7), 898–912. https://doi.org/10.1101/gad.373506

Secco, D., Whelan, J., Rouached, H., & Lister, R. (2017). Nutrient stress-induced chromatin changes in plants. Current Opinion in Plant Biology, 39, 1–7. https://doi.org/10.1016/j.pbi.2017.04.001

Seo, E., Lee, H., Jeon, J., Park, H., Kim, J., Noh, Y-S., & Lee, I. (2009). Crosstalk between Cold Response and Flowering in Arabidopsis Is Mediated through the Flowering-Time Gene SOC1 and Its Upstream Negative Regulator FLC. The Plant Cell, 21(10), 3185–3197. https://doi.org/10.1105/tpc.108.063883

Sequeira-Mendes, J., Aragüez, I., Peiró, R., Mendez-Giraldez, R., Zhang, X., Jacobsen, S. E., … Gutierrez, C. (2014). The Functional Topography of the Arabidopsis Genome Is Organized in a Reduced Number of Linear Motifs of Chromatin States. The Plant Cell, 26(6), 2351–2366. https://doi.org/10.1105/tpc.114.124578

Seyfferth, C., & Tsuda, K. (2014). Salicylic acid signal transduction: The initiation of biosynthesis, perception and transcriptional reprogramming. Frontiers in Plant Science, 5. https://doi.org/10.3389/fpls.2014.00697

Shafiq, S., Berr, A., & Shen, W-H. (2014). Combinatorial functions of diverse histone methylations in Arabidopsis thaliana flowering time regulation. The New Phytologist, 201(1), 312–322. https://doi.org/10.1111/nph.12493

Shah, J., Kachroo, P., Nandi, A., & Klessig, D. F. (2001). A recessive mutation in the Arabidopsis SSI2 gene confers SA- and NPR1-independent expression of PR genes and resistance against bacterial and oomycete pathogens. The Plant Journal: For Cell and Molecular Biology, 25(5), 563–574.

Shea, D. J., Itabashi, E., Takada, S., Fukai, E., Kakizaki, T., Fujimoto, R., & Okazaki, K. (2018). The role of FLOWERING LOCUS C in vernalization of Brassica: The importance of vernalization research in the face of climate change. Crop and Pasture Science, 69(1), 30. https://doi.org/10.1071/CP16468

Shen, Y., Wei, W., & Zhou, D-X. (2015). Histone Acetylation Enzymes Coordinate Metabolism and Gene Expression. Trends in Plant Science, 20(10), 614–621.

https://doi.org/10.1016/j.tplants.2015.07.005

Shi, Y. (2017). Mechanistic insights into precursor messenger RNA splicing by the spliceosome. Nature Reviews Molecular Cell Biology, 18(11), 655–670. https://doi.org/10.1038/nrm.2017.86

Shilatifard, A. (2012). The COMPASS Family of Histone H3K4 Methylases: Mechanisms of Regulation in Development and Disease Pathogenesis. Annual Review of Biochemistry, 81(1), 65–95. https://doi.org/10.1146/annurev-biochem-051710-134100

Shimotohno, A., & Scheres, B. (2019). Topology of regulatory networks that guide plant meristem activity: Similarities and differences. Current Opinion in Plant Biology, 51, 74–80. https://doi.org/10.1016/j.pbi.2019.04.006

Shin, J-H., & Chekanova, J. A. (2014). Arabidopsis RRP6L1 and RRP6L2 Function in FLOWERING LOCUS C Silencing via Regulation of Antisense RNA Synthesis. PLoS Genetics, 10(9), e1004612. https://doi.org/10.1371/journal.pgen.1004612

Shu, J., Chen, C., Thapa, R. K., Bian, S., Nguyen, V., Yu, K., … Cui, Y. (2019). Genome-wide occupancy of histone H3K27 methyltransferases CURLY LEAF and SWINGER in Arabidopsis seedlings. Plant Direct, 3(1), e00100. https://doi.org/10.1002/pld3.100

Shukla, S., Zhao, C., & Shukla, D. (2019). Dewetting Controls Plant Hormone Perception and Initiation of Drought Resistance Signaling. Structure, 27(4), 692-702.e3. https://doi.org/10.1016/j.str.2018.12.005

Simpson, G. G., Dijkwel, P. P., Quesada, V., Henderson, I., & Dean, C. (2003). FY Is an RNA 3′ End-Processing Factor that Interacts with FCA to Control the Arabidopsis Floral Transition. Cell, 113(6), 777–787. https://doi.org/10.1016/S0092-8674(03)00425-2

Singh, P., Yekondi, S., Chen, P-W., Tsai, C-H., Yu, C-W., Wu, K., & Zimmerli, L. (2014). Environmental History Modulates Arabidopsis Pattern-Triggered Immunity in a HISTONE ACETYLTRANSFERASE1–Dependent Manner. The Plant Cell, 26(6), 2676–2688. https://doi.org/10.1105/tpc.114.123356

Singh, V., Roy, S., Singh, D., & Nandi, A. K. (2014). Arabidopsis FLOWERING LOCUS D influences systemic-acquired-resistance-induced expression and histone modifications of WRKY genes. Journal of Biosciences, 39(1), 119–126. https://doi.org/10.1007/s12038-013-9407-7

Smirnova, E., Marquis, V., Poirier, L., Aubert, Y., Zumsteg, J., Ménard, R., … Heitz, T. (2017). Jasmonic Acid Oxidase 2 Hydroxylates Jasmonic Acid and Represses Basal Defense and Resistance Responses against Botrytis cinerea Infection. Molecular Plant, 10(9), 1159–1173. https://doi.org/10.1016/j.molp.2017.07.010

Smolle, M., & Workman, J. L. (2013). Transcription-associated histone modifications and cryptic transcription. Biochimica Et Biophysica Acta, 1829(1), 84–97. https://doi.org/10.1016/j.bbagrm.2012.08.008

Soares, L. M., & Buratowski, S. (2012). Yeast Swd2 Is Essential Because of Antagonism between Set1 Histone Methyltransferase Complex and APT (Associated with Pta1) Termination Factor. Journal of Biological Chemistry, 287(19), 15219–15231. https://doi.org/10.1074/jbc.M112.341412

Song, G., & Walley, J. W. (2016). Dynamic Protein Acetylation in Plant–Pathogen Interactions. Frontiers in Plant Science, 7. https://doi.org/10.3389/fpls.2016.00421

Song, Y. H., Ito, S., & Imaizumi, T. (2013). Flowering time regulation: Photoperiod- and temperature-sensing in leaves. Trends in Plant Science, 18(10), 575–583. https://doi.org/10.1016/j.tplants.2013.05.003

Song, Y. H., Lee, I., Lee, S. Y., Imaizumi, T., & Hong, J. C. (2012). CONSTANS and ASYMMETRIC LEAVES 1 complex is involved in the induction of FLOWERING LOCUS T in photoperiodic flowering in Arabidopsis: Interaction of AS1 with CO regulates FT expression. The Plant Journal, 69(2), 332–342. https://doi.org/10.1111/j.1365-313X.2011.04793.x

Song, Y., Ji, D., Li, S., Wang, P., Li, Q., & Xiang, F. (2012). The Dynamic Changes of DNA Methylation and Histone Modifications of Salt Responsive Transcription Factor Genes in Soybean. PLoS ONE, 7(7), e41274. https://doi.org/10.1371/journal.pone.0041274

Song, Young Hun. (2016). The Effect of Fluctuations in Photoperiod and Ambient Temperature on the Timing of Flowering: Time to Move on Natural Environmental Conditions. Molecules and Cells, 39(10), 715–721. https://doi.org/10.14348/MOLCELLS.2016.0237

Song, Z-T., Sun, L., Lu, S-J., Tian, Y., Ding, Y., & Liu, J-X. (2015). Transcription factor interaction with COMPASS-like complex regulates histone H3K4 trimethylation for specific gene expression in plants. Proceedings of the National Academy of Sciences, 112(9), 2900–2905. https://doi.org/10.1073/pnas.1419703112

Sonmez, C., Baurle, I., Magusin, A., Dreos, R., Laubinger, S., Weigel, D., & Dean, C. (2011). RNA 3' processing functions of Arabidopsis FCA and FPA limit intergenic transcription. Proceedings of the National Academy of Sciences, 108(20), 8508–8513. https://doi.org/10.1073/pnas.1105334108

Soppe, W. J., Bentsink, L., & Koornneef, M. (1999). The early-flowering mutant efs is involved in the autonomous promotion pathway of Arabidopsis thaliana. Development (Cambridge, England), 126(21), 4763–4770.

Spoel, S. H., & Dong, X. (2008). Making Sense of Hormone Crosstalk during Plant Immune Responses. Cell Host & Microbe, 3(6), 348–351. https://doi.org/10.1016/j.chom.2008.05.009

Springer, N. M., Napoli, C. A., Selinger, D. A., Pandey, R., Cone, K. C., Chandler, V. L., … Kaeppler, S. M. (2003). Comparative Analysis of SET Domain Proteins in Maize and Arabidopsis Reveals Multiple Duplications Preceding the Divergence of Monocots and Dicots. Plant Physiology, 132(2), 907–925. https://doi.org/10.1104/pp.102.013722

Srikanth, A., & Schmid, M. (2011). Regulation of flowering time: All roads lead to Rome. Cellular and Molecular Life Sciences, 68(12), 2013–2037. https://doi.org/10.1007/s00018-011-0673-y

Strahl, B. D., & Allis, C. D. (2000). The language of covalent histone modifications. Nature, 403(6765), 41–45. https://doi.org/10.1038/47412

Strahl, B. D., Grant, P. A., Briggs, S. D., Sun, Z-W., Bone, J. R., Caldwell, J. A., … Allis, C. D. (2002). Set2 Is a Nucleosomal Histone H3-Selective Methyltransferase That Mediates Transcriptional Repression. Molecular and Cellular Biology, 22(5), 1298–1306. https://doi.org/10.1128/MCB.22.5.1298-1306.2002

Sui, P., Shi, J., Gao, X., Shen, W-H., & Dong, A. (2013). H3K36 Methylation Is Involved in Promoting Rice Flowering. Molecular Plant, 6(3), 975–977. https://doi.org/10.1093/mp/sss152

Sun, B., Zhou, Y., Cai, J., Shang, E., Yamaguchi, N., Xiao, J., … Ito, T. (2019). Integration of Transcriptional Repression and Polycomb-Mediated Silencing of WUSCHEL in Floral Meristems. The Plant Cell, 31(7), 1488–1505. https://doi.org/10.1105/tpc.18.00450

Sun, C., Chen, D., Fang, J., Wang, P., Deng, X., & Chu, C. (2014). Understanding the genetic and epigenetic architecture in complex network of rice flowering pathways. Protein &

Cell, 5(12), 889–898. https://doi.org/10.1007/s13238-014-0068-6

Sun, Q., Csorba, T., Skourti-Stathaki, K., Proudfoot, N. J., & Dean, C. (2013). R-Loop Stabilization Represses Antisense Transcription at the Arabidopsis FLC Locus. Science, 340(6132), 619–621. https://doi.org/10.1126/science.1234848

Sureshkumar, S., Dent, C., Seleznev, A., Tasset, C., & Balasubramanian, S. (2016). Nonsense-mediated mRNA decay modulates FLM-dependent thermosensory flowering response in Arabidopsis. Nature Plants, 2(5), 16055. https://doi.org/10.1038/nplants.2016.55

Swiezewski, S., Liu, F., Magusin, A., & Dean, C. (2009). Cold-induced silencing by long antisense transcripts of an Arabidopsis Polycomb target. Nature, 462(7274), 799–802. https://doi.org/10.1038/nature08618

Takeuchi, T., Watanabe, Y., Takano-Shimizu, T., & Kondo, S. (2006a). Roles of jumonji and jumonji family genes in chromatin regulation and development. Developmental Dynamics, 235(9), 2449–2459. https://doi.org/10.1002/dvdy.20851

Talbert, P. B., & Henikoff, S. (2017). Histone variants on the move: Substrates for chromatin dynamics. Nature Reviews Molecular Cell Biology, 18(2), 115–126. https://doi.org/10.1038/nrm.2016.148

Tamada, Y., Yun, J-Y., Woo, S. chul, & Amasino, R. M. (2009). ARABIDOPSIS TRITHORAX-RELATED7 Is Required for Methylation of Lysine 4 of Histone H3 and for Transcriptional Activation of FLOWERING LOCUS C. The Plant Cell, 21(10), 3257–3269. https://doi.org/10.1105/tpc.109.070060

Tan, L., Zhang, C., Hou, X., Shao, C., Lu, Y., Zhou, J., … He, X. (2018). The PEAT protein complexes are required for histone deacetylation and heterochromatin silencing. The EMBO Journal, 37(19), e98770. https://doi.org/10.15252/embj.201798770

Tang, D., Wang, G., & Zhou, J-M. (2017). Receptor Kinases in Plant-Pathogen Interactions: More Than Pattern Recognition. The Plant Cell, 29(4), 618–637. https://doi.org/10.1105/tpc.16.00891

Tang, X., Lim, M-H., Pelletier, J., Tang, M., Nguyen, V., Keller, W. A., … Cui, Y. (2012). Synergistic repression of the embryonic programme by SET DOMAIN GROUP 8 and EMBRYONIC FLOWER 2 in Arabidopsis seedlings. Journal of Experimental Botany, 63(3), 1391–1404. https://doi.org/10.1093/jxb/err383

Tanny, J. C. (2014). Chromatin modification by the RNA Polymerase II elongation complex. Transcription, 5(5), e988093. https://doi.org/10.4161/21541264.2014.988093

Tao, Y., Xie, Z., Chen, W., Glazebrook, J., Chang, H-S., Han, B., … Katagiri, F. (2003). Quantitative nature of Arabidopsis responses during compatible and incompatible interactions with the bacterial pathogen Pseudomonas syringae. The Plant Cell, 15(2), 317–330. https://doi.org/10.1105/tpc.007591

Tao, Z., Hu, H., Luo, X., Jia, B., Du, J., & He, Y. (2019). Embryonic resetting of the parental vernalized state by two B3 domain transcription factors in Arabidopsis. Nature Plants, 5(4), 424–435. https://doi.org/10.1038/s41477-019-0402-3

Tao, Z., Shen, L., Gu, X., Wang, Y., Yu, H., & He, Y. (2017). Embryonic epigenetic reprogramming by a pioneer transcription factor in plants. Nature, 551(7678), 124–128. https://doi.org/10.1038/nature24300

Tarkowski, Ł. P., & Van den Ende, W. (2015). Cold tolerance triggered by soluble sugars: A multifaceted countermeasure. Frontiers in Plant Science, 6. https://doi.org/10.3389/fpls.2015.00203

Thalhammer, A., Hincha, D. K., & Zuther, E. (2014). Measuring Freezing Tolerance: Electrolyte Leakage and Chlorophyll Fluorescence Assays. In D. K. Hincha & E.

Zuther (Eds.), Plant Cold Acclimation (Vol. 1166, pp. 15–24). https://doi.org/10.1007/978-1-4939-0844-8_3

Thalhammer, A., Hincha, D. K., & Zuther, E. (2014). Measuring Freezing Tolerance: Electrolyte Leakage and Chlorophyll Fluorescence Assays. Methods in Molecular Biology, 1166,15-24. https://doi.org/10. 10.1007/978-1-4939-0844-8_3

Theißen, G., Melzer, R., & Rümpler, F. (2016). MADS-domain transcription factors and the floral quartet model of flower development: Linking plant development and evolution. Development, 143(18), 3259–3271. https://doi.org/10.1242/dev.134080

Theißen, G., Rümpler, F., & Gramzow, L. (2018). Array of MADS-Box Genes: Facilitator for Rapid Adaptation? Trends in Plant Science, 23(7), 563–576. https://doi.org/10.1016/j.tplants.2018.04.008

Thorstensen, T., Grini, P. E., Mercy, I. S., Alm, V., Erdal, S., Aasland, R., & Aalen, R. B. (2008). The Arabidopsis SET-domain protein ASHR3 is involved in stamen development and interacts with the bHLH transcription factor ABORTED MICROSPORES (AMS). Plant Molecular Biology, 66(1–2), 47–59. https://doi.org/10.1007/s11103-007-9251-y

Tian, B., & Manley, J. L. (2017). Alternative polyadenylation of mRNA precursors. Nature Reviews Molecular Cell Biology, 18(1), 18–30. https://doi.org/10.1038/nrm.2016.116

Tian, Y., Zheng, H., Zhang, F., Wang, S., Ji, X., Xu, C., … Ding, Y. (2019). PRC2 recruitment and H3K27me3 deposition at FLC require FCA binding of COOLAIR. Science Advances, 5(4), eaau7246. https://doi.org/10.1126/sciadv.aau7246

Tsang, J. C., Gao, X., Lu, L., & Liu, P. (2014). Cellular reprogramming by transcription factor engineering. Current Opinion in Genetics & Development, 28, 1–9. https://doi.org/10.1016/j.gde.2014.07.001

Tsuji, H., Saika, H., Tsutsumi, N., Hirai, A., & Nakazono, M. (2006). Dynamic and Reversible Changes in Histone H3-Lys4 Methylation and H3 Acetylation Occurring at Submergence-inducible Genes in Rice. Plant and Cell Physiology, 47(7), 995–1003. https://doi.org/10.1093/pcp/pcj072

Turck, F., Roudier, F., Farrona, S., Martin-Magniette, M.-L., Guillaume, E., & Buisine, N. (2007). Arabidopsis TFL2/LHP1 Specifically Associates with Genes Marked by Trimethylation of Histone H3 Lysine 27. PLoS Genetics, 3(6), 12. https://doi.org/10.1371/journal.pgen.0030086

Turnbull, C. G. N., Booker, J. P., & Leyser, H. M. O. (2002). Micrografting techniques for testing long-distance signalling in Arabidopsis. The Plant Journal, 32(2), 255–262. https://doi.org/10.1046/j.1365-313X.2002.01419.x

Uemura, M., & Joseph, R. A. (1995). Cold Acclimation of Arabidopsis thaliana. Plant Physiology, 109, 16.

Uknes, S., Mauch-Mani, B., Moyer, M., Potter, S., Williams, S., Dincher, S., … Ryals, J. (1992). Acquired resistance in Arabidopsis. The Plant Cell, 4(6), 645–656. https://doi.org/10.1105/tpc.4.6.645

Valencia-Morales, M. del P., Camas-Reyes, J. A., Cabrera-Ponce, J. L., & Alvarez-Venegas, R. (2012). The Arabidopsis thaliana SET-domain-containing protein ASHH1/ SDG26 interacts with itself and with distinct histone lysine methyltransferases. Journal of Plant Research, 125(5), 679–692. https://doi.org/10.1007/s10265-012-0485-7

Van Criekinge, W., & Beyaert, R. (1999). Yeast Two-Hybrid: State of the Art. Biological Procedures Online, 2, 1–38. https://doi.org/10.1251/bpo16

van Dijk, K., Ding, Y., Malkaram, S., Riethoven, J-J. M., Liu, R., Yang, J., … Fromm, M.

(2010). Dynamic Changes in Genome-Wide Histone H3 Lysine 4 Methylation Patterns in Response to Dehydration Stress in Arabidopsis thaliana. BMC Plant Biology, 10(1), 238. https://doi.org/10.1186/1471-2229-10-238

van Nocker, S., & Ludwig, P. (2003). The WD-repeat protein superfamily in Arabidopsis: Conservation and divergence in structure and function. BMC Genomics, 11. https://doi.org/10.1186/1471-2164-4-50

van Verk, M. C., Gatz, C., & Linthorst, H. J. M. (2009). Chapter 10 Transcriptional Regulation of Plant Defense Responses. In Advances in Botanical Research: Vol. 51. Advances in Botanical Research (pp. 397–438). https://doi.org/10.1016/S0065-2296(09)51010-5

Vandesompele, J., De Preter, K., Pattyn, F., Poppe, B., Van Roy, N., De Paepe, A., & Speleman, F. (2002). Accurate normalization of real-time quantitative RT-PCR data by geometric averaging of multiple internal control genes. Genome Biology, 3(7), RESEARCH0034. https://doi.org/10.1186/gb-2002-3-7-research0034

Varala, K., Li, Y., Marshall-Colón, A., Para, A., & Coruzzi, G. M. (2015). "Hit-and-Run" leaves its mark: Catalyst transcription factors and chromatin modification. BioEssays, 37(8), 851–856. https://doi.org/10.1002/bies.201400205

Veley, K. M., & Michaels, S. D. (2008). Functional Redundancy and New Roles for Genes of the Autonomous Floral-Promotion Pathway. Plant Physiology, 147(2), 682–695. https://doi.org/10.1104/pp.108.118927

Verhage, L., Angenent, G. C., & Immink, R. G. H. (2014). Research on floral timing by ambient temperature comes into blossom. Trends in Plant Science, 19(9), 583–591. https://doi.org/10.1016/j.tplants.2014.03.009

Villajuana-Bonequi, M., Elrouby, N., Nordström, K., Griebel, T., Bachmair, A., & Coupland, G. (2014). Elevated salicylic acid levels conferred by increased expression of ISOCHORISMATE SYNTHASE 1 contribute to hyperaccumulation of SUMO1 conjugates in the Arabidopsis mutant early in short days 4. The Plant Journal: For Cell and Molecular Biology, 79(2), 206–219. https://doi.org/10.1111/tpj.12549

Viola Lang and E. Tapio Palva, V. (1992). The expression of a rab-related gene, rabl8, is induced by abscisic acid during the cold acclimation process ofArabidopsis thaliana (L.). Heyn. Plant in Molecular Biology. 20(5),951-62

Völkel, P., & Angrand, P-O. (2007). The control of histone lysine methylation in epigenetic regulation. Biochimie, 89(1), 1–20. https://doi.org/10.1016/j.biochi.2006.07.009

Wagner, D. (2017). Key developmental transitions during flower morphogenesis and their regulation. Current Opinion in Genetics & Development, 45, 44–50. https://doi.org/10.1016/j.gde.2017.01.018

Wagner, E. J., & Carpenter, P. B. (2012). Understanding the language of Lys36 methylation at histone H3. Nature Reviews Molecular Cell Biology, 13(2), 115–126. https://doi.org/10.1038/nrm3274

Wakeel, A., Ali, I., Khan, A. R., Wu, M., Upreti, S., Liu, D., … Gan, Y. (2018). Involvement of histone acetylation and deacetylation in regulating auxin responses and associated phenotypic changes in plants. Plant Cell Reports, 37(1), 51–59. https://doi.org/10.1007/s00299-017-2205-1

Wang, D., Weaver, N. D., Kesarwani, M., & Dong, X. (2005). Induction of protein secretory pathway is required for systemic acquired resistance. Science (New York, N.Y.), 308(5724), 1036–1040. https://doi.org/10.1126/science.1108791

Wang, G-F., Seabolt, S., Hamdoun, S., Ng, G., Park, J., & Lu, H. (2011). Multiple roles of WIN3 in regulating disease resistance, cell death, and flowering time in Arabidopsis.

Plant Physiology, 156(3), 1508–1519. https://doi.org/10.1104/pp.111.176776

Wang, Guifeng, & Köhler, C. (2017). Epigenetic processes in flowering plant reproduction. Journal of Experimental Botany, erw486. https://doi.org/10.1093/jxb/erw486

Wang, Guohua, Wang, F., Huang, Q., Li, Y., Liu, Y., & Wang, Y. (2015). Understanding Transcription Factor Regulation by Integrating Gene Expression and DNase I Hypersensitive Sites. BioMed Research International, 2015, 1–7. https://doi.org/10.1155/2015/757530

Wang, H., Liu, C., Cheng, J., Liu, J., Zhang, L., He, C., … Zhang, Y. (2016). Arabidopsis Flower and Embryo Developmental Genes are Repressed in Seedlings by Different Combinations of Polycomb Group Proteins in Association with Distinct Sets of Cis-regulatory Elements. PLOS Genetics, 12(1), e1005771. https://doi.org/10.1371/journal.pgen.1005771

Wang, H-L. V., & Chekanova, J. A. (2017). Long Noncoding RNAs in Plants. In M. R. S. Rao (Ed.), Long Non Coding RNA Biology (Vol. 1008, pp. 133–154). https://doi.org/10.1007/978-981-10-5203-3_5

Wang, J-W. (2014). Regulation of flowering time by the miR156-mediated age pathway. Journal of Experimental Botany, 65(17), 4723–4730. https://doi.org/10.1093/jxb/eru246

Wang, L., Zhang, F., Rode, S., Chin, K. K., Ko, E. E., Kim, J., … Qiao, H. (2017). Ethylene induces combinatorial effects of histone H3 acetylation in gene expression in Arabidopsis. BMC Genomics, 18(1), 538. https://doi.org/10.1186/s12864-017-3929-6

Wang, W., Vinocur, B., & Altman, A. (2003). Plant responses to drought, salinity and extreme temperatures: Towards genetic engineering for stress tolerance. Planta, 218(1), 1–14. https://doi.org/10.1007/s00425-003-1105-5

Wang, X., Chen, J., Xie, Z., Liu, S., Nolan, T., Ye, H., … Yin, Y. (2014). Histone lysine methyltransferase SDG8 is involved in brassinosteroid-regulated gene expression in Arabidopsis thaliana. Molecular Plant, 7(8), 1303–1315. https://doi.org/10.1093/mp/ssu056

Wang, Y., Ding, Z., Liu, X., Bao, Y., Huang, M., Wong, C. C. L., … Cong, Y. (2018). Architecture and subunit arrangement of the complete Saccharomyces cerevisiae COMPASS complex. Scientific Reports, 8(1), 17405. https://doi.org/10.1038/s41598-018-35609-8

Wang, Z., Cao, H., Chen, F., & Liu, Y. (2014). The roles of histone acetylation in seed performance and plant development. Plant Physiology and Biochemistry, 84, 125–133. https://doi.org/10.1016/j.plaphy.2014.09.010

Wang, Z-W., Wu, Z., Raitskin, O., Sun, Q., & Dean, C. (2014). Antisense-mediated FLC transcriptional repression requires the P-TEFb transcription elongation factor. Proceedings of the National Academy of Sciences, 111(20), 7468–7473. https://doi.org/10.1073/pnas.1406635111

Wani, S. H., Kumar, V., Shriram, V., & Sah, S. K. (2016). Phytohormones and their metabolic engineering for abiotic stress tolerance in crop plants. The Crop Journal, 4(3), 162–176. https://doi.org/10.1016/j.cj.2016.01.010

Ward, E. R., Uknes, S. J., Williams, S. C., Dincher, S. S., Wiederhold, D. L., Alexander, D. C., … Ryals, J. A. (1991). Coordinate Gene Activity in Response to Agents That Induce Systemic Acquired Resistance. The Plant Cell, 3(10), 1085–1094. https://doi.org/10.1105/tpc.3.10.1085

Waterborg, J. H. (2011). Plant histone acetylation: In the beginning…. Biochimica et

Biophysica Acta (BBA) - Gene Regulatory Mechanisms, 1809(8), 353–359. https://doi.org/10.1016/j.bbagrm.2011.02.005

Whittaker, C., & Dean, C. (2017). The FLC Locus: A Platform for Discoveries in Epigenetics and Adaptation. Annual Review of Cell and Developmental Biology, 33(1), 555–575. https://doi.org/10.1146/annurev-cellbio-100616-060546

Wickland, D. P., & Hanzawa, Y. (2015). The FLOWERING LOCUS T/TERMINAL FLOWER 1 Gene Family: Functional Evolution and Molecular Mechanisms. Molecular Plant, 8(7), 983–997. https://doi.org/10.1016/j.molp.2015.01.007

Wight, W. D., Kim, K-H., Lawrence, C. B., & Walton, J. D. (2009). Biosynthesis and role in virulence of the histone deacetylase inhibitor depudecin from Alternaria brassicicola. Molecular Plant-Microbe Interactions: MPMI, 22(10), 1258–1267. https://doi.org/10.1094/MPMI-22-10-1258

Willing, E-M., Rawat, V., Mandáková, T., Maumus, F., James, G. V., Nordström, K. J. V., … Schneeberger, K. (2015). Genome expansion of Arabis alpina linked with retrotransposition and reduced symmetric DNA methylation. Nature Plants, 1(2), 14023. https://doi.org/10.1038/nplants.2014.23

Wils, C. R., & Kaufmann, K. (2017). Gene-regulatory networks controlling inflorescence and flower development in Arabidopsis thaliana. Biochimica et Biophysica Acta (BBA) - Gene Regulatory Mechanisms, 1860(1), 95–105. https://doi.org/10.1016/j.bbagrm.2016.07.014

Woloszynska, M., Le Gall, S., & Van Lijsebettens, M. (2016). Plant Elongator-mediated transcriptional control in a chromatin and epigenetic context. Biochimica et Biophysica Acta (BBA) - Gene Regulatory Mechanisms, 1859(8), 1025–1033. https://doi.org/10.1016/j.bbagrm.2016.06.008

Wong, M. M., Chong, G. L., & Verslues, P. E. (2017). Epigenetics and RNA Processing: Connections to Drought, Salt, and ABA? In R. Sunkar (Ed.), Plant Stress Tolerance (Vol. 1631, pp. 3–21). https://doi.org/10.1007/978-1-4939-7136-7_1

Worden, E. J., & Wolberger, C. (2019). Activation and regulation of H2B-Ubiquitin-dependent histone methyltransferases. Current Opinion in Structural Biology, 59, 98–106. https://doi.org/10.1016/j.sbi.2019.05.009

Wu, C-H., Derevnina, L., & Kamoun, S. (2018). Receptor networks underpin plant immunity. Science, 360(6395), 1300–1301. https://doi.org/10.1126/science.aat2623

Wu, Z., Ietswaart, R., Liu, F., Yang, H., Howard, M., & Dean, C. (2015). Quantitative regulation of FLC via coordinated transcriptional initiation and elongation. Proceedings of the National Academy of Sciences, 113(1), 218–223. https://doi.org/10.1073/pnas.1518369112

Xia, M., Liu, J., Wu, X., Liu, S., Li, G., Han, C., … Cao, X. (2013). Histone Methyltransferase Ash1l Suppresses Interleukin-6 Production and Inflammatory Autoimmune Diseases by Inducing the Ubiquitin-Editing Enzyme A20. Immunity, 39(3), 470–481. https://doi.org/10.1016/j.immuni.2013.08.016

Xia, S., Cheng, Y. T., Huang, S., Win, J., Soards, A., Jinn, T-L., … Li, X. (2013). Regulation of transcription of nucleotide-binding leucine-rich repeat-encoding genes SNC1 and RPP4 via H3K4 trimethylation. Plant Physiology, 162(3), 1694–1705. https://doi.org/10.1104/pp.113.214551

Xiao, J., & Wagner, D. (2015). Polycomb repression in the regulation of growth and development in Arabidopsis. Current Opinion in Plant Biology, 23, 15–24. https://doi.org/10.1016/j.pbi.2014.10.003

Xie, Y., Zhang, Y., Han, J., Luo, J., Li, G., Huang, J., … Chen, L. (2018). The Intronic cis Element SE1 Recruits trans-Acting Repressor Complexes to Repress the Expression of ELONGATED UPPERMOST INTERNODE1 in Rice. Molecular Plant, 11(5), 720–735. https://doi.org/10.1016/j.molp.2018.03.001

Xing, D., Zhao, H., Xu, R., & Li, Q. Q. (2008). Arabidopsis PCFS4, a homologue of yeast polyadenylation factor Pcf11p, regulates FCA alternative processing and promotes flowering time. The Plant Journal, 54(5), 899–910. https://doi.org/10.1111/j.1365-313X.2008.03455.x

Xiong, L., & Zhu, J-K. (2003). Regulation of Abscisic Acid Biosynthesis. Plant Physiology, 133(1), 29–36. https://doi.org/10.1104/pp.103.025395

Xu, F., Kuo, T., Rosli, Y., Liu, M-S., Wu, L., Chen, L.-F. O., … Pu, L. (2018). Trithorax Group Proteins Act Together with a Polycomb Group Protein to Maintain Chromatin Integrity for Epigenetic Silencing during Seed Germination in Arabidopsis. Molecular Plant, 11(5), 659–677. https://doi.org/10.1016/j.molp.2018.01.010

Xu, Lin, Zhao, Z., Dong, A., Soubigou-Taconnat, L., Renou, J-P., Steinmetz, A., & Shen, W-H. (2008). Di- and tri- but not monomethylation on histone H3 lysine 36 marks active transcription of genes involved in flowering time regulation and other processes in Arabidopsis thaliana. Molecular and Cellular Biology, 28(4), 1348–1360. https://doi.org/10.1128/MCB.01607-07

Xu, M., Hu, T., Smith, M. R., & Poethig, R. S. (2016). Epigenetic Regulation of Vegetative Phase Change in Arabidopsis. The Plant Cell, 28(1), 28–41. https://doi.org/10.1105/tpc.15.00854

Xu, Q., & Xie, W. (2018). Epigenome in Early Mammalian Development: Inheritance, Reprogramming and Establishment. Trends in Cell Biology, 28(3), 237–253. https://doi.org/10.1016/j.tcb.2017.10.008

Xu, R., Zhao, H., Dinkins, R. D., Cheng, X., Carberry, G., & Li, Q. Q. (2006). The 73 kD Subunit of the cleavage and polyadenylation specificity factor (CPSF) complex affects reproductive development in Arabidopsis. Plant Molecular Biology, 61(4–5), 799–815. https://doi.org/10.1007/s11103-006-0051-6

Xu, S., & Chong, K. (2018). Remembering winter through vernalisation. Nature Plants, 4(12), 997–1009. https://doi.org/10.1038/s41477-018-0301-z

Xu, Y., Gan, E-S., Zhou, J., Wee, W-Y., Zhang, X., & Ito, T. (2014). Arabidopsis MRG domain proteins bridge two histone modifications to elevate expression of flowering genes. Nucleic Acids Research, 42(17), 10960–10974. https://doi.org/10.1093/nar/gku781

Yamaguchi, A., Kobayashi, Y., Goto, K., Abe, M., & Araki, T. (2005). TWIN SISTER OF FT (TSF) Acts as a Floral Pathway Integrator Redundantly with FT. Plant and Cell Physiology, 46(8), 1175–1189. https://doi.org/10.1093/pcp/pci151

Yan, Q., Zhu, C., Guang, S., & Feng, X. (2019). The Functions of Non-coding RNAs in rRNA Regulation. Frontiers in Genetics, 10, 290. https://doi.org/10.3389/fgene.2019.00290

Yan, W., Chen, D., Smaczniak, C., Engelhorn, J., Liu, H., Yang, W., … Kaufmann, K. (2018). Dynamic and spatial restriction of Polycomb activity by plant histone demethylases. Nature Plants, 4(9), 681–689. https://doi.org/10.1038/s41477-018-0219-5

Yan, Y., Shen, L., Chen, Y., Bao, S., Thong, Z., & Yu, H. (2014). A MYB-Domain Protein EFM Mediates Flowering Responses to Environmental Cues in Arabidopsis. Developmental Cell, 30(4), 437–448. https://doi.org/10.1016/j.devcel.2014.07.004

Yan, Z., Liang, D., Liu, H., & Zheng, G. (2010). FLC: A key regulator of flowering time in Arabidopsis. Russian Journal of Plant Physiology, 57(2), 166–174.

https://doi.org/10.1134/S1021443710020020

Yang, H., Howard, M., & Dean, C. (2014). Antagonistic roles for H3K36me3 and H3K27me3 in the cold-induced epigenetic switch at Arabidopsis FLC. Current Biology: CB, 24(15), 1793–1797. https://doi.org/10.1016/j.cub.2014.06.047

Yang, H., Howard, M., & Dean, C. (2016). Physical coupling of activation and derepression activities to maintain an active transcriptional state at FLC. Proceedings of the National Academy of Sciences, 113(33), 9369–9374. https://doi.org/10.1073/pnas.1605733113

Yang, H., Mo, H., Fan, D., Cao, Y., Cui, S., & Ma, L. (2012). Overexpression of a histone H3K4 demethylase, JMJ15, accelerates flowering time in Arabidopsis. Plant Cell Reports, 31(7), 1297–1308. https://doi.org/10.1007/s00299-012-1249-5

Yao, X., Feng, H., Yu, Y., Dong, A., & Shen, W-H. (2013). SDG2-Mediated H3K4 Methylation Is Required for Proper Arabidopsis Root Growth and Development. PLoS ONE, 8(2), e56537. https://doi.org/10.1371/journal.pone.0056537

Yasuda, M., Ishikawa, A., Jikumaru, Y., Seki, M., Umezawa, T., Asami, T., … Nakashita, H. (2008). Antagonistic Interaction between Systemic Acquired Resistance and the Abscisic Acid–Mediated Abiotic Stress Response in Arabidopsis. The Plant Cell, 20(6), 1678–1692. https://doi.org/10.1105/tpc.107.054296

Yoo, S. K., Chung, K. S., Kim, J., Lee, J. H., Hong, S. M., Yoo, S. J., … Ahn, J. H. (2005). CONSTANS Activates SUPPRESSOR OF OVEREXPRESSION OF CONSTANS 1 through FLOWERING LOCUS T to Promote Flowering in Arabidopsis. Plant Physiology, 139(2), 770–778. https://doi.org/10.1104/pp.105.066928

Yoo, S. K., Wu, X., Lee, J. S., & Ahn, J. H. (2011). AGAMOUS-LIKE 6 is a floral promoter that negatively regulates the FLC/MAF clade genes and positively regulates FT in Arabidopsis: Control of FLC/MAF and FT expression by AGL6. The Plant Journal, 65(1), 62–76. https://doi.org/10.1111/j.1365-313X.2010.04402.x

You, Y., Sawikowska, A., Neumann, M., Posé, D., Capovilla, G., Langenecker, T., … Schmid, M. (2017). Temporal dynamics of gene expression and histone marks at the Arabidopsis shoot meristem during flowering. Nature Communications, 8(1), 15120. https://doi.org/10.1038/ncomms15120

Young, M. D., Willson, T. A., Wakefield, M. J., Trounson, E., Hilton, D. J., Blewitt, M. E., … Majewski, I. J. (2011). ChIP-seq analysis reveals distinct H3K27me3 profiles that correlate with transcriptional activity. Nucleic Acids Research, 39(17), 7415–7427. https://doi.org/10.1093/nar/gkr416

Yu, C.-W., Chang, K-Y., & Wu, K. (2016). Genome-Wide Analysis of Gene Regulatory Networks of the FVE-HDA6-FLD Complex in Arabidopsis. Frontiers in Plant Science, 7. https://doi.org/10.3389/fpls.2016.00555

Yu, C.-W., Liu, X., Luo, M., Chen, C., Lin, X., Tian, G., … Wu, K. (2011). HISTONE DEACETYLASE6 Interacts with FLOWERING LOCUS D and Regulates Flowering in Arabidopsis. Plant Physiology, 156(1), 173–184. https://doi.org/10.1104/pp.111.174417

Yu, S., Jordán-Pla, A., Gañez-Zapater, A., Jain, S., Rolicka, A., Östlund Farrants, A.-K., & Visa, N. (2018). SWI/SNF interacts with cleavage and polyadenylation factors and facilitates pre-mRNA 3′ end processing. Nucleic Acids Research, 46(16), 8557–8573. https://doi.org/10.1093/nar/gky438

Yu, X., & Michaels, S. D. (2010). The Arabidopsis Paf1c Complex Component CDC73 Participates in the Modification of FLOWERING LOCUS C Chromatin. Plant Physiology, 153(3), 1074–1084. https://doi.org/10.1104/pp.110.158386

Yuan, L., Liu, X., Luo, M., Yang, S., & Wu, K. (2013). Involvement of Histone Modifications in Plant Abiotic Stress Responses: Histone Modifications in Plant Abiotic Stress Responses. Journal of Integrative Plant Biology, n/a-n/a. https://doi.org/10.1111/jipb.12060

Yuan, Wen, Xu, M., Huang, C., Liu, N., Chen, S., & Zhu, B. (2011). H3K36 Methylation Antagonizes PRC2-mediated H3K27 Methylation. Journal of Biological Chemistry, 286(10), 7983–7989. https://doi.org/10.1074/jbc.M110.194027

Yuan, Wenya, Luo, X., Li, Z., Yang, W., Wang, Y., Liu, R., … He, Y. (2016). A cis cold memory element and a trans epigenome reader mediate Polycomb silencing of FLC by vernalization in Arabidopsis. Nature Genetics, 48(12), 1527–1534. https://doi.org/10.1038/ng.3712

Yun, J.-Y., Tamada, Y., Kang, Y. E., & Amasino, R. M. (2012). ARABIDOPSIS TRITHORAX-RELATED3/SET DOMAIN GROUP2 is Required for the Winter-Annual Habit of Arabidopsis thaliana. Plant and Cell Physiology, 53(5), 834–846. https://doi.org/10.1093/pcp/pcs021

Zehring, W. A., Lee, J. M., Weeks, J. R., Jokerst, R. S., & Greenleaf, A. L. (1988). The C-terminal repeat domain of RNA polymerase II largest subunit is essential in vivo but is not required for accurate transcription initiation in vitro. Proceedings of the National Academy of Sciences of the United States of America, 85(11), 3698–3702. https://doi.org/10.1073/pnas.85.11.3698

Zentner, G. E., & Henikoff, S. (2013). Regulation of nucleosome dynamics by histone modifications. Nature Structural & Molecular Biology, 20(3), 259–266. https://doi.org/10.1038/nsmb.2470

Zhang, G., Zhao, F., Chen, L., Pan, Y., Sun, L., Bao, N., … Xu, L. (2019). Jasmonate-mediated wound signalling promotes plant regeneration. Nature Plants, 5(5), 491–497. https://doi.org/10.1038/s41477-019-0408-x

Zhang, H., Gao, L., Anandhakumar, J., & Gross, D. S. (2014). Uncoupling transcription from covalent histone modification. PLoS Genetics, 10(4), e1004202. https://doi.org/10.1371/journal.pgen.1004202

Zhang, K., Sridhar, V. V., Zhu, J., Kapoor, A., & Zhu, J-K. (2007). Distinctive Core Histone Post-Translational Modification Patterns in Arabidopsis thaliana. PLOS ONE, 2(11), e1210. https://doi.org/10.1371/journal.pone.0001210

Zhang, Xiaoyu, Bernatavichute, Y. V., Cokus, S., Pellegrini, M., & Jacobsen, S. E. (2009). Genome-wide analysis of mono-, di- and trimethylation of histone H3 lysine 4 in Arabidopsis thaliana. Genome Biology, 10(6), R62. https://doi.org/10.1186/gb-2009-10-6-r62

Zhang, Xiuren, Henriques, R., Lin, S-S., Niu, Q-W., & Chua, N-H. (2006). Agrobacterium-mediated transformation of Arabidopsis thaliana using the floral dip method. Nature Protocols, 1(2), 641–646. https://doi.org/10.1038/nprot.2006.97

Zhang, Xudong, Chen, S., & Mou, Z. (2010). Nuclear localization of NPR1 is required for regulation of salicylate tolerance, isochorismate synthase 1 expression and salicylate accumulation in Arabidopsis. Journal of Plant Physiology, 167(2), 144–148. https://doi.org/10.1016/j.jplph.2009.08.002

Zhang, Yinglu, Rataj, K., Simpson, G. G., & Tong, L. (2016). Crystal Structure of the SPOC Domain of the Arabidopsis Flowering Regulator FPA. PLOS ONE, 13. https://doi.org/10.1371/journal.pone.0160694

Zhang, Yong, Gu, L., Hou, Y., Wang, L., Deng, X., Hang, R., … Cao, X. (2015). Integrative genome-wide analysis reveals HLP1, a novel RNA-binding protein, regulates plant

flowering by targeting alternative polyadenylation. Cell Research, 25(7), 864–876. https://doi.org/10.1038/cr.2015.77

Zhao, D., Zhang, X., Guan, H., Xiong, X., Shi, X., Deng, H., & Li, H. (2016). The BAH domain of BAHD1 is a histone H3K27me3 reader. Protein & Cell, 7(3), 222–226. https://doi.org/10.1007/s13238-016-0243-z

Zhao, J., Hyman, L., & Moore, C. (1999). Formation of mRNA 3J Ends in Eukaryotes: Mechanism, Regulation, and Interrelationships with Other Steps in mRNA Synthesis. MICROBIOL. MOL. BIOL. REV., 63, 41.

Zhao, S., Zhang, B., Yang, M., Zhu, J., & Li, H. (2018). Systematic Profiling of Histone Readers in Arabidopsis thaliana. Cell Reports, 22(4), 1090–1102. https://doi.org/10.1016/j.celrep.2017.12.099

Zhao, W., Neyt, P., Van Lijsebettens, M., Shen, W-H., & Berr, A. (2019). Interactive and noninteractive roles of histone H2B monoubiquitination and H3K36 methylation in the regulation of active gene transcription and control of plant growth and development. The New Phytologist, 221(2), 1101–1116. https://doi.org/10.1111/nph.15418

Zhao, W., Shafiq, S., Berr, A., & Shen, W-H. (2015). Genome-wide gene expression profiling to investigate molecular phenotypes of Arabidopsis mutants deprived in distinct histone methyltransferases and demethylases. Genomics Data, 4, 143–145. https://doi.org/10.1016/j.gdata.2015.04.006

Zhao, Y., & Garcia, B. A. (2015). Comprehensive Catalog of Currently Documented Histone Modifications. Cold Spring Harbor Perspectives in Biology, 7(9), a025064. https://doi.org/10.1101/cshperspect.a025064

Zhao, Z., Yu, Y., Meyer, D., Wu, C., & Shen, W-H. (2005). Prevention of early flowering by expression of FLOWERING LOCUS C requires methylation of histone H3 K36. Nature Cell Biology, 7(12), 1256–1260. https://doi.org/10.1038/ncb1329

Zheng, S., Hu, H., Ren, H., Yang, Z., Qiu, Q., Qi, W., … Du, J. (2019). The Arabidopsis H3K27me3 demethylase JUMONJI 13 is a temperature and photoperiod dependent flowering repressor. Nature Communications, 10(1), 1303. https://doi.org/10.1038/s41467-019-09310-x

Zhong, P., Li, J., Luo, L., Zhao, Z., & Tian, Z. (2019). TOP1α regulates FLOWERING LOCUS C expression by coupling histone modification and transcription machinery. Development, 146(4), dev167841. https://doi.org/10.1242/dev.167841

Zhou, X., Sen, I., Lin, X-X., & Riedel, C. G. (2018). Regulation of Age-related Decline by Transcription Factors and Their Crosstalk with the Epigenome. Current Genomics, 19(6), 464–482. https://doi.org/10.2174/1389202919666180503125850

Zhu, X., Ma, H., & Chen, Z. (2011). Phylogenetics and evolution of Su(var)3-9 SET genes in land plants: Rapid diversification in structure and function. BMC Evolutionary Biology, 11(1), 63. https://doi.org/10.1186/1471-2148-11-63

Zhu, Y., Dong, A., & Shen, W-H. (2012). Histone variants and chromatin assembly in plant abiotic stress responses. Biochimica et Biophysica Acta (BBA) - Gene Regulatory Mechanisms, 1819(3–4), 343–348. https://doi.org/10.1016/j.bbagrm.2011.07.012

Zong, W., Zhong, X., You, J., & Xiong, L. (2013). Genome-wide profiling of histone H3K4-tri-methylation and gene expression in rice under drought stress. Plant Molecular Biology, 81(1–2), 175–188. https://doi.org/10.1007/s11103-012-9990-2

Introduction Générale

Chez les eucaryotes, l'ADN portant l'information génétique s'associe aux protéines histones pour former la chromatine dans le noyau et renforcer la stabilité du génome tout en veillant à sa bonne transcription. Les modifications post-traductionnelles covalentes des histones jouent un rôle important dans la modulation de la structure de la chromatine et ont été impliquées dans le contrôle de multiples processus développementaux chez les plantes. Ces modifications sont mises en place par différentes enzymes dites de modification des histones. Parmi elles, les membres du groupe Trithorax (TrxG) responsables de la méthylation de l'histone H3 sur la lysine 4 (H3K4) et / ou 36 (H3K36), deux marques corrélées à la transcription active, ont été impliqués dans le contrôle de divers processus cellulaires tels que la transcription (Berr *et al.*, 2016).

Au cours de mon projet de thèse, je me suis concentré sur l'étude de deux membres de la famille TrxG chez *Arabidopsis thaliana*, dénommés SET DOMAIN GROUP 8 (SDG8) et SDG26 au travers de trois aspects :

- **Comment *SDG8* en relation avec l'ARN polymérase II contribue à l'immunité inerte de la plante par la régulation de gènes liés à la voie de signalisation de l'acide salicylique (SA) ?**
- **Comment *SDG26* est impliqué dans la réponse au stress abiotique en lien avec l'acide abscissique (ABA) ?**
- **Comment *SDG26* régule certains gènes essentiels de la floraison au travers d'un nouveau complexe multi-protéique ?**

Résultats et Discussion

SDG8 par son activité histone méthyltransférase potentialise l'induction transcriptionnelle efficace de gènes liés à l'immunité inerte chez Arabidopsis

Alors que de nombreux articles se sont intéressés aux rôles joués par les histones méthyltransférases dans le contrôle d'étapes importantes liées au développement des plantes (*i.e.* la gamétogenèse, le développement des graines, la germination, la détermination du devenir cellulaire, l'induction de la floraison et la vernalisation ; Fletcher, 2017), il existe encore relativement peu d'études portant sur leur implication dans la réponse aux stress (Ramirez-Prado et al., 2018). En utilisant *sdg8-1*, un mutant de perte de fonction de l'histone méthyltransférase SDG8 impliquée dans la di- et tri-méthylation en H3K36 (H3K36me2 et H3K36me3), nous avons mis en évidence la contribution de la méthylation en H3K36, en relation avec l'ARN polymérase II, dans l'immunité d'*Arabidopsis*. En effet, nous avons montré que même si *sdg8-1* présentait une sensibilité plus élevée aux différentes souches du pathogène bactérien *Pseudomonas syringae*, le mécanisme de défense gène-contre-gène semblait toujours opérationnel chez le mutant, mais avec une efficacité moindre par rapport à des plantes sauvages. Par des analyses de métabolomique, nous avons démontré que le taux d'acide salicylique (SA), une hormone de défense des plantes, était anormalement élevé dans des conditions de croissance normales chez le mutant, que son augmentation en début d'infection était similaire à celle observée chez les plantes sauvages, mais que son taux chutait rapidement à un stade ultérieur d'infection. De manière concomitante, la transcription de plusieurs gènes liés à la défense le long de la voie de signalisation SA n'était pas induite de manière efficace. En utilisant du SA exogène comme stimulus, nous avons en outre remarqué que l'inefficacité d'induction de ces gènes n'était pas strictement due à la non-accumulation de SA observée chez *sdg8-1* à des stades avancés d'infection. Au regard de la chromatine, les niveaux globaux de certaines marques de méthylation H3 dites activatrices (H3K4me3 et H3K36me3) ou répressives (H3K27me3) au regard de la transcription se sont révélés stables après un traitement SA chez des plantes sauvages, alors qu'au niveau de certains gènes de défense, leur induction par du SA était corrélée à une augmentation de la quantité d'ARN polymérase II (ARNPII) et de méthylation en H3K4 et H3K36. Fait intéressant,

de tels changements étaient absents chez le mutant *sdg8-1*. Enfin, confirmant la corrélation entre l'augmentation du recrutement de ARNPII et l'augmentation de la méthylation en H3K4 et H3K36, nous avons constaté que la protéine SDG8 pouvait interagir physiquement avec les différentes formes phosphorylées du domaine C-terminal de l'ARNPII. Nous proposons donc que le couplage physique entre SDG8, par son activité d'histone méthyltransférase, et l'ARNPII soit fonctionnellement crucial pour permettre l'induction transcriptionnelle forte de certains gènes de défense. En résumé, nos résultats démontrent le rôle fondamental joué par SDG8 chez Arabidopsis pour assurer une immunité durable.

SDG26 participe à la régulation de la réponse aux stress abiotiques par l'intermédiaire de la voie de la biosynthèse et du catabolisme de l'acide abscissique chez Arabidopsis

SDG26 est un autre membre de la famille TrxG chez *Arabidopsis* qui a jusqu'à maintenant principalement été étudié au regard du phénotype de floraison tardive causé par sa mutation (Xu et *al.*, 2007). Cependant, des analyses *in silico* nous ont permis de mettre en évidence son implication potentielle dans la réponse aux stress abiotiques (*e.g.* dans des donnés publiques de microarray *SDG26* apparaît transcriptionnellement induit par divers stress abiotiques; la séquence promotrice de SDG26 contient des éléments cis-régulateurs reconnus par des facteurs de transcription liés aux stress abiotiques). Sur la base de ces informations, nous avons décidé d'explorer l'implication de *SDG26* dans la réponse au stress abiotiques. Avant tout nous avons décidé de mieux caractériser le gène *SDG26*. En plus du transcrit classique SDG26 nommé SDG26-a/b étudié jusqu'ici et codant une protéine de 492 aa (55,3 kDa), nous avons identifié un second transcrit appelé SDG26-c codant pour une protéine putative de 253 aa (28,8 kDa). Nous avons détecté les deux transcrits dans différents tissus d'Arabidopsis, bien que SDG26-c soit environ dix fois moins exprimé que SDG26-a/b. De plus, la protéine correspondant à SDG26-a/b est principalement retrouvée dans le noyau, alors que celle correspondant à SDG26-c est retrouvée au niveau de la membrane plasmique. Des tests de complémentation nous ont permis de constater que seul SDG26-a/b permettait de complémenter le phénotype de

floraison tardive du mutant *sdg26*. Des lignées *sdg26* transgéniques stables portant la séquence génomique de SDG26 fusionnées à la GFP ou à 10xMyc sous le contrôle du promoteur 35S ou sous le contrôle du promoteur natif de *SDG26* ont également été produites et ont permis de complémenter le phénotype de *sdg26*. Dans ces lignées génomiques, les deux transcrits étaient toujours détectés mais seule la protéine codée par SDG26-a/b était observée. En conclusion, nous supposons que le transcrit SDG26-c serait la cible du NMD (nonsense-mediated mRNA decay), un mécanisme capable de reconnaitre et de dégrader les ARNm portant un codon stop prématuré afin d'empêcher la synthèse de protéines tronquées. En outre, nous avons pu constater par des analyses d'hybridation *in situ* et des tests de coloration GUS, que SDG26 devait jouer différents rôles tout au long de la croissance et du développement de la plante.

Par la suite, en étudiant l'inductibilité de SDG26 par différents stress et différentes hormones liées au stress abiotique (*i.e.* ABA, kinétine ou ACC), nous avons découvert que *SDG26* était induit spécifiquement par un stress thermique à 4°C et un stress hydrique. Cette induction a également pu être confirmée par des tests de coloration à l'aide de lignées exprimant le gène *GUS* sous le contrôle du promoteur de *SDG26*. En outre, le mutant *sdg26* présente un retard de germination en condition normale et une sensibilité moindre à l'ABA par rapport au contrôle sauvage. Fait intéressant, en utilisant une approche métabolomique, nous avons constaté que le niveau d'ABA endogène était significativement plus bas chez *sdg26* par rapport au contrôle sauvage et que ce niveau n'augmentait que légèrement suite à une stimulation par le froid. Soutenant ce résultat et en accord avec les données de microarray publiées précédemment (Liu *et al.*, 2016), plusieurs gènes impliqués dans la biosynthèse et le catabolisme de l'ABA (*e.g. ABA1, ABA* et *AAO3* ; *CYP707A3* et *CYP707A4*, respectivement) ont été trouvés dérégulés chez *sdg26*. Plus en aval, certains gènes liés au froid dépendants de l'ABA (*e.g.* les gènes *CBF*) ont été trouvés régulés à la baisse chez *sdg26*, tandis que les gènes indépendants de l'ABA étaient inchangés. Ces différents résultats semblent indiquer que *SDG26* régule positivement la réponse au stress froid en renforçant la voie de biosynthèse de l'ABA et en inhibant la voie de dégradation de l'ABA.

SDG26 participe au control des gènes de régulation de la floraison *FLC* et *SOC1* au sein d'un complexe multiprotéique

Les mutants pour les histones méthyltransférases SDG8 (Zhao et al., 2005) et SDG25 (Berr et al., 2009) présentent un phénotype de floraison précoce, alors que le mutant pour SDG26 présente lui un phénotype de floraison tardive (Xu *et al.*, 2007). Afin de mieux appréhender le positionnement génétique de ces histone méthyltransférases le long des voies de signalisation de la floraison, nous avons entrepris une approche génétique en croisant les mutants *sdg8*, *sdg25* et *sdg26* avec des mutants pour des gènes de floraison critiques tels que *FLOWERING LOCUS C* (*FLC*), ou les intégrateurs floraux *SUPPRESSOR OF OVEREXPRESSION OF CO 1* (*SOC1*) et *FLOWERING LOCUS T* (*FT*). Les analyses du temps de floraison et de l'expression des gènes de la floraison nous ont permis de confirmer que SDG8 et SDG25 inhibaient la floraison *via* l'activation de *FLC*. Nous avons également constaté une régulation mutuelle entre *SOC1* et *FT* puisque *SOC1* était régulée à la baisse chez le mutant *ft* et que *FT* était régulée à la hausse dans le mutant *soc1*. Corrélée à cette régulation mutuelle, nous avons constaté que la mutation *FT* affectait le dépôt de certaines marques d'histone sur *SOC1* et inversement. Outre ces résultats, un effet synergique a été observé entre *sdg26* et les mutants *soc1* et *ft*, alors que la mutation de *FLC* permettait de complémenter le phénotype de floraison tardive de *sdg26*. Il convient également de noter que la chromatine de *SOC1* dans le double mutant *flc sdg26* se comportait de la même manière que dans le simple mutant *sdg26*, avec une diminution des niveaux de H3K4me3 et H3K36me3 et une augmentation du niveau de H3K27me3. Ensemble, ces résultats indiquent que la répression de *SOC1* médiée par FLC pourrait se faire partiellement par le biais de l'SDG26. Auparavant, il a été montré que le phénotype de floraison tardive du mutant *sdg26* était complémentée par une phase de vernalisation (*i.e.* phase pouvant être défini comme l'acquisition ou l'accélération de la capacité à fleurir suite à un traitement au froid ; Berr et al., 2015). En dehors de cela, en considérant les phénotypes de floraison des mutants simples *sdg26*, *flc* et double *flc sdg26* et les corrélations moléculaires entre *sdg26* et *flc*, nos résultats renforcent la forte implication de SDG26 dans la voie de signalisation de la floraison dite autonome.

En outre, en utilisant une approche protéomique confirmée par d'autres méthodes (co- immunoprécipitation, BiFC et / ou double-hybride chez la levure), plusieurs

partenaires protéiques de SDG26 ont été identifiés. Sur cette base, un complexe a été construit autour de SDG26, contenant le facteur de transcription LD (LUMINIDEPENDENS), l'histone H3K4 déméthylase FLD (FLOWERING LOCUS D), un composant du complexe transcriptionnel COMPASS, APRF1/S2La. Par une approche génétique et après l'analyse du phénotype de floraison, nous avons constaté que les mutants doubles *sdg26 fld*, *sdg26 ld* et *sdg26 aprf1* étaient similaires aux mutants simples *fld*, *ld* et *aprf1*, suggérant ainsi que l'effet épistatique des mutations de *FLD*, *LD* et *APRF1*/*S2La* sur *sdg26*. Confortant davantage l'existence de ce complexe protéique, nous avons découvert par des analyses d'immunoprécipitation de la chromatine que la liaison de SDG26 au niveau de la chromatine de *FLC* nécessitait LD, FLD et APRF1/S2La. De manière surprenante, SDG26 peut également se lier à *SOC1* (connu pour être réprimé directement par FLC), et la liaison de SDG26 à *SOC1* nécessite également LD, FLD et APRF1/S2La. En analysant le comportement de certaines marques d'histones au niveau de la chromatine de *FLC* et *SOC1*, l'acétylation de H3 et le niveau de H3K4me3 chez les mutants *ld* et *fld* présentaient un pic au niveau du site d'initiation et de terminaison de la transcription, alors que chez le mutant *aprf1*, ces mêmes marques étaient enrichies du côté de l'extrémité 3 'de *FLC*. A l'inverse, aucun changement pour l'acétylation de H3 et le niveau de H3K4me3 au niveau de *FLC* n'était observable chez le mutant *sdg26*. En plus des modifications des marques actives observées chez certains mutants, tous les mutants présentaient une diminution du niveau de la marque répressive H3K27me3 sur *FLC*. Des transcrits antisens collectivement dénommés COOLAIR sont produits à partir d'un promoteur situé dans la région 3 'en aval de *FLC* et participent à la régulation négative de la transcription de *FLC*. Nos analyses par qPCR nous ont permis de montrer que les transcrits distaux COOLAIR poly (A) et les transcrits COOLAIR totaux étaient induits dans les mutants simples *fld*, *sdg26* et double *fld sdg26*. Dans l'ensemble, nos résultats indiquent que LD est un élément central d'un complexe comprenant à la fois des activateurs (APRF1 / S2La et SDG26) et un répresseur (FLD) de la transcription. Ce complexe est recruté au niveau de la chromatine de *FLC* et de *SOC1* pour réprimer *FLC* et pour induire *SOC1*, respectivement, sachant que FLC est connue comme étant un répresseur de *SOC1*. Bien que la manière dont le complexe active la transcription de *SOC1* ne soit pas encore totalement claire, nous supposons que la régulation de ces deux gènes par un seul et même complexe protéique pourrait servir à équilibrer leur régulation transcriptionnelle afin de garantir un temps de floraison optimal.

Conclusion

Pour résumer, les résultats de ma thèse soutiennent encore d'avantage le rôle important joué par la méthylation de l'histone et les histone-méthyltransférases dans différents processus liés à la réponse au stress et aux transitions développementales chez Arabidopsis. Après détection, la stimulation d'une voie de signalisation d'un stress donné a généralement pour effet de hiérarchiser les processus de défense par rapport aux processus cellulaires liés à la croissance, et cet équilibrage se doit d'être précisément régulé afin de fournir suffisamment de ressources pour la survie et la reproduction. La position des histone-méthyltransférases à la jonction entre réponse au stress et transition développemental pourrait donc servir cet équilibre afin de garantir la survie de la plante.

Université de Strasbourg

École Doctorale des Sciences de la Vie et de la Santé STRASBOURG

Xue ZHANG

Implications fonctionnelles de deux histone méthyltransferases dans les réponses aux stress et la régulation de la floraison chez *Arabidopsis thaliana*

Résumé

La méthylation des histones par des histone-méthyltransférases est essentielle à la régulation de la transcription. Chez les végétaux, plusieurs méthyltransférases jouent un rôle central dans différents processus cellulaires. Lors de ma thèse, j'ai étudié la fonction biologique de deux d'entre elles dans le contrôle des réponses à plusieurs stimuli chez Arabidopsis thaliana. Premièrement, mes résultats ont permis de démontrer que SDG8, une méthyltransférase spécifique de H3K36, contrôlait la transcription de NPR1, un acteur central de l'immunité induite par l'acide salicylique, et en lien avec la RNAPII permettait l'induction transcriptionnelle efficace de plusieurs gènes de défense suite à leur stimulation. Deuxièmement, j'ai démontré que SDG26, une méthyltransférase proche de SDG8, jouait un rôle important dans la réponse aux stress abiotiques. J'ai découvert ainsi que SDG26 régulait la réponse au froid en activant directement la transcription des gènes SOC1 et CBF en se liant à leur chromatine et en déposant H3K36me3. Sachant que l'acide abscissique (ABA) joue un rôle important dans la réponse aux stress abiotiques, j'ai pu constater que SDG26 contrôlait l'accumulation d'ABA en régulant l'expression de gènes liés à son homéostasie. Enfin, j'ai confirmé par une approche génétique que SDG26 était un élément appartenant à la voie de floraison dite autonome. Au sein d'un complexe multi-protéique comprenant l'histone déméthylase FLD, le facteur de transcription homéobox LD, ainsi qu'un composant de COMPASS, APRF1, SDG26 semble contrôler la transcription du répresseur de floraison, FLC, ainsi que de sa cible, l'activateur de floraison SOC1, afin de réguler précisément la transition florale.

Mots-clés: méthylation d'histones, SDG8, SDG26, transcription génique, immunité, stress dû au froid, floraison, Arabidopsis thaliana

Summary

Histone methylation catalyzed by histone methyltransferase is essential in transcriptional regulation of gene expression. Histone methyltransferases are known to play crucial roles in multiple cellular processes in plants. My PhD work investigated the biological function of two histone methyltransferases in controlling plant responses to various environmental stimuli in Arabidopsis thaliana. In the first part, my results demonstrated that the H3K36-methyltransferase SDG8 transcriptionally regulates NPR1, a central player in salicylic acid-mediated immunity and co-acts with the RNAPII to enable the efficient transcriptional induction of several defense genes upon stimulation. In the second part, my work unraveled that SDG26, another ortholog of the animal H3K36-methyltransferase, plays an important role in plant response to abiotic stresses. By focusing on cold stress, SDG26 was shown to regulate the cold stress response by directly activating the transcription of SOC1 and CBF genes through binding their chromatin and depositing H3K36me3. Interestingly, SDG26 mastered the accumulation of ABA by regulating the expression of ABA homeostasis-related genes, suggesting an involvement of ABA pathway in the cold response. In the last part, using a genetic approach my work established SDG26 as an autonomous flowering pathway component. Accordingly, SDG26 was found in a multiple-protein complex comprising the histone demethylase FLD, the homeobox-domain transcription factor LD, as well as a putative COMPASS component APRF1. This multiple-protein complex was found in controlling the repression of the major flowering repressor FLC as well as the activation of the flowering activator SOC1 to precisely regulate the floral transition.

Keywords: histone methylation, SDG8, SDG26, gene transcription, immunity, cold stress, flowering, *Arabidopsis thaliana*